MONTAN UNIVERSITÄT
WWW.UNILEOBEN.AC.AT

Dissertation

von

Muhammad Imran Irfan M.Sc.

Anthropogenic versus geogenic contamination of the Vordernbergerbach valley, Steiermark, Austria.

A geochemical, mineralogical and geophysical study.

Ausgeführt zum Zwecke der Erlangung des akademischen Grades eines Doktors der montanistischen Wissenschaften

Durchgeführt am Lehrstuhl Allgemeine und Analytische Chemie an der Montanuniversität Leoben unter der Erstbetreuung von A.o. Univ. Prof. Mag. Dr. Thomas Meisel

Leoben, Juli 2012

Eidesstattliche Erklärung:

Ich erkläre an Eides statt, dass ich diese Arbeit selbständig verfasst, andere als die angegebenen Quellen und Hilfsmittel nicht benutzt und mich auch sonst keiner unerlaubten Hilfsmittel bedient habe.

Affidavit:

I declare in lieu of oath, that I wrote my thesis and performed and associated research myself, using only literature cited in this volume.

Muhammad Imran Irfan M.Sc.

Leoben, Juli 2012

Acknowledgements

I want to pay my humble thanks to my academic advisor A.o. Univ. Prof. Mag. Dr. Thomas Meisel at the Chair of General and Analytical Chemistry, Montanuniversität Leoben, for his kind, guiding and professional supervision who gave me an opportunity to write this thesis providing the perfect working conditions and scientific support. Words cannot describe my feeling of gratitude for him.

I want to pay thanks to A.o.Univ. Prof. Dr. Robert Scholger, at the Chair of Geophysics, Montanuniversität Leoben, for his technical guidance and support. I am grateful for his cooperation during measurements at Geophysics Lab, Montanuniversität Leoben.

I am thankful to Dr. Federrica Zaccarini, Dr. Johann Raith and Dr. Hassan Neinavaie for their guidance and technical support during mineralogical study at the Chair of Mineralogy, Montanuniversität Leoben.

I wish to pay thanks to Dany Sarvad M.Sc., at the University of Quebec at Chicoutimi, Canada, who performed analysis on my samples with the help of laser ablation, I am thankful for his guidance and assistance.

Additionally, I am very grateful to all of my colleagues at the Chair of General and Analytical Chemistry, Montanuniversität Leoben, especially Karin Schober, Hubert Falk and Friedrich Pichler, Thomas Christof and Wolfgang Neff who provided me assistance, moral support and perfect working conditions to accomplish this project.

I am thankful to OeAD and HEC-Pakistan who funded this project and I am grateful to the Chair of General and Analytical Chemistry, who organized everything to make it possible.

Moreover, I am grateful to my loving parents Sher Muhammad and Rabia Bibi who always have been encouraging me and praying for me. I feel lack of vocabulary to pay gratitude to them.

Dedication

I dedicate my work to my loving parents, who have been encouraging and guiding me throughout my life. I find myself the luckiest person of the world having such loving parents. I am grateful to my uncle Rafique's family especially aunt Nasreen, who has a big contribution in my educational carrier. I am thankful to my loving family members and friends who are assets of my life.

Table of Contents

Zusammenfassung

In dieser Studie wurden umfassende geochemische, mineralogische und geophysikalische Untersuchungen von Sedimenten des Vordernberger Baches sowie an Böden- und Staubproben, im Bezirk Leoben, Steiermark, Österreich durchgeführt. Die Bachsedimentproben wurden ausgehend von den Quellen am Polster/Präbichl (1500 m.ü.M) bis zur Mündung in die Mur im Stadtgebiet von Leoben gesammelt.

Der Einfluss sowohl der historischen Bergbau-, Vehüttungsaktivitäten als auch der modernen Stahlproduktion auf die Zusammensetzung der Bachsedimente, waren ein Hauptaspekt der Untersuchungen. Die Erfassung der magenetischen Suszeptibilität als Methode zur Katierung des Ausmaßes der Kontamination durch einen anthropogenen Einfluss hat sich als ausgesprochen nützlich erwiesen.

Erhöhte Gehalte an Schwermetallen wurden insbesonders in den Sedimenten der Lokalitäten Vordernberg und Donawitz festgestellt. Zudem wurden auch in Bodenproben aus der Judaskreuzsiedlung/Donawitz Kontaminationen festgestellt, wobei die Gehalte von Ni, Cr, Zn und Pb über den Grenzwerten liegen. Die Schwermetalle sind in enger Beziehung zu magnetischen Partikeln anthropogenen Ursprungs. Mikroskopische und Mikrosondenuntersuchungen lassen erkennen, dass diese Partikel sich vor allem aus Magnetite, aber auch Hämatit, Schlacke, Zunder, Sinter und Röstgut zusammensetzen. Auffällig waren kugelförmige Magnetite mit Durchmessern von kleiner 10 bis ca. 100 µm in der Schwermineralfraktion aller Proben. Die Erscheinungsformen dieser kugelförmigen Partikel reichen von hohl, dickwandig bis kompakt mit glatter bis sehr strukturierter Oberfläche. Die Häufigkeiten dieser magnetischen Partikel in den Schwermineralfraktion (0.1 bis 0.71 mm und einer Dichte > 2.9 g/cm^3) sind höher in den Proben von Friedauwerk und Donawitz als in der Probe von Gmeingrube/Trofaich.

Erstmals wurde auch ein Laserablation-ICP-MS für die Untersuchung der Schwermetallgehaltverteilung in den magnetischen Partikeln eingesetzt. Es zeigte sich, dass Cr und Ni gleichmäßig in diesen Partikeln verteilt ist, wohingegen Pb nur an der Oberfläche der meisten Partikel gefunden wurde. Die Untersuchungen der Bodenproben und frischen Staubproben zeigen, dass sich die chemische Zusammensetzung und die Erscheinungsform der Partikel in den letzten 60 Jahren nicht verändert haben.

Im Gegensatz zu dem historisch bedingten Eintrag vom anthropogenen Material im Bereich Vordernberg und Trofaich, wurde rezent in Bereich Donawitz zusätzlich noch technogener Apatit, Magnesioferrit und Ferrosilizium eingetragen.

Eine Überwachung der Luftimmissionen im Bereich Donawitz ist auch gegenwärtig notwendig, es zeigt sich aber, dass der Einsatz von einfachen geophysikalischen Instrumenten für die Quantifizierung und Ausbreitung der Kontaminationen gut geeignet ist.

Abstract

A comprehensive geophysical, geochemical and mineralogical study of sediments from alpine river Vordernbergerbach (Styria) starting from its origin (1500 m above sea level) till its confluence point with river Mur at Leoben (540 m above sea level) has been made. The impact of historical mining activity, iron smelting and modern steel production plant has been investigated. Magnetic susceptibility measurements proved a suitable tool to mark the contaminated areas due to heavy metals deposition by iron and steel production plant due to association of heavy metals with spherical magnetite of anthropogenic nature identified with the help of EMPA. Geochemical analysis of Vordernbergerbach sediments and soil collected from Judaskreuzsiedlung near the steel production plant Donawitz/Leoben show a higher heavy metal content at contaminated sites in particular at the localities of Vordernberg and Donawitz/Leoben. The concentration of heavy metals (Cr and Ni) content was found beyond safe limit in the Vordernberg region in sediments. Nickel, Cr, Pb, and Zn concentrations were found to be beyond the safe limit in soil near the Donawitz steel plant. Heavy metals were found associated with anthropogenic particles like magnetites mainly, but also hematites, slag, scale, sinter and roasting ore when analyzed with the help of optical microscopy and electron microprobe analysis (EMPA). A detailed mineralogical study of the heavy mineral fraction of the sediments revealed the fact, that heavy metal are associated with spherical magnetites with a range of diameters from <10 µm to 100 µm having a variety of morphology including hollow, compact, rimmed and smooth surfaces. Relative abundance of heavy minerals (0.1 to 0.71 mm and >2.9 g/cm^3) was found much higher at contaminated sites at Friedauwerk and Donawitz/Leoben when compared to Gmeingrube. For the first time Laser ablation coupled with ICP-MS was applied to identify the distribution of heavy metals within the carrier particles magnetites mainly. Heavy metals like Cr and Ni were found within the spherical particles and in flakes or scales, while lead was identified as a veneer covering the particles of anthropogenic origin, in soil and dust samples with the help of laser ablation mapping. The lead covering the anthropogenic particles is persisted over ~60 years in the soil. Recent input of heavy metals by the Voest-alpine plant has added more anthropogenic particles/minerals such as apatite, magnesioferrite and ferrosilicon to the list of anthropogenic particles by smelters which can be observed in other regions of with historic iron production. For this reason monitoring of anthropogenic immissions is still necessary, but can be conducted with simple instrumentation such as magnetic susceptibility tools.

1. Introduction

Some species of heavy metals, e.g., nickel, chromium and lead etc. have adverse effect on human health. Industrial processes like combustion of fossil fuels, municipal waste incineration, cement production and metallurgical processes are responsible for emission of ferromagnetic particles along with toxic heavy metals. Ferromagnetic particles are formed during industrial process, e.g., oxidation of iron sulphides in coal results in production of ferromagnetic particles. Ferromagnetic particles especially magnetite and hematite after emission get transported and ultimately deposited along with heavy metals. Industrial emissions are always a matter of concern for human health. Recently magnetic susceptibility device has been used as in-situ device to highlight the contaminated spots. Heavy metal's association with ferromagnetic particles facilitates this device to establish a correlation between magnetic susceptibility values and content of heavy metals. Some researchers have already reported a good correlation of heavy metals with magnetic susceptibility in area closer to steel production plant in Donawitz/Leoben. Hanesch, Scholger et al. (2003) and Blaha, Appel et al. (2008) have found a correlation of magnetic susceptibility with concentration of heavy metals in leaf and soil samples in the contaminated region of Leoben and surroundings. The target of this study was to distinguish between anthropogenic and geogenic contamination of river sediments and soil due to heavy metals. This thesis involved a geophysical, geochemical and mineralogical study in detail. Moreover the target of this study was to find the distribution of heavy metals, e.g., nickel, chromium in carrier particles in a historic context.

1.1. Nickel

Nickel ($_{28}$Ni) is a silvery white metal and belongs to the transition elements. It is hard, ductile and takes on high polish.

1.1.1. Occurrence and production

Earth's crust contains roughly 0.016 % of nickel, making it the 24th most abundant metal. Two types of ore deposits are vital for nickel mining. The first are laterites where the principal ore minerals are nickeliferous limonite: (Fe, Ni)O(OH) and garnierite (a hydrous nickel silicate): $(Ni,Mg)_3Si_2O_5(OH)$. The second are magmatic sulphide deposits where the

principal ore mineral is pentlandite: $(Ni,Fe)_9S_8$. 72 % of nickel contained resources in the world are laterite and about 28 % are sulphides (Dalvi et al., 2004). However, due to requirement of less energy, pyrometallurgical extraction of Ni from sulphide ore is easier than from other ores (McNear Jr et al., 2007). 58 % of the nickel production in the world is being done by processing the sulphide ore while 42 % of Nickel is being produced from laterite. China contributes 70 % of world's nickel production (Dalvi et al., 2004). According to annual report of MMC Norilsk Nickel for 2010, it has contributed 297,000 tonnes of nickel production which is 20 % of all global nickel production for 2010 (MMC Norilsk Nickel, 2010). Other major deposits of nickel are found in New Caledonia, Australia, Cuba, Philippines and Indonesia (Dalvi et al., 2004). The deposits in tropical areas are typically laterites. These laterites are produced by the intense weathering of ultramafic igneous rocks and the resulting secondary concentration of nickel bearing oxide and silicate minerals. Recently known deposits in western Turkey are especially important and convenient for European smelters, steelmakers and factories. Riddle, Oregon is the only locality in the United States known for commercial mining of nickel, where several square miles of nickel-bearing garnierite (hydrous nickel silicate) surface deposits are located. Most of the nickel of planet earth, is supposed to be concentrated in the earth's core as it is evidenced by iron meteorites that present the core of small planets. Till 2003, eight time increase in the production of Ni as compared to its production in 1950 has been reported (Dalvi et al., 2004)

1.1.2. Anthropogenic sources

Heavy metals can be present naturally in the soil either being originated from parent bed rock material in soil or due to volcanic activities. In addition to the natural presence, there are many anthropogenic sources which contribute towards the environmental pollution for example, fertilizers, pesticides, industrial activities such as mining and emission of dust particulates from industries (Desenfant et al., 2004). The amount of trace metals (in thousand tons per year) which are contributed to the biosphere *(terrestrial + aquatic input – atmospheric emission)* in 1983 are shown in Table 1 (Nriagu and Pacyna, 1988).

Trace elements	Amount (103 tons)
Zn	2,340
Cu	2150
Pb	1,160
Ni	470
As	120
Mo	110
Se	79
Sb	72
V	71
Cd	30
Hg	11

Table 1 Contribution of trace metals to the biosphere (1983)

1.1.2.1. Nickel in air

Pollutants enter in the air, water and soil. Anthropogenic sources of nickel which contaminates the air include coal and oil burning for heat or power generation, incineration of waste and sewage sludge, nickel mining, steel manufacturing, electroplating, cement factories, fossil fuel refining, Ni-Cd battery disposal etc. (Nriagu and Pacyna, 1988). Typical ambient air contains concentration of nickel which ranges from 6-25 ng /m^3 Ni (Williams, 2001). In polluted air, the predominant nickel compounds appear to be nickel sulphate, oxides, sulphides, and, to some extent, metallic nickel (WHO, 1991). Nickel subsulphides are carcinogenic (Goodarzi et al., 2008). The small respirable particles containing Ni_3S_2 are hazardous to human health (Environmental Protection Agency, 1991).

1.1.2.2. Nickel in water

In aquatic system nickel is present due to natural erosion of soil and rocks. The average content of nickel (Ni^{2+} mainly) present in water is 1-50 µg/L (Williams, 2001). Beside the natural erosion of soil and rocks, nickel concentration in surface water may be due to anthropogenic sources. The anthropogenic sources of heavy metals to contaminate aquatic ecosystem include domestic waste water effluents discharging heavy metals like As, Cr, Ni, Mn and Cu, dumping of sewage sludge (As, Pb and Mn), non-ferrous metal smelting units (Pb, Ni, Se and Cd), coal burning power plants (Se, As and Hg) iron and steel production responsible for addition of heavy metals like Cr, Mo, Sb and Zn (Nriagu and Pacyna, 1988).

For example, the concentration levels of nickel in waters and sediments occurring nearby the Sudbury area, Canada, are elevated due to long term smelting in that region. And due to leaching from adjacent soil containing metal saturation, it is supposed that nickel elevation will remain far into the future Nriagu et al. cited by (Doig and Liber, 2007).

1.1.2.3. Nickel in soil

The amount of nickel present in soil depends mainly on the mineralogical composition of the soil and ranges from 2 to 50 mg/kg or even more. But beside the mineral composition, anthropogenic sources contribute a lot for increased nickel level in soil cited in (Çıftcı et al., 2007). For example soil adjacent to the Ni refinery in Port Colborne, Ontario, Canada is polluted through aerial deposition of Ni which exceeded the Ni concentration in 29 km^2 of land high above than Canadian Ministry of Environment's remedial action level of 200 mg/kg for phytotoxicity (McNear Jr et al., 2007). Organic soil closer to this refinery found contaminated high enough ranging 600 to 6455 mg/kg resulting problems in vegetable production for at least two decades (Frank et al., 1982).

Sewage sludge contains heavy metals and produce unwanted environmental impacts (for example, toxicity in plants and microbes) with food chain and ground water contamination when used as fertilizer and for landfills. Uptake of heavy metals so entering in food chain is a potential threat to animals and human health. Nickel concentration exceeded 10 time for the soil limit due to sewage sludge addition in experimented Polish soil is observed (Sprynskyy et al., 2007).

1.1.3. Applications

Nickel is a very reactive element but in common with massive forms of chromium, aluminum and titanium metals nickel is very slow to react with air. Due to its permanence in air and its inertness to oxidation, it is used in coins, for plating iron, brass, for chemical apparatus, and in certain alloys. It is magnetic and is very frequently accompanied by cobalt as in some coins. Nickel and cobalt are also found in meteoric iron.

A finely divided form of nickel 'Raney nickel' is frequently used as a catalyst for the hydrogenation. Nickel is chiefly valuable due to its use in alloys and super alloys, e.g., stainless steel (Dalvi et al., 2004) and German silver/Nickel silver (an alloy composed of 60 % of Cu, 20 % of Ni and 20 % of Zn).

Nickel consumption can be summarized as: nickel steels (60 %), nickel-copper alloys and nickel silver (14 %), malleable nickel, nickel clad, inconel and other superalloys (9 %), plating (6 %), nickel cast irons (3 %), heat and electric resistance alloys, such as Nichrome (3 %), nickel brasses and bronzes (2 %), others (3 %) (Wikipedia).

1.1.4. Toxicity

Heavy metals, e.g., As, Zn, Cd, Pb, Ni, Cr, Hg and Cu are toxic (Evanko and Dzombak, 1997; Wuana and Okieimen, 2011). They may reduce the crop production. Heavy metals after being adsorbed in soil change in other chemical forms with varying bioavailability (original ref in (Wuana and Okieimen, 2011). The decision of benefit or toxicity of an element related to human and its environment depends upon the well-defined chemical form of an element, its concentration and exposure level. There are ample evidences to suggest that, rather than total dissolved metal concentration the free (hydrated) ion activity of divalent cationic metals is a better predictor of metal toxicity/bioavailability (original ref (Doig and Liber, 2007). As for most metals, the toxicity of nickel is dependent on the route of exposure and the solubility of the nickel compound. Nickel may be absorbed as the soluble nickel ion (Ni^{+2}) while sparingly soluble nickel compounds may be phagocytised. Nickel exposure to human being in our daily life is often via atmosphere, water and some foods containing nickel, e.g., chocolate, soy beans, nuts, oat meals. The daily intake of nickel varies between 100 to 800 µg in food items (Williams, 2001). Exposure to nickel metal and soluble compounds should not exceed 0.05 mg/cm³ in nickel equivalents per 40-hour work week. Nickel subsufides (Goodarzi et al., 2008) nickel sulfide (Ni_2S_3) fume and dust is believed to be carcinogenic mainly for nasal and lungs cancer for the workers employed in high temperature roasting of sulfide ores (WHO, 1991; Williams, 2001). A detailed study about the exposure levels via different mediums is described by environmental ministry of Canada (Leece and Rifat, 1998).

Increased tumors incidences and positive results in genotoxicity assays in several species and strains of animal for multiple routes of administration have been seen due to nickel subsulfate (WHO, 1991). Respiratory risk due to mixture of nickel oxide and nickel sulphides and lung cancers due to separate nickel oxides are reported in refinery workers (Williams, 2001).

Nickel carbonyl, [$Ni(CO)_4$], is an extremely toxic gas which has a greater exposure there in pyrometallurgical and hydrometallurgical units for extraction of Ni from ores. Nickel carbonyl is highly toxic due to toxicity of metal and the carbonyl's ability to give off extremely toxic carbon monoxide gas which can damage hemoglobin. Chronic effects, e.g., rhinitis, sinusitis and asthma have been reported in Ni refinery and nickel plating workers. It is explosive in air. It can cause frontal headache, nausea, vomiting, insomnia and irritability. The lowest toxic concentration (TCLo) for nickel carbonyl is 0.007 mg/m^3 (WHO, 1991). Sensitized

individuals may show an allergy to nickel affecting their skin, also known as dermatitis. In several countries it is found that 10 % female and 1 % male are nickel sensitive. And among those nickel sensitive persons 40-50 % have vesicular hand eczema, which in some cases may even lead to loss of working ability (WHO, 1991). Contact allergy is some time due to use of nickel in jewelry intended for pierced ears. But it requires long time nickel-skin contact till the corrosion of nickel containing items (jewelry) and sweat of skin may react with each other (Williams, 2001).

1.1.5. Natural background level of nickel

Natural concentration of nickel in soil depends upon parent soil material. Anthropogenic sources can cause an increase in the natural level of nickel in soils. For uncontaminated soils average value of nickel can be 20-40 mg/kg (Hemetsberger, 2006). Normal or geogenic value for Styrian soil is 60 mg/kg (Krainer, 2000). The limit values for nickel either proposed or existing in agricultural soils in some European countries are different, e.g., 15 mg/kg in Denmark, 35 mg/kg in Holland and 30 Germany (soils with pH>60), further details in (Walterson).

1.2. Chromium

Chromium ($_{24}Cr$) is a steel-gray, lustrous, hard metal that takes a high polish and has a high melting point. It is also odorless, tasteless, and malleable. It is 21st most abundant element in the earth's crust cited in (Mukherjee, 1998).

1.2.1. Occurrence and production

Chromium is mined from chromitite ore $(Mg,Fe)(Al,Cr,Fe)_2O_4$ (Darrie, 2001) mainly present as chromite ($FeCr_2O_4$) with impurities such as Mg and Al (Vitale et al., 1997) i.e. Composition of chromites may vary in 15-65 % of chromic oxide content (Darrie, 2001). Chromium is widely used in metallurgical, chemical and refractory industries. According to International Chromium Development Association (1999) 85 % of total estimated world annual consumption 12.5 million tonnes is used for metallurgical purposes, 8 % for chemicals and 7 % is used by refractories (Darrie, 2001). According to U.S. Geological Survey report (2012), main producer countries of the chromium for 2007-2010 are South Africa (34 %) and Kazakhstan (17 %), Russia (9 %), China (5 %) and other contribute 35 % (Papp, 2012).

Though native chromium deposits are rare, but, some native chromium metal has been discovered. The Udachnaya Mine (Russia) produces samples of the native metal and

diamond also. Chromium is obtained commercially by heating the ore in the presence of aluminum or silicon (Wikipedia). The extraction of chromium from its ore is described in paper, see (Darrie, 2001)

Naturally occurring chromium is composed of three stable isotopes; with ^{52}Cr being the most abundant (83.789 % naturally) (Wolf et al., 2007).

1.2.2. Biological role

Trivalent chromium (Cr^{3+}) is an essential nutrient which is required in trace amounts (50-200 µg/day) for metabolism of glucose (Agency for Toxic Substances and Disease Registry, 2000). Its deficiency can cause problem like impaired fertility, triglycerides and cholesterol level increasing the risk for diabetes and heart disease, impaired glucose tolerance etc. (Agency for Toxic Substances and Disease Registry, 2000; Yang et al., 2006).

1.2.3. Anthropogenic sources

Concentration of elements in soil mainly depends upon the mineralogical composition of soil. The natural process like weathering of ultramafic rocks can release significant amount of chromium to the soil and waters. In US the average chromium level in the soil is found 37 mg/kg and an elevated chromium level to 5900 mg/kg in the foothills of Sierra Nevada Mountains situated in California due to presence of ultramafic rocks (Wolf et al., 2007). Beside the natural process there are several anthropogenic sources which contaminate our environment. Anthropogenic sources include leather tanning industries, smelter (Shtiza et al., 2005) and refineries, cement industries, dyes and paint industries, textile industries (Georgeaud et al., 1997; Wolf et al., 2007) and fuel combustion (Agency for Toxic Substances and Disease Registry, 2000). John F. Papp has described in detail about anthropogenic sources and their contribution for chromium in environment (Papp, 1994). According to an estimate, 1,723 metric tons of chromium emission annually is being deposited from coal and oil combustion. Chrome plating sources contribute 700 metric tons of Cr^{6+} emission each year in atmosphere. For example in USA, fuel combustion and steel production emit about 64 % (Cr^{3+}) of its total atmospheric chromium emission, while 32 % (Cr^{6+}) is due to chrome plating, chemical manufacturing units and chromate inhibitor using chemical cooling towers (Agency for Toxic Substances and Disease Registry, 2000).

Smelters produce ferrochromium, slag and gas dust as by-products and pollutes the environment. Windblown dust particles originating directly from the smelter chimneys or from slag dumps and from the slag used in the road construction contribute additionally.

Moreover the rivers which drain off the industrial area pollutes the water and soil with heavy metals cited in (Shtiza et al., 2005). Chromite ore processing residue (COPR) wastes are produced mainly by 'high lime process' forbidden in Europe since late 1960s but still in progress in India, Pakistan, Russia and China (Darrie, 2001). Porto Romano (Albania) released about 100 tonnes of COPR waste in just 20 years (1972-1992) and contaminated the environment a lot with chromium. Total chromium (24,409 mg/kg) contains 75 % to 90 % of Cr^{3+} while remaining 10 % to 25 % is Cr^{6+} (Shtiza et al., 2009). The measured chromium concentration in waters near Albanian Smelter is up to 168 mg/l (Shtiza et al., 2008) which is 3000 times higher than Environmental Quality Standards (EQS) (Shtiza et al., 2009). Due to chromate and dichromate chemical production in New Jersey over a period of 7 decades (1905-1976) a huge amount of waste in the area has been accumulated. Ninteen sites from Hudson County, New Jersey containing 1-50 % Cr^{6+} content out of 10,000 mg/kg total chromium are reported (Burke et al., 1991). COPR was deposited due to local chemical work during 1830 to 1968 in an area of Glasgow, that area has been investigated and higher concentration of chromium 91 mg/l predominantly existing in form of Cr^{6+} as CrO_4^{2-} is reported (Farmer et al., 2002).

1.2.4. Toxicity

Assessment of environmental and physiological impact of an element depends upon its exposure level, quantity and well defined chemical form of that element i.e. speciation.
Chromium was added to the list of hazardous heavy elements in 1995 due to the possible presence of Cr^{6+} which is potentially carcinogenic form of chromium (Williams, 2001). Cr^{3+} is considered less or non-toxic specie of chromium while Cr^{6+} is 100 times more toxic than Cr^{3}. Cr^{6+} is more toxic due to the higher oxidation potential and the ease with which it penetrates biological membranes (Gómez and Callao, 2006). Hexavalent chromium is toxic and mutagen when inhaled, while is dangerous in solution form as it causes skin allergy called dermatitis and is carcinogenic as well (Agency for Toxic Substances and Disease Registry, 2000; Tirez et al., 2003). High concentration of Cr often is associated with other heavy metals such as Ni and due to their adverse effect on human health and environment, they are of greater importance. According to Turner and Rust (1971) to 0.5 mg/kg concentration of Cr^{6+} in solution and 5 mg/kg in soils are phytotoxic (Shtiza et al., 2009; Shtiza et al., 2005).

1.2.5. Limits of chromium

Level of chromium depends upon soil type. Defined average value for Cr in soil is 50 mg/kg (Hemetsberger, 2006). Normal or geogenic value for Styrian soil is 80 mg/kg (Krainer, 2000). The limit values for chromium either proposed or existing in agricultural soils in some European countries are different, e.g., 30 mg/kg in Denmark, 100 mg/kg in Holland and 100 Germany (soils with pH>6) for more details (Walterson).

1.3. Deposition of heavy metals in industrial areas

As described above that industrial activities increase the concentration level of heavy metals in environment. Increased level of heavy metals concentration is a matter of concern for human health and environment/ ecosystem. These facts have attracted the attention of researchers to have a check and balance on the level of contamination due to heavy metals especially in the areas near industries. To find the impact of industries and other anthropogenic sources, concentration of heavy metals in dust, water, sediments and soil are investigated. For example, industrial activities, e.g., nonferrous solid waste processing have resulted contamination of Pb higher than action limits (100 mg/kg dry soil) in an area of greater concern being very populated. Soluble Pb in water and higher values of Pb in dust and soil than normal back ground level has been found. Increased level of Pb values in blood of children (particularly susceptible) living in Pantelimon, the nearest town to these industries, have been examined (Velea et al., 2009). Pollution of an area due to iron smelting industry at Papankulam-Madavarvilagam, Tamilnadu, India due has been reported (Arunachalam et al., 2009).

Concentration of heavy metals in ground water near mining area at Dhanbad was investigated, and among measured metals (Cr, Mn, Cu, Cd, Fe, Pb and Zn) the concentrations of Fe and Mn were found higher than the permissible level at few points but in general they were below the accepted permissible limits (Prasad and Jaiprakas, 1999).

Impact of iron smelting industry at Papankulam-Madavarvilagam, Tamilnadu, India, has been investigated and it is found that it is polluting the area with heavy metals and effecting the ecosystem (Arunachalam et al., 2009).

There are many metal factories in an area Aliağa closer to Izmir city of Turkey. The values of heavy metals, e.g., Fe, Cr, Ni, Zn, Pb, Ti, Mn and Cu are found higher in soil, sediments and water sample in the vicinity. Higher concentration of heavy metals is due to these metal factories (Sponza and Karaoğlu, 2002). The Northern part of the Czech Republic is one of the most industrially polluted areas in Europe due to mainly combustion of brown coal

containing high content of heavy metals and pyrite (Hanesch and Scholger, 2002; Kapička et al., 1999). Because heavy metals have adverse effects on human health and are crucial for environmental measures thus mapping and monitoring of heavy metals is necessary.

2. Geophysical and geochemical study of river sediments

Heavy metals can be present in the environment naturally or they may be emitted by industries. Heavy metals are generally produced along with the ferromagnetic particles (mostly magnetite and hematite) as a result of various industrial processes, e.g., oxidation of iron sulfide in coal during combustion of fossil fuels, cement production, waste incineration and metallurgical processes. Production of heavy metals and magnetic particles may take place together but they may be present as separate particles too. So correlation between pollutants and magnetic particles is complex and different for different processes. It is not easy to say that how far magnetic susceptibility measurement on its own can inform us about the pollution (Hanesch and Scholger, 2002). But magnetic tools can be used to highlight the contaminated spots. Geophysical and geochemical study together can help to find the correlation of heavy metals and magnetic signals.

2.1. Magnetization and magnetic susceptibility

Magnetic moment of any electron consists of orbital moment and spin moment. The magnetic moments of an atom, ion or macroscopic sample have the tendency for compensation to reduce its energy. The number of magnetic moments M as a result of imperfect compensation in a unit volume dV is known as magnetization and is denoted with J.

According to definition $J = M / dV$ [A/m].

Magnetization which occurs as a response of an externally applied magnetic field H_a is known as induced magnetization. The ratio between induced magnetization and external magnetic field is called magnetic volume susceptibility which is denoted with k.

$k = J_i / H_a$

Dividing volume susceptibility by density gives specific susceptibility.

$\chi = k / \rho$ [m^3/kg]

2.1.1. Diamagnetism

In diamagnetic materials all the magnetic moments are compensated thus shows magnetization antiparallel to the external field. Diamagnetic materials show very small and negative volume susceptibility which is temperature independent. All kind of materials have diamagnetic properties but they are so weak that ferromagnetism and paramagnetism become dominant. Examples of diamagnetic materials are mineral, quartz, water and carbonates(Hemetsberger, 2006).

2.1.2. Paramagnetism

There are number of uncompensated magnetic spin moments in paramagnetic materials. The spin moments in paramagnetic materials are irregularly oriented and have no interference at normal room temperature. Magnetization J for such material is zero if there is no external magnetic field applied. Applying external field can cause the spin moments go in such an orientation that it results magnetic moment M and an induced magnetization J_i parallel to applied field H_a. Volume susceptibility of paramagnetic materials is small and positive. As temperature change can change the orientation of spin moments, magnetic susceptibility of paramagnetic materials is function of absolute temperature T. According to Curie's law, paramagnetic susceptibility decreases with increase of temperature. $K_{para} = C / T$ where C is Curie constant and has specific value for every paramagnetic material (Hemetsberger, 2006).

2.1.3. Ferromagnetism

If a lot of uncompensated magnetic moments of paramagnetic ions create strong interactions among moments causing the parallel alignment of elementary magnetic moments of atoms in neighborhood within small space (magnetic domains). Iron, nickel, cobalt and their alloys show strict parallel alignment of all uncompensated magnetic moments. Ferromagnetic materials are able to show spontaneous magnetization even if external field is not applied. They are strongly temperature dependent. Complete magnetic order of such material can be seen at 0 K. The magnetic order beyond Curie temperature T_c fully lost and material start showing paramagnetic behavior (Hemetsberger, 2006).

2.1.4. Antiferromagnetism

In materials showing antiferromagnetism, magnetic moments are arranged in regularly antiparallel directions. The order exists at low temperature generally. Antiferromagnetic materials don't show spontaneous magnetization in absence of external applied field. External applied field causes rotation and inversion of Weiss domains (magnetic domains) leading to magnetization which is parallel to the applied field. Antiferromagnetic properties depend upon temperature. Magnetic susceptibility of antiferromagnetic materials is maximum at certain temperature called Néel-temperature (T_n), above this temperature magnetic susceptibility values change according to Curie-Weiss Law:

$k_{antif} = C/ (T+ T_n)$ where C is Curie constant and T is absolute temperature.

Hematite and goethite are common minerals which show antiferromagnetic behavior.

2.1.5. Ferrimagnetism

When the antiparallel moments are not equal then their summation does not show total compensation in absence of external magnetic field. Such phenomenon is recognized as ferrimagnetism. This is the most important magnetic behavior of natural material. Magnetic susceptibility k_{ferri} depends on temperature. k_{ferri} is maximum at Curie temperature above that it is described with following equation according to Curie-Weiss law: $k_{ferri} = C/ (T + T_c)$ (Hemetsberger, 2006)

2.2. Heavy metals and magnetic susceptibility measurements

Heavy metals have affinity to form metallic bonding with ferrous material which leads to increase in magnetic susceptibility. Heavy metals are incorporated in ferrimagnetic material during combustion process or they get adsorbed on the surface of ferrimagnetic material already existing in the environment (Chaparro et al., 2004a; El Baghdadi et al., 2011). Pollutants are generally related with magnetic particles, so magnetic measurements can be used as a proxy for chemical methods (Hanesch and Scholger, 2002). A correlation between magnetic data and concentration of heavy metals, e.g., Cd, Pb and Fe in soil near magnisite mining at St. Jacob, Austria has been reported (Maier and Scholger, 2004). Correlation between magnetic susceptibility measurements and concentration of heavy metals, e.g., Fe determined by chemical analysis for the soil samples near Bradford, England closer to a high quality iron production (1789-1957) unit Low Moor Iron Works has been studied. A pronounced positive correlation between concentration of heavy metals (Fe, Cu, Mn and Ni) content and magnetic data is observed (Schmidt et al., 2005). Lead, Zn, Cu and Ba concentration were found highly correlated with magnetic susceptibility in a study made on urban soil in the arid region of Isfahan, Iran (Karimi et al., 2011). Correlation of heavy metals Pb, Cu, Zn, Se, Sc, Mo, Fe, and Bi concentration with magnetic susceptibility have been observed in soil samples from the cities like Xuzhou (Wang and Qin, 2005) and significance correlation of Cr, Cu, Pb and Zn concentration and magnetic susceptibility in topsoil from and Luoyang, China (Lu et al., 2007) has been reported. Concentration of Fe, Mn, Pb, Zn and Ni were reported in good correlation with magnetic susceptibility for metallurgical dust and similarly correlation of magnetic susceptibility in fly ash in Poland with heavy metals concentration (Strzyszcz and Magiera, 1998) is seen. Magnetic study and its correlation with heavy metals, e.g., Cr and Sr concentration in soil samples taken from Merida, state of Yucatan, Southern Mexico containing ferrimagnetic minerals (magnetic

carriers) have been reported (Reyes et al., 2011). Clear but less pronounced correlation between magnetic data and heavy metals, e.g., Pb and Zn concentration in an area with less input of anthropogenic magnetic particles in soil at Upper Silesia, Poland (Heller et al., 1998) has been described. Topsoil of Mexico City is investigated to find any relationship of concentration of heavy metals with magnetic indications. In investigated topsoil of Mexico City correlation between magnetic indications and heavy metals Cu and Zn and iron oxides concentration and common anthropogenic source for them is reported (Morton-Bermea et al., 2009). In Beni Mellal City Morocco, the topsoil is observed for the magnetic susceptibility and high positive correlation with Pb concentration, moderately positive correlation with concentration of Cu and Zn while slightly negative relationship for Cd concentration with magnetic susceptibility values is observed and reason for imperfect correlation is linked to grain size (El Baghdadi et al., 2011). Region of Tallinn, Estonia was studied thoroughly. Central part of the city showed a strong correlation in the values for magnetic susceptibility and concentration of Cr, Pb, Zn and Cu which are higher due to industries and heavy traffic in that part. Moreover significance correlation of magnetic susceptibility and concentration of Ni, Pb and Cu for soil of Tallin region but less pronounced correlation with concentration of Ni, Cr and Mo in urban Tallin is observed (Bityukova et al., 1999). A strong positive correlation of MS with concentration of heavy metals i.e. Cr, Ni, Pb and Cu and correlation of MS values with pollution load index (PLI) in top soils along coastal area Izmit Gulf and Izaytas (Turkey) has been reported (Canbay et al., 2010). Magnetic susceptibility measurements were applied for spatial distribution of anthropogenic particles in soils around a coal-burning power plant in the Czech Republic (Kapička et al., 1999). Magnetic susceptibility is suitable for mapping the areas which are contaminated due to heavy metals besides the traditional geochemical mapping (Bityukova et al., 1999; Hanesch and Scholger, 2002; Maier and Scholger, 2004). Measuring magnetic susceptibility (MS) is non-destructive, economical and fast method to report the heavy metal loaded areas (Blaha et al., 2008; Hu et al., 2008; Maier and Scholger, 2004; Schmidt et al., 2005), as compared to the chemical analysis which requires more time for sample collection, preparation and is costly too (Desenfant et al., 2004; Jordanova et al., 2003; Schmidt et al., 2005) and it facilitates to select the better sampling sites for conventional chemical analysis (Blaha et al., 2008; Reyes et al., 2011). Related study is made by many workers in different countries. Mapping dust distribution by measuring magnetic measurements of tree leaves near industrial unit (Georgeaud et al., 1997; Hanesch et al., 2003). In a detail study of magnetic concentration parameters and their strong correlation with concentration of heavy metals Cr, V, Zn, Fe and Pb in Shougang industrial area, western Beijing this fact is revealed that magnetic

measurements are suitable to map the areas which are loaded with heavy metals (Hu et al., 2008). In urban area of Kathmandu City, Nepal, geochemical analysis of tree leaves showed the correlation of concentration of heavy metals especially Cu, Zn and Pb with magnetic measurements (Gautam et al., 2005). Researchers have been trying to use magnetic susceptibility meter as tool to map the areas with higher heavy metal contents and to study the related topics like the influence of soil moisture on magnetic values (Maier et al., 2006), lithological and pedological impact on magnetic susceptibility (Hanesch et al., 2007) etc. Aquatic systems work as collectors of organic and inorganic pollutants including toxic and heavy metals which get accumulated in suspended and bottom sediments and then enter in the food chains of aquatic system becoming hazardous for population (Jordanova et al., 2003). So analyzing stream sediments is worthy for health issues. Stream sediments are better to observe for the purpose to know the natural mineralogy and heavy metals of lithogenic, pedogenic and anthropogenic origions. Although there can be the chances of dilution and alteration of sediments going downstream, still riverbed provides useful informations for geological anomalies and pollution sources in the area (Desenfant et al., 2004). Soil (Hanesch et al., 2007) and sediments show the loading of pollutants over a long period of time (Hanesch et al., 2003). Correlation between magnetic measurements and heavy metals Zn and Pb deposition due to anthropogenic sources on stream sediments in the Arc river (Desenfant et al., 2004) while Zn, Cd and Cr in sediment samples taken from lake (Etang de Berre), France showed good correlation with magnetic data (Georgeaud et al., 1997). Preliminary magnetic study on stream sediments Del Gato and El Pescado Buenos Aires Province, Argentina is made and impact of industrial and urban activities is studied by magnetic measurements (Chaparro et al., 2003; Chaparro et al., 2004a).

Detailed geochemical and magnetic study on sediment samples taken from East Lake, Wuhan city, China suggested that there is strong link between magnetic susceptibility and concentration level of heavy metal (Pb) but in this case study anhysteretic remanent magnetization (ARM) was found better parameter to report high concentration of heavy metals Pb, Zn and Cu correlated with ARM deposited due to anthropogenic sources like, Wuhan Iron and Steel Company (WISC), Qingshan Thermal Power Plant (QTPP) and traffic (Yang et al., 2007). A detailed magnetic study of feature and concentration dependent magnetic parameters i.e. para and anti ferrimagnetic, their characteristics as grain size distribution, soft or hard magnetic carrier on the stream sediments of cross city stream in Northeast of Buenos Aires Province, in the Greater La Plata area loaded with pollutant from urban, industrial and diffuse sources has been made and two different groups of sediment

cores are distinguished. From which vertical distribution of sediments has recent (last 20-40 years) anthropogenic influence. Moreover it was observed that four measured magnetic parameters (magnetic susceptibility, anhysteric remanent magnetization, S-ratio and κARM/κ) show good positive correlation with heavy metals but among these parameters correlation of heavy metals with grain size and magnetic feature-dependent parameters (κARM/κ and S-ratio) is more significant than for magnetic concentration-dependent parameters (Chaparro et al., 2004b). Sediments of the largest river of the Czech Republic, the Moldau river and near by soils have been observed and a positive correlation between magnetic susceptibility and concentration of heavy metals, e.g., Cu and Zn in upper 300 km. Increase in magnetic signal in the river sediments is due to the anthropogenic activities like sawmill, technical construction and sewage treatment plant. But the area near Slapy dam which is magnetic anomaly is turned ambiguous for magnetic signals to be interperated as anthropogenic marker in last 80 km downstream (Knab et al., 2006). Danube, the largest river basins in Europe is the reciepient of huge amount of various contaminating substances coming from point and diffuse anthropogenic sources, e.g., industries, agriculture, mining steel and petrochemical units. Moreover Balkan war and dam breakage at Baia Mare gold mining company in February 2000 must have contributed to an increase the level of contamination in it. Magnetic susceptibility meters i.e. MS2D, KT-5 and SM30 have been applied on sediments of this river in northwestern Bulgaria for the field magnetic study. It is found that all three showed similar pattern for the measurements of magnetic susceptibility (Jordanova et al., 2003). Magnetic parameters, e.g., magnetic susceptibility, anhysteric remanent magnetisation were found in moderate and good correlation with heavy metals, e.g., Zn, Cr, Ni and Fe in sediments from Cauvery and Palaru River, India (Chaparro et al., 2008). Magnetic parameters are suggested suitable indicator of heavy metals deposited due to traffic related pollution at road Autovia 2, Argentina. Magnetic parameteres and geochemical analysis for urban road side soil in Lishui city, China were made to find the heavy metals pollution due to traffic in the area. A significance positive correlation of magnetic parameters and heavy metals like Ni, Cr, Pb, Fe, Zn, Cu, and Cd is reported. In a case study from Finland, magnetic and geochemical analysis along with microstructural study of road dust sample, magnetic measurements were found helpful tool for environmental monitoring (Bućko et al., 2010). Investigation on a spatial variability of magnetic susceptibility, on core soil from polluted and less polluted forest near steel mill Leoben, Austria is made. Significance correlation of heavy metals, e.g., Pb and Zn with magnetic suscpetibilty is reported (Blaha et al., 2008).

2.3. Sampling

Sampling location, procedure and preparation is described as following.

2.3.1. Sampling area

The University of Leoben (Montanuniversität Leoben) is situated in the heart of Austrian province called Styria/Steiermark. Due to the abundance of iron ore (Siderite $FeCO_3$) mining, iron and steel production have been the main industry in the region of Leoben for last 3 centuries. Austrian second largest steel production plant is situated very close to the center of Leoben. The main wind direction and the site within a mountain valley make this vicinity of the town center to the steel plant unfavorable. On the other hand, industrial activity makes the area ideal for the study of environmental impact due to the industrial emissions. The largest outcrop of ultramafic materials (the serpentinite of Kraubath) almost 30 km upstream of Leoben and the use of gravel from the serpentinite quarries as gravel in particular during the long winter periods has lead our attention to the actual sources of Cr and Ni contaminations in the region of Leoben.

2.3.2. Stream sediment collection

The river Vordernbergerbach starting from its origin point (at 1500 m above sea level) near Leobener Hütte (Präbichl) coming downstream to the confluence point of the Vordernbergerbach with the Mur River in Leoben at 540 m above sea level has been investigated. River sediments from 24 different sampling points within the Vordernbergerbach were collected. Sampling locations were planned to investigate the heavy metals and their real point or diffused, anthropogenic or geogenic sources in the whole area, taking 2nd order streams in account. Where there was an input due to 2nd order stream in mainstream, samples upstream and downstream (i.e. before and after the junction of 2nd order stream into the Vordernbergerbach) were collected. Plenty of samples were collected near each residential and industrial plant. As the target is to measure the concentration of heavy metals in stream sediments, so sampling tools used were totally metal free. Sampling sites were named after the nearest localities of Präbichl *(PB1-PB7)*, Vordernberg *(VB1-VB6)*, Trofaiach *(TF1-TF6)*, St. Peter Freinstein *(SP1-SP3)* and Leoben *(LE1-LE2)*. Some information related each sampling site i.e. sample description, GPS coordinates, date, time, number of subsamples, distance for subsamples within each sample site and magnetic susceptibility values was recorded in the accompanying protocol. For each sampling site several available and accessible subsampling points within distance of few meters were collected and combined as one sample after measuring magnetic susceptibility values for each subsampling point. Magnetic susceptibility meter used in the field was a MS2

Bartington with a loop sensor. For each subsample 2-3 times or even more times magnetic susceptibility values were obtained. For example, for the 5th sample, notation *PB/5/IV(30 m)/091118/S/O* describes the detail; *PB/5* stands for sample # 5 in area of Präbichl, *IV(30 m)* means 4 (Roman *IV)* subsampling points within distance of *30 m* were collected on *Nov 18, 2009,* while S/O stands for sediments/original. However the sample notations, e.g., PB1, PB2 and so on are easier and enough to understand about the sample. Subsampling portions were collected in bucket and then were sieved below 2 mm either on the site or in the lab. Water required for wet sieving was taken from the river for each sample except one sampling site PB1 where there was no water available as the river bed was dried out. Dry sediment sample PB1 was sieved using milli-Q water in the lab. Description of protocols is given in appendix.

2.4. Instruments used for geochemical analysis

Depending upon the sample nature, limit of detection of instrument and objectives of study, and the measurement uncertainty, different analytical techniques can be used to determine total concentration of chromium and nickel. A comprehensive survey for such methods and instruments used for the determination of the total chromium content in different samples during 2000 to 2006 has been summarized by Gómez and Callao (Gómez and Callao, 2006). For our purpose of measuring total concentration of chromium, nickel and other elements of interest following instruments were used.

- A wavelength dispersive X-ray fluorescence spectrophotometer (WD-XRF AXIOS)
- Inductively coupled plasma mass spectrometer (ICP-MS Agilent Technologies 7500 cx)

The XRF is a well-established technique for elemental analysis in a variety of (liquids and solids) samples having many advantages over other techniques. It is non-destructive and does not require time consuming sample preparation as required for other analytical methods (Valentinuzzi et al., 2006).

Inductively coupled plasma mass spectrometry (ICP-MS) is a highly sensitive analytical instrument. Its features like the ability of multi-element detection, isotopic information, the calculation procedure despite the loss of analyte etc. make the instrument applicable widely for the determination of total concentration of elements as well as their speciation.

2.5. Sample preparation

Stream sediments were sieved by wet sieving method into two fractions which were a coarse (*150µm* to *2mm*) fraction and a fine (*<150µm*) fraction. Fine fraction after being sieved was decanted and then dried in an oven at a temperature less than *30 °C*. The dried

fine fraction was used for further analysis while the coarse fraction was stored in paper bags. The dried fine fraction from each sample was grinded with a porcelain ball mill in lab at institute of mineral processing (Montanuniversität Leoben) at 140 rpm for almost 100 minutes. Then grinded material was stored in labeled glass bottles.
Duplicates of each sample were prepared. As analytical instruments i.e. XRF and ICP-MS are applied for the determination of concentration of elements, samples are prepared according to the requirement of analytical instrument. Fused glass beads and pressed powder pellets were prepared for analysis with XRF and Na_2O_2 digestion method is adopted for dissolving the total metal content in the sample in solution before being analyzed with ICP-MS. The detail procedure is described in following.

2.5.1. Fused glass beads

Grinded sediment samples are dried at 105 °C in oven and then subjected into the platinum crucible. Platinum crucible of having known (weighted) amount of sample is kept in muffle furnace at 1000 °C for loss on ignition (LOI). When, after few hours constant weight of sample is acquired, ignited sample is kept into the desiccator for cooling. One gram of ignited but cooled sample is then mixed with 8 g of di-lithium tetraborate ($Li_2B_4O_7$). The mixture is homogenized well with a glass stirrer. The platinum crucibles were adjusted in 'Fusion Machine type VAA2' and left it till the time it required to complete its automatic program P1 for fused beads formation. The glass beads were marked accordingly and analyzed with the XRF.

2.5.2. Pressed powder pellets

Four grams of very fine, dried (at 105 °C) sample is mixed with 1g of wax. The mixture is homogenized very well by shaking machine for about 4 minutes at 30 rpm. The homogenized mixture is then pressed to form its pressed pellet with the help of hydraulic laboratory pressing machine 'PE-MAN'. The applied pressure was ~100 kN.

2.5.3. Na_2O_2 sintering

Sodium peroxide (Na_2O_2) method of digesting sample is highly effective because Na_2O_2 is rapid in attacking mineral and resulting sinter residue gets dissolved easily. Na_2O_2 decomposes to NaOH and O_2 and does not introduce elements that cause significant instrument memory (Meisel et al., 2002). The Na_2O_2 sintering technique is preferable over other due to its characteristics. This simple, inexpensive technique can digest sample containing refractory minerals with highly reproducible and reliable results. Moreover the

higher total dissolved solids compared to acid digestion techniques and higher blanks do not affect the quality of the result (Meisel et al., 2002).

2.5.3.1. Procedure for Na_2O_2 sintering

100 mg (0.1 g) of dried (at 105 °C) and samples were weighed into glassy carbon crucibles and each of them were mixed thoroughly with about 0.6 g of fine powered Na_2O_2 by a glass stirrer. The carbon crucibles were heated in muffle furnace at 480 °C for 30 minutes. After it they were allowed to cool down to room temperature. The crucibles were washed from outside with Milli-Q water to remove any kind of possible dirt deposition from the furnace. Carbon crucibles were kept in Teflon beakers covered with glass lids and these Teflon beakers were kept on hot plate (90 ºC) along with magnetic stirrer stirring at 250 rpm for 30 minutes. Milli-Q water was added drop-wise in the crucibles till the reaction ceased and no more vapors seen on glass lids which earlier were being accumulated. Following reaction takes place in Na_2O_2 digestion method.

$$2\ Na_2O_2 + 2\ H_2O \longrightarrow 4\ NaOH + O_2$$

The solution was poured to the 50 ml PP centrifugation tubes and centrifuged at 4000 rpm for 5 minutes. The clear solution from centrifugation tubes was poured into a 100 ml volumetric flask. While 2 ml of conc. HCl (reagent grade) was added to the all crucibles to get sinter cake dissolved. Three ml of 3 mol/l HCl was added to the residue obtained after centrifugation. The dissolved material obtained after addition of 2 ml conc. HCl to carbon crucibles was mixed with the solution in centrifuging tube. All the solutions were poured from centrifuge tube, Teflon beaker and carbon crucible into the respective labeled flasks. The solution was diluted with milli-Q water up to exactly 100 ml after rinsing beaker, crucible and centrifuging tube into the respective volumetric flasks. The flasks were closed with their stoppers, the solutions are mixed by gentle shaking and clear solutions were poured into the tubes for further treatment required for analysis by ICP-MS. One ml from this solution was taken for ICP-MS measurements
and further diluted upto 5 ml total, with 1 % of HNO_3. 100 µl of In/Re (100 ppb) and 50 µl of Ge (1ppm) were added as internal standards. Blank solution and MUS (in house RM) (detail about MUS is given in 2.7) were also treated similarly before final measurements with the ICP-MS.

2.6. Magnetic susceptibility measurements on river sediments

Magnetic susceptibility values for all 24 sediment samples were determined in the field and in the lab as well. Magnetic Susceptibility meter MS2-Bartington with a loop sensor was used to measure the magnetic susceptibility in the field during sediment sample collection from Vordernbergerbach. The magnetic susceptibility values were noted for each sub-sampling points within each sampling site before sediment collection and mixing them in the marked bucket. On each subsampling point several readings were made. An average of magnetic susceptibility values of all sub sampling points within one sampling site is taken as indicator of magnetic susceptibility for the vicinity of that sampling site. These magnetic susceptibility values measured in field are volume susceptibility values (κ). Volume susceptibility measurements in the field done are noted in sampling protocol so all the values can be seen in appendix section while the average on each subsampling point (SSP) and average of volume magnetic susceptibility on each sampling site with RSD (%) are given in Table 2 and shown in (Graph 1).

However magnetic susceptibility measurements in the lab were carried out on MS2 meter (Bartington). The exact sample mass was recorded and magnetic susceptibility values on MS2 display (κ) were noted. Mass specific magnetic susceptibility (κ) was calculated with the following formula.

$$X = \frac{\kappa \,.\, 10}{Mass\ of\ sample\ (g)}$$

Where κ (Greek k or kappa) is the value displayed on display of MS2 meter.

Magnetic susceptibility measurements carried out, in the field is an indication of the magnetic signal of the sediments in that region and it represents the magnetic measurements of sediments as whole (i.e. coarser and fine fractions) without discrimination of size fraction. While magnetic susceptibility values determined in lab were done only on fine fraction (below 150 µm) of sediment samples.

Moreover, sediments were not equally available on each subsampling points within one sampling site, so the mean values for magnetic values in the field may be different from magnetic values in the lab. They are described in the results section below.

	
Magnetic susceptibility meter MS2 (Bartington) with loop sensor (in field) Photo captured by Friedrich Pichler (FriPi)	Magnetic susceptibility meter MS2 (Bartington) (lab)

2.6.1. Results and discussion

S. No.	Sample ID	Mean values of magnetic susceptibility values on each subsampling point (SSP), in the field, on MS2 meter with loop sensor							Volume magnetic susceptibility (κ) SI (10^{-5})	
		SSP1	SSP2	SSP3	SSP4	SSP5	SSP6	SSP7	Average	RSD %
1	PB1	4	3	3	2	2			3	36
2	PB2	10	7	5	6	7	5		7	26
3	PB3	4	5	6	3	8	3	6	5	36
4	PB4	3	3	9	5	4			5	52
5	PB5	31	22	68	22				36	62
6	PB6	25	28	10	21	22	50		26	51
7	PB7	44	26	43	67				45	37
8	VB1	21	24	58	36				35	49
9	VB2	126	64	68	105				91	33
10	VB3	108	112	684	170				269	104
11	VB4	198	595	471					421	48
12	VB5	347	571	276					398	39
13	VB6	576	114	473	916	338			483	61
14	TF1	667	753	431	428	208			497	43
15	TF2	48	46	27	136	45			60	71
16	TF3	47	49	627					241	139
17	TF4	42	81	48					57	37
18	TF5	5	4						5	26
19	TF6	122							122	4
20	SP1	10							10	1
21	SP2	16	19	20	23				20	16
22	SP3	10	9	48	38	95	32		39	82
23	LE1	150	142	453	274	45			213	74
24	LE2	303	622	188					371	61

Table 2 Magnetic susceptibility measured in the field

S.No.	Location	Sample mass (g)	Magnetic susceptibility values				Mass specific magnetic susceptibility (X) $[10^{-8}m^3/kg]$	RSD %
			Magnetic susceptibility readings on MS2 meter (in lab)					
1	PB1	4.83	11.6	11.7	11.1	11.5	24	3
2	PB2	4.69	13.0	13.0	12.5	12.8	27	2
3	PB3	4.84	12.3	12.2	11.6	12.0	25	3
4	PB4	4.48	18.0	18.1	17.0	17.7	40	3
5	PB5	4.47	25.9	25.9	24.7	25.5	57	3
6	PB6	4.68	48.0	48.0	46.5	47.5	101	2
7	PB7	4.71	49.5	49.5	49.5	49.5	105	0
8	VB1	4.60	39.7	39.9	39.9	39.8	87	0
9	VB2	4.64	60.3	60.4	60.6	60.4	130	0
10	VB3	4.52	68.1	68.9	68.1	68.4	151	1
11	VB4	4.59	211.0	211.2	204.9	209.0	456	2
12	VB5	4.46	157.0	161.1	161.1	159.7	358	1
13	VB6	4.64	244.4	248.8	248.8	247.3	533	1
14	TF1	3.76	27.4	27.6	27.7	27.6	73	1
15	TF2	5.44	30.3	30.5	30.5	30.4	56	0
16	TF3	4.81	22.6	22.6	22.7	22.6	47	0
17	TF4	4.45	20.2	20.5	20.7	20.5	46	1
18	TF5	5.21	10.2	10.4	10.5	10.4	20	1
19	TF6	4.81	13.1	13.2	13.3	13.2	27	1
20	SP1	4.77	16.4	16.6	16.7	16.6	35	1
21	SP2	5.93	13.1	13.2	13.2	13.2	22	0
22	SP3	5.19	13.1	13.1	13.2	13.1	25	0
23	LE1	5.45	70.1	70.2	70.0	70.1	129	0
24	LE2	4.78	42.8	42.8	43.2	42.9	90	1

Table 3 Mass specific magnetic susceptibility values of sediments samples (from Vordernbergerbach) measured in lab

The bias on mass specific magnetic susceptibility measurements calculated from the standard reference material and its certified values is 2 %.

Generally, volume susceptibility measurements in the field can be correlated with the mass specific magnetic susceptibility measurements determined in the lab by taking the density factor in account because of their relationship i.e.

$$\kappa = X \,.\, \rho$$

Where ρ represents the density, κ represents the volume magnetic susceptibility and X represents the mass specific magnetic susceptibility.

Density of fine fraction (<150 µm) is approximated to 1 g/cm^3 (1000 kg/m^3). Ideally if the magnetic signals are contributed equally from coarser and fine fractions at each spot or if magnetism is the character of fine fraction only and if the amount taken from each subsampling point is equal, then there might be a perfect correlation of magnetic values in the field and in the lab.

But in the case of this study, volume susceptibility measurements (field values) must not be necessarily similar or comparable to the magnetic susceptibility values determined in the lab because of several reasons. As described earlier that volume susceptibility values of samples measured in field represent the contribution of magnetic signal from pebbles, gravels and

sediments of both fractions (coarser 150 µm – 2mm and fine <150 µm), while mass specific magnetic susceptibility measurements determined in the lab for case study represent the magnetic susceptibility of fine fraction (<150 µm) only.

As the loop sensor only gives signal for the material exactly under the loop, and the material which is few centimeters away from it can have different magnetic signals so several measurements on each subsampling point (SSP) covering the spot of sediment collection were done to have a better idea of the magnetic susceptibility in the vicinity of each sampling point. So a greater variance for the average value of magnetic susceptibility (in field) is a consequence that is why the relative standard deviation (RSD) values are higher for volume magnetic susceptibility. Moreover, the availability of amount of sediments on each SSP was not equal which again is a cause for the average volume magnetic susceptibility values to be different from the average mass specific magnetic susceptibility measurements done in the lab.

In addition to the presence of metallic pieces, nails and needles etc. can highly affect the field values but sieved fine fraction is exempted from these sources of variance in the indication on the instrument.

S.No.	Locations	Coordinates		Volume susceptibility values (κ)		Mass susceptibility values (X)	
				In field		Lab	
				SI [10^{-5}]		(10^{-8} m^3/kg)	
		N	E	Average	RSD%	Average	RSD%
1	PB1	47° 32.134′	14° 58.358′	3	36	24	3
2	PB2	47° 31.995′	14° 58.775′	7	26	27	2
3	PB3	47° 31.896′	14° 58.597′	5	36	25	3
4	PB4	47° 31.096′	14° 58.413′	5	52	40	3
5	PB5	47° 30.832′	14° 58.436′	36	62	57	3
6	PB6	47° 30.649′	14° 58.608′	26	51	101	2
7	PB7	47° 30.382′	14° 59.005′	45	37	105	0
8	VB1	47° 30.043′	14° 59.326′	35	49	87	0
9	VB2	47° 29.846′	14° 59.442′	91	33	130	0
10	VB3	47° 29.475′	14° 59.644′	269	104	151	1
11	VB4	47° 29.123′	14° 59.487′	421	48	456	2
12	VB5	47° 28.945′	14° 59.339′	398	39	358	1
13	VB6	47° 28.508′	14° 59.234′	483	61	533	1
14	TF1	47° 27.246′	14° 59.804′	497	43	73	1
15	TF2	47° 26.365′	15° 0.000′	60	71	56	0
16	TF3	47° 25.498′	15° 0.270′	241	139	47	0
17	TF4	47° 25.488′	15° 0.382′	57	37	46	1
18	TF5	47° 25.515′	15° 0.160′	5	26	20	1
19	TF6	47° 24.733′	15° 1.372′	122	4	27	1
20	SP1	47° 23.431′	15° 2.280″	10	1	35	1
21	SP2	47° 23.457′	15° 2.267′	20	16	22	0
22	SP3	47° 23.16′	15° 2.747′	39	82	25	0
23	LE1	47° 22.692′	15° 4.765′	213	74	129	0
24	LE2	47° 22.800′	15° 5.365′	371	61	90	1

Table 4 Magnetic susceptibility measurements in field and in lab

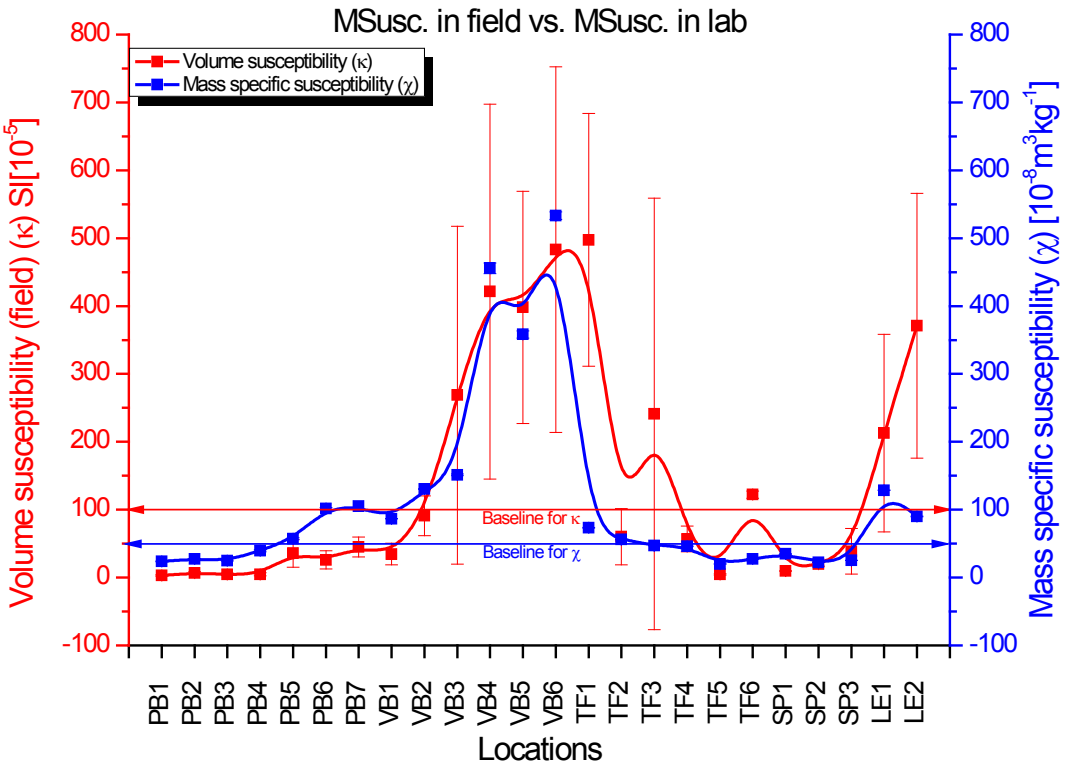

Graph 1 Magnetic susceptibility measurements of sediment samples (Vordernbergerbach) measured in lab and in field

Due to already mentioned reasons, it is not necessary for mass specific susceptibility measurements done in the lab to be in perfect or significant correlation with the values measured in the field in the case of this study. These reasons are hindrances for us to establish any statistical factor to correlate the magnetic susceptibility values in the field and in the lab.

However, higher values of volume magnetic susceptibility than mass specific magnetic for locations PB1 to VB2, VB4, SP1 and SP2 show that magnetic particles are more concentrated in fine fraction and magnetic signal is only character of fine fraction. For sampling points, Vordernberg (VB3-VB6), and Trofaiach TF2, TF4 and Sankt Peter/Freienstein SP3 are in close range of average values for the measurements done in lab and in the field which shows that either fine fraction or coarser fraction contribute equal signal of magnetism or only the fine fraction is responsible for the magnetic signals. When the volume susceptibility (in field) is higher than the baseline 100 SI [10^{-5}] then it is considered interesting and hot spot. For studied river sediments, the base line for mass specific susceptibility of fine fraction (<150 µm) defined is 50 [$10^{-8}m^3/kg$]. In the studied area, Vordernberger and Leoben regions have high magnetic susceptibility values ranging from 100 to 750 SI [10^{-5}] and 50 to 550 SI [10^{-5}] respectively. There is a greater difference

between magnetic susceptibility values in the field for the samples LE2 and that in the lab. Some possible reasons of this greater difference are different amount of sediments taken from subsampling points, some magnetic particles or error sources (nails. needles etc.) in the coarser fraction or discarded fraction (>150µm).

Magnetic susceptibility values in the lab are either in the same range or even higher than the magnetic susceptibility values in the field for most of the samples which shows that the fine fraction is better representative of magnetic particles as compared to the coarser fraction i.e. that magnetic minerals or particles are present mostly in the fine fraction of the collected sediments. Generally, there is similar trend for magnetic susceptibility values in the field and in the lab proving that magnetic susceptibility meter is a useful tool to indicate the hot spots for sampling, e.g., in our case study higher magnetic signals in Vordernberg and Leoben regions which were identified as hot spots.

2.6.2. Conclusions

- Magnetic susceptibility meter is useful device to indicate the hot spot for sample collection and is equally applicable in the field and in the lab to measure the magnetic susceptibility values. In our case study Vordernberg and Leoben areas are associated with higher values of magnetic susceptibility ranging 100-750 SI [10^{-5}] and 50-550 SI [10^{-5}]. The reason for these higher signal in these regions are the historical iron production plants in area of Vordernberg, Trofaiach and steel production plant Voest alpine in the area of Leoben.
- Some problems, e.g., different amount of sediments collected from subsampling point within each sampling point, coarser fraction (between 2mm and 150 µm) or discarded fraction (<150 µm) possibly containing some magnetic minerals or source error restrict to create any statistical correlation between volume magnetic susceptibility values in the field and mass specific magnetic susceptibility values of only fine fraction measured in the lab.
- For most of the samples, magnetic susceptibility values measured in the field and in the lab either in the same range or higher values in the lab than in the field convince that fine fraction is a better choice than coarse fraction to determine the concentration of heavy metals and hence mass specific magnetic susceptibility values measured in the lab must be preferred for further consideration especially when only fine fraction is being focused.

2.7. Geochemical measurements of sediment samples

An 'in house' reference material from 13 samples (PB1-VB6) was prepared and named as MUS (Montanuniversität Sediment). The very fine grinded sediments from fine fraction (<150 µm) were mixed and homogenized, then splitted and stored in labeled plastic bottles. 10 splits were selected, 10 fused glass beads (1 bead from each split), 5 pressed pellets (1 from each 5 out of 10 selected split, because both sides of pellet is measured as duplicate) and 10 Na_2O_2 digested solutions (duplicates from 5 splits) were prepared. To measure the concentration of elements with the XRF, two calibration programs i.e. GeoWSU and Protrace Geo were adopted for the fused glass beads and pressed pellets of MUS respectively. REE method of concentration determination with the help of ICP-MS used in our lab was applied on each Na_2O_2 digested MUS split. The best fitting values for all split measured, decided on the basis of best agreement of concentration values (with minimum RSD %) of measured and published values of reference material GBW 07309 i.e. stream sediment powder (National Research Center for Certified Reference Materials, Office of CRMs, No. 18, Bei San Huan Dong Lu, Hepingjie, Beijing 100013, China) were assigned to MUS. Then MUS was used as quality control material for further chemical analysis all 24 collected sediment samples.

Similarly, fused glass beads in duplicates for each sediment sample (PB1-LE2), single pellet for each sample because surface of each side (top and down) of a pellet acts as a duplicate of same sample preparation and duplicate solution (sintered with Na_2O_2) of each sample were prepared. GeoWSU for beads, Protrace Geo for pressed pellets and 'geol01' (relevant method of concentration determination by ICP-MS used in our lab) methods to determine the concentration of elements were applied. For major elements the concentration of elements measured with XRF while for REE (rare earth elements) the concentration measured with ICP-MS are reliable. Additionally, the closest values of measured MUS to assigned MUS values for each element, was the criteria to select the concentration values of elements (for sediment samples i.e. PB1-LE2) among available modes of concentration determination i.e. Geo WSU, Protrace Geo (both by XRF) and geol01 (by ICPMS). If the concentration values for any element by different modes were in agreement with each other and with reference material as well, then the SSP of those concentration values obtained with more than one mode is taken.

S.No.	Locations	Fe_2O_3	RSD	Cr	RSD %	Ni	RSD	Zn	RSD	Pb	RSD %
		%	%	mg/kg	%	mg/kg	%	mg/kg	%	mg/kg	%
1	PB1	6.48	1	79.9	1	43.3	3	32.2	0	14.6	8
2	PB2	5.91	2	74.2	0	34.3	2	59.6	1	30.8	16
3	PB3	6.33	2	84.2	1	41.2	1	43.2	2	15.4	8
4	PB4	6.17	1	66.7	2	36.2	2	40.0	3	18.7	20
5	PB5	5.92	1	78.0	1	42.7	1	41.2	1	24.9	1
6	PB6	7.31	2	70.5	2	45.2	2	71.8	0	36.9	2
7	PB7	6.54	1	85.8	7	48.9	1	76.7	5	23.6	27
8	VB1	5.99	1	75.3	1	44.9	4	44.0	2	16.6	12
9	VB2	6.02	3	93.6	8	62.8	10	53.2	3	21.5	15
10	VB3	6.04	1	102	1	62.1	9	60.5	1	27.1	10
11	VB4	7.13	1	156	1	85.0	4	128	2	60.1	0
12	VB5	6.80	2	151	5	72.0	2	126	1	55.8	1
13	VB6	7.27	1	191	2	91.3	0	108	0	59.5	3
14	TF1	8.52	1	188	4	68.7	1	83.4	1	46.4	3
15	TF2	7.53	2	171	2	68.7	1	75.2	1	44.2	7
16	TF3	7.35	1	128	2	73.4	6	95.2	0	38.6	6
17	TF4	6.76	1	164	2	95.5	2	104	1	29.7	2
18	TF5	6.45	1	127	1	57.6	1	83.5	2	17.4	2
19	TF6	6.75	4	150	1	71.2	1	102	7	26.2	9
20	SP1	6.44	0	142	2	62.7	1	79.7	2	29.9	11
21	SP2	6.01	2	115	2	58.6	0	70.5	1	22.2	21
22	SP3	6.26	2	120	2	61.7	1	89.2	0	29.6	8
23	LE1	10.7	2	173	1	66.6	0	236	1	70.0	7
24	LE2	9.60	4	125	2	64.7	1	381	1	79.5	0

Table 5 Concentration of elements in sediments from Vordernbergerbach

Duplicate test portion for each location were measured with different calibration program for concentration measurement i.e. GeoWSU used for fused glass beads, Protrace Geo for pellets (both pellets and beads measured with the XRF) and Na_2O_2 sintered solutions were subjected to ICP-MS measurement.

Major elements with XRF can be measured well, but trace elements and rare earth elements were measured with ICP-MS. To have detailed information about the composition of sediments, all three modes were applied. Only few elements were discussed here and data for selected elements is being presented here in Table 5, but the concentration tables for each element, measured with different techniques are reported in of thesis. Among all options of measured concentration, only the best fitting concentration values, having the least bias of data and the least variance were selected. As duplicate test portions were measured for each mode of measurement, so average of selected (on the basis of less bias and much closeness of measured and expected/assigned concentration of MUS) is taken and RSD is reported, shown in Table 5. The samples were collected in two different sampling sessions, two batches of samples PB1-VB6 (13 samples) and TF1-LE2 (11 samples) were

measured in different times with the XRF but for the ICP-MS they were measured together. Background level of concentration for elements is decided as the average of first seven samples (PB1-PB7) taken from region of Präbichl because these locations are not contaminated sites as there is neither residential nor industrial source of contamination in this area. The following Graph 2 to Graph 6 were made on OrginPro 8.5G choosing B-spline. As baseline and safe limits for sediments were not found so the values for safe limits and background defined for soils were taken into the account.

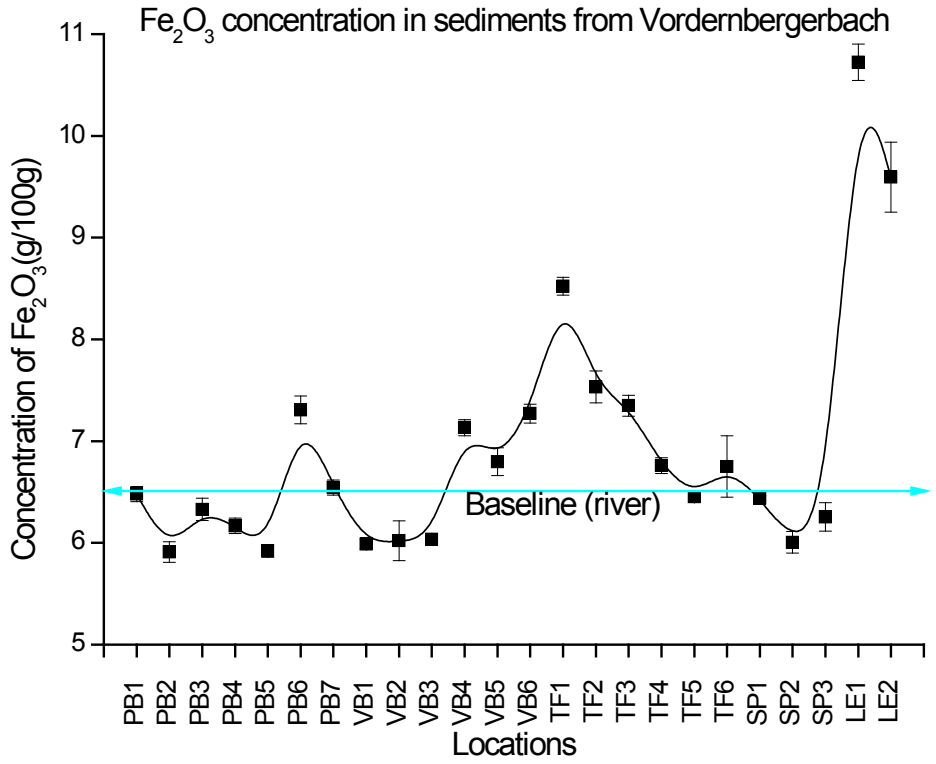

Graph 2 Concentration of Fe_2O_3 in sediments of Vordernbergerbach

Concentration of Fe_2O_3 is measured with the XRF using GeoWSU and Protrace Geo calibration programs and with the ICP-MS using geol 01 method for duplicate sample portions and duplicate sample solutions respectively. The selected averages of concentration among measured options have 2 % RSD. The average bias of the data calculated from assigned values of MUS and measured MUS along with samples is 0.01 %. The baseline for Fe_2O_3 is 6.5 g/100g in the river Vordernbergerbach is decided on the basis of average of 1st 7 samples belonging to Präbichl as no anthropogenic sources were situated there. Any area having concentration of Fe_2O_3 more than baseline can be marked as contaminated area. In the investigated river, the area of Vordernberg and Leoben are found to be contaminated. A clear increase in the area of Vordernberg (VB4-TF1) is observed as shown in Graph 2. TF1

sample is collected from river sediments at Friedauwerk, and the concentration of Fe_2O_3 is found higher at this point, near to this point it decreases gradually till we reach location TF5 where the concentration of Fe_2O_3 is closer to baseline. In region of St. Peter/Freinstein, the concentration of Fe_2O_3 is normal and equal to base line value. The most contaminated area is Leoben, where concentration of Fe_2O_3 reaches to 11 g/100g.

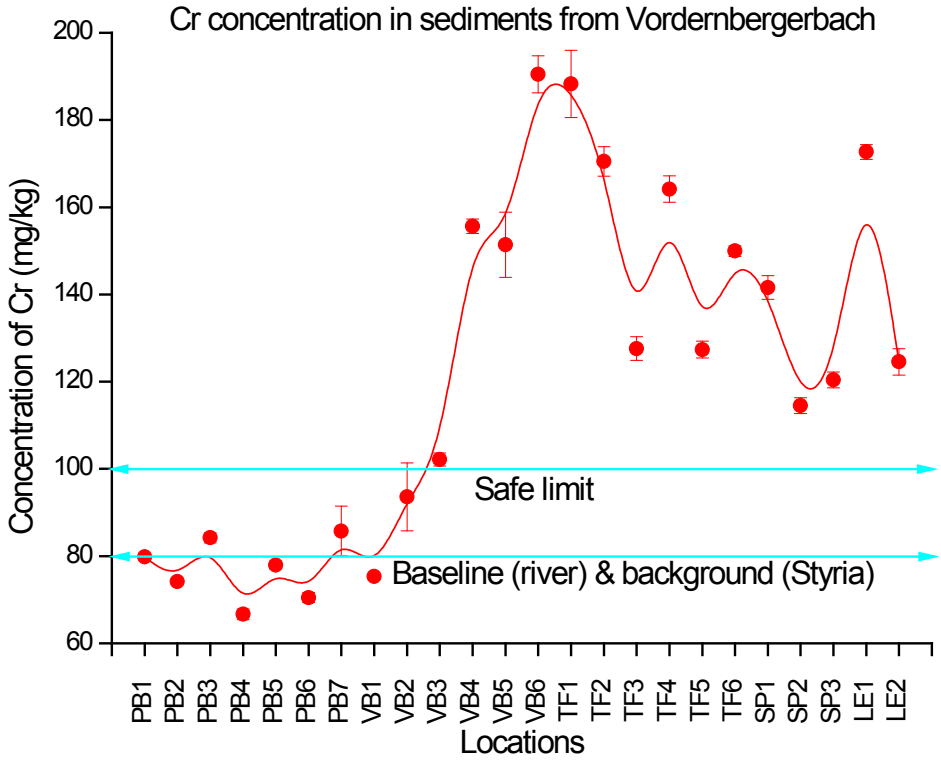

Graph 3 Concentration of chromium in sediments of Vordernbergerbach

Concentration of Cr is measured with XRF using Protrace Geo mode. Duplicate samples measured for each location have RSD 2 % while bias of the data calculated from MUS measured and assigned values is 3 %. Baseline for Cr in sediments is 80 mg/kg. This level of Cr concentration is present is Styrian soil. The whole area after Präbichl coming downstream towards Leoben (VB3-LE2) is identified as contaminated as concentration of Cr is higher than the safe limits (100 mg/kg). Maximum Cr concentration up to 190 mg/kg is found at TF1 (at Friedauwerk) and in Leoben its concentration is determined as 170 mg/kg as shown in Graph 3. Area in between these highly contaminated spots, i.e., downstream region of Trofaiach is relatively less contamination of chromium. While in St. Peter/Freinstein, the Cr concentration in river sediments is closer to safe limits.

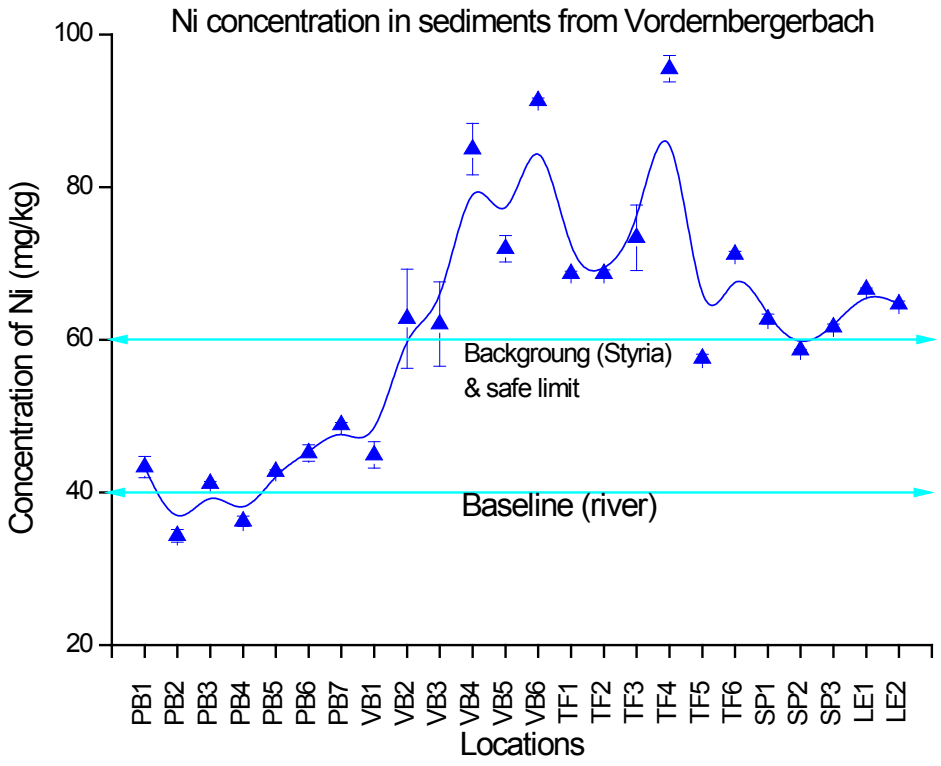

Graph 4 Concentration of nickel in sediments of Vordernbergerbach

Concentration of Ni was measured with ICP-MS using geol01 method. Duplicate samples measured for each location; have overall 2 % average RSD while the average bias of data is 8 %. Baseline for Ni in the sediments of this river under investigation is 40 mg/kg. 60 mg/kg concentration of Ni is considered normal for Styrian soil and is a safe limit as well (Krainer, 2000). In investigated river (Vordernbergerbach) sediments overall area after Präbichl (Vordernberg to Leoben) is found contaminated and the areas of Vordernberg-Trofaiach (VB3-TF2) and Leoben (LE1-LE2) are found beyond the safe limit as shown in Graph 4. Sediment samples taken from St. Peter/Freienstein (SP1-SP3) showed concentration values closer to the safe limits.

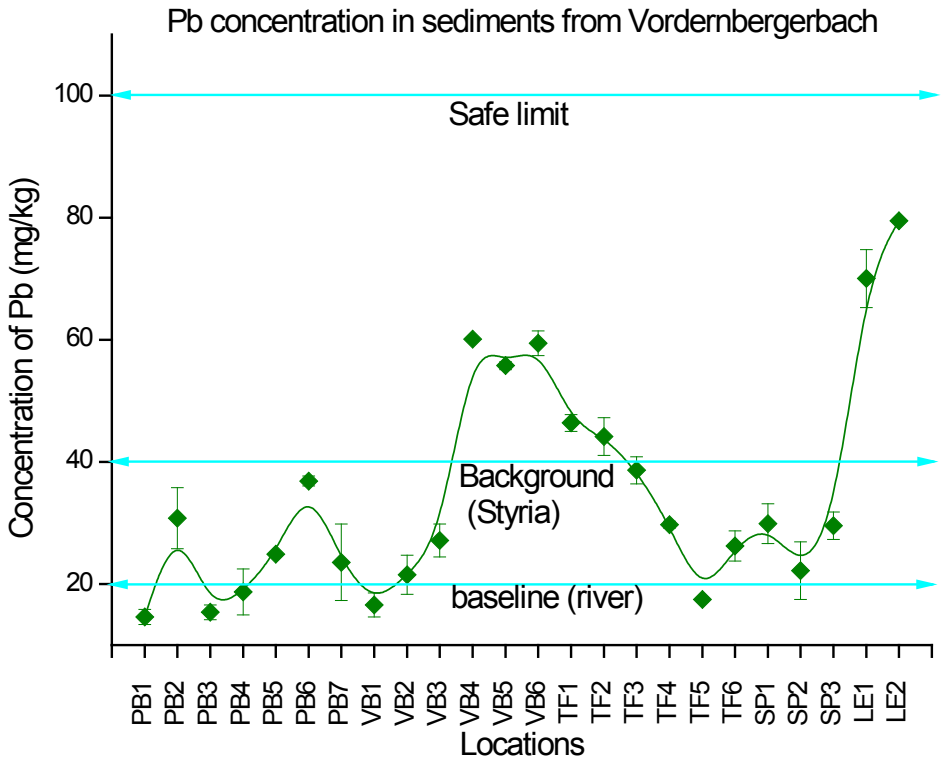

Graph 5 Concentration of lead in sediments of Vordernbergerbach

Concentration of Pb is measured with XRF using GeoWSU programm. Duplicate samples measured for each location have average RSD 8 % while the average bias for is 4%. Baseline for Pb in the sediments of this river is 20 mg/kg. Styrian soils contain 40 mg/kg of Pb in average (Krainer, 2000). So, Vordernberg with 60 mg/kg concentration of Pb and Leoben having Pb concentration level upto 80 mg/kg are marked as contaminated areas. However concentration of Pb is below safe limit (100 mg/kg)(Krainer, 2000) in whole area as shown in Graph 5.

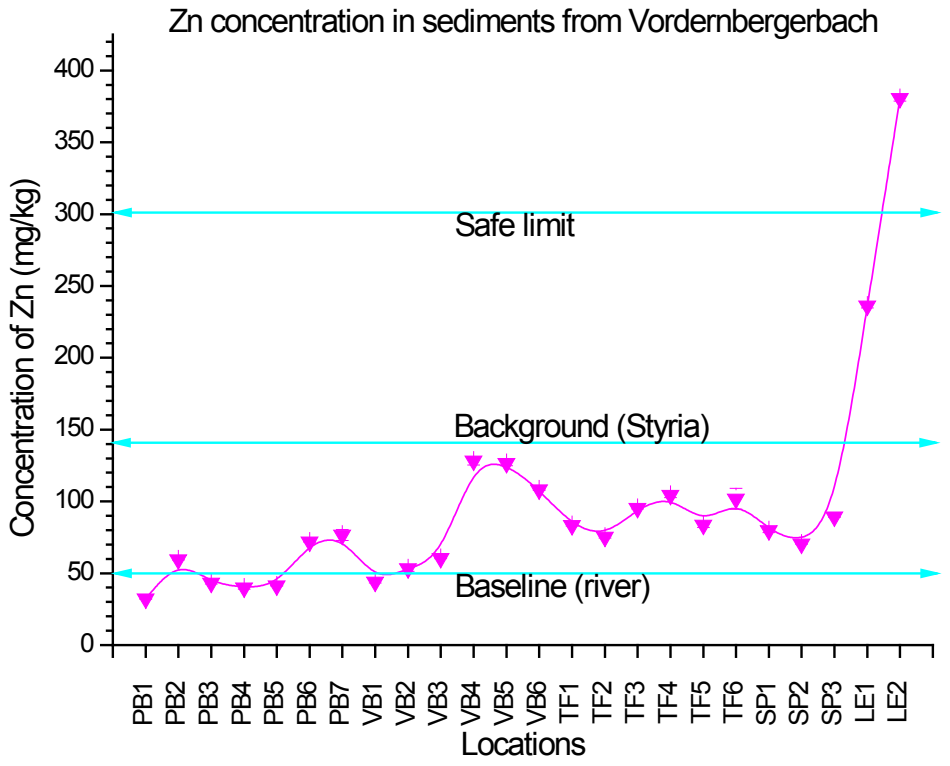

Graph 6 Concentration of zinc in Vordernbergerbach

Concentration of Zn is measured with XRF using GeoWSU. Duplicate samples measured for each location have overall 2 % RSD while the average bias of data is 12%. Most of the area is between baseline (50 mg/kg) and background level of zinc in Styrian soil (140 mg/kg) (Krainer, 2000). Areas of Vordernberg and Trofaiach have relatively higher concentration than baseline but much below than safe limit as shown in Graph 6. Maximum concentration in studied river is found near Leoben which is 2 folds than its concentration in Vordernberg and Styrian background level. Leoben is the only area found where zinc concentration is found higher enough to cross the safe limit that is 300 mg/kg (Krainer, 2000).

Elevated level of concentration can be either geogenic or due to anthropogenic activity. Iron production had been in progress in the region near Friedauwerk, which remained actively progressive from 17-19th century. This might be the reason of high level of concentration of Cr, Fe_2O_3, and Ni etc. in the region of VB3-TF2. While higher level of concentration in region of Leoben is thought due to steel production unit in Donawitz. However, to further investigate the possible (anthropogenic or geogenic) source/s of contamination of sediments due to heavy metals mineralogical study of sediments is made.

2.8. Magnetic susceptibility values and concentration of elements

Graph 2 to Graph 6 show that the areas of Vordernbergerbach and Leoben (LE1-LE2) are contaminated due to heavy metals containing higher concentration level of heavy metals in these areas as compared to the other areas, e.g., Präbichl, St. Peter Freinstein and lower Trofaiach (TF3-TF6). These areas were highlighted in magnetic susceptibility measurements as well. Mostly heavy metals and magnetic particles may be produced together but they may be present as separate particles too. So this correlation between pollutants and magnetic particles is complex and different for different processes which are responsible for heavy metal contamination. It is not easy to say that how far magnetic susceptibility measurement on its own can inform us about the pollution (Hanesch and Scholger, 2002). However in the case of study on Vordernbergerbach sediments, magnetic measurements and concentration of heavy metals in different regions fit together showing that magnetic particles are the carrier of heavy metals.

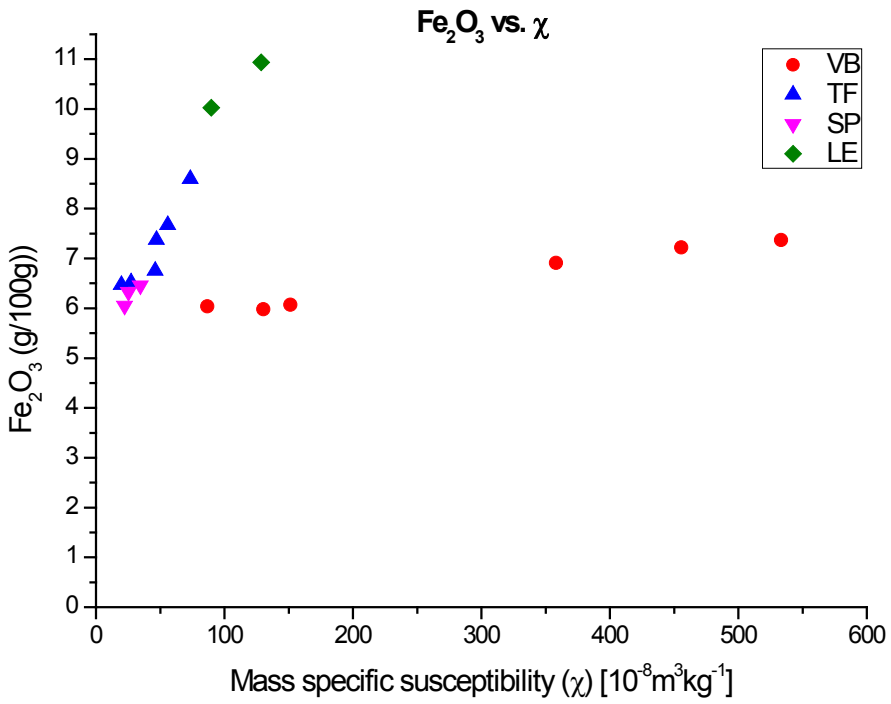

Graph 7 Correlation between mass specific magnetic susceptibility (x) measurements and Fe_2O_3 content

In detail, trends of correlation between heavy metals and magnetic susceptibility measurements (Graph 7-Graph 11) in different areas are found different. Different trends for different areas show that the heavy metals in different areas are derived from different origin. Graph 7 shows that Fe_2O_3 in Vordernberg area has iron content which is highly

magnetic while in Trofaiach and St. Peter/Freienstein, the iron content is higher but present in nonmagnetic form, e.g., iron bearing non-magnetic minerals e.g. fine silicates, trend for only two points in Leoben, is not very clear here for Fe_2O_3 but different origin is indicated in Graph 8-Graph 11. In scatter plots (Graph 7-Graph 11) the samples from Präbichl are not included considering them as baseline.

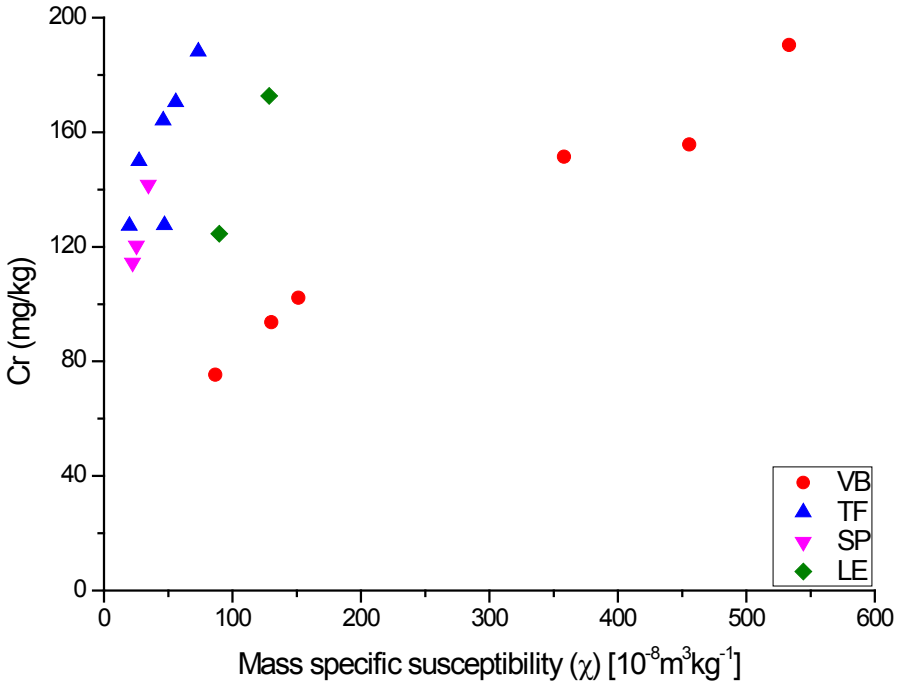

Graph 8 Correlation between mass specific magnetic susceptibility (x) measurements and chromium content

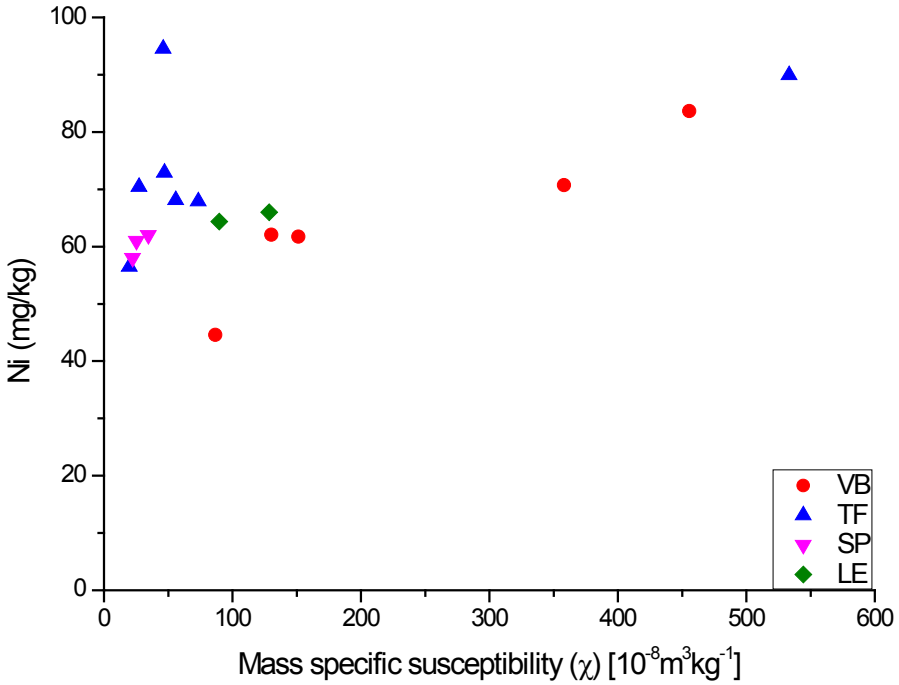

Graph 9 Correlation between mass specific magnetic susceptibility (x) measurements and nickel content

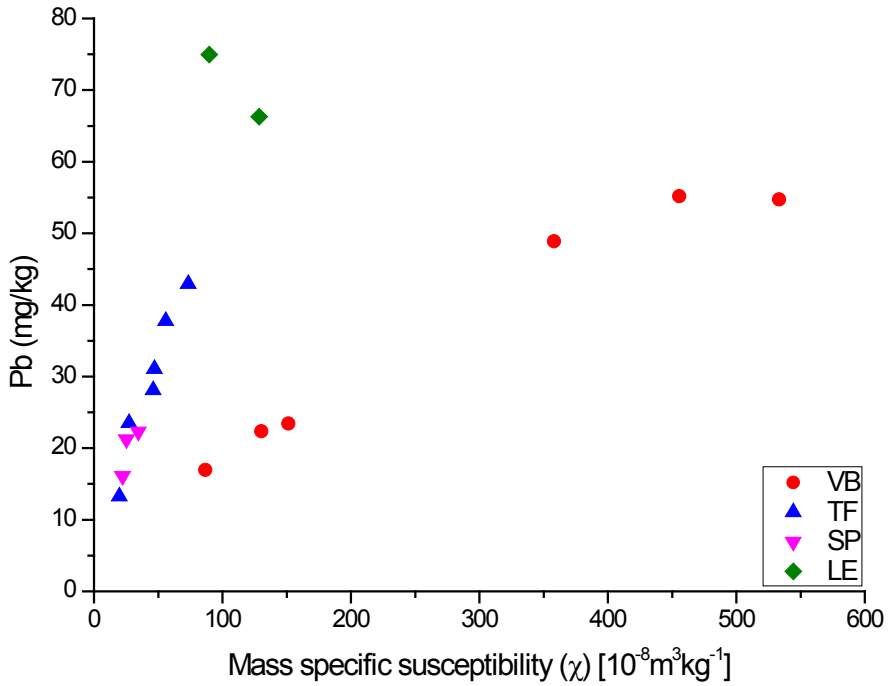

Graph 10 Correlation between mass specific magnetic susceptibility (x) measurements and lead content

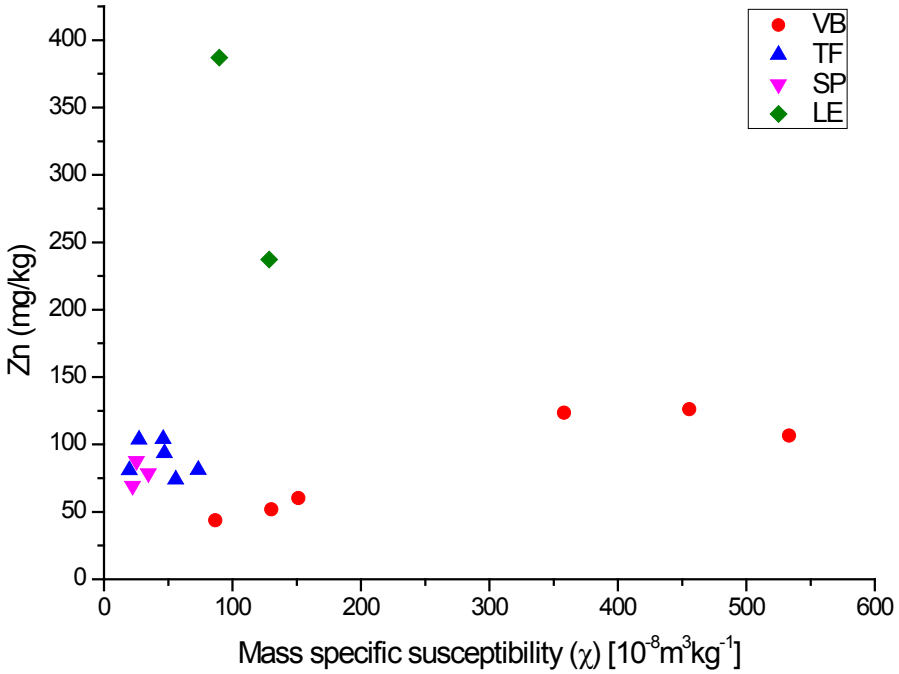

Graph 11 Correlation between mass specific magnetic susceptibility (x) measurements and zinc content

2.8.1. Conclusion

- Concentration of heavy metals and magnetic susceptibility measurements are higher at the contaminated spots it reveals the fact that magnetic susceptibility device is quick and economical device which helps to mark the contaminated sites due to heavy metals association with magnetic particles.
- Trofaiach and St. Peter/Freienstein contain iron bearing non-magnetic minerals while Vordernberg area contains iron which shows high magnetic properties.
- Average concentration of chromium on contaminated spots is 190 mg/kg at Friedauwerk location (TF1), 170 mg/kg in Leoben region (LE1) and 140 mg/kg in lower Trofaiach region (TF3-TF6) higher than safe limits (100 mg/kg) for soil.
- Nickel concentration at contaminated Vordernberg near Friedauwerk (TF1) is 90 mg/kg which is more than safe limit for nickel (60 mg/kg).
- Although in Vordernberg area (VB3-TF2) the concentration of Pb and Zn are higher than the background for Styrian soils, they are below the safe limits 100 mg/kg and 300 mg/kg respectively.

- The most likely source for these contaminated sites Vordernberg and Leoben may be anticipated iron activity which had been in progress for few centuries in the area of Vordernberg and current steel production unit in Leoben respectively. But to differentiate between anthropogenic or geogenic sources of contamination mineralogical study is required.
- Scatter plots between magnetic susceptibility measurements and heavy metals indicates different origin or association of heavy metals with different minerals in contaminated areas Vordernberg and Leoben with respect to non-contaminated or less contaminated areas.

3. Mineralogical Study

To find out the real anthropogenic or geogenic source/s of contamination of river sediments due to heavy metals, a mineralogical study was made.

3.1. Sampling

For this purpose three sampling locations were selected which corresponds to the above mentioned places TF1, TF6 and LE1. The exact locations were shown in maps (1-3).

S. No.	Locations	Coordianates	Corresponding position for geochemical data	Sample ID for mineralogical samples	Volume magnetic susceptibility (in field) (k) SI [10-5]			RSD%
					on MS2 meter		Mean	
1	Annabrücke	N47° 22.688′ E15° 04.757′	LE1	LE1	426.9	428,2	383	62
					96.3	96,9		
					629.6	620,2		
2	Gmeingrube	N47° 24.572′ E15° 01.616′	TF6	SP1	127.8		59	100
					27.7			
					22.9			
3	Friedauwerk	N47° 27.373′ E14° 59.687′	TF1	FW1	65.2	62.3	70	48
					36.9	36.7		
					111.3	110.9		

Table 6 Sample locations collected for mineralogical study and magnetic susceptibility in the field

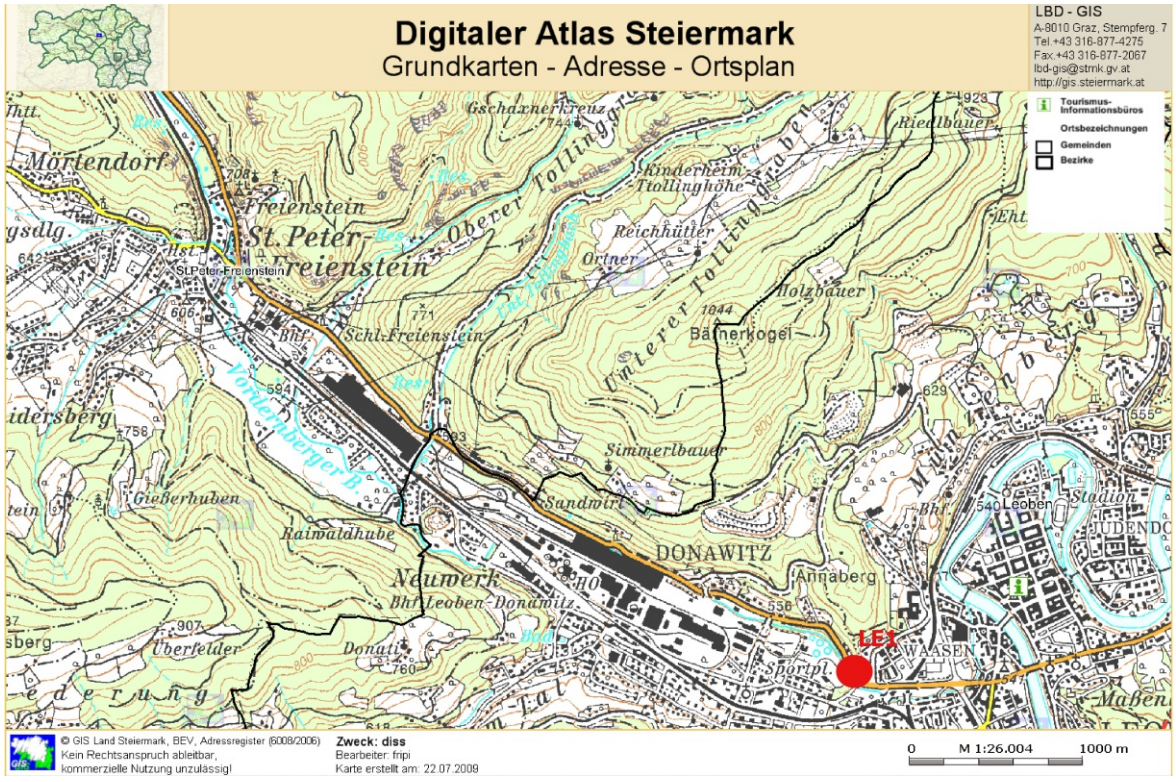

Map 1 Sampling point LE1 for mineralogical study at Donawitz/Leoben

Map 2 Sampling point SP1 for mineralogical study at Gmeingrube

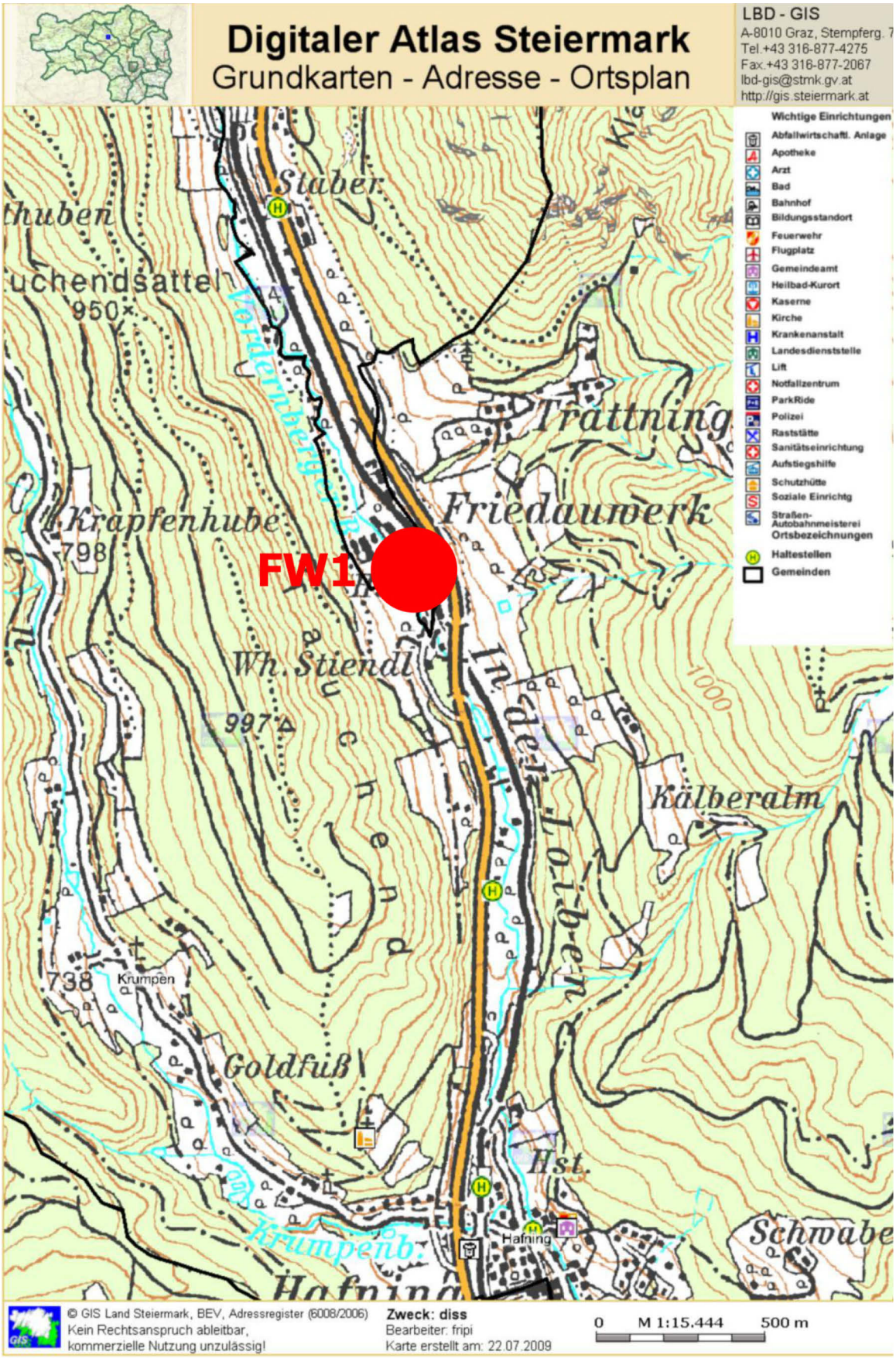

Map 3 Sampling point FW1 for mineralogical study at Friedauwerk

3.1.1. Panning

Sediments on each location were sieved through 1.40 mm sieve. The amount of sieved sediments taken for pre-concentration of heavy minerals contained in it was recorded as 4 kg and 8 kg for LE1 and SP1 respectively, weight of sieved stuff taken at FW1 was not noted. The fraction less than 1.40 mm was further washed with river water and fine material was simply discarded to get the pre concentrate of sediments containing heavy minerals. Water was removed and then wet samples were packed in the marked bags.

3.1.2. Heavy liquid separation

Subsequently, the samples were subjected to sieve analysis with 0.71/0.1 mm. Then sink-float analysis using sodiumpolytungstate with density of 2.9 g/cm^3 was performed at chair of mineral processing. Material with density greater than 2.9 g/cm^3 and grain size smaller than 0.71 mm was separated. Then magnetic and non-magnetic fractions of material (>2.9 g/cm^3 and >0.71/0.1mm) were separated with the help of a hand magnet. Polished section from magnetic fractions and thin section from non-magnetic sections were prepared for further analysis under microscope and Electron Micro-Probe Analyzer (EMPA) at the chair of mineralogy.

S. No.	Sample ID	Mass of sediments > 0.71mm in concentrate	0.71/0.1 mm 1/2 TP Riffled			< 0.1 mm	% age of heavy mineral (0.71/0.1 mm and density>2.9 g/cm^3) in sieved fraction (0.71/0.1 mm)
			Total	>2.9 g/cm^3	< 2.9 g/cm^3		
		Mass (g)	Mass (g)	Mass (g)	Mass (g)	Mass (g)	%
1	LE1	8.22	101.14	32.98	64.75	1.49	33
2	SP1	21.48	94.15	12.47	81.02	1.49	13
3	FW1	34.35	164.7	68.11	96.68	0.73	41

Table 7 Amounts of fractions in sediments (concentrate) as a result of heavy liquid separation

It is mention worthy here, that the amount of sample taken for the sample at Gmeingrube (SP1) was double than that taken for Donawitz/Leoben for preconcentration. Moreover, the amount of heavy mineral is much less than that of other locations.

3.2. Analysis

Polished sections and thin sections were prepared and analyzed at the Chair of Mineralogy (Montanuniversität Leoben) with following instruments.

- Electron Micro-Probe Analyzer JEOL JXA 8200
- Reflection microscope

Polished sections (magnetic heavy minerals) and thin sections (non-magnetic minerals) were observed with the reflection microscope. Minerals were identified on the basis of shape, color and brightness of the minerals. Heavy minerals look much brighter than other. Minerals of interest in polished sections were encircled with the help of diamond tip. Mineralogy of these particles were verified with the help of quantitative and qualitative analysis using EMPA. Shape, color, brightness, spectrum and quantitative data and stoichiometric ratio altogether were used to interpret the mineralogy. The relative abundance of each mineral was observed by optical assessment with the help of reflection microscope and recorded manually. Decision of origin of minerals was also based on optical observation of physical features of minerals, for example geogenic magnetite has octahedral structure and anthropogenic magnetite has spherical structure. Moreover typical anthropogenic particles contain mineral of anthropogenic origin.

Typical anthropogenic particles present in area are as following:

- Spherical particles
- Tinder/scale
- Roasting ore
- Sinter
- Iron furnace slag
- Steel mill slag

Minerals in above mentioned typical anthropogenic particles are anthropogenic for example magnetite and hematite in sinter; magnetite and wüstit (wuestite) in scale or slag are also anthropogenic.

3.2.1. Mineralogy of sediments in Donawitz/Leoben (LE1)

In microscopic study following phases of minerals were observed.

Predominantly high occurrence of metallic iron, magnetite of anthropogenic origin as they are spherical mostly, geogenic magnetite have octahedral structure, hematite anthropogenic because they are present in sinter, chromite (type I and II) of geogenic nature, calcium ferrite, (Ca,Al)-Ferrite), anthropogenic wüstit (in tinder, slag and reduction products), iron hydroxide, titanium minerals (ilmenite, rutile and titanite) of geogenic origin, olivine mixed

crystals (anthropogenic), calcium silicate (anthropogenic, found in slag), epidot minerals (geogenic), pyrite (geogenic) and glass phases (mostly ingredients of slag, thus anthropogenic) is seen.

Average occurance of ferrosilicon (mostly anthropogenic), magnesioferrite, RO-phases (Mn, Ca, Fe, Mg, Mix oxides) of anthropogenic nature, carbonates (siderite and ankerite) of geogenic origin, garnet, chlorite and amphibole (all three geogenic), apatite (mostly anthropogenic), chromspinel (mostly with chromite washed out), and maghemite is observed.

Occasionally presence of metal as titanium, Ti-nitride, graphite, melilite mixed crystals, corundum (anthropogenic), magnetic gravels, spinel (anthropogenic) serpentine, diopsid, Xenotime, periclase and zircon have been identified.

Note: Relative abundance of different minerals is seen within the same sample

Relative abundance of typical anthropogenic particles in stream sediments (Vordernbergerbach) at Donawitz/Leoben is given in Table 8.

Globular	++++
Scale/tinder	++++
Roasting ore	+++
Sinter gut	++++
Blast furnace slag	+++++
Steel work slag	++++

Table 8 Relative abundance of typical anthropogenic particles in river sediments at Donawitz/Leoben

Legends

Occasional +

Less ++

Average +++

A lot of ++++

Excess +++++

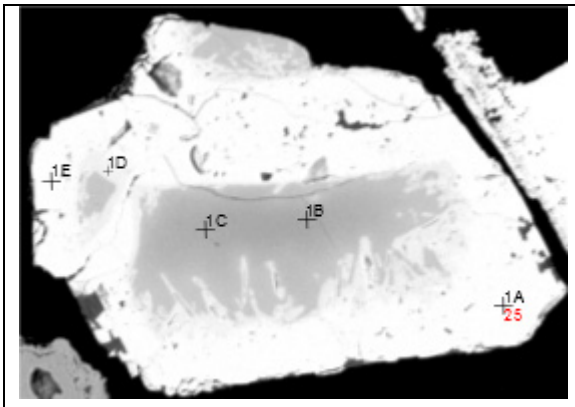

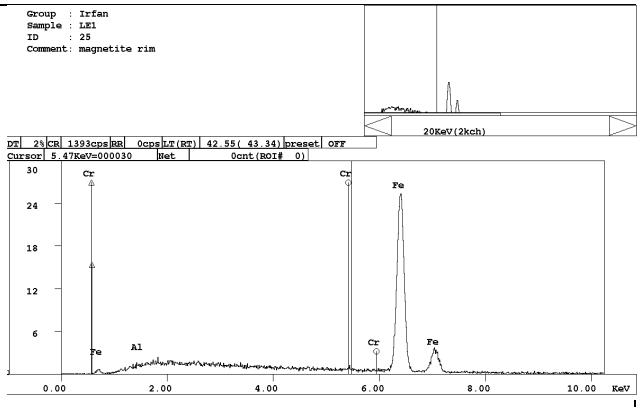

LE1C6-1 Chromite (1B-1E) having magnetite rim around (1A)

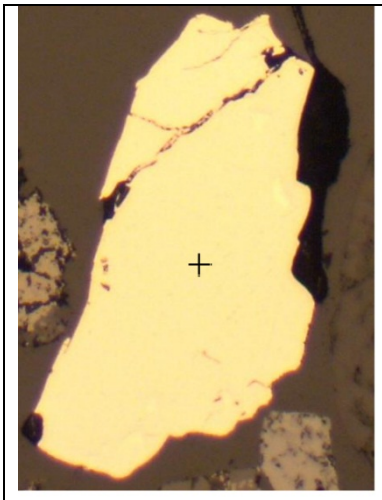

Ferrosilicon containing Ni and Cr (LE1C1-2)

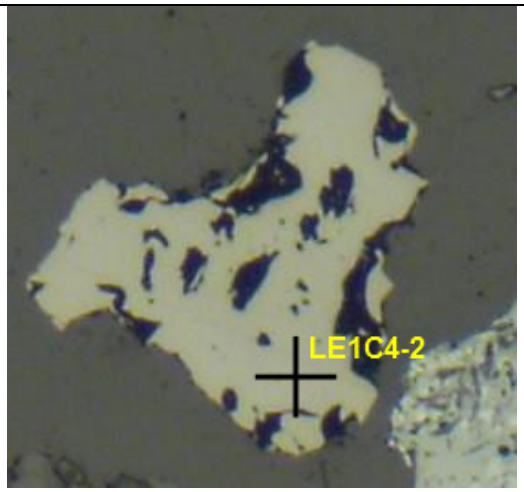

Anthropogenic magnetite containing nickel

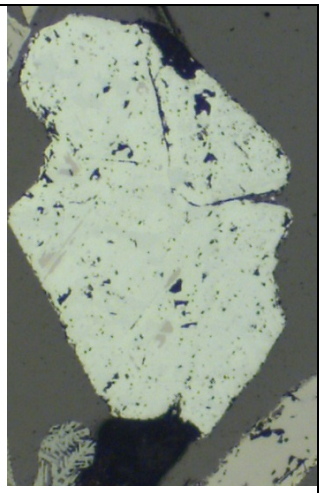

Hematite (LE1C4-3)

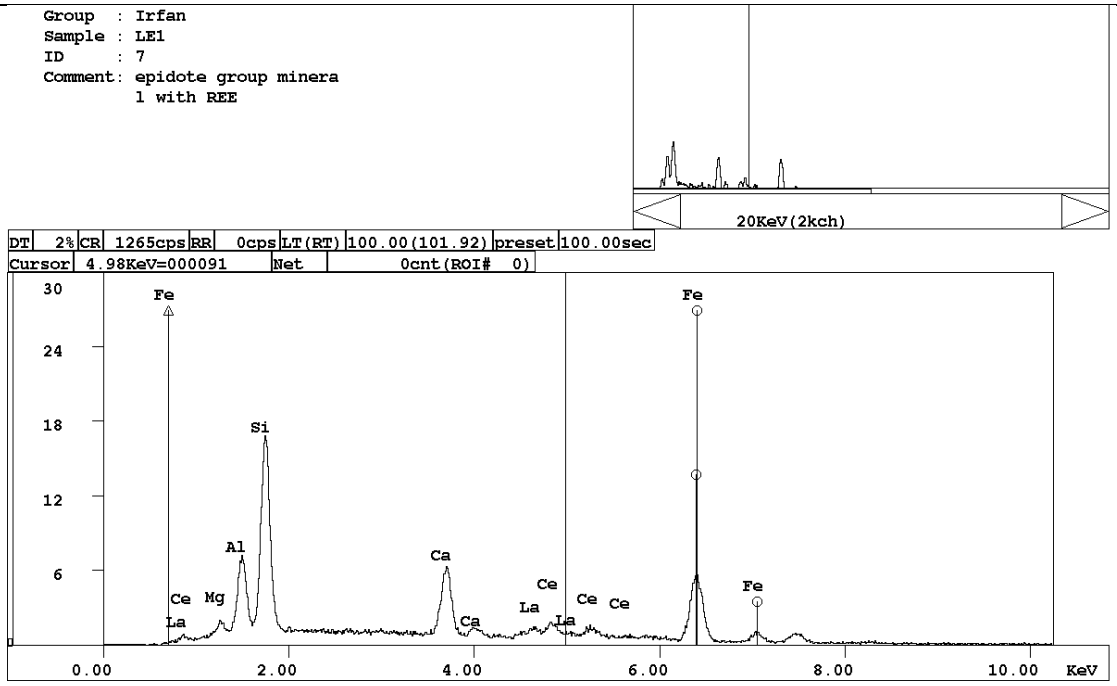

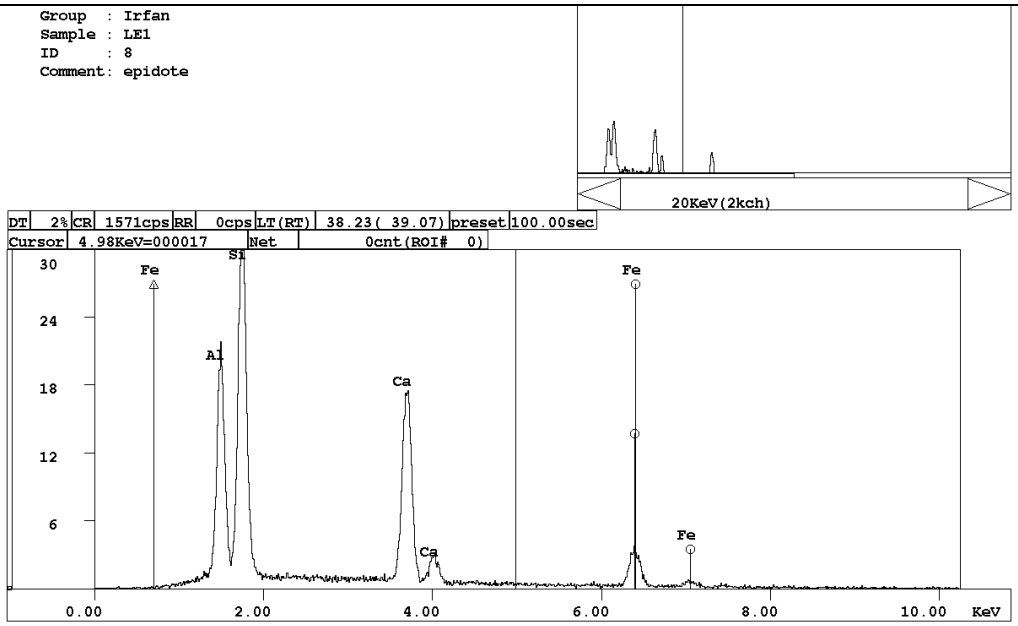

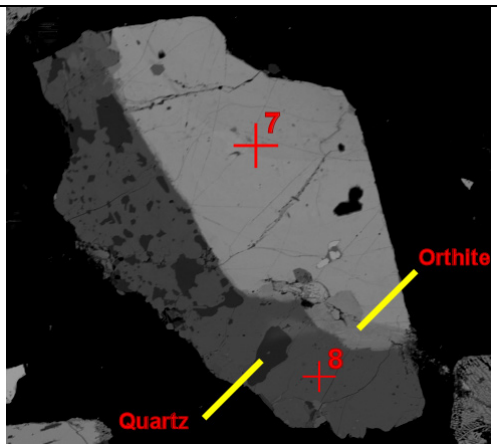

Epidote group mineral (Apatite), SiO_2 forming a ring around Apatite

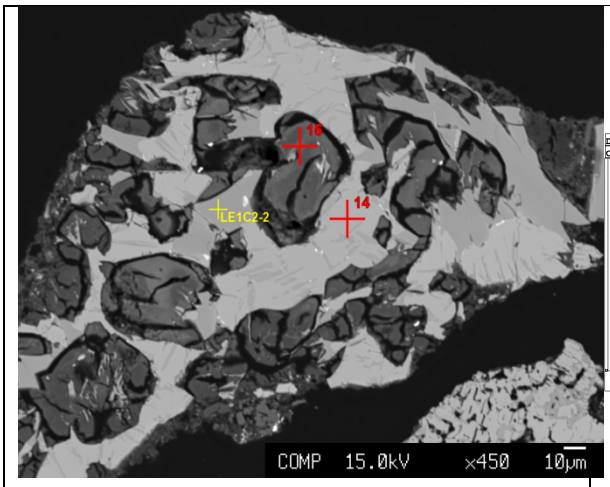

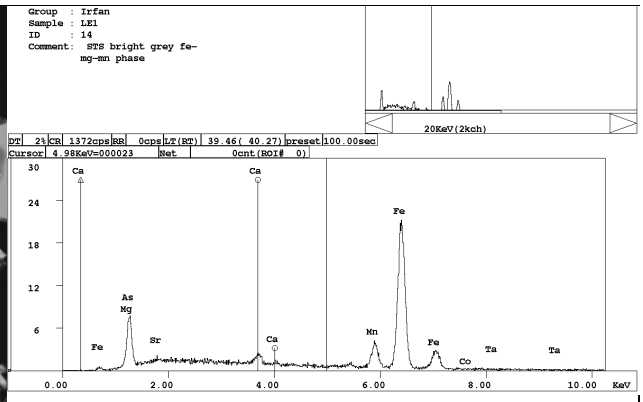

Steel work slag containing Ni in it (LE1C2-2) observed in quantitative analysis, darker phase contains Mg, Al, Ca, Si and Fe (EDS 15) while bright phase contains more Fe, Mn and Mg (EDS 14).

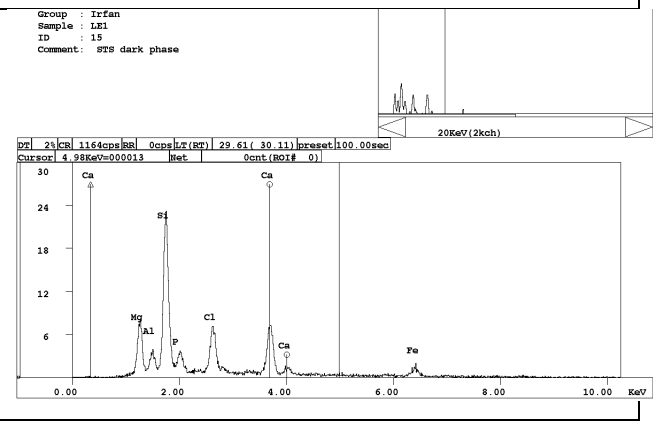

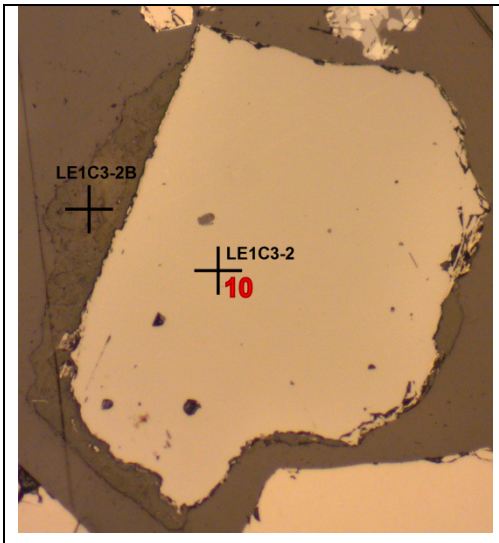

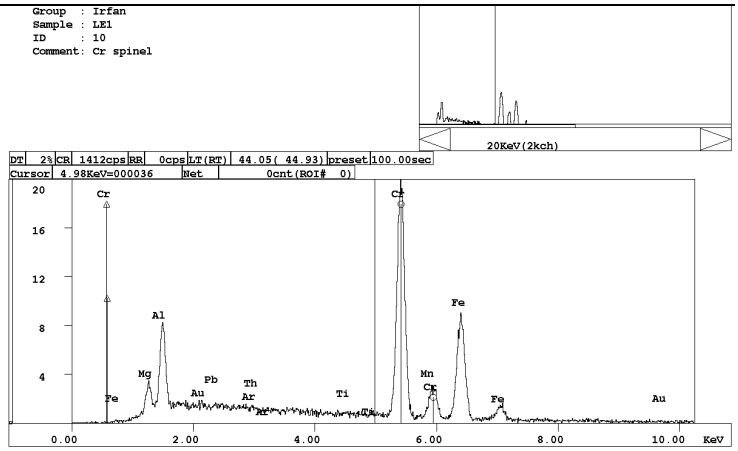

LE1C3-2 Chromspinel surrounded by Mg-Si phase containing Ni in it (LE1C3-2B)

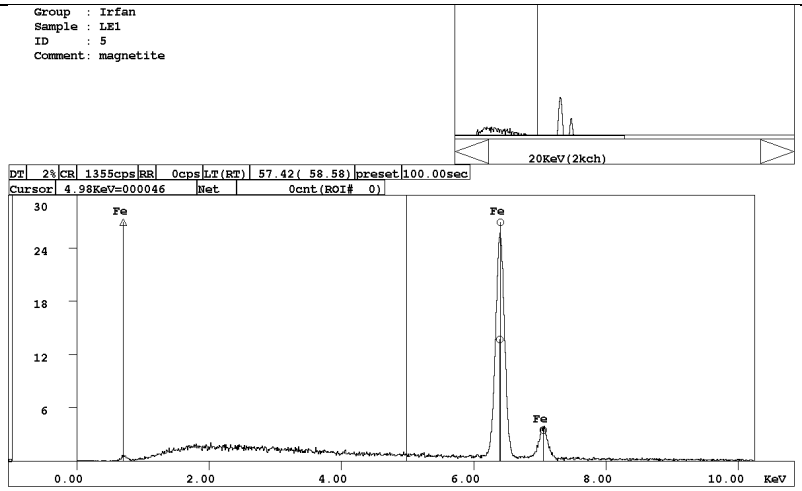

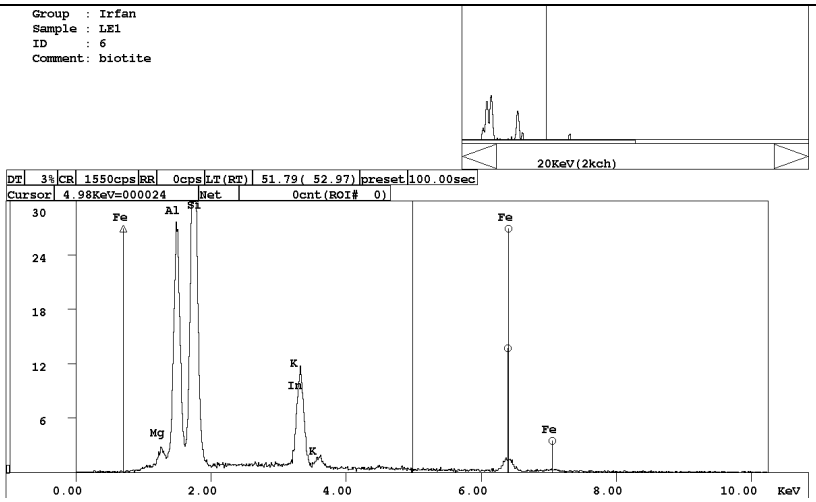

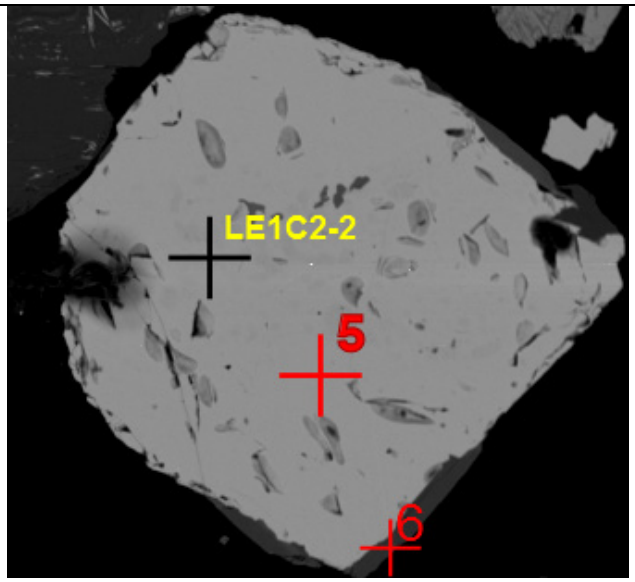

Ni containing anthropogenic magnetite (LE1C2-2) along with biotite (6)

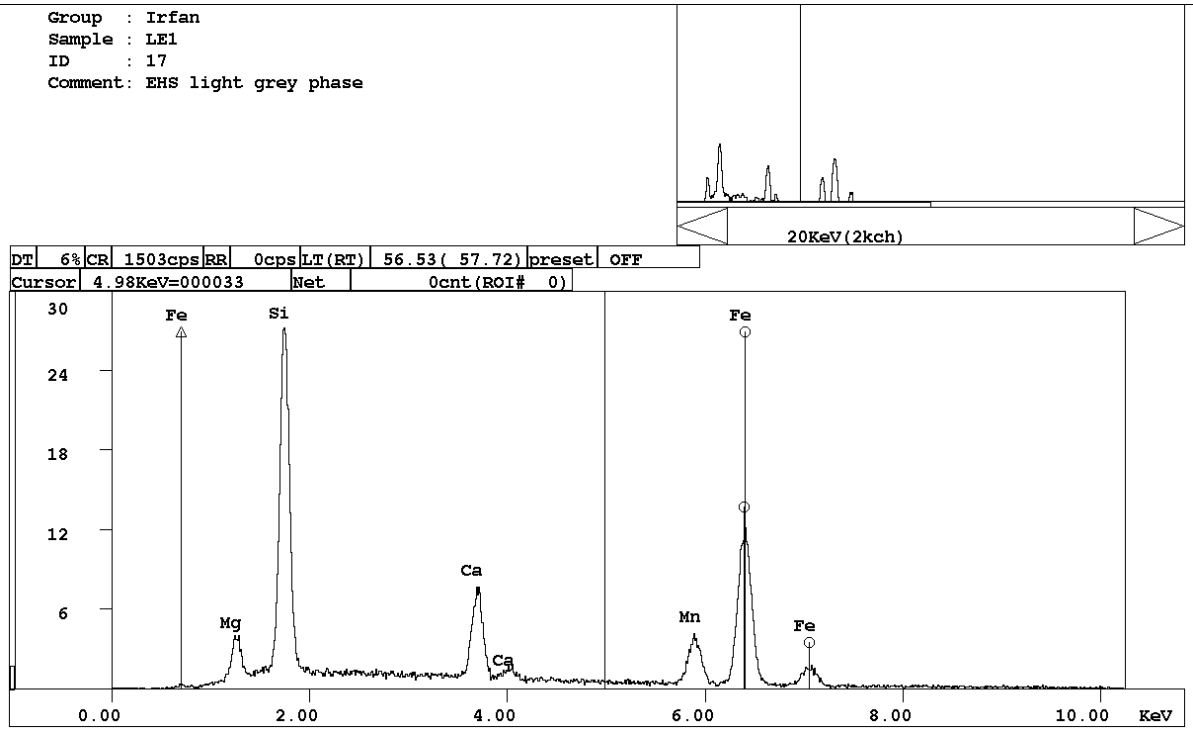

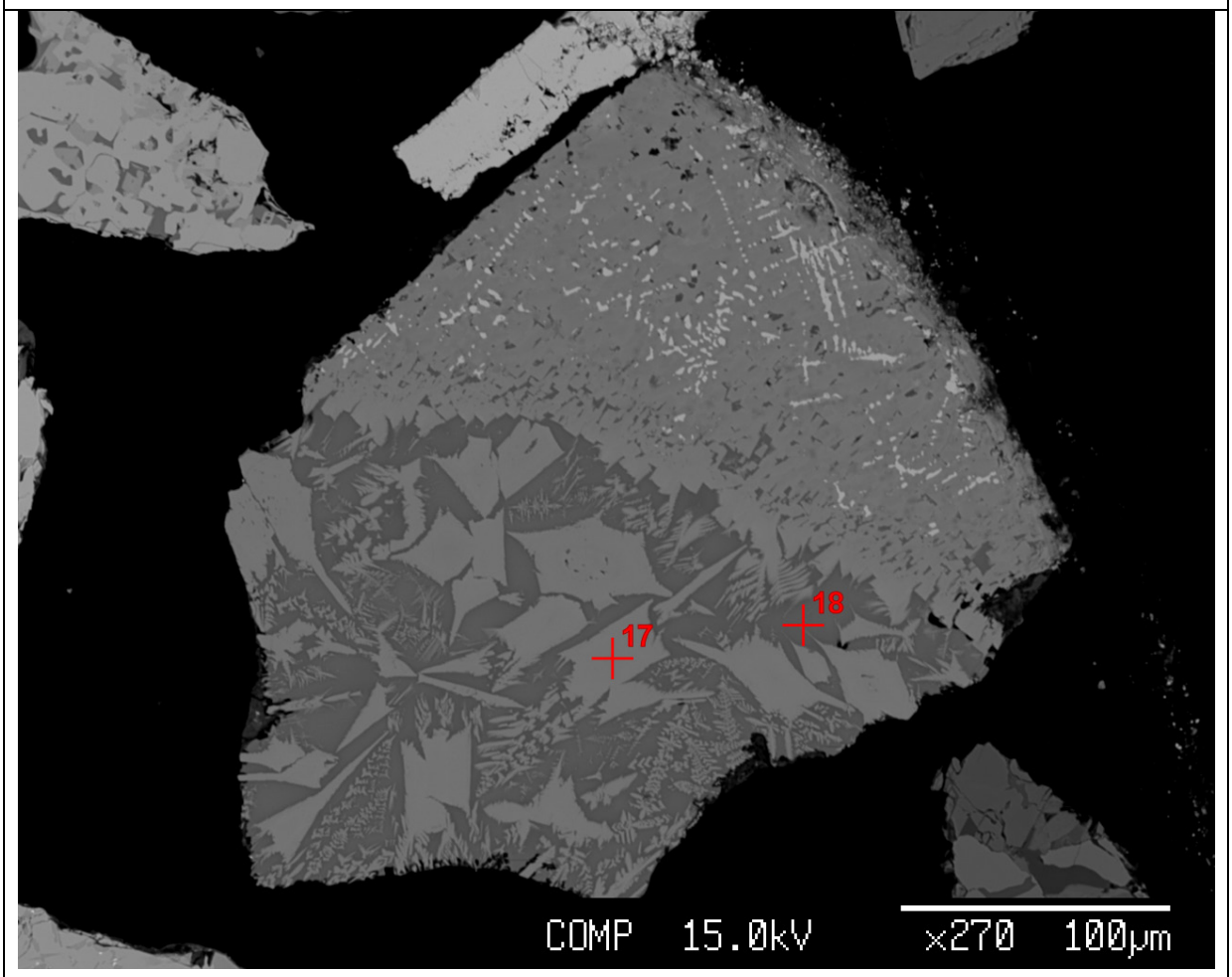

Blast furnace/iron work slag

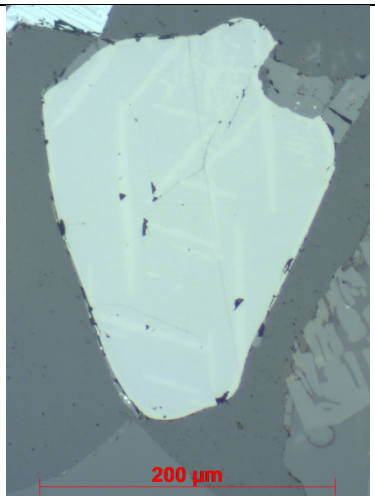	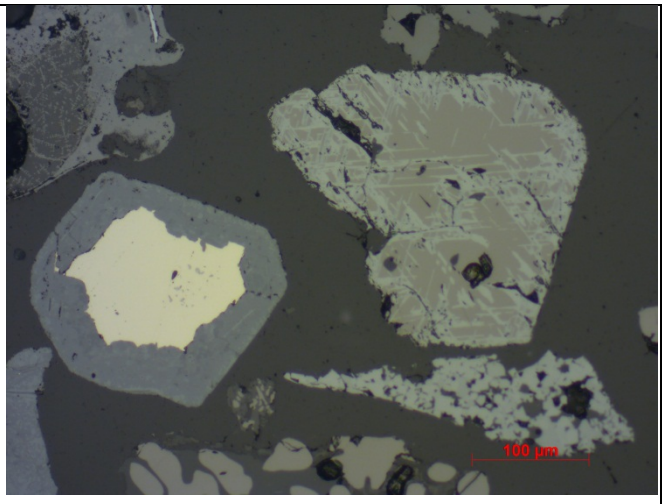
Rutile (TiO2)	Pyrite

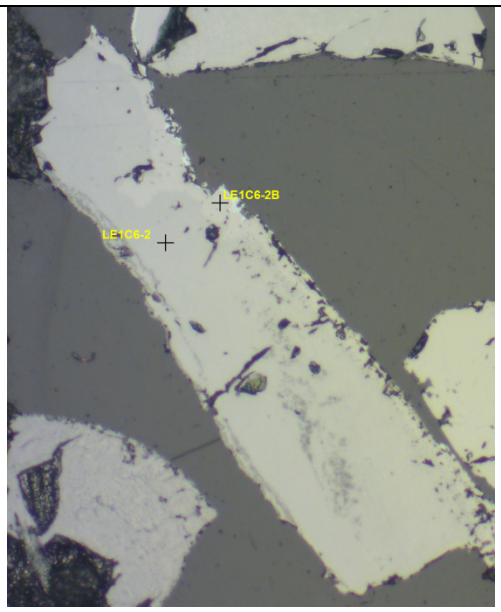	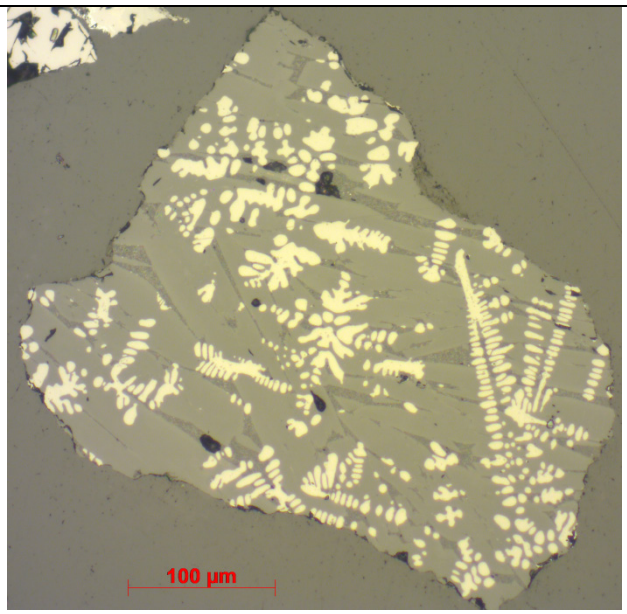
Tinder getting oxidized	Blast furnace slag containing dendrites of magnetite crystals

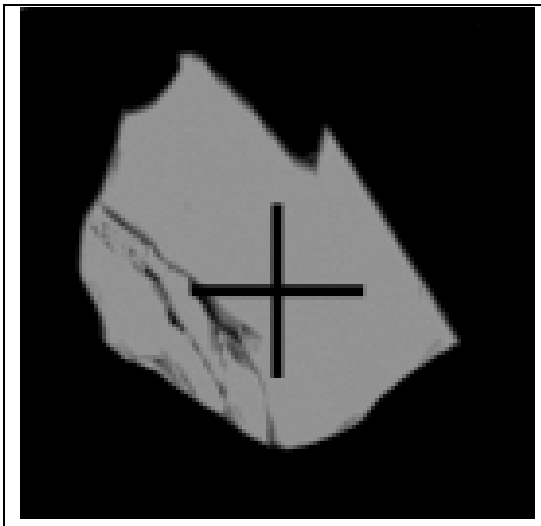	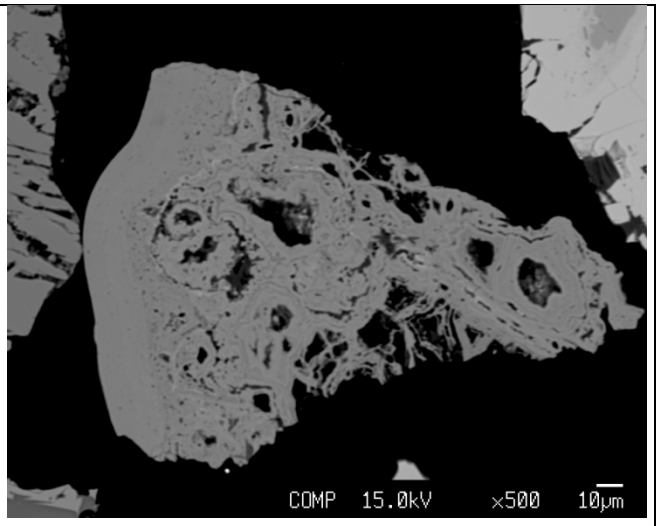
(LE1C6-5) Hematite containing Ni	(LE1C6-4) Ni containing $Fe(OH)_2$
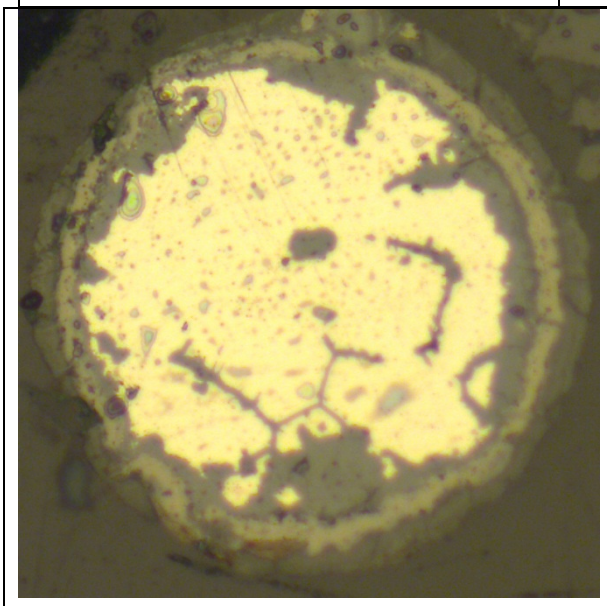	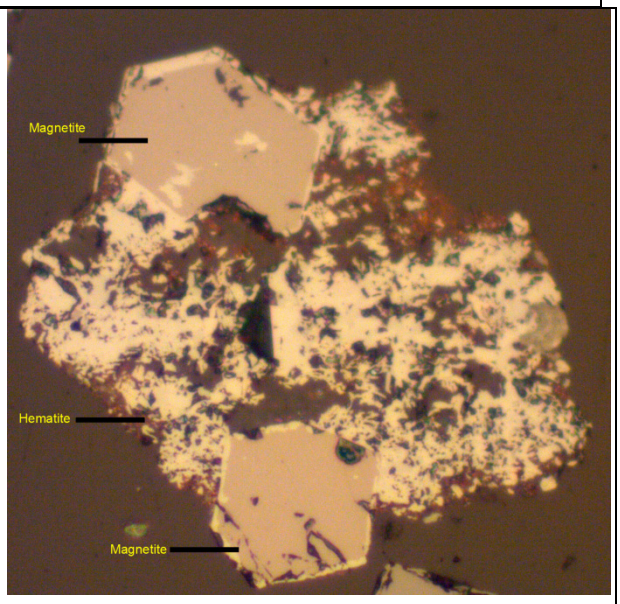
Metallic iron surrounded by wüstit and is getting converted into $Fe(OH)_2$	Geogenic hematite bearing geogenic magnetite

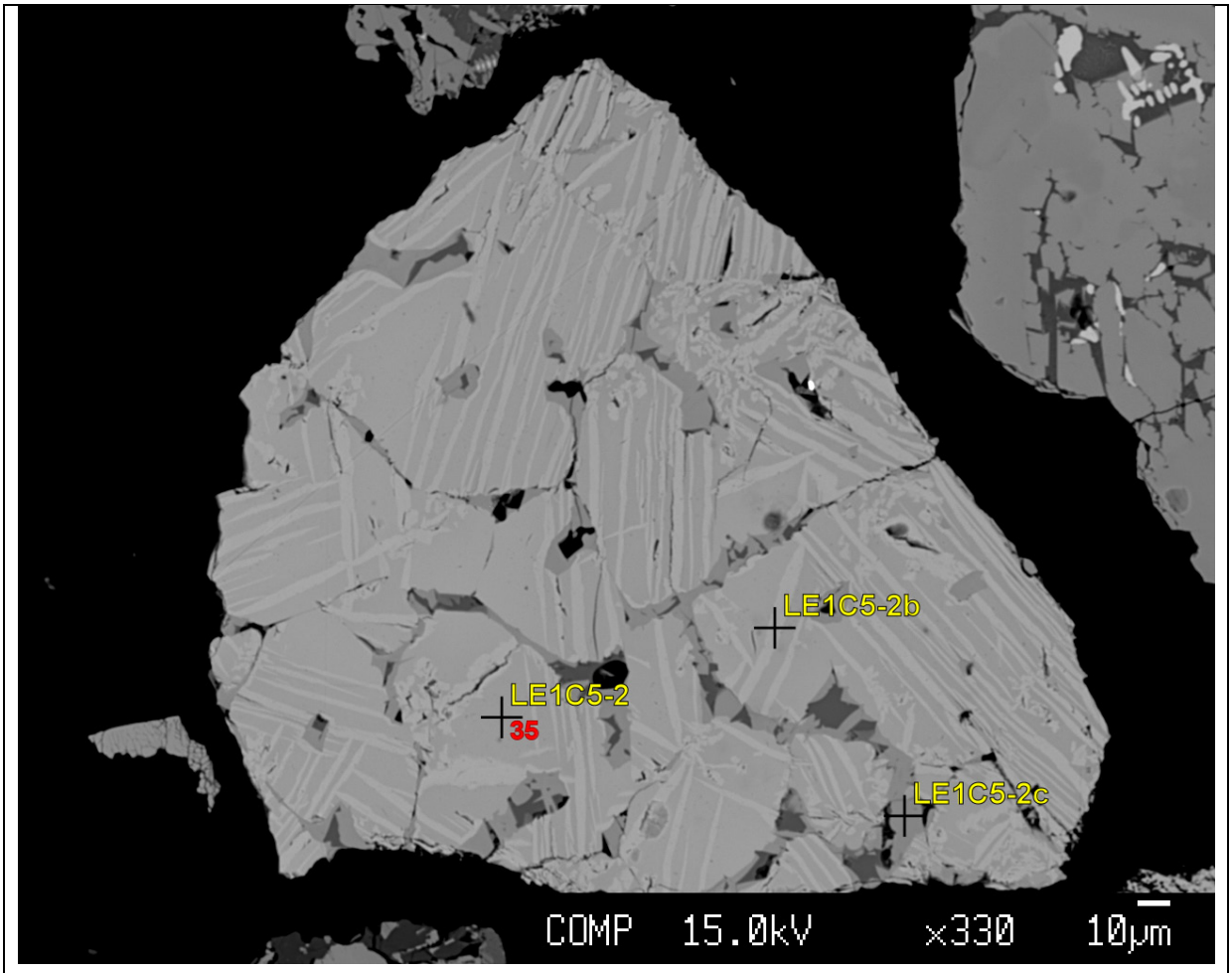

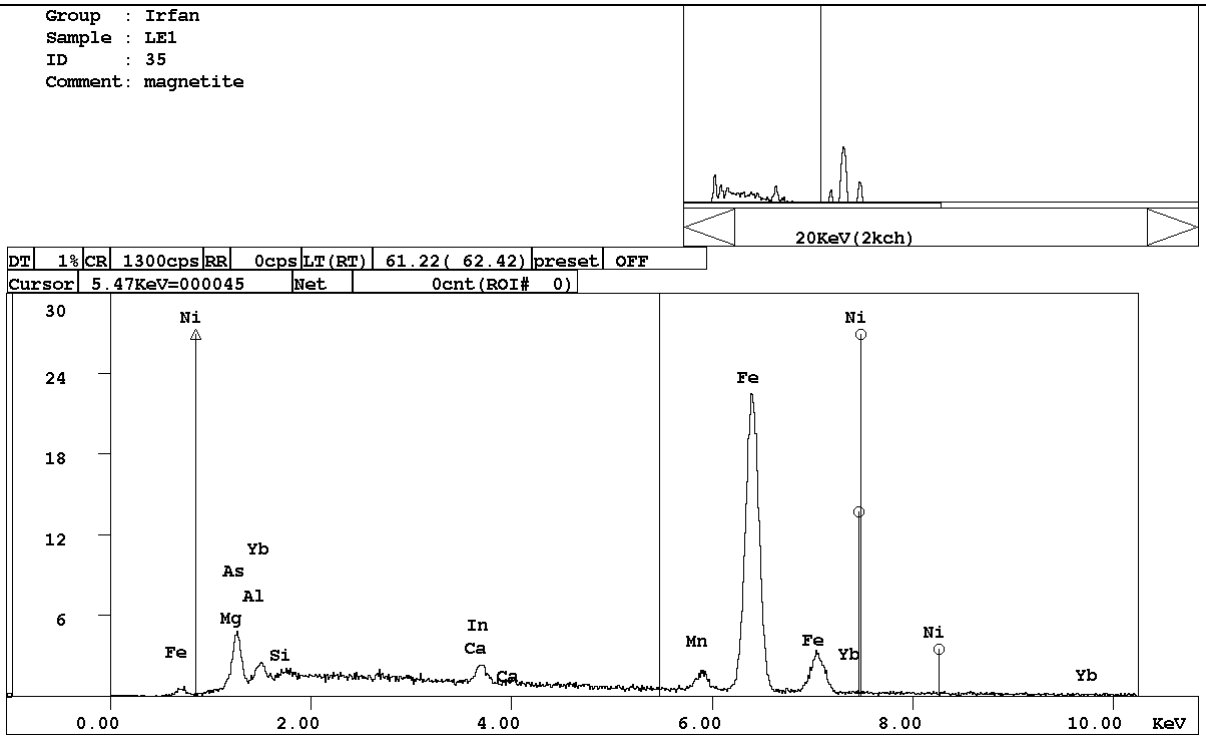

Magnetite (LE1C5-2)

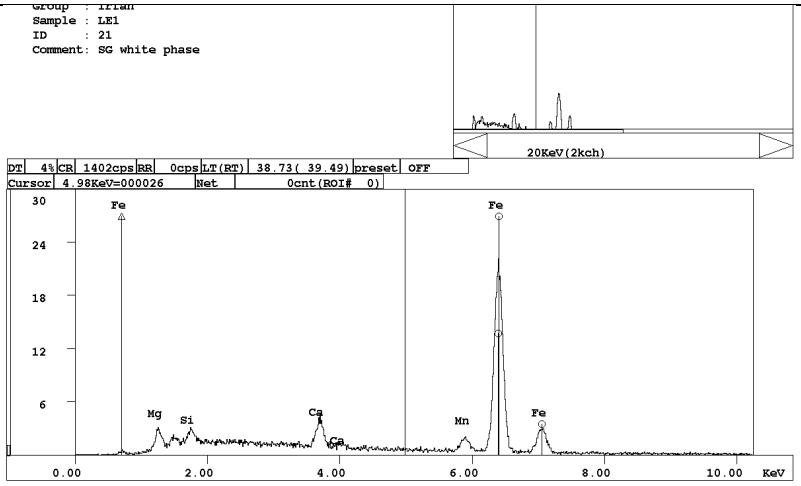

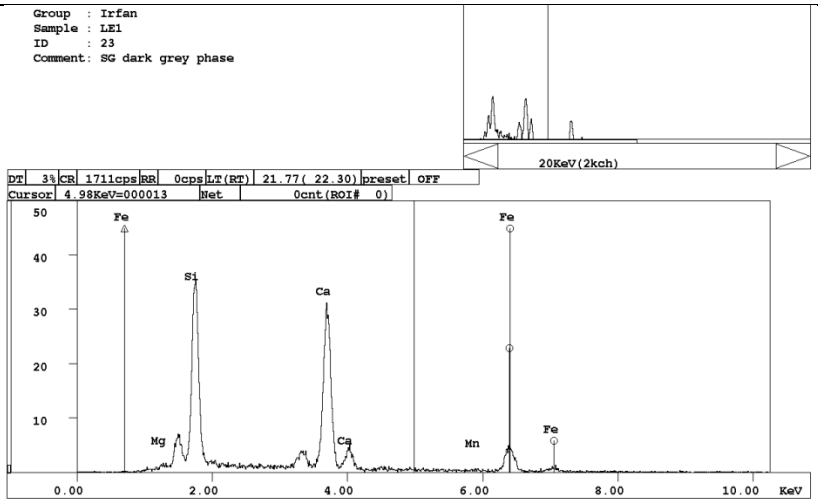

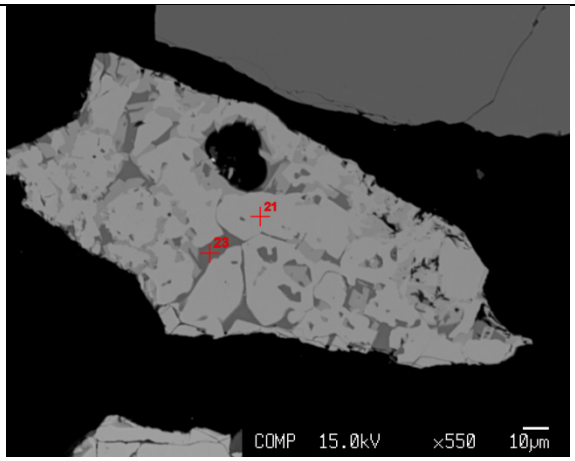

Sinter having different phases, dark with more Ca and Si but less Fe, white with more Fe and less Ca and Si.

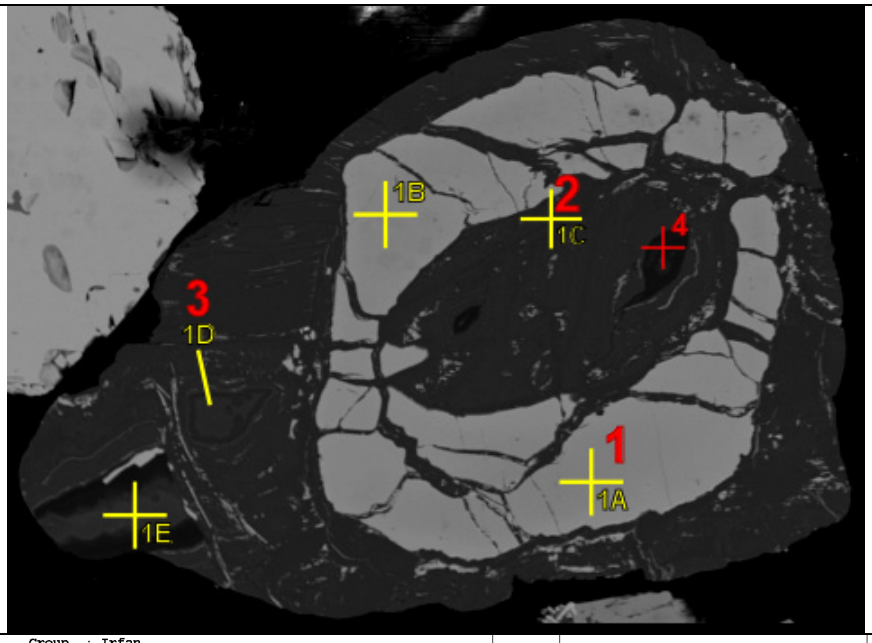

Group : Irfan
Sample : LE1
ID : 1
Comment: Chromite

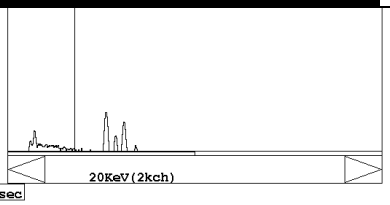

DT 2% CR 1424cps RR 0cps LT(RT) 79.13(80.79) preset 100.00sec
Cursor 3.68KeV=000095 Net 0cnt(ROI# 0)

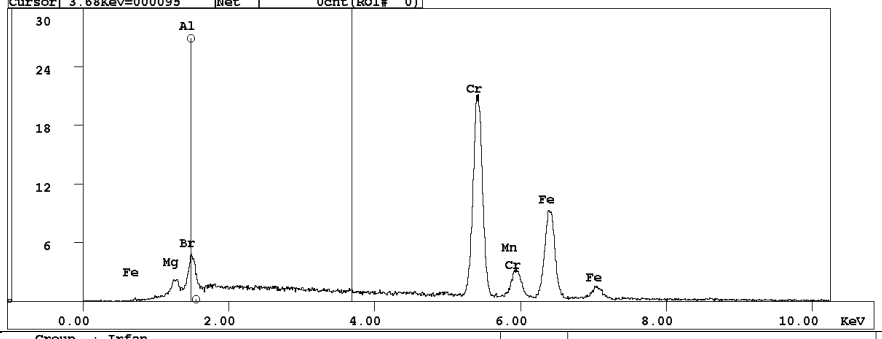

Group : Irfan
Sample : LE1
ID : 2
Comment: Serpentine?

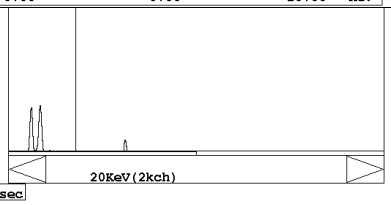

DT 2% CR 1272cps RR 0cps LT(RT) 99.40(101.21) preset 100.00sec
Cursor 3.68KeV=000056 Net 0cnt(ROI# 0)

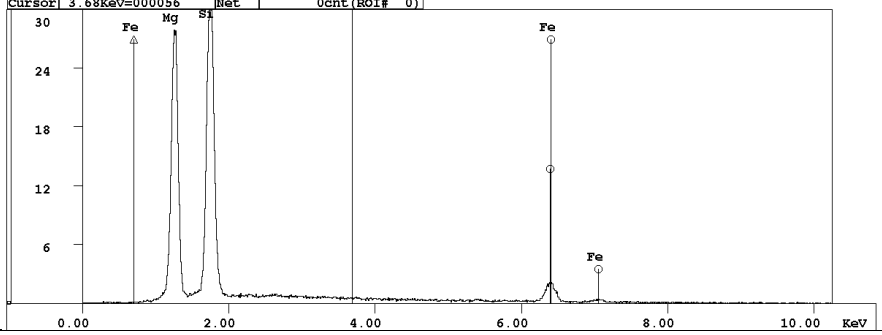

Chromite (LE1C2) in Donawitz/Leoben

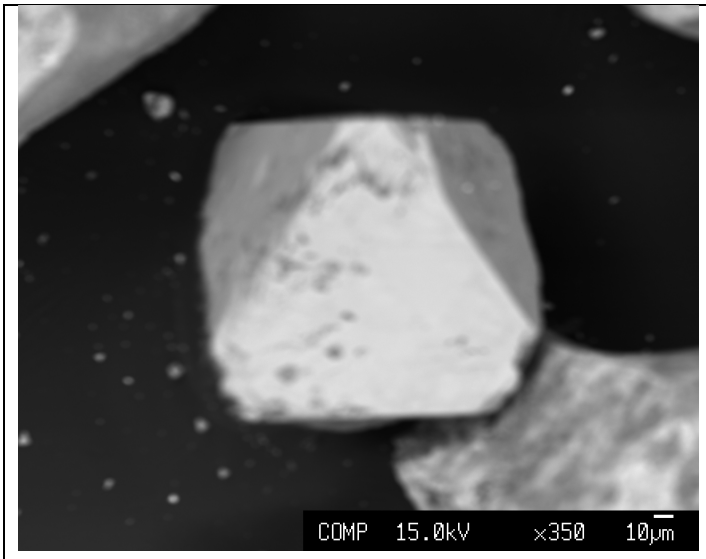	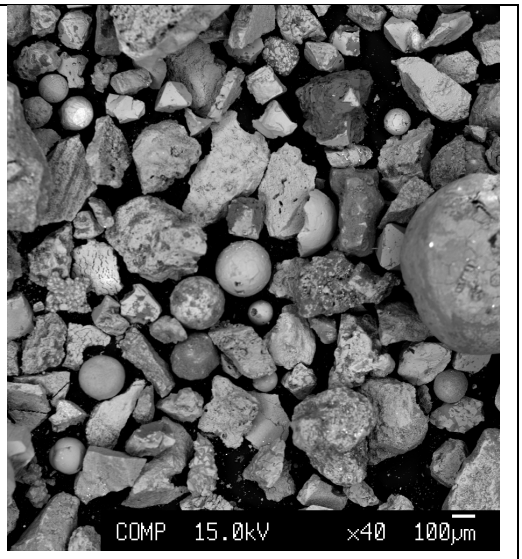
Geogenic magnetite (rarely found in Leoben)	Spherical particles (magnetite) in abundance

3.2.2. Mineralogy of sediments near Gmeingrube (SP1)

Predominant high abundance of metallic iron, magnetite (mostly anthropogenic, due to shape), hematite (mostly geogenic), chromite (type I mostly) as it does not contain zinc, calcium ferrite, (Ca,Al)-Ferrite), wüstit, RO-phases, olivine mixed crystals, glass phase, chlorite, epidote minerals, garnet, siderite, amphibole and titanium minerals is seen in mineralogical study.

Average occurrence of spinel (anthropogenic), chromspinel (mostly conversion products from chromites), maghemite, magnetic gravels (of anthropogenic origin) present in sinter and slag, graphite (anthropogenic and geogenic), pyrite and zoisite is observed.

Occasionally present minerals include pyrolusite, corundum (anthropogenic), Ti-nitride, serpentine, olivine (anthropogenic), chloritoide and pentlandite, which have been identified in mineralogical study.

Note: Relative abundance of different minerals is seen within the same sample

Relative abundance of typical anthropogenic particles in stream sediments (Vordernbergerbach) at Gmeingrube is given in Table 9.

Globular	++++
Scale/tinder	++
Roasting ore	+++
Sinter gut	--
Blast furnace slag	+++++
Steel work slag	++++

Table 9 Relative abundance of typical anthropogenic particles in river sediments at Gmeingrube

Legends

Nil	--
Occasional	+
Less	++
Average	+++
A lot of	++++
Excess	+++++

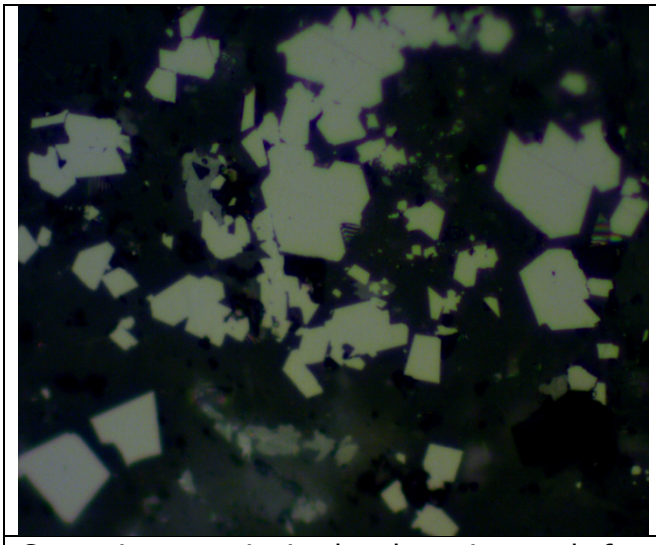

Geogenic magnetite in abundance in sample from Gmeingrube (SP1)

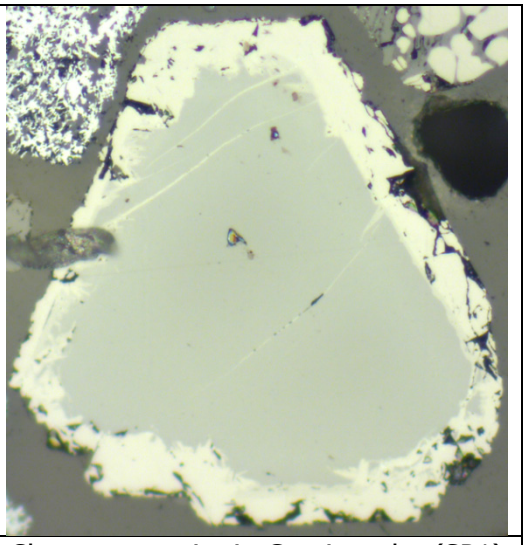

Chrommagnetite in Gmeingrube (SP1)

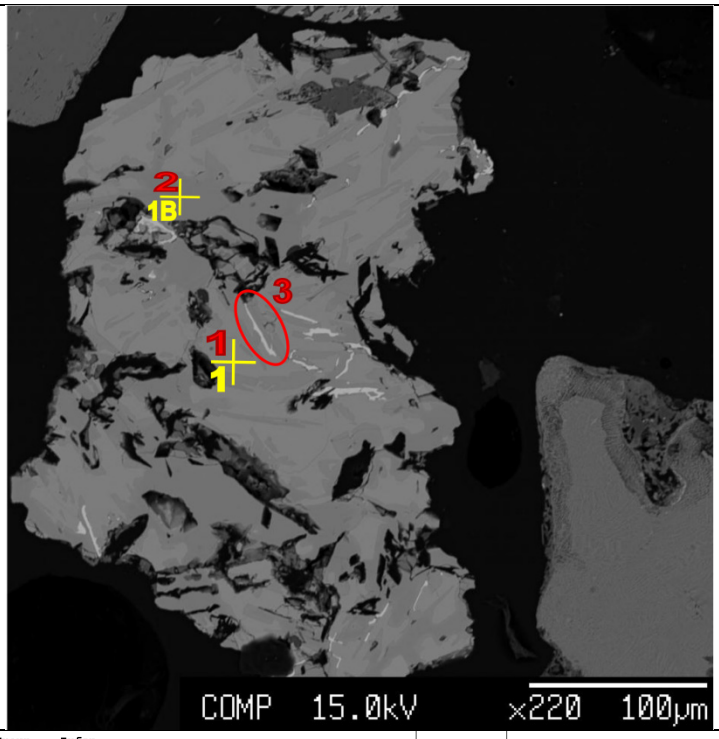

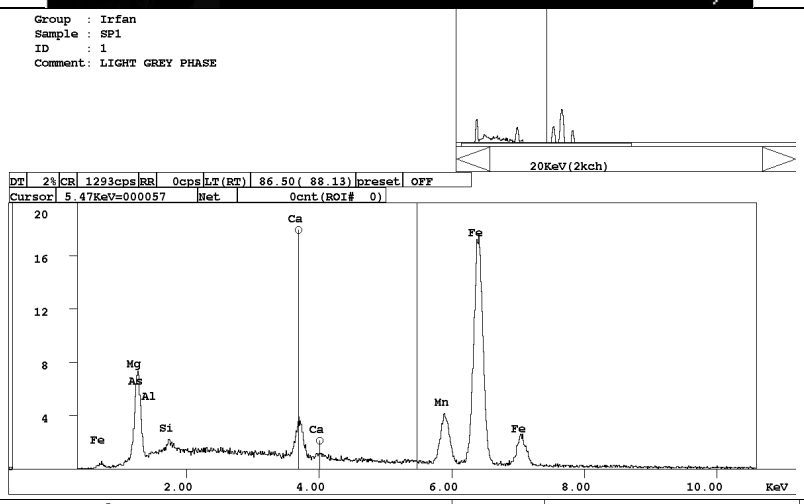

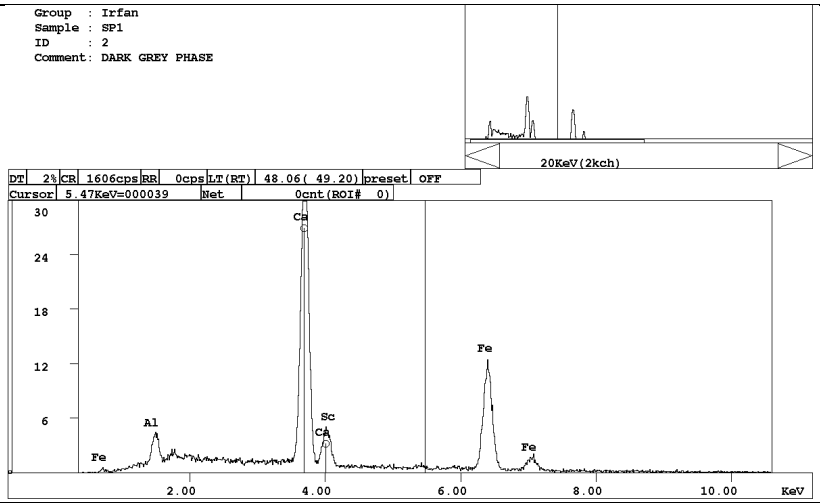

Steel work slag in Gmeingrube (SP1C1)

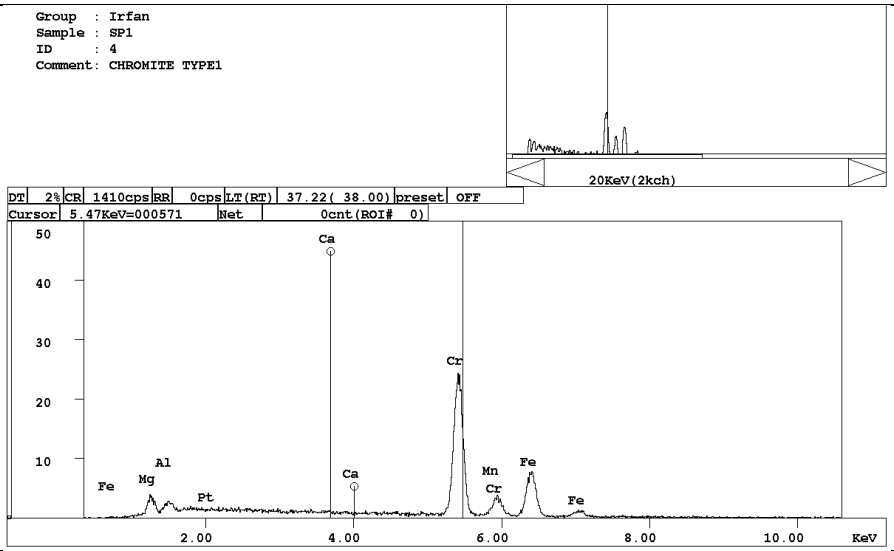

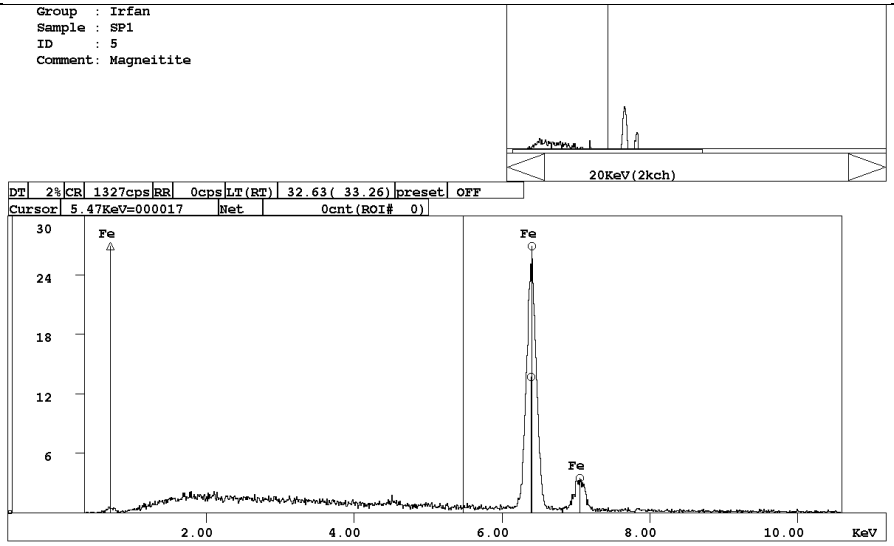

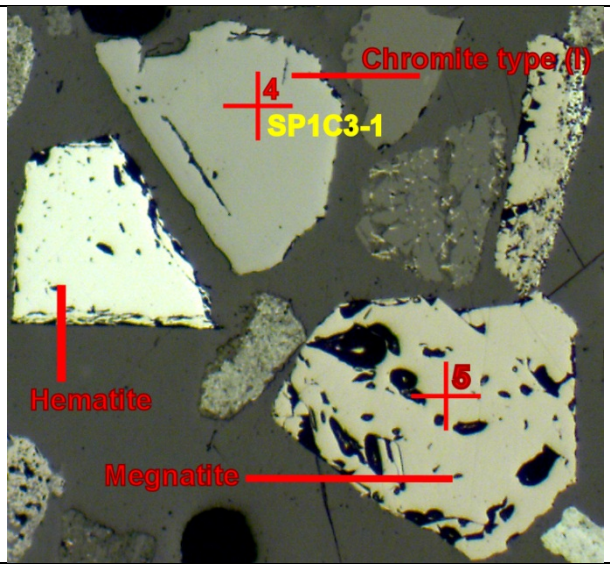

Chromite type (I) in Gmeingrube (SP1) along with hematite and magnetite

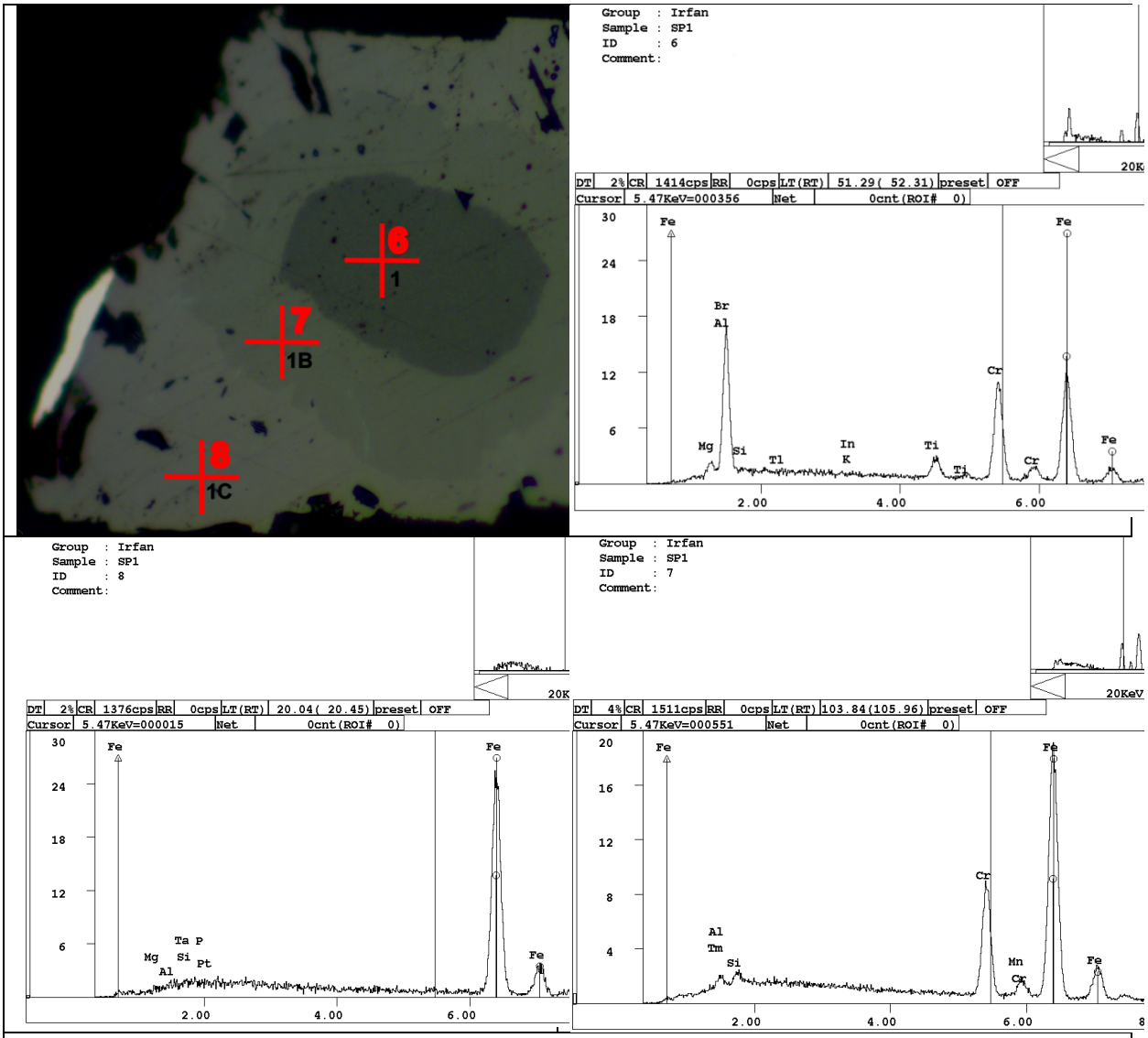

Cr-spinel (1B), chromite type II (1) and chrommagnetite (1C) in Gmeingrube (SP1C2)

3.2.3. Mineralogical study of sediments near Friedauwerk (FW1)

Predominant high occurring metallic iron, magnetite (mostly anthropogenic) in slag, chromite (mostly geogenic), wüstit (geogenic, present in tinder/scale), iron hydroxide, iron carbonates (mostly siderite of geogenic nature), highly Mn rich olivine mixed crystals and pyrite are observed.

Average high abundance of hematite (almost equal amount of anthropogenic and geogenic origin), calcium ferrite, (Ca-Al) ferrite, spinel (anthropogenic mostly but some time geogenic), RO-phases (Ca,Mg,Mn,Fe)-mixoxide±chrom, titanium minerals, graphite, melilite mixed crystals, and an average amount of garnet and glass phases are seen.

Occasional presence of pyrolusite, magnetic gravels, copper gravels, zinc, apatite, maghemite, amphibole, epidote minerals, tourmaline, chlorite, biotite, zircon and metallic tin is seen.

Note: Relative abundance of different minerals is seen within the same sample

Relative abundance of typical anthropogenic particles in stream sediments (Vordernberger-bach) at Friedauwerk is given in Table 10.

Globular	++++
Scale/tinder	++
Roasting ore	++
Sinter gut	--
Blast furnace slag	+++++
Steel work slag	++

Table 10 Relative abundance of typical anthropogenic particles in river sediments at Friedauwerk

Legends

Nil	--
Occasional	+
Less	++
Average	+++
A lot of	++++
Excess	+++++

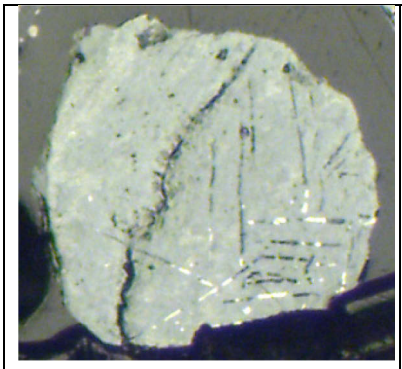	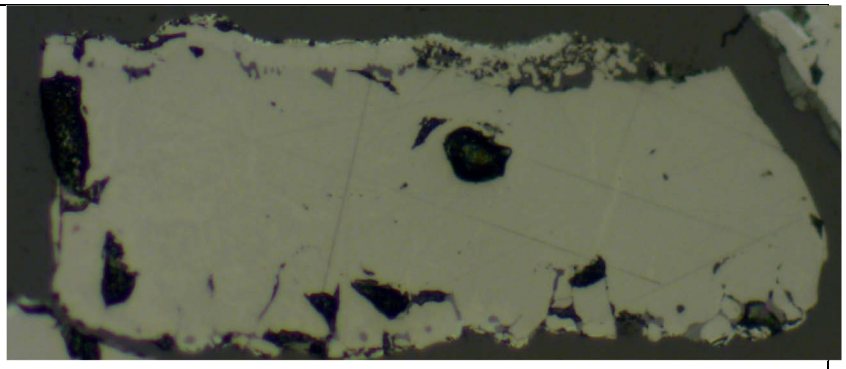
$Fe(OH)_2$	Tinder in sediments at Friedauwerk (FW1C2)
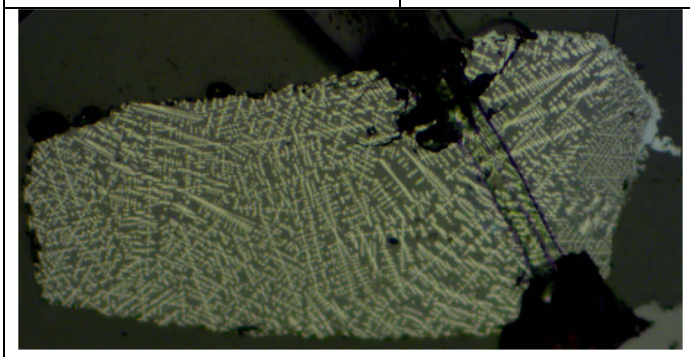	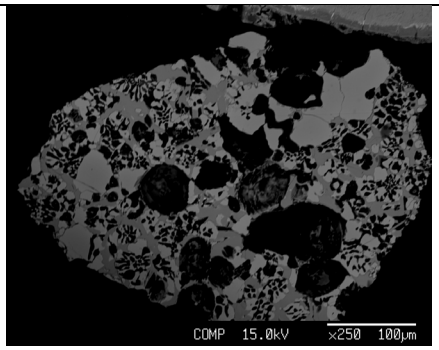
Blast furnace slag with dendrites of magnetite in sediments at Friedauwerk (FW1C2)	Steel work slag in sediments at Friedauwerk (FW1C2)

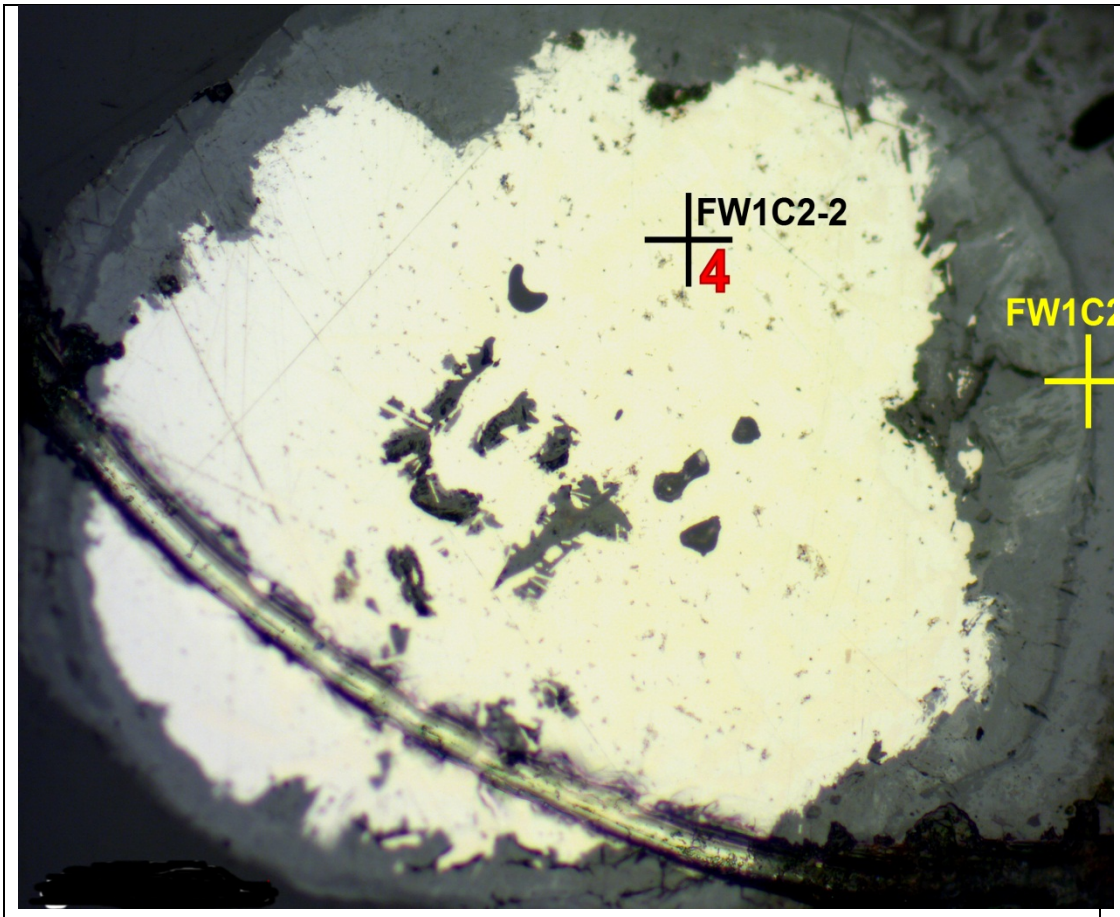

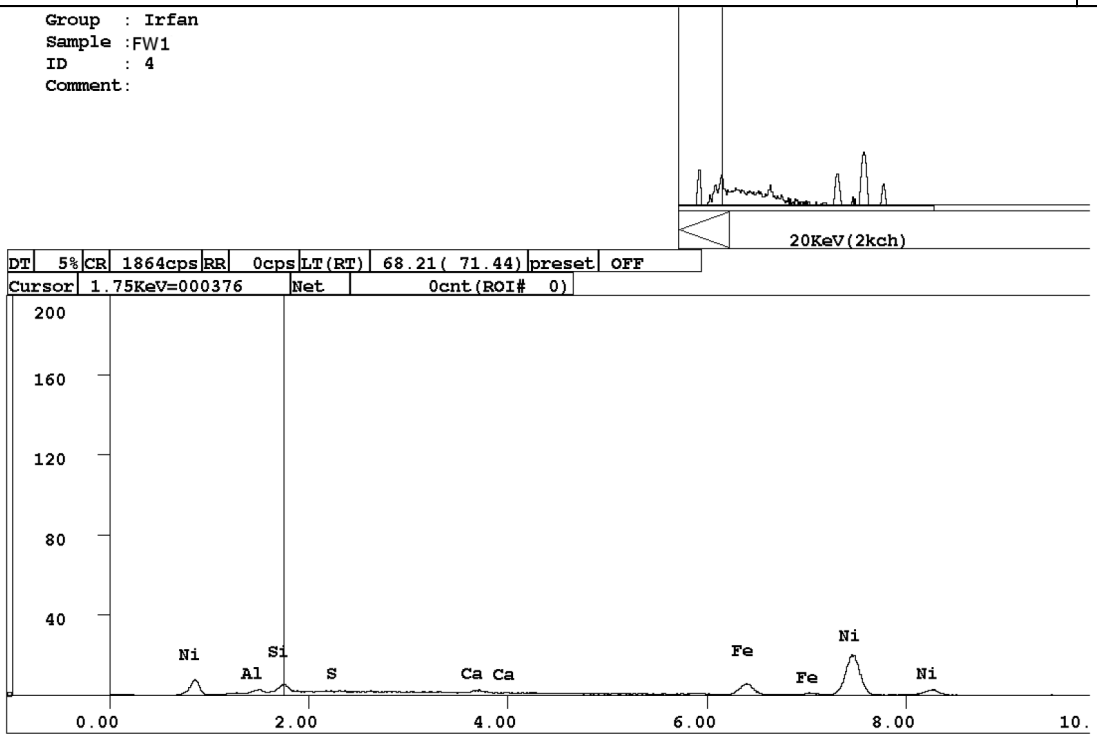

Iron hydroxide contains nickel shown in EDS at marked point (4)

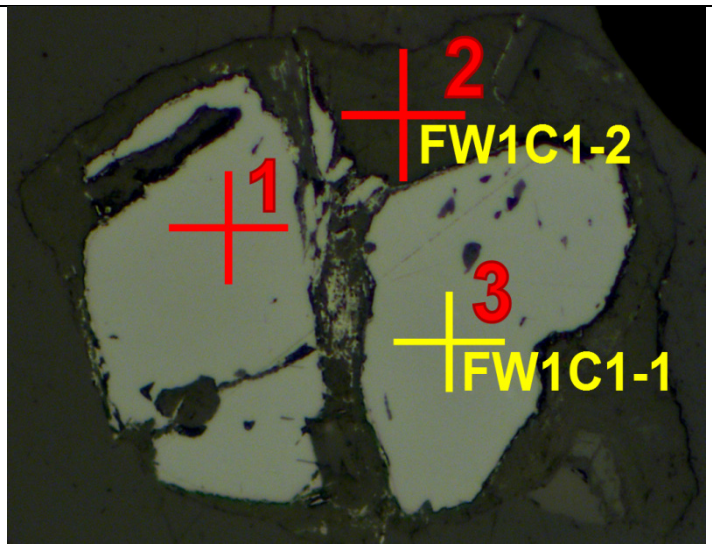

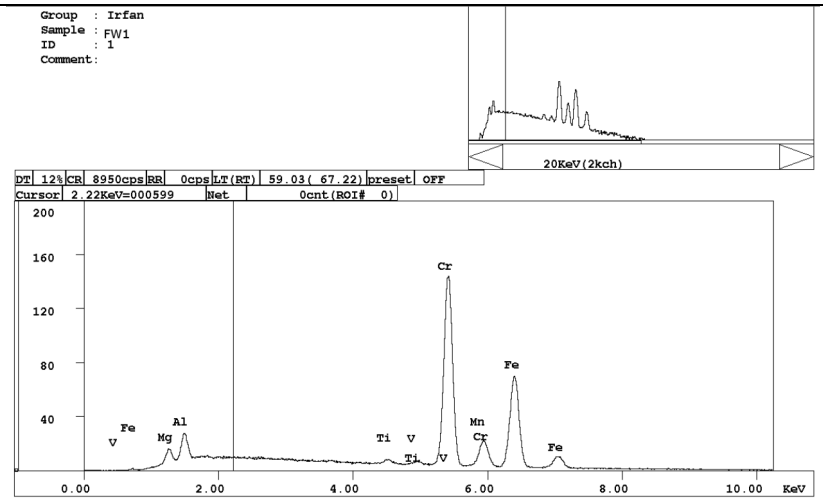

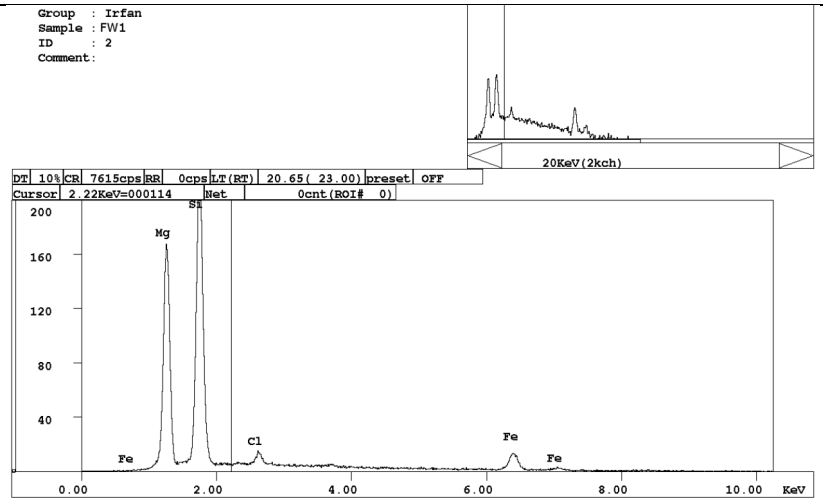

Chromite type (I) shown at marked points (1 and 3) with serpentine at marked point (2)

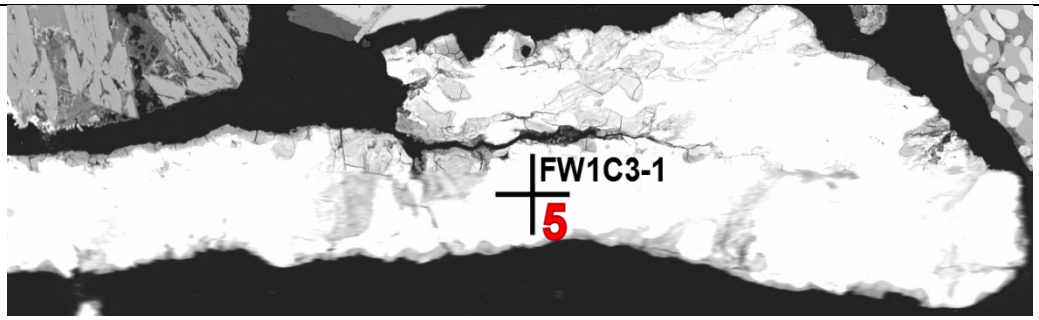

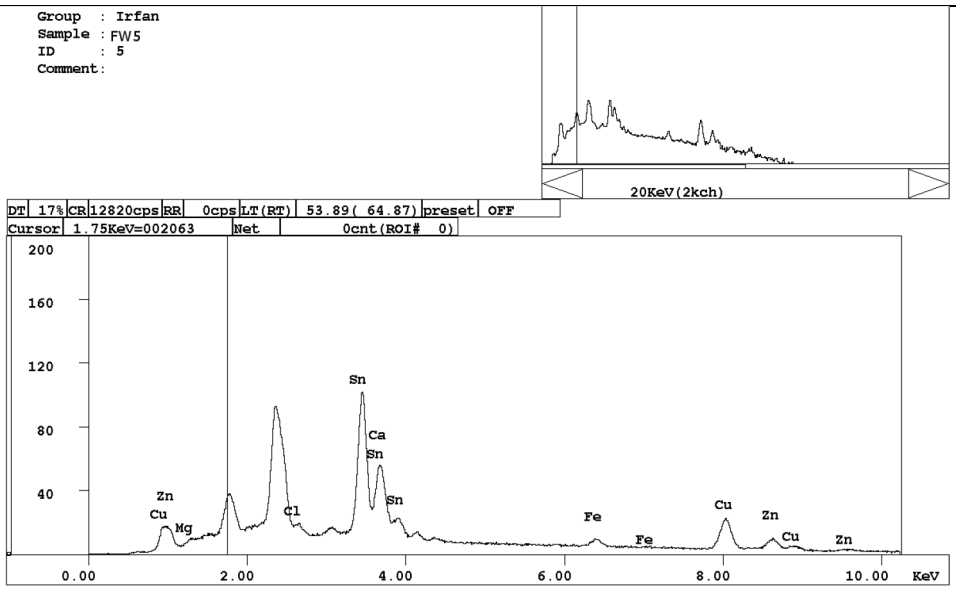

Sn-Zn bronze of anthropogenic origin in sediments at Friedauwerk

No.	Mg	P	Ni	Cr	Al	Pb	Zn	Fe	Si	Ti	Mn	V	Total	Comment	Identification of particles
1	0.037	0.163	0.024	0.608	0.000	0.037	0.015	93.132	12.176	0.019	0.204	0.167	106.582	LE1C1-2	Ferrosilicon
2	3.523	0.000	0.000	0.205	0.771	0.045	0.000	39.696	0.003	0.123	11.820	0.010	56.196	LE1C1-1	Chromite
3	0.011	0.053	0.000	0.000	0.524	0.036	0.000	33.475	1.989	0.118	1.374	0.000	37.580	LE1C1-3	Iron
4	1.748	0.000	0.000	35.446	2.370	0.007	0.587	28.281	0.000	0.183	0.439	0.301	69.362	LE1C2-1a	Chromite (type II)
5	1.583	0.006	0.024	35.318	1.733	0.100	0.573	29.107	0.047	0.155	0.438	0.287	69.371	LE1C2-1b	Chromite
6	19.470	0.000	0.166	0.246	0.009	0.000	0.000	6.279	18.334	0.000	0.097	0.000	44.601	LE1C2-1c	Chromite
7	18.965	0.000	0.000	0.023	0.000	0.000	0.084	8.667	18.413	0.029	0.034	0.009	46.224	LE1C2-1d	Chromite
8	21.741	0.008	0.004	0.000	0.000	0.005	0.000	3.015	0.003	0.000	0.475	0.000	25.251	LE1C2-1e	Chromite
9	0.000	0.000	0.008	0.000	0.035	0.013	0.000	74.342	0.026	0.006	0.022	0.060	74.512	LE1C2-2	Magnetite
10	2.684	0.000	0.000	33.382	4.763	0.050	0.537	25.760	0.004	0.175	0.315	0.277	67.947	LE1C3-2	Chromite
11	19.271	0.062	0.052	0.084	0.097	0.001	0.014	7.484	17.592	0.029	0.103	0.000	44.789	LE1C3-2b	Chromite (Mg.Si phase)
12	3.305	0.010	0.000	0.192	0.000	0.016	0.000	32.650	0.101	0.035	33.890	0.045	70.244	LE1C3-1	Ca-Mn-Fe-Mg phase (steel slag)
13	0.228	0.090	0.000	0.277	3.676	0.103	0.049	25.633	1.046	3.151	1.806	0.172	36.231	LE1C3-1b	Ca-Al-Fe-phase (steel slag)
14	0.235	0.111	0.008	0.231	3.255	0.000	0.000	29.348	0.798	2.422	0.551	0.130	37.089	LE1C4-1	Steel work slag
15	9.399	0.005	0.000	0.415	0.000	0.000	0.077	59.713	0.013	0.014	7.535	0.054	77.225	LE1C4-1b	Steel work slag
16	0.035	0.000	0.006	0.000	0.000	0.000	0.067	74.265	0.014	0.000	0.035	0.087	74.509	LE1C4-2	Magnetite
17	0.000	0.000	0.000	0.000	0.056	0.032	0.114	71.279	0.000	0.008	0.084	0.002	71.575	LE1C4-3	Hematite
18	3.332	0.008	0.000	0.000	0.027	0.000	0.088	35.023	14.072	0.020	7.917	0.025	60.512	LE1C4-4	Blast furnace slag
19	0.212	0.199	0.000	0.000	6.345	0.000	0.000	16.223	18.757	0.635	1.903	0.028	44.302	LE1C4-4b	Blast furnace slag
20	2.806	0.017	0.000	0.000	0.511	0.133	0.090	63.620	0.067	0.030	3.198	0.020	70.492	LE1C4-5	Sinter
21	0.935	0.321	0.000	0.000	2.159	0.000	0.021	37.630	9.167	0.134	0.961	0.000	51.328	LE1C4-5b	Sinter
22	3.739	0.000	0.144	22.469	8.294	0.003	0.367	29.033	0.000	2.019	0.498	0.220	66.786	LE1C6_1b	Chromite/Chrommagnetite
23	0.000	0.000	0.045	0.465	0.012	0.008	0.000	73.738	0.037	0.000	0.029	0.062	74.396	LE1C6_1a	Chromite/Chrommagnetite
24	0.013	0.025	0.017	18.657	0.409	0.013	3.368	49.626	0.035	0.065	0.670	0.082	72.980	LE1C6_1d	Chromite/Chrommagnetite
25	0.008	0.000	0.028	0.535	0.011	0.089	0.092	73.542	0.000	0.000	0.035	0.075	74.415	LE1C6_1e	Chromite/Chrommagnetite
26	2.848	0.007	0.126	22.406	8.206	0.004	0.337	30.805	0.028	2.049	0.546	0.184	67.546	LE1C6_1c	Chromite/Chrommagnetite
27	0.000	0.018	0.020	0.000	0.000	0.092	0.018	77.309	0.000	0.014	0.914	0.004	78.389	LE1C6_2	Scale/Tinder
28	0.016	0.008	0.000	0.003	0.018	0.055	0.021	73.034	0.000	0.000	0.803	0.014	73.972	LE1C6_2b	Scale/Tinder

No.	Mg	P	Ni	Cr	Al	Pb	Zn	Fe	Si	Ti	Mn	V	Total	Comment	Identification of particles
29	4.307	0.000	0.008	0.001	0.041	0.018	0.007	36.559	14.787	0.014	9.193	0.016	64.951	LE1C6_3	Blast furnace slag
30	0.110	0.367	0.009	0.000	0.137	0.074	0.003	62.431	0.905	0.003	0.184	0.000	64.223	LE1C6_4	Fe (OH)2
31	0.152	0.338	0.000	0.000	0.010	0.036	0.081	60.653	0.913	0.000	0.457	0.014	62.654	LE1C6_4b	Fe (OH)2
32	0.000	0.000	0.032	0.005	0.091	0.159	0.037	71.132	0.000	0.020	0.011	0.000	71.487	LE1C6_5	Hematite
33	1.126	0.063	0.000	0.000	0.029	0.063	0.000	30.642	14.474	0.048	10.642	0.000	57.087	LE1C5_1	Blast furnace slag
34	4.366	0.000	0.020	31.867	6.412	0.003	0.141	20.066	0.209	0.872	0.189	0.642	64.787	chromite std	Chromite Standard
35	4.820	0.012	0.002	0.000	0.917	0.023	0.000	62.186	0.036	0.041	2.808	0.000	70.845	LE1C5_2	Magnetite
36	0.684	0.011	0.000	0.003	0.630	0.026	0.000	68.330	0.005	0.014	0.766	0.032	70.501	LE1C5_2b	Magnetite
37	1.604	0.000	0.000	0.008	2.780	0.042	0.000	45.940	5.016	0.132	0.987	0.000	56.509	LE1C5_2c	Magnetite
38	3.701	0.002	0.163	22.927	8.326	0.050	0.172	28.720	0.016	1.986	0.431	0.214	66.708	LE1C6_1 CHROMITE	Chromite
39	2.215	0.009	0.024	7.016	2.641	0.023	0.697	24.702	0.064	0.169	0.419	0.001	37.980	LE1C2-1a	Chromite
40	2.129	0.001	0.031	7.419	2.039	0.018	0.669	25.661	0.012	0.142	0.426	0.000	38.547	LE1C2-1a	Chromite
41	7.404	0.000	0.000	0.005	0.000	0.043	0.041	8.803	17.685	0.000	0.047	0.008	34.036	LE1C2-1d	Chromite
42	26.522	0.000	0.325	0.000	0.000	0.040	0.061	5.828	19.526	0.005	0.086	0.009	52.402	olivin std 34	Olivine Standard
43	0.039	0.019	0.023	0.009	0.081	0.124	0.000	73.951	0.085	0.031	0.037	0.101	74.500	LE1c2_2	Magnetite
44	6.550	0.013	0.000	0.015	10.295	0.106	0.003	17.678	18.564	0.035	0.341	0.000	53.600	Grt Std	Garnet Standard
45	4.498	0.000	0.040	32.123	6.751	0.005	0.103	20.254	0.165	0.842	0.207	0.648	65.636	chromite std	Chromite Standard
46	0.028	0.004	0.000	0.038	0.026	0.060	0.040	71.571	0.207	0.065	0.004	0.075	72.118	mgt std	Magnetite Standard
47	0.059	0.000	0.000	0.053	0.024	0.053	0.000	71.903	0.027	0.033	0.000	0.095	72.247	mgt std	Magnetite
48	0.023	0.008	0.000	0.000	0.027	0.000	0.071	73.521	0.031	0.036	0.014	0.071	73.802	LE1c2_2	Magnetite
49	2.132	0.067	0.003	0.009	0.254	0.000	0.050	8.556	0.761	0.037	0.443	0.000	12.312	LE1C1-4	Rim outside iron
50	9.208	0.008	0.000	0.174	0.002	0.046	0.112	56.719	0.000	0.010	9.827	0.000	76.106	SP1C1-1	Light grey phase in steel work slag
51	0.089	0.043	0.000	0.565	2.274	0.040	0.004	34.318	0.307	0.096	0.366	0.125	38.227	SP1C1-1B	Dark grey phase in steel work slag
52	3.256	0.000	0.043	40.577	1.049	0.022	0.288	23.060	0.000	0.217	0.340	0.151	69.003	SP1C3-1	Chromite type I
53	0.001	0.000	0.007	0.002	0.003	0.100	0.005	0.007	0.073	0.001	0.004	0.005	0.208	SP1C2-1	Chromite type II
54	0.000	0.000	0.004	0.000	0.002	0.033	0.008	0.012	0.058	0.005	0.002	0.007	0.131	SP1C2-1b	Chromite type II

No.	Mg	P	Ni	Cr	Al	Pb	Zn	Fe	Si	Ti	Mn	V	Total	Comment	Identification of particles
55	0.002	0.000	0.007	0.000	0.001	0.036	0.009	0.011	0.055	0.005	0.000	0.005	0.131	SP1C2-1c	Chromite type II
56	2.100	0.000	0.118	32.740	3.007	0.014	0.399	29.463	0.000	0.536	0.369	0.297	69.043	FW1C1-1	Chromite
57	19.078	0.045	0.127	0.057	0.070	0.074	0.041	6.965	18.264	0.000	0.044	0.000	44.765	FW1C1-2	Serpentine
58	0.230	0.028	0.012	0.073	6.976	0.000	0.000	24.646	0.537	1.216	1.076	0.150	34.944	FW1C2-1	Blast furnace slag
59	7.355	0.000	0.000	0.869	0.001	0.075	0.090	28.697	0.001	0.000	19.016	0.000	56.104	FW1C2-1B	Blast furnace slag
60	0.013	0.000	0.002	0.001	0.000	0.049	0.034	57.509	2.592	0.018	0.068	0.007	60.293	FW1C2-2	$Fe(OH)_2$
61	0.006	0.000	0.000	0.003	0.004	0.045	0.000	110.024	0.000	0.015	0.000	0.001	110.098	FW1C2-2B	$Fe(OH)_2$
62	3.871	0.001	0.125	22.666	8.296	0.034	0.224	28.861	0.048	2.013	0.500	0.201	66.840	LE1C6_1 CHROMITE INNER CORE	Chromite

Table 11 Quantitative analysis of heavy minerals with EMPA (raw data) all data in g/100g

	Mg.Std 46	mgt std	mgt std	LE1C2-2	LE1C4-5	LE1C6-1a	LE1C6-1e	LE1C6-2b	LE1C5-2	LE1c2-2
oxide	g/100g	g/100g	g/100g	g/100g	g/100g	g/100g	g/100g	g/100g	g/100g	g/100g
SiO_2	-	0.443	0.058	0.056	0.021	0.079	-	0.079	0.143	-
TiO_2	0.110	0.108	0.055	0.010	0.015	-	-	-	0.050	-
Al_2O_3	0.050	0.049	0.045	0.066	0.089	0.023	0.021	0.023	0.966	0.034
Cr_2O_3	0.060	0.056	0.077	-	0.013	0.680	0.782	0.680	-	0.004
Fe_2O_3	68.102	67.310	68.438	70.735	67.842	69.922	69.864	69.922	69.060	70.407
FeO	30.801	31.510	30.922	31.993	30.576	31.947	31.747	31.947	19.706	30.605
MnO	0.010	0.005	-	0.028	0.034	0.037	0.045	0.037	4.129	1.037
MgO	0.050	0.046	0.098	-	0.033	-	0.013	-	4.653	0.027
total weight	**99.183**	**99.527**	**99.693**	**102.888**	**98.624**	**102.688**	**102.472**	**102.688**	**98.707**	**102.114**
cations	atoms	atoms	atoms	atoms	atoms	atoms	atoms	atoms	atoms	atoms
Si	-	0.017	0.002	0.002	0.001	0.003	-	0.003	0.005	-
Ti	0.003	0.003	0.002	0.000	0.000	-	-	-	0.001	-
Al	0.002	0.002	0.002	0.003	0.004	0.001	0.001	0.001	0.043	0.002
Cr	0.002	0.002	0.002	-	0.000	0.020	0.023	0.020	-	0.000
Fe^{3+}	1.989	1.956	1.988	1.992	1.993	1.973	1.976	1.973	1.944	1.998
Fe^{2+}	1.000	1.017	0.998	1.001	0.998	1.002	0.998	1.002	0.616	0.965
Mn	0.000	0.000	-	0.001	0.001	0.001	0.001	0.001	0.131	0.033
Mg	0.003	0.003	0.006	-	0.002	-	0.001	-	0.259	0.001
Total cations	3.000	3.000	3.000	3.000	3.000	3.000	3.000	3.000	3.000	3.000
Total no. of oxygen	**4.000**	**4.000**	**4.000**	**4.000**	**4.000**	**4.000**	**4.000**	**4.000**	**4.000**	**4.000**

Table 12 Composition of magnetite in sediments determined by quantitative analysis on EMPA

	Standard used			Chromites found in Leoben area (LE1)								Gmeingrube	Friedauwerk
				LE1C2		**LE1C3**	**LE1C6**					**SP1C3**	**FW1C1**
Oxides/elements	**Chromite std 53-IN-8**			**LE1C2-1a**	**LE1C2-1b**	**LE1C3-2**	**LE1C6-1b**	**LE1C6-1d**	**LE1C6-1c**	**LE1C6_1** (chromite)	**LE1C6-1** (CHROMITE INNER CORE)	**SP1C3-1**	**FW1C1-1**
Cr_2O_3	49.31	46.58	46.95	51.81	51.62	48.79	32.84	27.27	32.75	33.51	33.13	59.31	47.85
Al_2O_3	12.83	12.12	12.76	4.48	3.27	9.00	15.67	0.77	15.51	15.73	15.68	1.98	5.68
TiO_2	1.60	1.45	1.40	0.31	0.26	0.29	3.37	0.11	3.42	3.31	3.36	0.36	0.89
FeO	25.48	22.11	22.26	27.56	27.62	25.78	26.80	34.55	29.23	26.92	26.56	23.51	27.48
Fe_2O_3	2.95	4.11	4.22	9.81	10.92	8.18	11.73	32.55	11.56	11.15	11.75	6.85	11.59
MgO	6.12	7.24	7.46	2.90	2.63	4.45	6.20	0.02	4.72	6.14	6.42	5.40	3.48
MnO	0.14	0.06	0.08	0.36	0.36	0.21	0.51	0.76	0.57	0.42	0.51	0.20	0.29
NiO	0.08	0.03	0.05	-	0.03	-	0.18	0.02	0.16	0.21	0.16	0.05	0.15
Total	**98.51**	**93.70**	**95.18**	**97.21**	**96.71**	**96.70**	**97.30**	**96.05**	**97.92**	**97.39**	**97.56**	**97.66**	**97.41**
Formula units based on 32 oxygens and Fe^{2+}/Fe^{3+} assuming full site occupancy (Concentrations are given in mass percent unit)													
Cr	10.61	10.44	10.33	12.06	12.18	11.03	7.08	6.75	7.10	7.22	7.11	13.63	11.01
Al	4.12	4.05	4.19	1.55	1.15	3.03	5.04	0.29	5.01	5.05	5.02	0.68	1.95
Ti	0.33	0.31	0.29	0.07	0.06	0.06	0.69	0.03	0.70	0.68	0.69	0.08	0.20
Fe^{3+}	0.61	0.88	0.88	2.17	2.45	1.76	2.41	7.67	2.38	2.29	2.40	1.50	2.54
Fe^{2+}	5.81	5.26	5.19	6.86	6.99	6.22	6.20	10.12	6.79	6.22	6.13	5.75	6.79
Mg	2.48	3.06	3.09	1.27	1.17	1.90	2.52	0.01	1.93	2.49	2.60	2.34	1.51
Mn	0.03	0.01	0.02	0.09	0.09	0.05	0.12	0.20	0.13	0.10	0.12	0.05	0.07
Ni	0.02	0.01	0.01	-	0.01	-	0.04	0.01	0.04	0.05	0.03	0.01	0.04
Total	**24.01**	**24.01**	**24.01**	**24.08**	**24.10**	**24.05**	**24.09**	**25.07**	**24.09**	**24.08**	**24.09**	**24.04**	**24.10**
$100Mg/Mg^{+}Fe^{2+}$	25.02	32.88	32.98	15.11	14.34	20.51	22.41	0.10	16.34	22.11	23.31	36.38	17.28
$100Cr/Cr^{+}Al$	72.05	72.05	71.17	88.58	91.36	78.43	58.42	95.95	58.61	58.82	58.63	95.25	84.96
$100Fe^{3+}/Cr^{+}Al^{+}Fe^{3+}$	3.94	5.71	5.73	13.77	15.53	11.12	16.57	52.16	16.45	15.70	16.52	9.47	16.38

Table 13 Quantitative analysis of chromite minerals with EPMA all data in g/100g

Minerals	**LE**	**SP**	**FW**
Metalic iron	++++	++++	++++
Magnetite	++++	++++	++++
Hematite	++++	++++	++++
Chromite	++++ type I, II	++++ type I	++++
Calciumferrite	++++	++++	++
(Ca,Al)-ferrite	++++	++++	+++
Wustite	++++	++++	++++
Iron hydroxide	++++		++++
Titanium mineral (ilmenite, rutile, titanium)	++++	++++	+++
Olivine		+	
Olivinmixed crystal	++++	++++	++++
Calciumsilicate	++++		
Epidotminerals	++++	++++	
Pyrite	++++	+++	++++
Glass phases	++++	++++	+++
Ferrosilicon	+++		
Magnesioferrite	++++	--	--
RO-phases (Mn,Ca,Fe,Mg-mixoxides)	+++	+++	+++
Carbonates	+++		++++
Siderite	+++	++++	
Ankerite	+++	++++	++
Garnate	+++		+++
Chlorite	+++	++++	+
Amphibole	+++	++++	
Maghemite	+++	+++	
Chromspinel	+++	+++	
Apatite	+++		
Titanium	+		
Ti-Nitride	+	+	
Graphite	+	+++	+
Melilithmix crystal	+	--	+++
Corrundum	+	+	
Magnetic gravels	+	++	+
Spinel	+	+++	+++
Serpentine	+	+	
Diopsid	+		
Periklas	+		
Zircon	+	--	+
Zoisite		+++	
Pyrolusite		+	+
Chlorotoid		+	
Pentlandite		+	
Copper gravels			+

Minerals	LE	SP	FW
Metallic zinc			+
Tourmaline			+
Biotite			+
Tin	+		+

Table 14 Relative abundance of different minerals within each sample and their antropogenic or geogenic nature (predominantly abundant ++++) (Moderately high/average +++) (occasional +) (anthropogenic shown in red color) (geogenic shown in black)

3.3. Observations

- Results obtained from mineralogical study show that the sources of heavy metals in studied areas are not only anthropogenic but geogenic as well. Ca-ferrite, Ca-Al ferrite, ferrosilicon, magnetite, hematite, iron hydroxide, steel mill slag and iron work slag/blast furnace slag are the anthropogenic mineral or particles which carry the heavy metals as shown in Table 11-Table 14. Chromite, olivine, serpentine and rutile are the geogenic minerals which also carry heavy metals, as mentioned in Table 11-Table 14.
- High magnetic signals and concentration of heavy metals at the location Donawitz/Leoben obtained in geophysical and geochemical data, is related with the abundance of heavy minerals i.e., the carrier of heavy metals. Similarly the concentrations of the elements at location Friedauwerk (TF1 for geochemical data) and Gmeingrube (SP1 for geochemical data) correspond well to the abundance of heavy metal carrier minerals. Table 14 should not mislead to the comparison of minerals abundance with respect to sampling location, as these relative abundances of different minerals within same samples were mentioned, but the relative abundances with respect to different locations, i.e., 33% heavy minerals (size 0.71/0.1mm, density>2.9 g/cm^3) of total heavy minerals material (size 0.71/0.1mm) at Donawitz, 13% at Gmeingrube and 41% at Friedauwerk was obtained (see Table 7). Moreover, the amount of sediments used in panning was also different e.g. for Gmeingrube ~8 kg and for Donawitz/Leoben ~4 kg while for Friedauwerk it was not recorded.
- The nature of similar kind of minerals at two locations Friedauwerk and Gmeingrube but addition of new anthropogenic minerals e.g. apatite, magnesioferrite and ferrosilicon is responsible for the different trend of magnetic signals vs. heavy metals than that of other areas e.g. Trofaiach and St. Peter Freienstein. Anthropogenic apatite and Ca-P-silicate contain heavy metals like V, Cr, Ni, Mn and Fe.
- The relative abundance of anthropogenic particles (within the same sample for each location) like steel work slag and roasting ore (carrier of heavy metals) was found

relatively higher at Donawitz/Leoben than in other regions. The sinter (the carrier of heavy metals) was only found at Donawitz/Leoben. Steel work slag is comparatively higher in Donawitz/Leoben, it contains Ca-ferrite, RO-phases which are (Ca,Mg,Mn,Fe)mixed oxides which are anthropogenic and carry heavy metals. As a consequence concentration level of heavy metals is higher at this site and is of anthropogenic nature mainly.

- Sediments at Gmeingrube contain chromite type I while at Donawitz/Leoben chromite type II (with zinc).
- Hematites at Gmeingrube are mostly geogenic but at Donawitz/Leoben and Friedauwerk the abundance of anthropogenic hematites is more than geogenic ones.
- Quality of the measurements on EMPA was controlled by using the standard magnetite, chromite and olivine minerals. Total sum (of stoichiometric calculation) of oxides more than 100% for samples and for the standard magnetite was obtained which is usually obtained on EMPA, when an iron rich material is analyzed. The results obtained for quantitative analysis magnetite (Table 11-Table 13) are acceptable. However summation of oxides for chromite was not 100 %, thus for chromites data can be considered as semi-quantitative, as total of stoichiometric calculation was bit less, i.e., ~98%.
- Magnetic susceptibility measurements at Friedauwerk and Gmeingrube (positionTF1 and TF6 respectively for geophysical and geochemical data) are not remarkably different and the similar trend (for this region TF1-TF6) of concentration of elements versus magnetic susceptibility (Graph 8-Graph 11) and explain the same kind of minerals present at both locations but different trend for Vordernberg region. It is suggested that a mineralogical study on sample taken from the Vordernberg region needs to be done to understand the reason of different trend of magnetic susceptibility versus concentration of elements in the diagrams.

3.4. Conclusion

From mineralogical study it can be concluded that in the studied river the historical mining and iron production activity at Friedauwerk and recent steel production at Donawitz/Leoben have resulted in anthropogenic deposition of heavy metals which are associated with magnetite (mostly spherical) and hematite. In addition to apatite, magnesioferrite and ferrosilicon are the recent additions of anthropogenic minerals due to recent activity of steel production at Donawitz/Leoben. Beside anthropogenic particles, a contribution of heavy metals due to geogenic minerals, e.g., chromite, olivine, serpentine cannot be ignored.

4. Study of soil and dust from Judaskreuzsiedlung/Donawitz

In the geochemical, geophysical and mineralogical studies on sediments of the Vordernbergerbach, it is observed that area adjacent to steel production plant 'Voest-alpine' is contaminated, due to anthropogenic contribution of heavy metals mainly. To identify the carrier particles of heavy metals and distribution of heavy metals in carrier particles study on soil and dust samples was also made.

Judaskreuzsiedlung is a residential allotment situated near (less than 1 km away from) the steel production plant 'Voest alpine' in Donawitz/Leoben. The houses in Judaskreuzsiedlung (JKS) were built in the 1950's hence the soil records the deposition of the last 60 years.

4.1. Soil and dust sample collection

Soil samples were collected from two plots (No. 6 and No. 8) in the Judaskreuzsiedlung on Aug 11, 2008 and named as *JKS 6* and *JKS 8* respectively. Recent anthropogenic activity leads to the deposition of heavy metals on the top surface of a soil profile. So, two layers *0-5 cm* and *5-10 cm* depth were selected. 7 sample points in *JKS 6* were selected and samples of both depths on all 7 points were collected. 8 sampling points from *JKS 8* were selected which comprises of both top and lower layers of *0-5 cm* and *5-10 cm* respectively. Notation T stands for top surface (*0-5 cm*) and L for lower layer (*5-10 cm*).

For the study of more recent deposition of heavy metals, dust sample from the roof of house No. 4 was also collected and named as *JKS 4*.

All the samples were collected in plastic bags and were labeled accordingly before being brought to the lab for further procedure of measurement.

4.2. Sample preparation

Dust sample collected from *JKS 4* was sieved and divided into two fractions which were a coarser fraction (*125 µm* to *250 µm*) and fine fraction (*< 125 µm*) and named as *4DC* and *4DF* respectively. Polished sections of both fractions were prepared but 4DF is only observed with laser ablation mapping.

Soil samples were dried at room temperature in the lab by spreading the samples on clean paper sheets with marking. After drying, samples were sieved below *2 mm* and stones, pebbles and gravels were removed. Samples were 1st grinded manually in a mortar followed by splitting. One split (about *40g*) portion of splitted sample was grinded very finely with agate ball mill and stored in plastic vials for analysis and remaining splits were combined together and stored in labeled plastic bags. Duplicate pressed pellets, fused glass

beads and Na_2O_2 digestion solutions of soil samples were prepared similarly as described previously (for sediments).

4.3. Magnetic Separation

Several selected samples from JKS6 and JKS8 were taken and magnetic separation was performed. Weighted amount of soil samples were dissolved in milli-Q water and stirred keeping a hand magnet outside of the beaker to get the magnetic particles sticking to the beaker as shown in picture below. Magnetic particles were then extracted with handmade μ-needle on which we may induce magnetic field by joining it with a hand magnet. Removal of hand magnet from this μ-needle leads the extract to get detatched. Moreover, the extract was removed from needle by drops of milli-Q water, into a small container. Then milli-Q water was decanted and dried to get only magnetic fraction. Non-magnetic fraction remains in the beaker, similarly water from beaker was evaporated to get non-magnetic fraction.

a- Concentrate of magnetic material with hand magnet, after dissolving soil in milli-Q water

b- Extraction of magnetic material with μ-metal needle

No glass bead, or pressed powder pellet was prepared from the magnetic and non-magnetic fraction, only Na_2O_2 digestion solutions of them were prepared. Some un-dissolved residual

particles with normal (already described) procedure of Na_2O_2 digestion of magnetic fraction were observed, to dissolve them 2 ml additional concentrated HCl was added and samples were kept stirring on hot plate (100 °C) for 1 extra hour to get a clear solution which otherwise was not obtained. The residues were most likely magnetites.

4.4. Measurements

Geochemical analysis of soil samples were performed on following instruments

- X-ray fluorescence spectrophotometer (WD-XRF AXIOS)
- Inductively coupled plasma mass spectrometer (ICP-MS Agilent Technologies 7500 cx)
- EMPA JEOL JXA 8200
- Laser ablation (ArF excimer 193nm Resonetics RESOlution M-50) coupled to mass spectrometer (Agilent 7700x ICP-MS) at the University of Quebec in Chicoutimi (Canada)

Geophysical measurements were performed on following instruments

- Magnetic susceptibility meter MS2-Bartington
- Multi-Function Kappabridge (AGICO) (for Curie point determination)

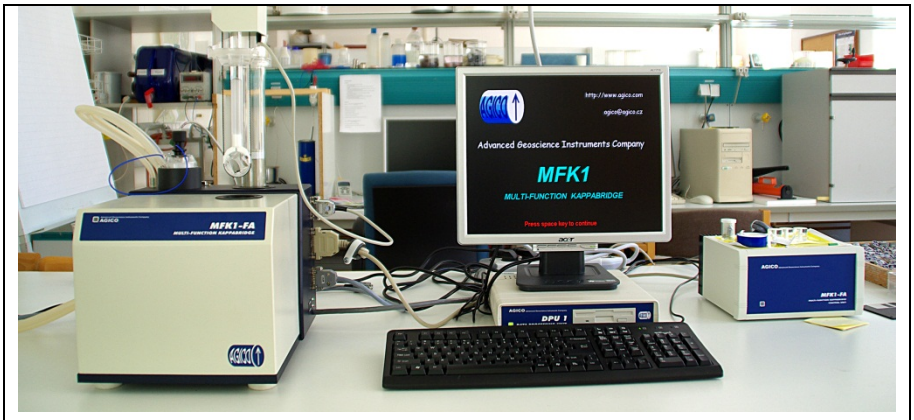

Multi-function Kappabridge (MFK1-FA) AGICO

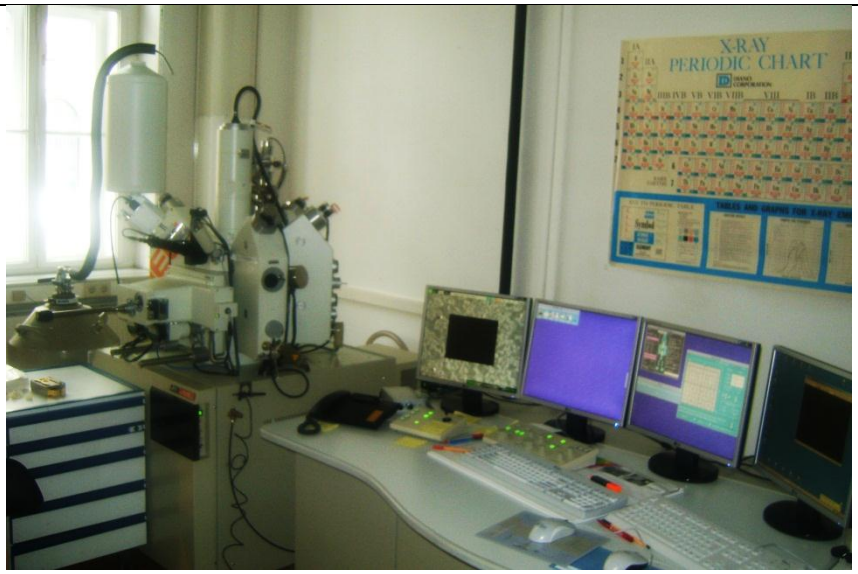

Electron micro probe analyser (EMPA) JEOL JXA 8200

S.No	Sample ID	Weight of sample			Magnetic fraction				Non-magnetic fraction			X of total sample	Mean of Mass Specific total susceptibility	Another un-separated sample portion		
S.No	Sample ID	Unseparated	Magnetic fraction	Non-magnetic fraction	% age of magnetic fraction in soil	uncorrected volume susceptibility values	Mass specific magnetic susceptibility (**X**) of magnetic fraction	Mean **X** for magnetic fraction	uncorrected volume susceptibility values	**X** for NM fraction	Mean **X** for NM	**X** of total sample	Mean of **X** for total sample	Sample weight	Uncorrected volume susceptibility values	Mass specific magnetic susceptibility (**X**)
		g	g	g	%	$[10^{-5}]$SI	10^{-8} m^3/kg		$[10^{-5}]$SI	10^{-8} m^3/kg				g	$[10^{-5}]$SI	10^{-8} m^3/kg
1	6T1a	2.00	0.54	1.36	**27**	590	10906	**11146**	94	694	**612**	3605	**3575**	3.63	1373	**3787**
2	6T1b	2.00	0.54	1.41	**27**	615	11386		75	531		3545				
3	6T3a	2.00	0.47	1.48	**23**	432	9176	**9994**	67	452	**483**	2554	**2509**	3.45	927	**2685**
4	6T3b	2.00	0.37	1.58	**18**	400	10811		81	514		2463				
1	6T5a	2.00	0.38	1.89	**19**	306	8098	**7845**	42	221	**240**	1534	**1615**	4.22	810	**1919**
2	6T5b	2.00	0.39	1.58	**19**	292	7592		41	260		1696				
7	6T7a	2.00	0.29	1.62	**14**	302	10425	**9888**	56	347	**328**	1879	**1857**	3.9	758	**1943**
8	6T7b	2.00	0.33	1.62	**16**	308	9352		50	310		1834				
3	6L1a	2.00	0.68	1.29	**34**	681	9948	**9897**	49	379	**388**	3705	**3666**	4.54	1828	**4023**
4	6L1b	2.01	0.68	1.31	**34**	667	9846		52	398		3626				
11	6L7a	2.00	0.26	1.69	**13**	300	11617	**11326**	58	343	**326**	1833	**1825**	3.14	618	**1971**
12	6L7b	2.00	0.28	1.68	**14**	304	11035		52	309		1818				

Table 15 Magnetic separation and susceptibility data for JKS6 soil

S.No	Sample ID	Weight of sample			Magnetic fraction				Non-magnetic fraction			X of total sample	Mean of Mass Specific total susceptibility	Another unseparated sample portion		
S.No	Sample ID	Unseparated	Magnetic fraction	Non-magnetic fraction	% age of magnetic fraction in soil	uncorrected volume susceptibility values	Mass specific magnetic susceptibility (X) of magnetic fraction	Mean X for magnetic fraction	uncorrected volume susceptibility values	X for NM fraction	Mean X for NM	X of total sample	Mean of X for total sample	Sample weight	uncorrected volume susceptibility values	Mass specific magneticsusceptibility (X) of unseparated
		g	g	g	%	$[10^{-5}]$SI	10^{-8} m^3/kg		$[10^{-5}]$SI	10^{-8} m^3/kg				g	$[10^{-5}]$SI	10^{-8} m^3/kg
1	8T3a	2.11	0.32	1.74	**15**	356	11125	**10537**	91	523	**497**	2167	**2189**	4.3	999	**2323**
2	8T3b	2.29	0.41	1.81	**18**	406	9949		86	471		2211				
3	8T4a	2.05	0.6	1.37	**29**	488	8172	**8525**	98	714	**734**	2973	**3033**	3.15	1000	**3176**
4	8T4b	2.03	0.56	1.38	**27**	496	8879		104	753		3092				
5	8T7a	2.05	0.48	1.50	**24**	496	10241	**10520**	118	786	**784**	3100	**3218**	3.09	1027	**3324**
6	8T7b	2.1	0.53	1.54	**25**	568	10799		120	783		3336				
7	8L2a	2.01	0.44	1.51	**22**	397	9012	**8816**	77	511	**512**	2433	**2434**	5.14	1418	**2756**
8	8L2b	2.01	0.46	1.48	**23**	397	8621		76	513		2435				
9	8L5a	2.01	0.62	1.34	**31**	428	6937	**6912**	76	569	**603**	2579	**2574**	2.39	652	**2729**
10	8L5b	2.02	0.6	1.35	**30**	416	6887		86	637		2569				
11	8TL6a	2.19	0.58	1.56	**26**	578	9970	**10386**	98	625	**638**	3152	**3167**	3.30	1123	**3408**
12	8TL6b	2.17	0.53	1.59	**24**	572	10801		104	651		3181				

Table 16 Magnetic separation and susceptibility data for JKS8 soil

Observations on mass specific susceptibility measurements follow as:

- 98 % of soil set for separation is recovered in two fractions namely magnetic and non-magnetic fraction.
- It is observed that soil in Judaskreuzsiedlung contains more than 20 % of magnetic fraction.
- There was not remarkable difference of magnetic content in top and lower layer. Even some time the lower layer had a higher magnetic content than the top layer as in case of sample 6T1 and 6L1 (JKS6, top and lower layers at sampling point #1 respectively), lower layer contains 34 % and top layer contains 27 % of magnetic content in it.
- Mass specific susceptibility values of soil at JKS6 for un-separated measured samples lie in the range of 1500 to 3500 (10^{-8} m^3/kg), for magnetic fractions lie from 8500 to 11000 (10^{-8} m^3/kg) while for non-magnetic fraction from 250 to 550 (10^{-8} m^3/kg).
- Mass specific susceptibility measurements of soil at JKS8 for un-separated measured samples lie in the range of 2000 to 3000 (10^{-8} m^3/kg), for magnetic fractions lie from 7000-11000 (10^{-8} m^3/kg) and for non-magnetic fraction from 500-800 (10^{-8} m^3/kg).
- To check the heterogeneity of samples, magnetic susceptibility of another test portion for each selected (separated) sample was measured the RSD overall found was less than 8 % on the basis of precision.
- Homogeneity of un-separated soil samples was checked by mass specific magnetic susceptibility measurements and RSD found on the basis of precision of duplicate samples, is found 2 %.

Geochemical analysis of soil sample was performed with XRF and ICP-MS. Geo27 and Protrace Geo modes of measurements were adopted for fused glass beads and pressed pellets respectively. Na_2O_2 sintered solution of soil samples were measured with ICP-MS using geol01 method of measurement. 100 µl of In/Re (100 ppb) and 50 µl of Ge (1ppm) were used as internal standard. GBW 07403 (soil powder) National Research Center for Certified Reference Materials, Office of CRMs, No.18, Bei San Huan Dong Lu, Hepingjie, Beijing 100013, China) was used as quality control material along with measurements of JKS soil samples and blanks. The best fit (the least bias and the most precise) concentration data among measured (Geo27, Protrace Geo, geol01), for each element is selected. Average of duplicates (selected values) and precision based RSD % are related with concentration of some selected elements, from JKS 6 and JKS 8 are

reported in Table 17 and Table 18 respectively. For magnetic and non-magnetic fractions, concentration is measured only on ICP-MS.

4.5. Results

S.No.	Sample ID		Fe_2O_3 g/100g	RSD %	Cr mg/kg	RSD %	Ni mg/kg	RSD %	Pb mg/kg	RSD %	Zn mg/kg	RSD %
1	Unseparated top layer (0-5 cm)	6T1	17.7	0.1	170	0.02	76.9	0.05	155	3	619	12
2		6T2	14.8	0.2	131	0.01	65.3	0.03	123	2	482	1
3		6T3	14.0	0.1	143	0.00	63.3	0.01	125	3	528	20
4		6T4	13.2	0.1	136	0.05	56.0	0.00	104	2	435	18
5		6T5	11.0	0.7	150	0.02	62.4	0.01	89.7	3	282	5
6		6T6	10.7	0.5	128	0.03	56.8	0.05	77.5	3	295	3
7		6T7	10.9	0.2	143	0.05	55.6	0.00	93.0	3	411	21
8	Unseparated lower layer (5-10 cm)	6L1	18.7	0.2	183	0.01	78.5	0.01	163	4	621	1
9		6L2	14.3	0.7	127	0.02	58.2	0.05	115	2	445	4
10		6L3	14.2	0.2	139	0.01	61.0	0.04	117	2	447	1
11		6L4	13.3	0.4	123	0.03	54.7	0.02	101	2	360	1
12		6L5	10.3	1.7	144	0.04	60.5	0.03	75.5	1	274	1
13		6L6	11.6	0.1	123	0.01	54.2	0.03	84.5	0	325	1
14		6L7	10.9	0.0	140	0.01	58.0	0.07	95.1	3	340	0
15	Magnetic fraction	6T1M	37.4	3.0	243	0.05	116	0.01	222	3	565	1
16		6T3M	38.3	2.7	184	0.06	104	0.00	205	3	544	6
17		6T5M	31.2	1.9	192	0.06	103	0.02	168	3	447	2
18		6T7M	35.1	2.7	217	0.06	112	0.00	181	3	489	7
19		6L1M	35.1	2.0	205	0.06	113	0.02	266	3	620	0
20		6L7M	40.0	2.2	221	0.06	123	0.02	182	3	540	10
21	Non-magnetic fraction	6T1NM	9.80	0.8	125	0.01	48.5	0.09	124	3		
22		6T1NM	9.70	0.7	160	0.02	66.0	0.09	123	3		
23		6T3NM	8.44	1.3	111	0.01	46.5	0.10	118	3		
24		6T5NM	6.91	1.6	133	0.04	49.9	0.04	74.1	3	157	6
25		6T7NM	8.86	0.6	94	0.02	55.3	0.04	158	3		0
26		6T7NM	6.55	2.8	118	0.04	55.5	-	78.7	3	186	12
27		6L1NM	9.52	0.8	172	0.02	67.0	0.02	139	3		
28		6L5NM	8.95	1.5	108	0.01	-		103	3		
29		6L7NM	6.46	2.1	173	0.05	51.6	0.03	76.0	3	181	12

Table 17 Concentration of elements in soil from Judaskreuzsiedlung (JKS6)

S. No.	Sample ID		Fe_2O_3 g/100g	RSD %	Cr mg/kg	RSD %	Ni mg/kg	RSD %	Pb mg/kg	RSD %	Zn mg/kg	RSD %
1	Unseparated top layer (0-5 cm)	8T1	14.4	0.1	122	0.02	80.2	0.07	123	3	444	5
2		8T2	16.1	0.9	136	0.00	61.9	0.04	145	3	429	2
3		8T3	12.8	1.4	133	0.02	59.0	0.03	107	3	360	0
4		8T4	16.2	0.3	148	0.01	60.4	0.00	155	3	451	2
5		8T5	14.4	0.2	122	0.03	56.9	0.03	124	3	365	0
6		8T7	16.5	0.8	172	-	72.0	0.03	176	3	653	0
7	Unseparated lower layer (5-10 cm)	8L1	13.7	0.4	129	0.05	58.4	0.03	119	3	395	0
8		8L2	15.0	7.0	116	0.02	75.1	0.04	120	3	441	2
9		8L3	12.3	0.6	112	0.01	57.3	0.08	100	2	357	0
10		8L4	15.7	0.2	142	0.01	68.2	0.05	139	3	417	1
11		8L5	14.4	1.3	109	0.00	62.0	0.03	121	3	427	1
12		8L7	10.8	0.4	142	0.04	57.4	0.01	95.4	3	325	1
13	0-10 cm	8TL6	16.3	0.2	141	0.03	66.8	0.05	157	3	465	1
14	composite	8MIX	13.9	0.5	143	0.04	60.0	-	146	3	629	9
15	Magnetic fraction	8T3M	32.9	2.8	163	0.02	107	0.01	178	3	507	0
16		8T4M	27.0	12.4	127	0.04	100.0	0.02	169	3	454	4
17		8T7M	34.0	2.7	181	0.03	92.9	0.02	267	3	728	6
18		8L2M	26.2	13.1	121	0.02	91.3	0.03	153	3	415	17
19		8L5M	20.6	11.4	103	0.02	93.3	0.02	136	3	341	9
20		8TL6M	36.7	2.5	163	0.05	100	0.01	235	3	545	3
21	Non-magnetic fraction	8T3NM	7.48	5.3	101	0.04	48.8	0.04	84.6	3	163	20
22		8T4NM	8.44	11.5	92	0.03	51.8	0.02	97.2	3	198	3
23		8T7NM	8.92	8.7	100	0.02	48.1	0.02	134	3	280	0
24		8L2NM	6.98	10.5	81	0.02	42.7	0.02	78.3	3	168	2
25		8L5NM	7.96	1.6	86	0.02	48.0	0.03	93.1	3	215	3
26		8TL6NM	8.05	1.6	120	0.04	42.9	0.03	120	3	214	28

Table 18 Concentration of elements in soil from Judaskreuzsiedlung (JKS8)

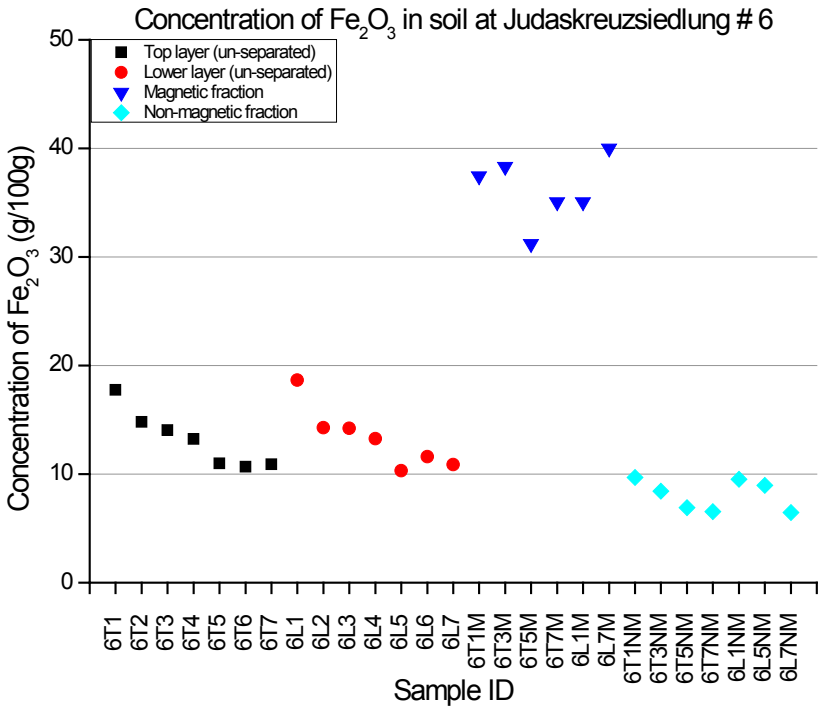

Graph 12 Concentration of Fe2O3 in soil at Judaskreuzsiedlung # 6

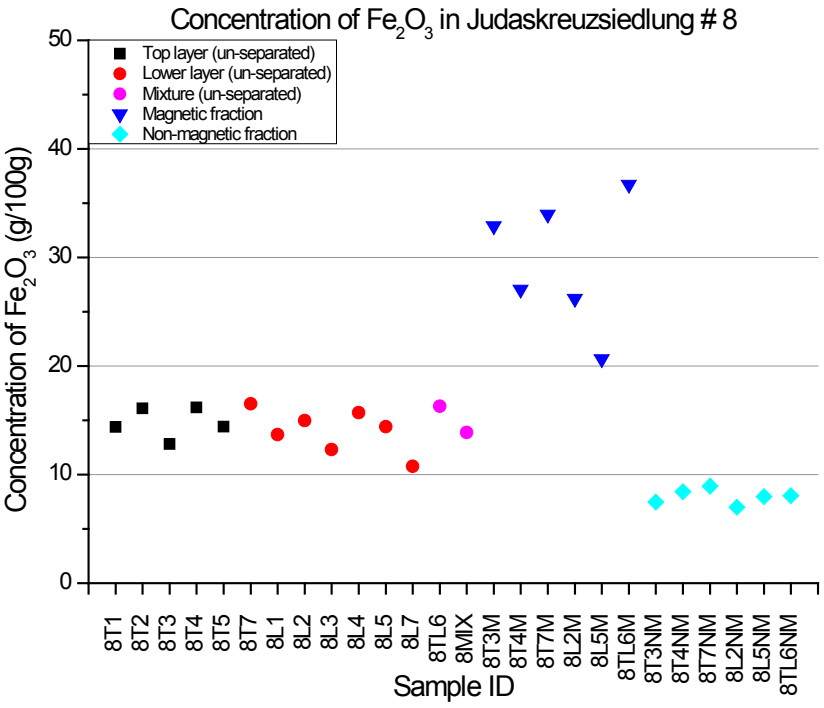

Graph 13 Concentration of Fe2O3 in soil at Judaskreuzsiedlung # 8

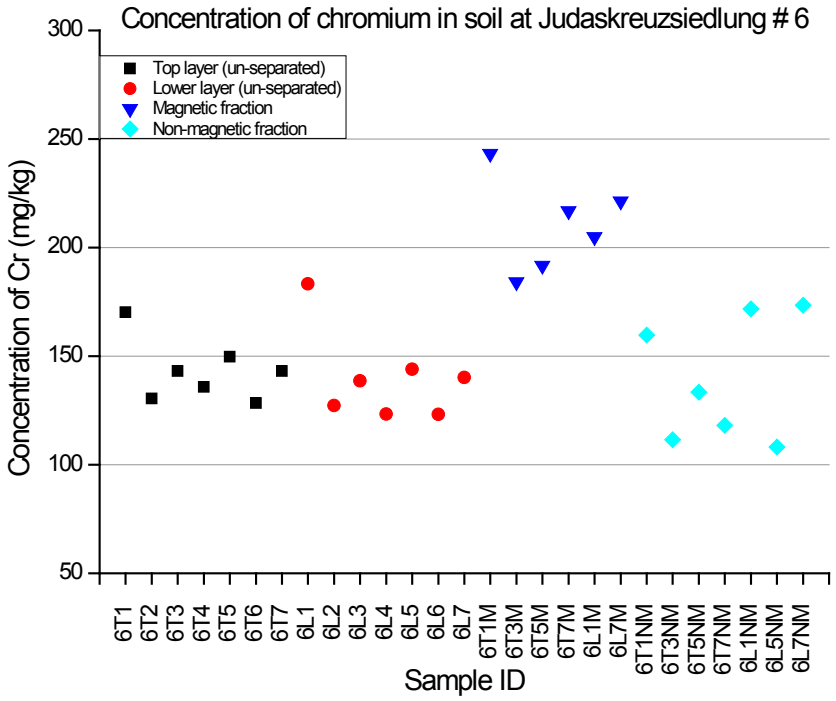

Graph 14 Concentration of chromium in soil at Judaskreuzsiedlung # 6

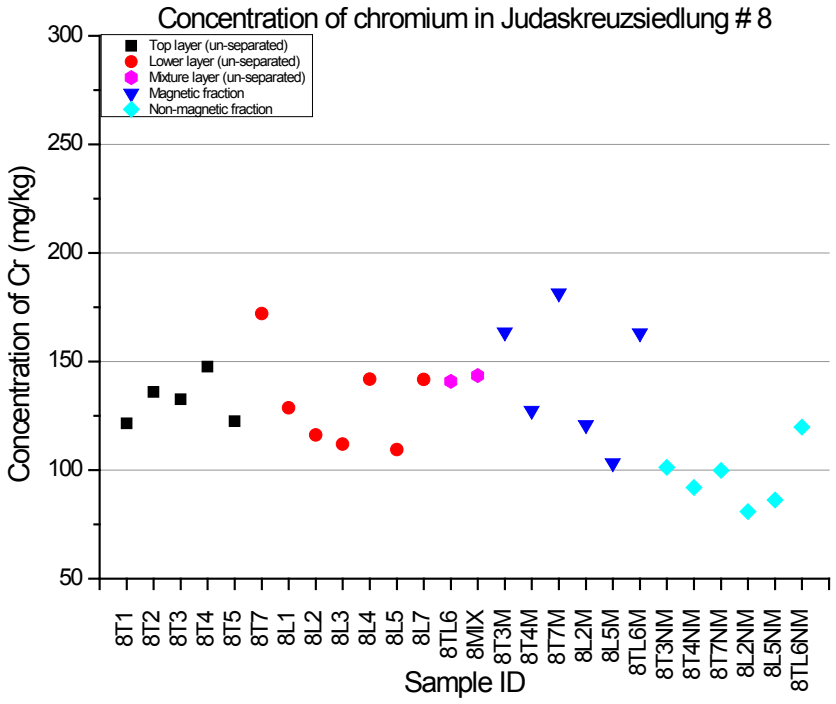

Graph 15 Concentration of chromium in soil at Judaskreuzsiedlung # 8

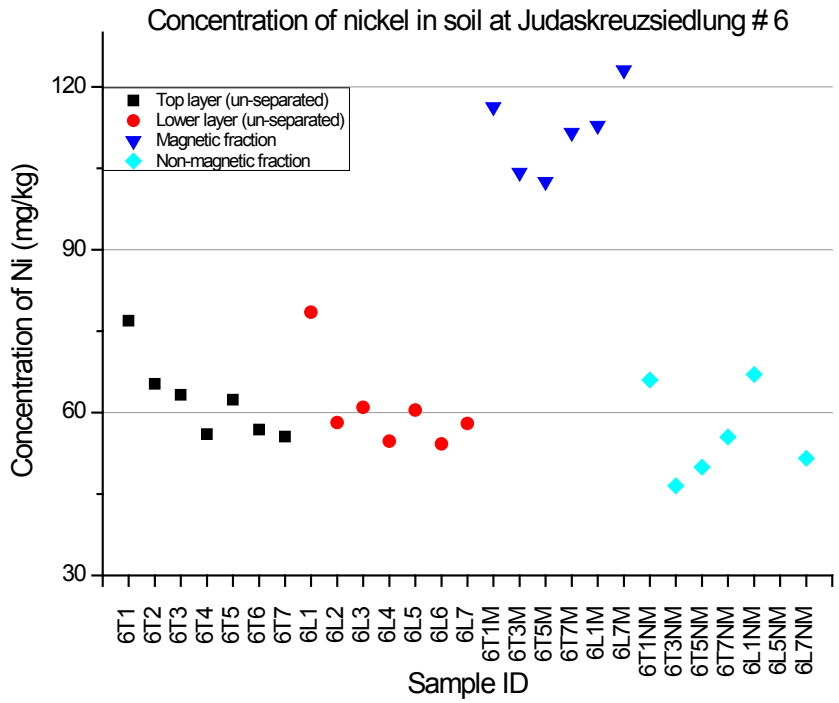

Graph 16 Concentration of nickel in soil at Judaskreuzsiedlung # 6

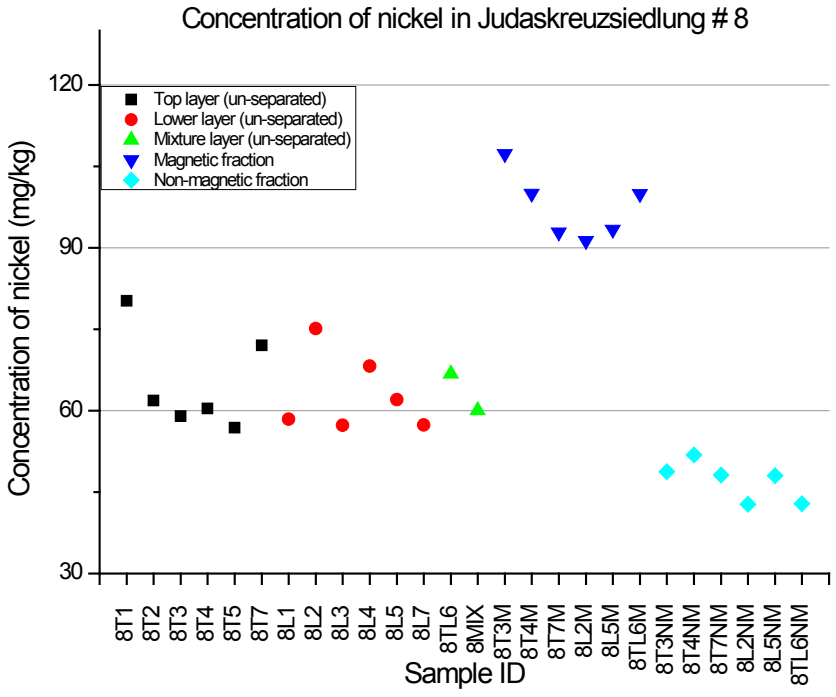

Graph 17 Concentration of nickel in soil at Judaskreuzsiedlung # 8

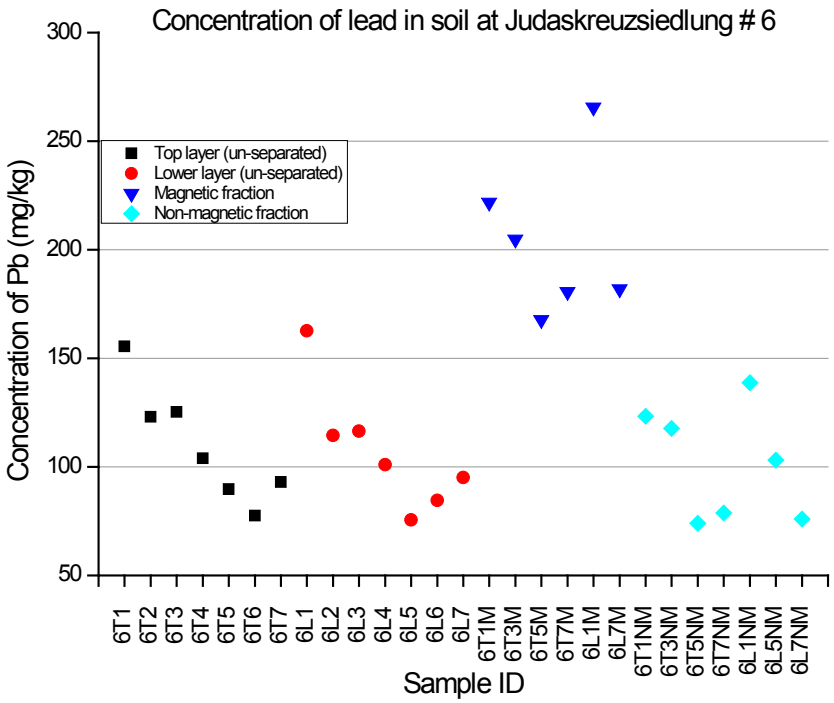

Graph 18 Concentration of lead in soil at Judaskreuzsiedlung # 6

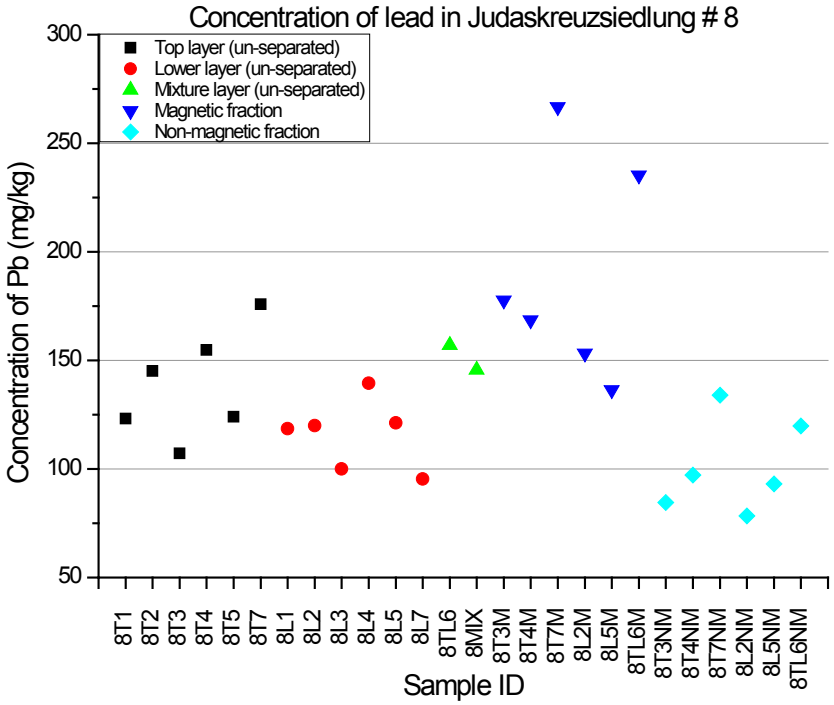

Graph 19 Concentration of lead in soil at Judaskreuzsiedlung # 8

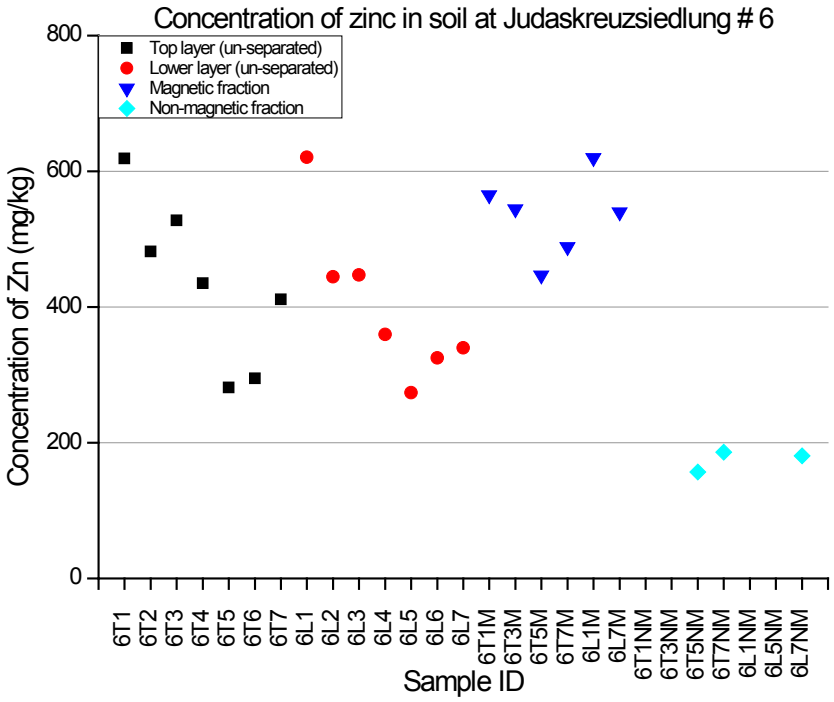

Graph 20 Concentration of zinc in soil at Judaskreuzsiedlung # 6

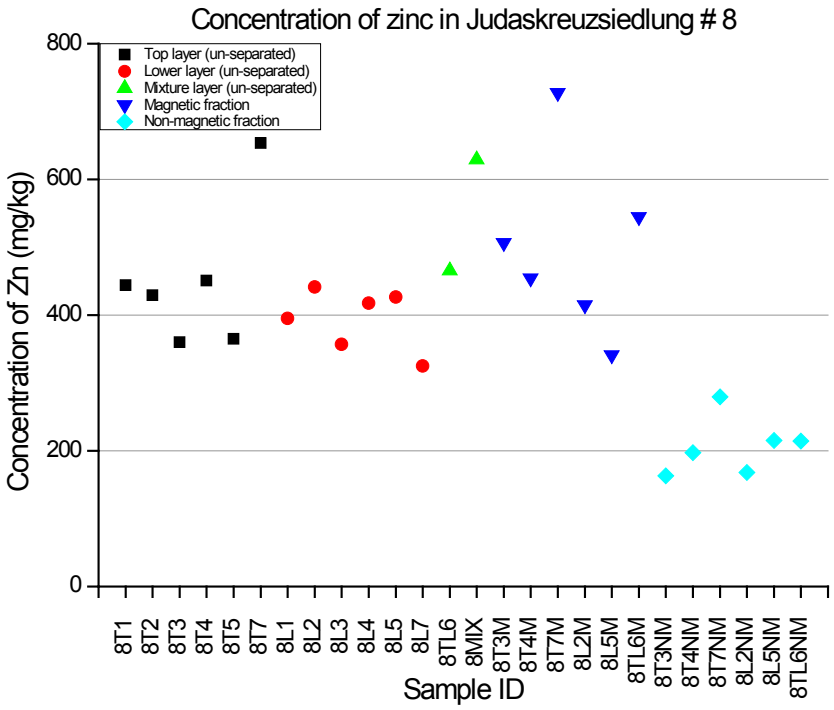

Graph 21 Concentration of zinc in soil at Judaskreuzsiedlung # 8

Graph 12 and Graph 13 show that the concentration of Fe_2O_3 in soil samples at Judaskreuzsiedlung (6 and 8) about 15 g/100g and less than 10 g/100g in non-magnetic fraction, while more than g/100g in the magnetic fraction. There is not remarkable

difference between concentrations of Fe_2O_3 in top (0-5 cm) and lower layer (5-10) cm. It means that the extent of deposition of Fe_2O_3 over a longer period of time ~60 years is similar.

Concentration of chromium determined in the area lies near 130 mg/kg on average. Concentration of chromium in magnetic fraction and non-magnetic fraction as compared to un-separated soil is complex here, in JKS 6, magnetic fraction shows higher concentration of chromium while difference of its concentration in un-separated and non-magnetic fraction is not remarkable. On the other hand in JKS8, non-magnetic fraction has lower concentration of chromium but magnetic fraction and un-separated soil has chromium concentration in similar range. It indicates that concentration of chromium in this area is not only due to the particles which are highly magnetic, but chromium is being contributed by different sources as shown in Graph 14 and Graph 15. Similar kind of trend for concentration of zinc and lead is seen Graph 18-Graph 21. Average values for concentration of the lead and zinc in soils at Judaskreuzsiedlung are 120 mg/kg higher than the safe limits 100 mg/kg and 430 mg/kg higher than the safe limits 300 mg/kg respectively (Krainer, 2000).

Graph 16 and Graph 17 show the concentration of nickel is 60 mg/kg in un-separated soil and more than 90 mg/kg in magnetic fraction while non-magnetic fraction contains less than 60 mg/kg concentration of nickel. It shows that magnetic particles are the main carrier of nickel.

Correlation between mass specific magnetic susceptibility and concentration of heavy metals is seen, in both soils moreover, as expected heavy metals are attached with iron bearing mineral phases. So correlation of iron oxide (Fe_2O_3) and heavy metals is also checked.

Correlation between elements and magnetic susceptibility

4.5.1.1. JKS6

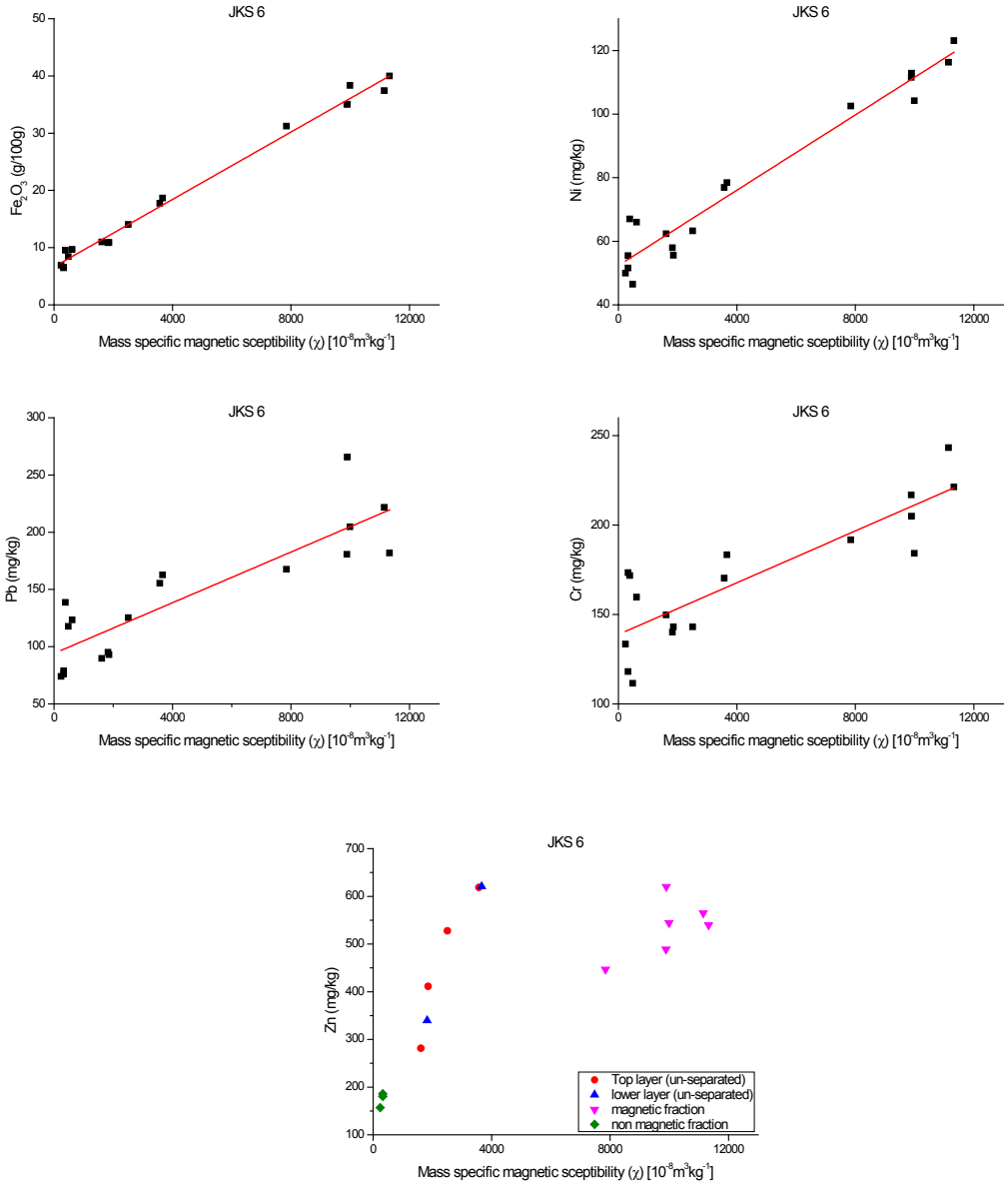

Graph 22 Correlation between concentration of elements and mass specific susceptibility in JKS 6 soil

4.5.1.2. JKS8

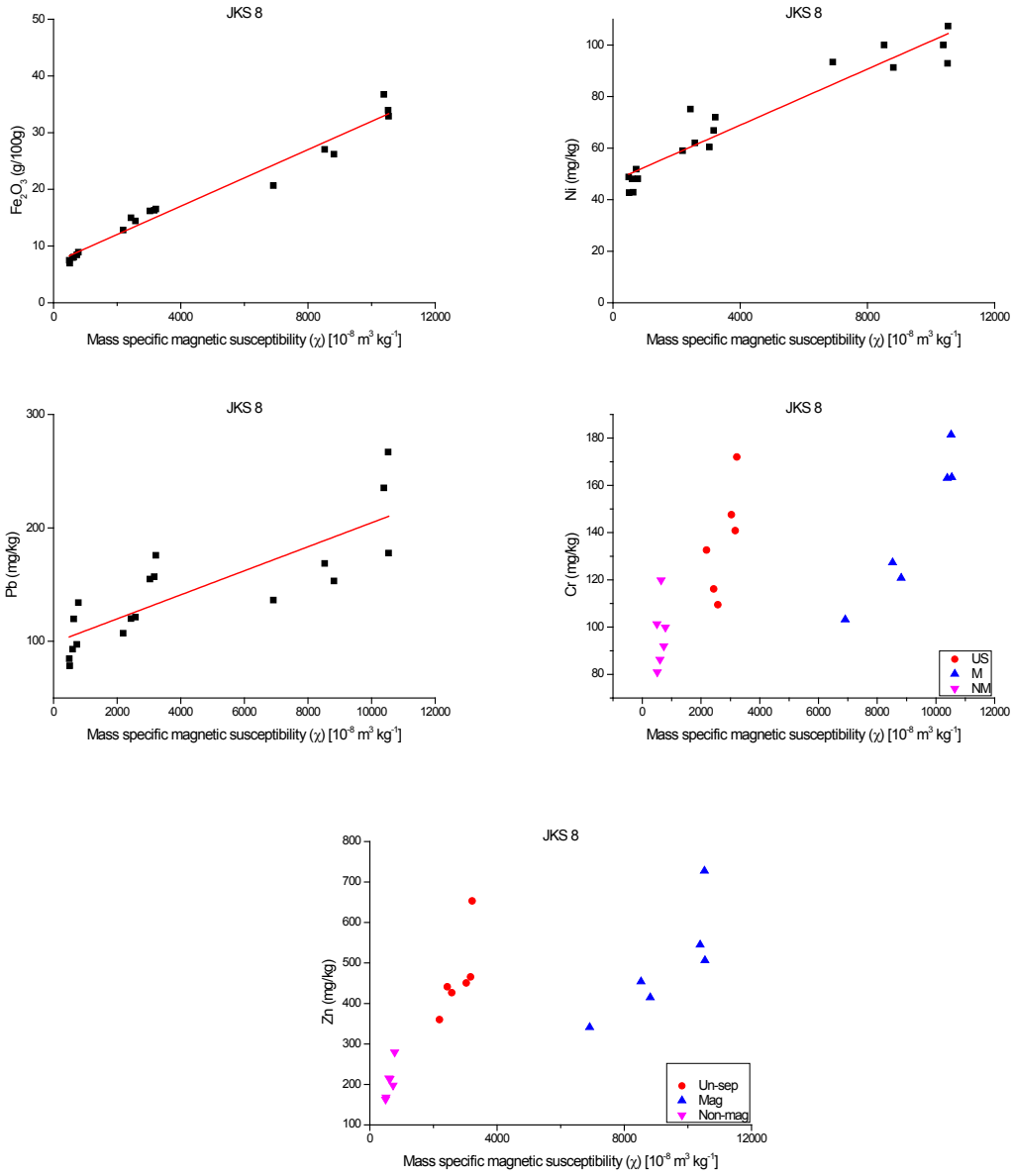

Graph 23 Correlation between concentration of elements and mass specific susceptibility in JKS 8 soil

4.5.2. Correlation between concentration of Fe_2O_3 and other elements (JKS 6 and JKS 8)

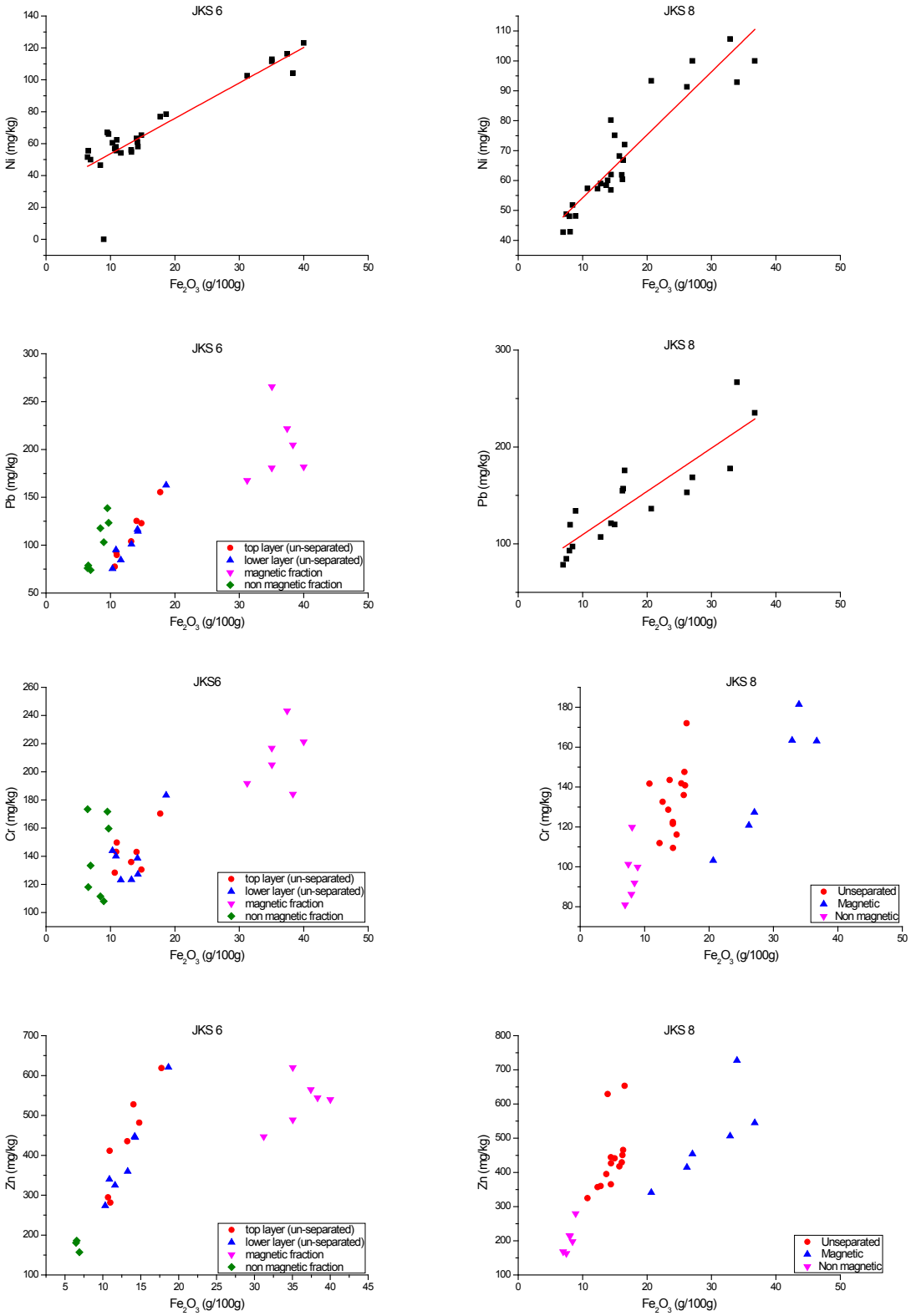

Graph 24 Correlation between concentration of Fe2O3 and other elements (JKS 6 and JKS 8)

The correlation curves show that there is a perfect correlation between magnetic susceptibility and concentration of Fe_2O_3. The correlation of Fe_2O_3 content with Ni and Pb contents is significant. The correlation of chromium with Fe_2O_3 and magnetic susceptibility is positive and good but it shows a dual kind of trend for correlation for magnetic and non-magnetic/un-separated samples. Similar behavior for zinc is observed. Correlation coefficients for JKS 6 and JKS 8 are given in the Table 19 and Table 20.

	Pearson Corr.	Magnetic Susceptibility $10^{-8}m^3/kg$	Fe_2O_3 g/100g	Cr (mg/kg)	Ni (mg/kg)	Pb (mg/kg)	Zn (mg/kg)
Magnetic Susceptibility $10^{-8}m^3/kg$		1.000					
	Sig.	--					
Fe_2O_3 g/100g	Pearson Corr.	0.996	1.000				
	Sig.	<0.001	--				
Cr (mg/kg)	Pearson Corr.	0.859	0.837	1.000			
	Sig.	<0.001	<0.001	--			
Ni (mg/kg)	Pearson Corr.	0.975	0.900	0.892	1.000		
	Sig.	<0.001	<0.001	<0.001	--		
Pb (mg/kg)	Pearson Corr.	0.871	0.887	0.802	0.817	1.000	
	Sig.	<0.001	<0.001	<0.001	<0.001	--	
Zn (mg/kg)	Pearson Corr.	0.690	0.703	0.582	0.673	0.822	1.000
	Sig.	0.004	<0.001	0.004	<0.001	<0.001	--

Table 19 Pearson correlation coefficients among magnetic susceptibility and concentration of elements (JKS6)

	Pearson Corr.	Magnetic Susceptibility $10^{-8}m^3/kg$	Fe_2O_3 (g/100g)	Cr (mg/kg)	Ni (mg/kg)	Pb (mg/kg)	Zn (mg/kg)
Magnetic Susceptibility $10^{-8}m^3/kg$		1.000					
	Sig.	--					
Fe_2O_3 (g/100g)	Pearson Corr.	0.984	1.000				
	Sig.	<0.001	--				
Cr (mg/kg)	Pearson Corr.	0.655	0.674	1.000			
	Sig.	0.003	<0.001	--			
Ni (mg/kg)	Pearson Corr.	0.956	0.924	0.547	1.000		
	Sig.	<0.001	<0.001	0.004	--		
Pb (mg/kg)	Pearson Corr.	0.823	0.878	0.798	0.726	1.000	
	Sig.	<0.001	<0.001	<0.001	<0.001	--	
Zn (mg/kg)	Pearson Corr.	0.701	0.695	0.858	0.632	0.818	1.000
	Sig.	0.001	<0.001	<0.001	0.001	<0.001	--

Table 20 Pearson correlation coefficients among magnetic susceptibility and concentration of elements (JKS8)

Correlation between iron oxide and other elements show the same trends which have been observed between magnetic susceptibility and element content. Generally heavy metals are

thus associated with iron minerals. To find out the dominating mineral phase, Curie temperature with a Multi-Function Kappabridge (AGICO) was determined.

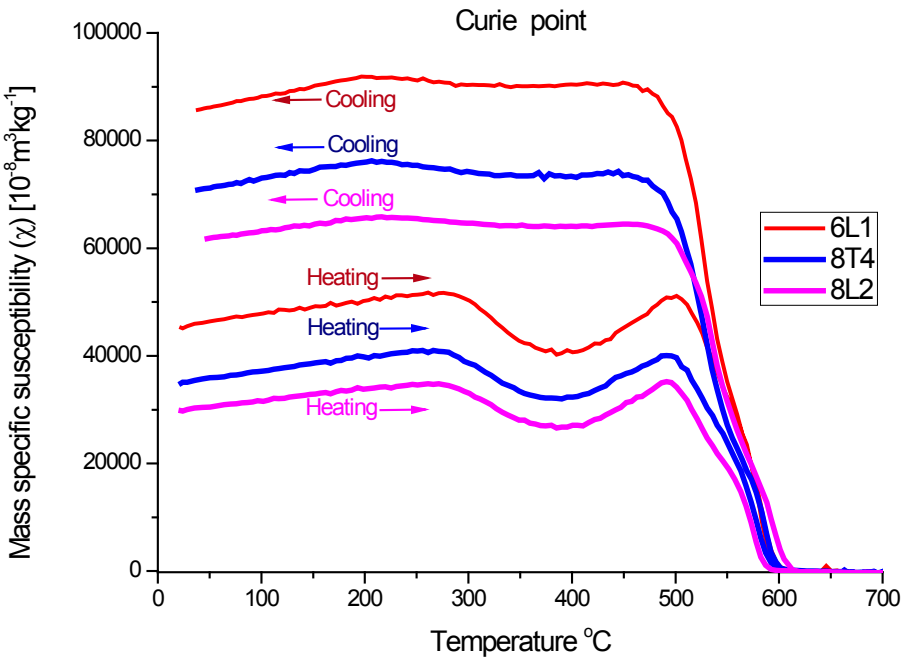

Graph 25 Curie point determination for soil at Judaskreuzsiedlung (Leoben)

Typical Curie curves of susceptibility changes with the change in temperature. Graph 25 shows that soil contains magnetite as dominating phase in it. Curie temperature for it is (~585 °C).

4.6. EMPA Study of soil samples

Magnetic particles were observed under EMPA JEOL JXA 8200. Back scatter images are shown below. Excess of spherical particles in magnetic fractions are found.

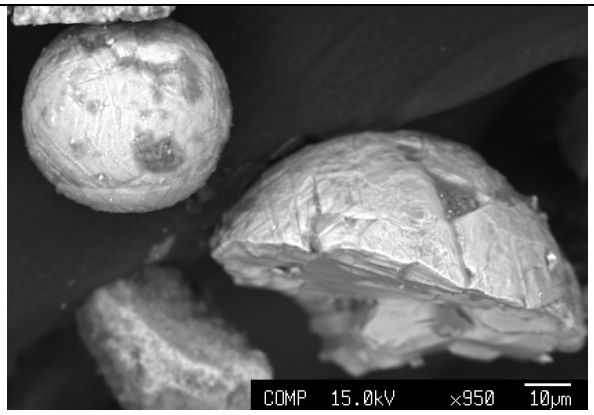	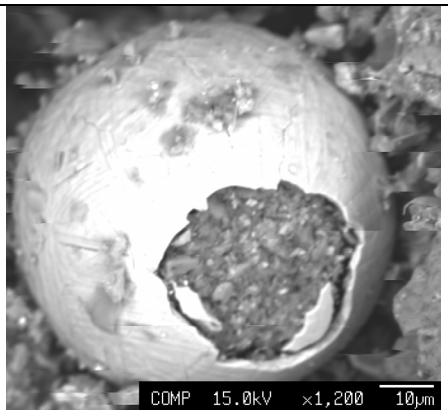
Broken piece of compact spherule, scale bar 10 μm	Spherule surface of 2μm thick wall, scale bar 10 μm

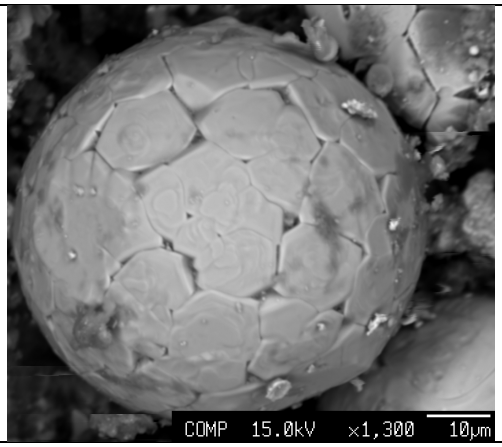

Spherule with patched surface, scale bar 10 µm

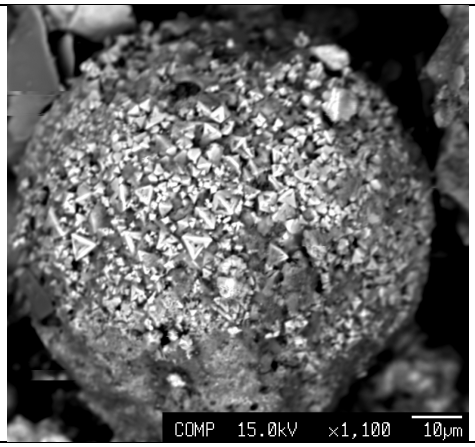

Spherule having building units of pyramid structure, scale bar 10 µm

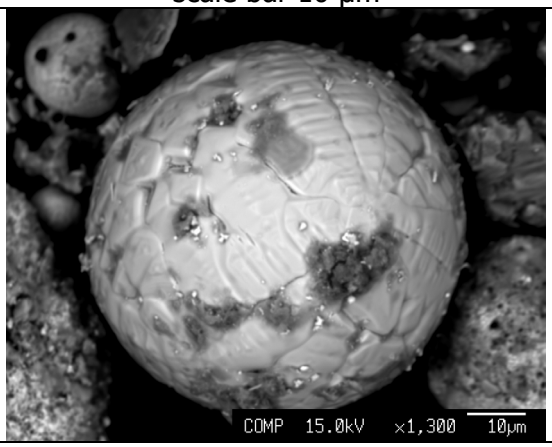

Spherule with patches and having flakes on surface, scale bar 10 µm

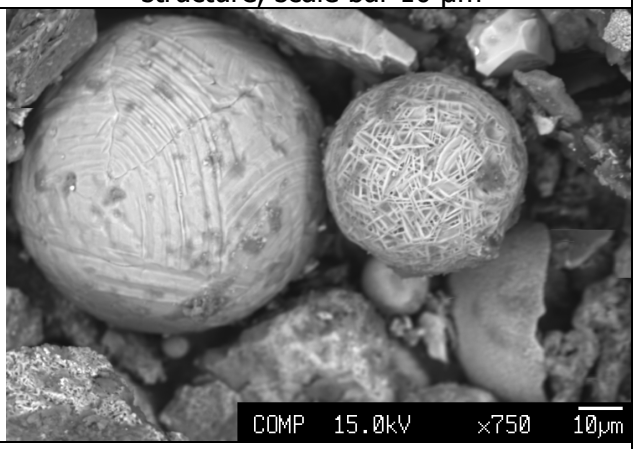

Spherule with angular rimmed surface, scale bar 10 µm

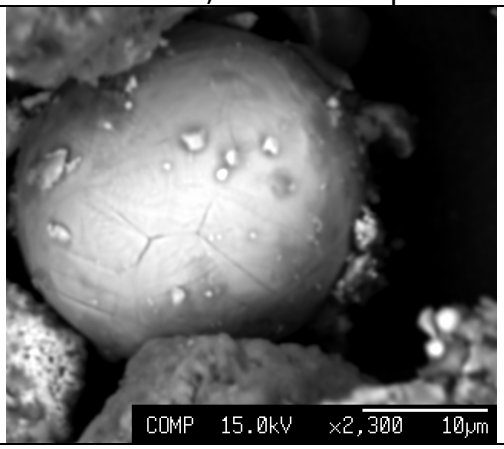

Spherule having flakes on surface, scale bar 10 µm

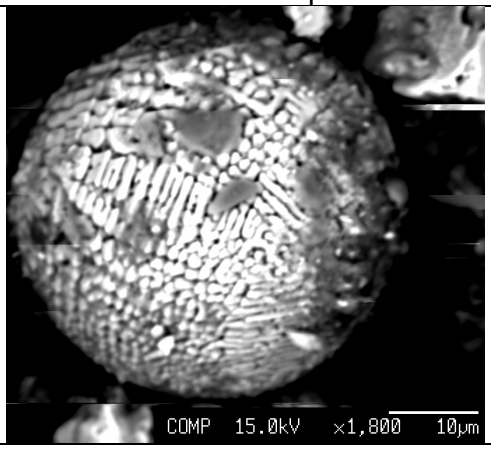

Spherule like 'golf ball', scale bar 10 µm

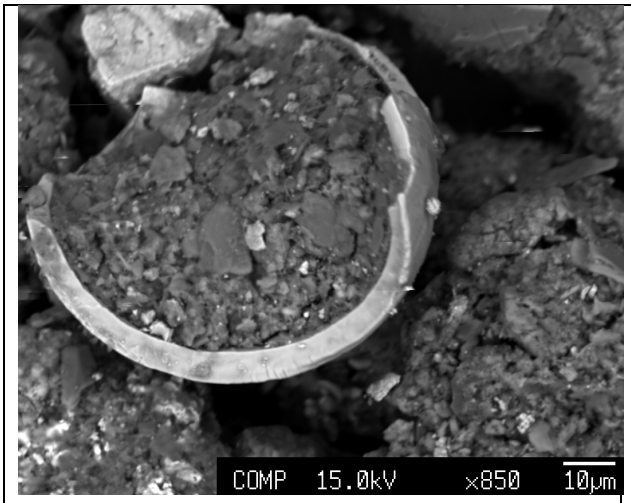

A broken spherule, scale bar 10 µm

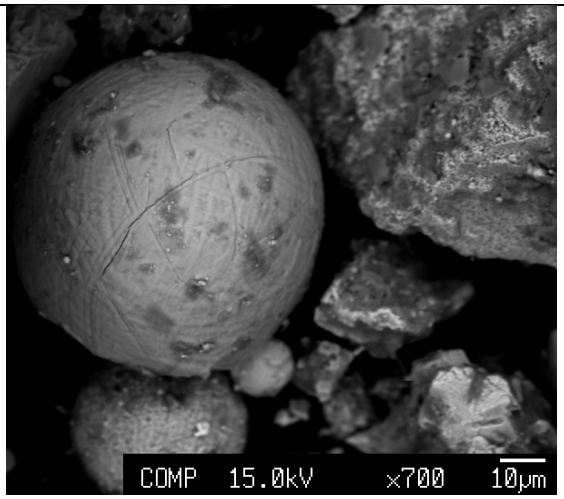

Spherules of different sizes and morphology with rims on surface, scale bar 10 µm

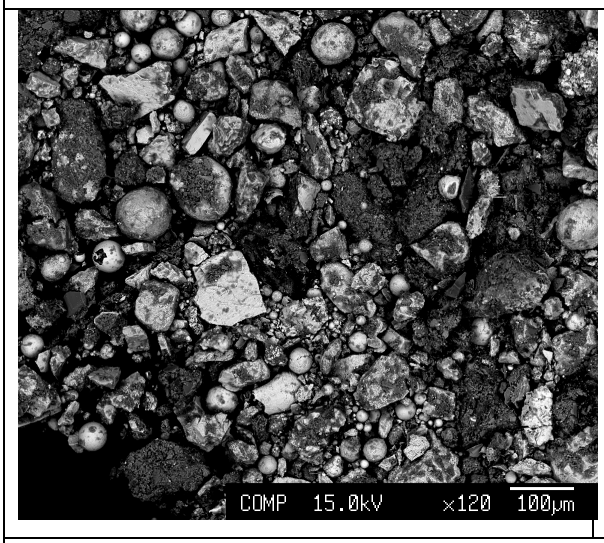

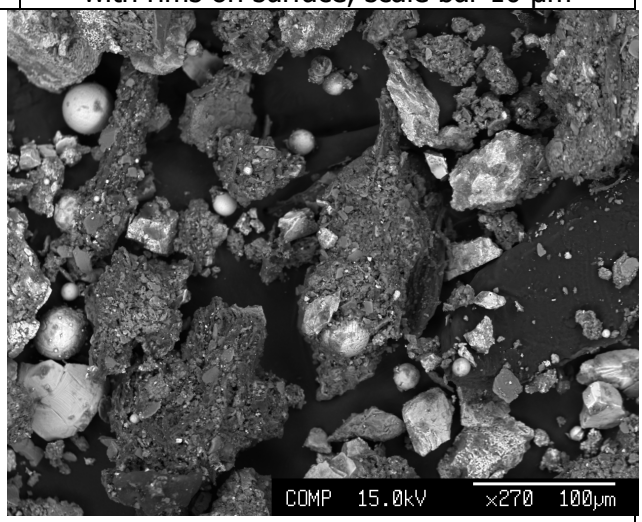

Abundant of spherical particles with different diameters, scale bar 100 µm

Although non-spherical particles (scale etc.) were also present, the majority of particles in magnetic fraction are spherical. These spherules are identified as magnetite of anthropogenic origin and carrier of heavy metals. As grinded soil samples were observed under EMPA, so the exact upper range of diameter is not reported here, but in observed grinded samples spherules of diameter ranging from few µm (<10 µm) to 100 µm have been identified. Morphology of these spherules show a large variety. Hollow, compact, spherules with angular rimmed surface, with patches and some like golf balls, some spherules having flakes on surface are seen. Some spherules having building units of pyramidal structure were also identified. Spherules with soft to rough surface for Leoben, emitted from anthropogenic source in the area have already been reported (Blaha et al., 2008; Hemetsberger, 2006)

4.7. Laser Ablation Mapping

To see the distribution of heavy metals within spherical magnetite, mapping on soil samples with laser ablation coupled with an ICP-MS was performed. Laser ablation analysis was performed at LabMaTer (Laboratoire Matériaux Terrestres), University of Quebec in Chicoutimi (Canada) by Dany Sarvad.

4.7.1. Analytical procedure and instrumentation

Laser ablation (ArF excimer 193nm Resonetics RESOlution M-50) coupled to mass spectrometer (Agilent 7700x ICP-MS) equipped with a double rough pump system to increase sensitivity were used for analysis. The beam size was set to 7 µm with a displacement speed of 7.5 µm/s, pulsing at 15Hz and the energy was set to 5 mJ/pulse. High purity helium (650mL/min) was used as carrier gas in the ablation cell and 1ml/min of high purity nitrogen was added to the line to increase the sensitivity. The argon nebulizer was set to 0.85~0.95ml/min based on best sensitivity and to ensure oxide formation below 0.5 % - 1 % using $^{254}UO/^{238}U$ as monitor. The dwell time was set to 5ms for all isotopes. A 20s gas blank was acquired before each line of analysis and the background was subtracted from the signal. The software IOLITE (University of Melbourne, Australia) was used to generate the map images, calculate concentrations and limits of detection. Multiple parallel line-scans were carried out to obtain the maps and 1µm separation between the edges of each line was left to avoid duplication of ablated area. The USGS glasses GSE-1g was used to calibrate and GSD-1g was analyzed as an unknown to verify the calibration. Working values used for the glasses were from GeoREM website (Max-Planck Institute, Germany) as they were available in date of May 2011. Limits of detection are <1-5ppm in most traces element and <100ppm in majors based GSD-1g fully-quantitative determination. Because the analyzed samples were composed of various phases and that the composition of the phases were unknown, no internal standard could be used to monitor the ablation yield. The yield can vary significantly from phase as it is mainly driven by the efficiency of the laser in ablating the phases and the ionization of the ablated particles in the plasma as well. Thus, only semi-quantitative results can be obtained. Figure 1 presents a micro-photography of a sample (MAP-2-C) after ablation. It is clear that the depth of ablation was changing following phases which obliviously affect the yield. GSD-1g was also analyzed as an unknown i.e. using the standard-less method to verify the semi-quantitative technique. The results obtained for GSD-1g are compared with working values in Graph 26-Graph 27 and are from major elements (>1 % concentrations) and traces elements respectively. The

results show that the results can significantly vary in GSD-1g despite similar matrix, with relative standard deviation on the mean at around 25 % for most elements as based on 14 replicate analyses over 4 days of data acquisition. To compare the effect of standard-less with fully-quantitative, all the GSD-1g were also calculated using ^{57}Fe as internal standard. Results are compared with working value in Graph 28-Graph 29, and the standard deviation on mean are significantly lower at 5-15 % as expected from the fully quantitative technique. Exception are for Au, Tl, As and Zn, those being heterogeneous or close to limit of detection.

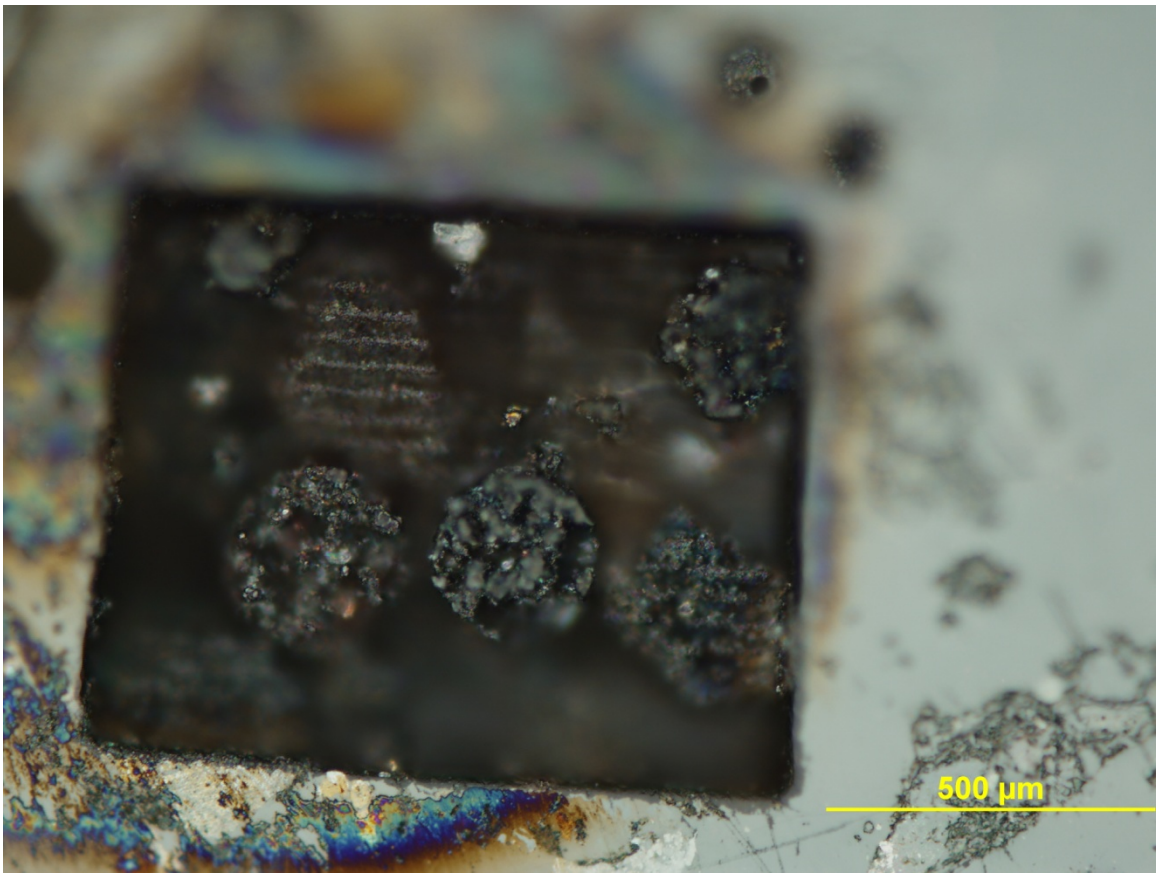

Figure 1 Micro-photography of Map-2-C after ablation

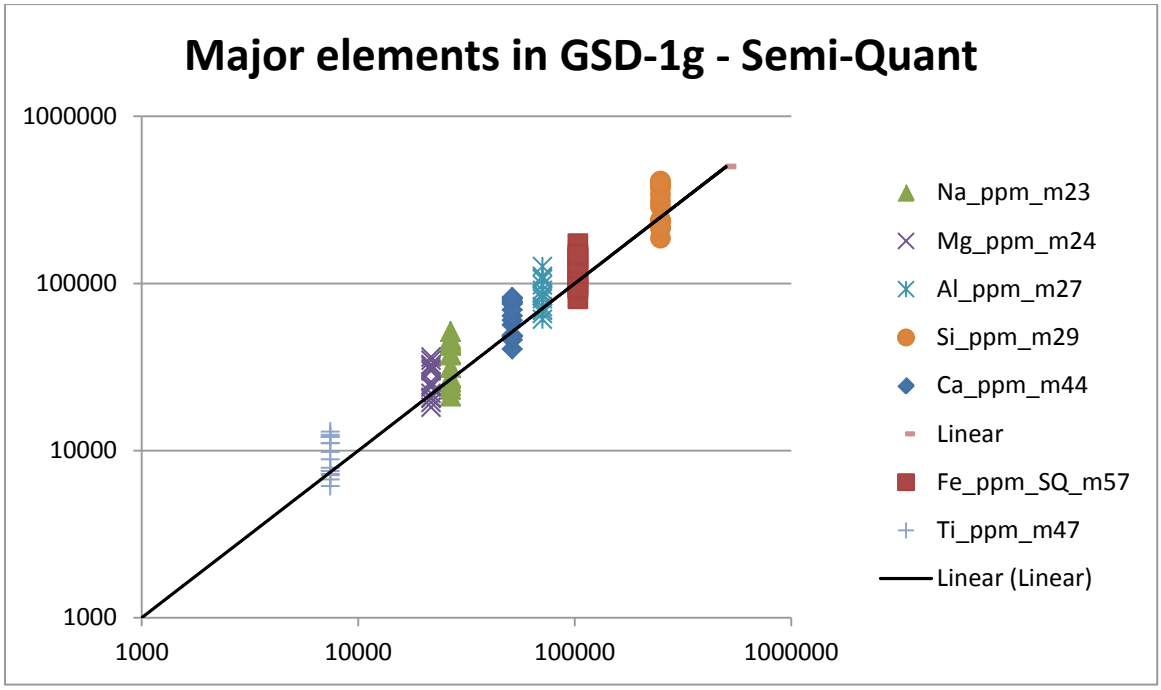

Graph 26 Major elements in GSD-1g using GSD-1e as calibrant (without internal standard), Semi-Quant (laser ablation)

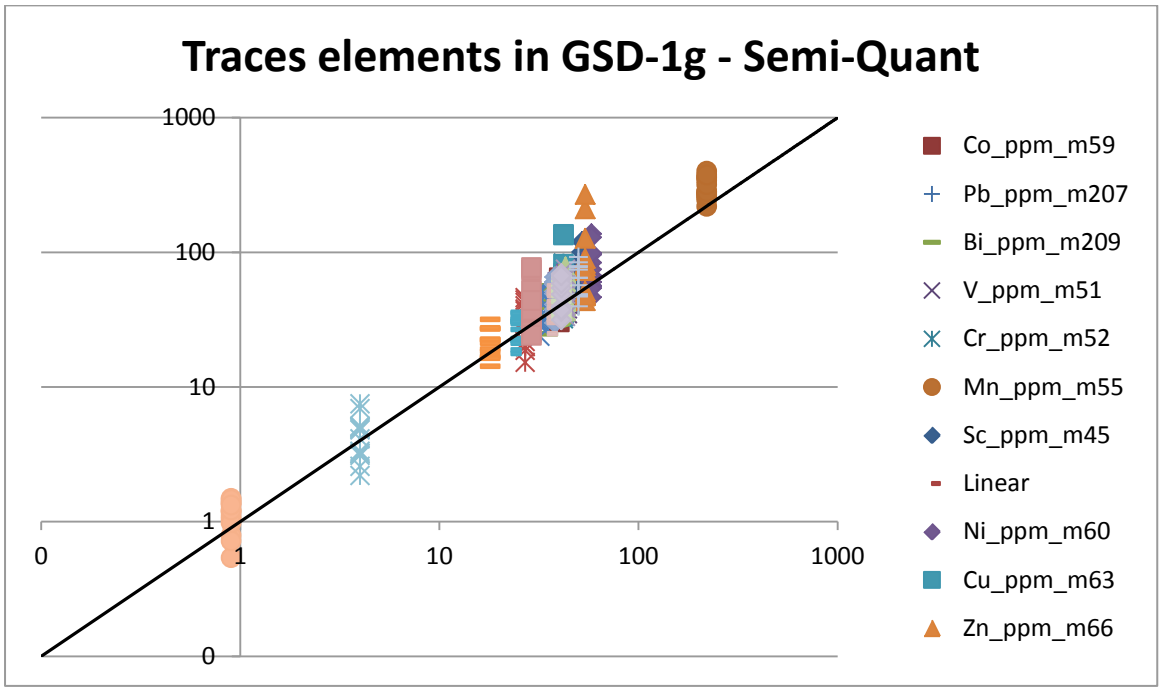

Graph 27 Trace elements in GSD-1g using GSD-1e as calibrant (without internal standard)- Semi-Quant (laser ablation)

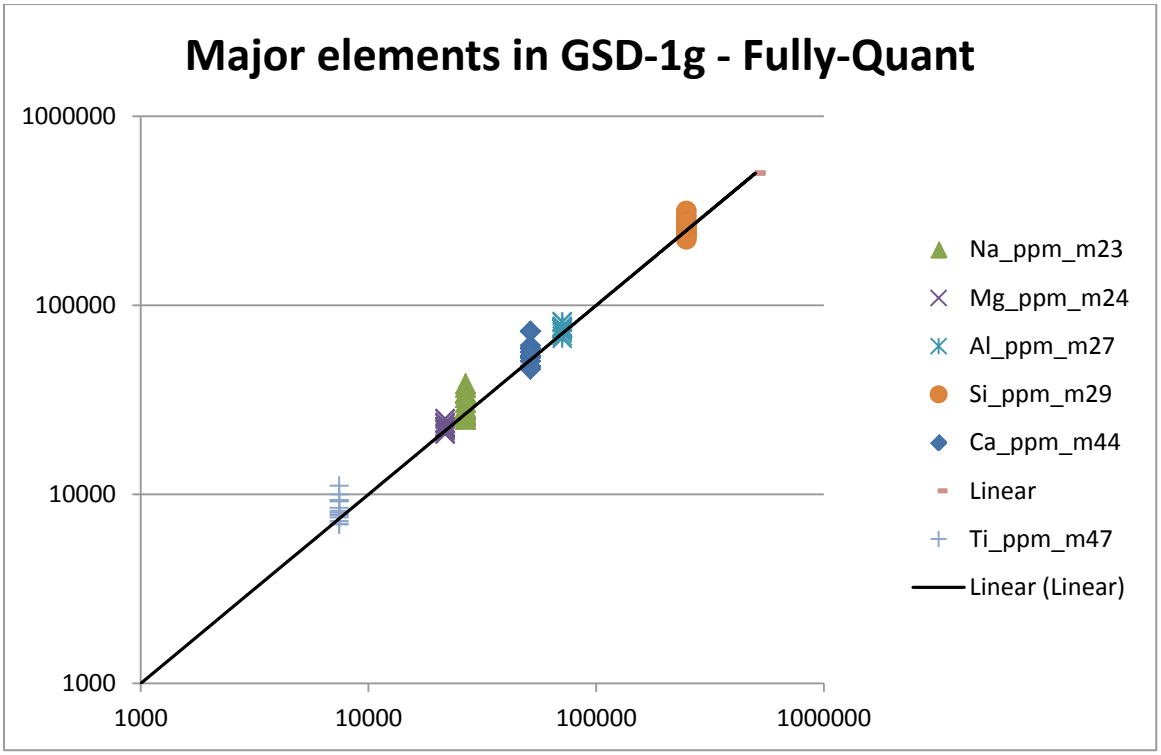

Graph 28 Major elements in GSD-1g using GSD-1e as calibrant (with internal standard) - Fully-Quant (laser ablation)

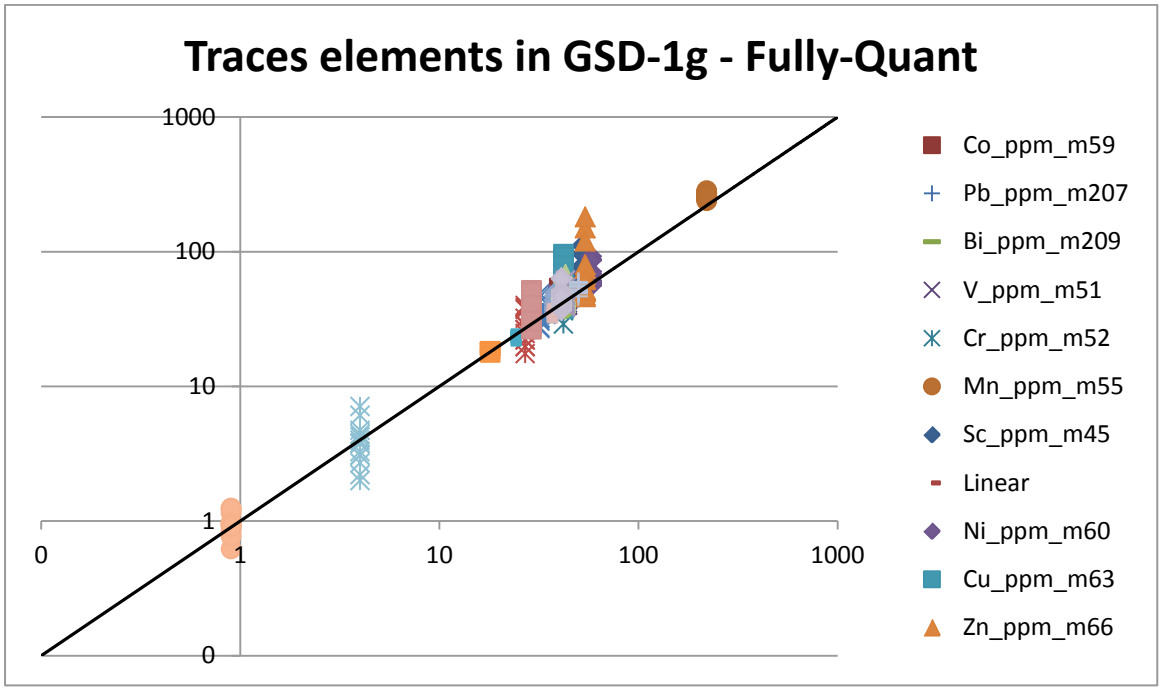

Graph 29 Major elements in GSD-1g using GSD-1e as calibrant (with internal standard) - Fully-Quant (laser ablation)

4.7.2. Mapping of soil samples with laser ablation

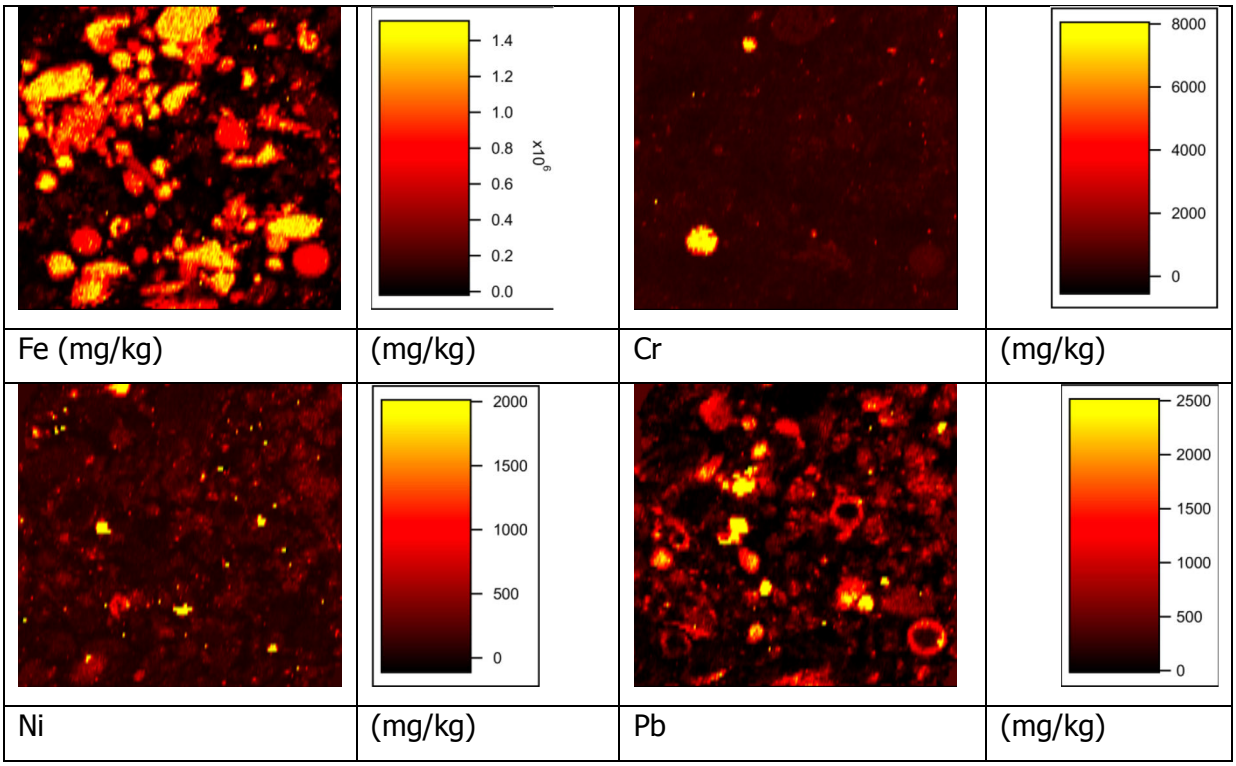

Fe (mg/kg)	(mg/kg)	Cr	(mg/kg)
Ni	(mg/kg)	Pb	(mg/kg)

Figure 2 Spherical particle with high Cr content covered by Pb, nickel in spherical and non-spherical particles (sample 1G)

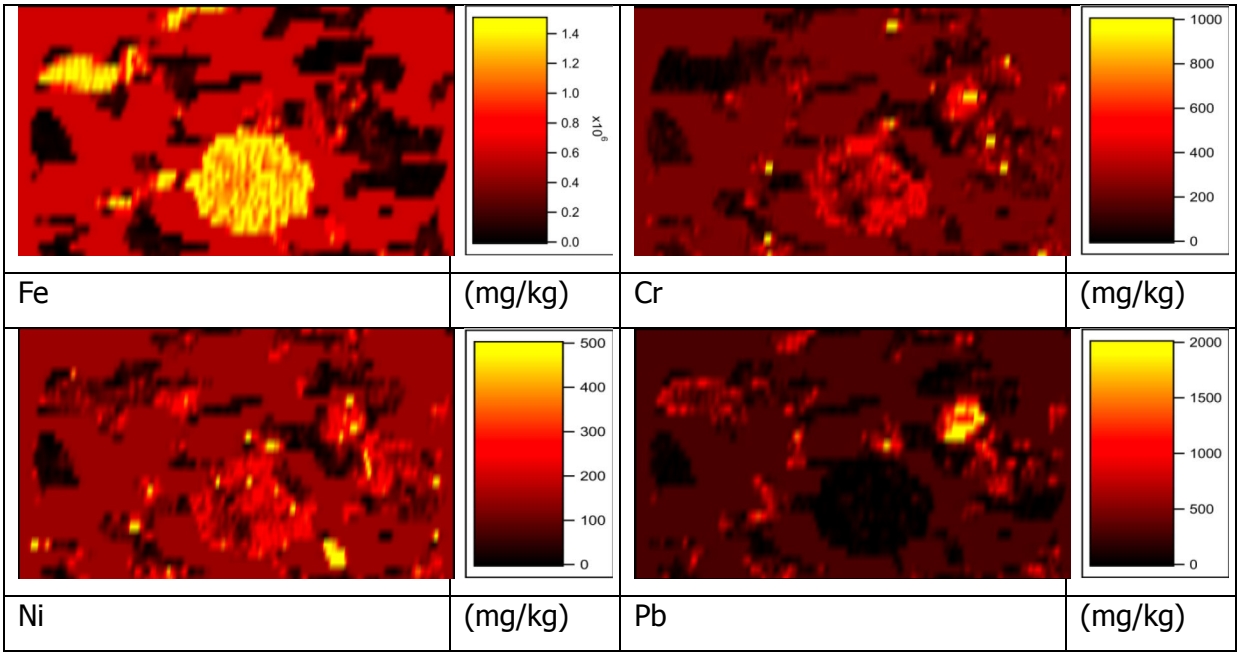

Fe	(mg/kg)	Cr	(mg/kg)
Ni	(mg/kg)	Pb	(mg/kg)

Figure 3 Magnetite with chromium and nickel in it, lead inside particles (sample 2D)

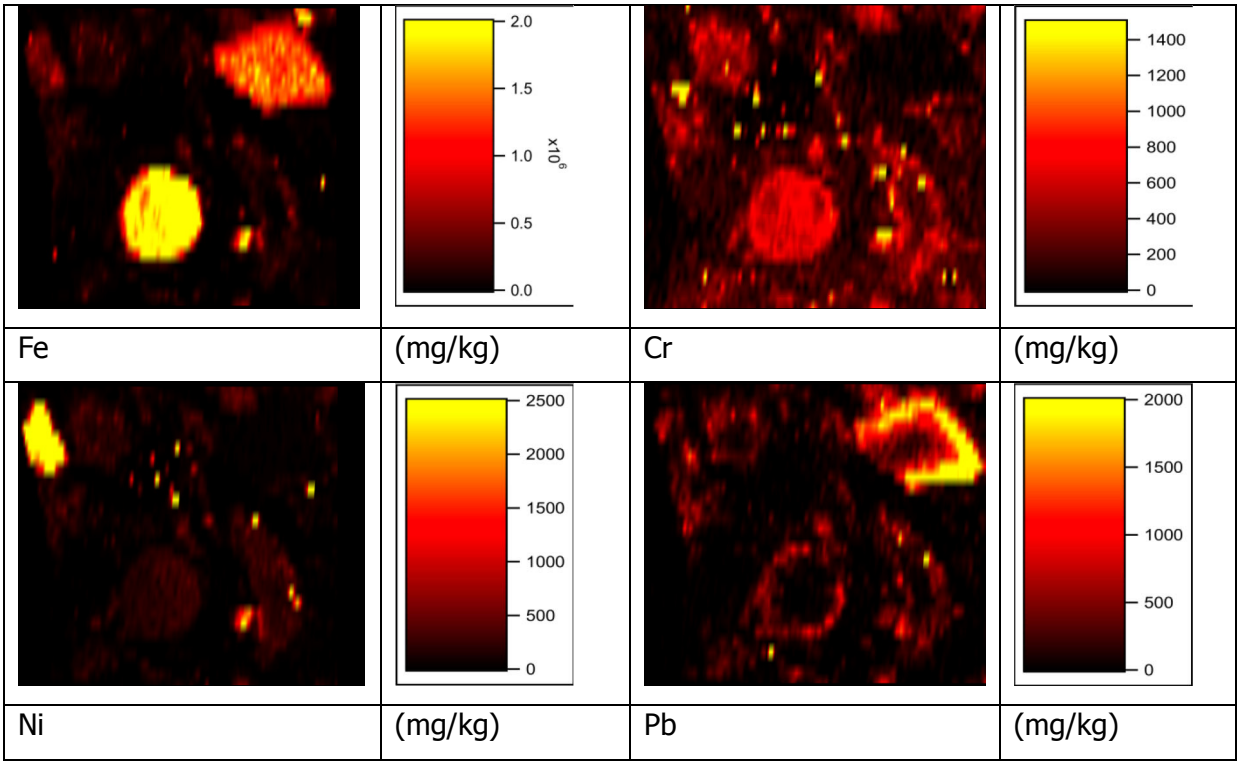

Fe	(mg/kg)	Cr	(mg/kg)
Ni	(mg/kg)	Pb	(mg/kg)

Figure 4 Nickel in spherical and as scale/flake (3E1)

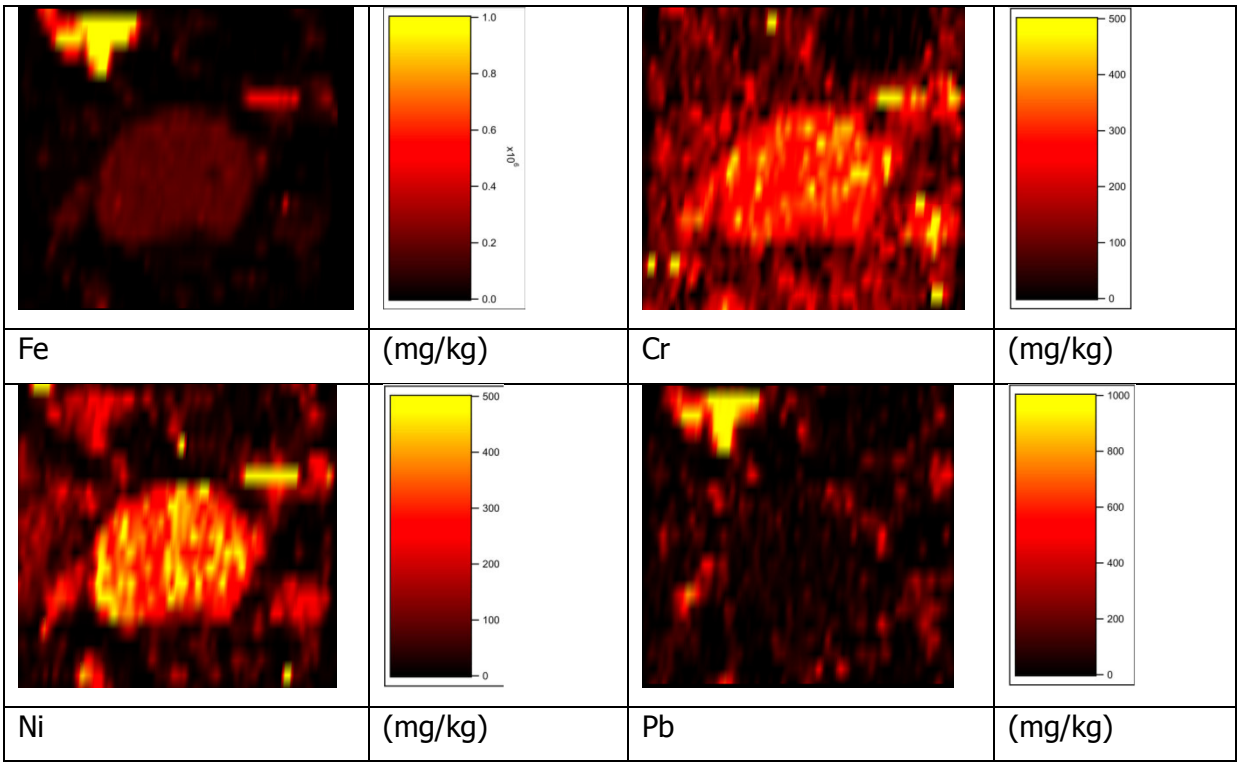

Fe	(mg/kg)	Cr	(mg/kg)
Ni	(mg/kg)	Pb	(mg/kg)

Figure 5 Nickel and chromium in spherical (broken) magnetite without Pb covering (3E2)

4.7.3. Mapping of dust sample (<125 µm)

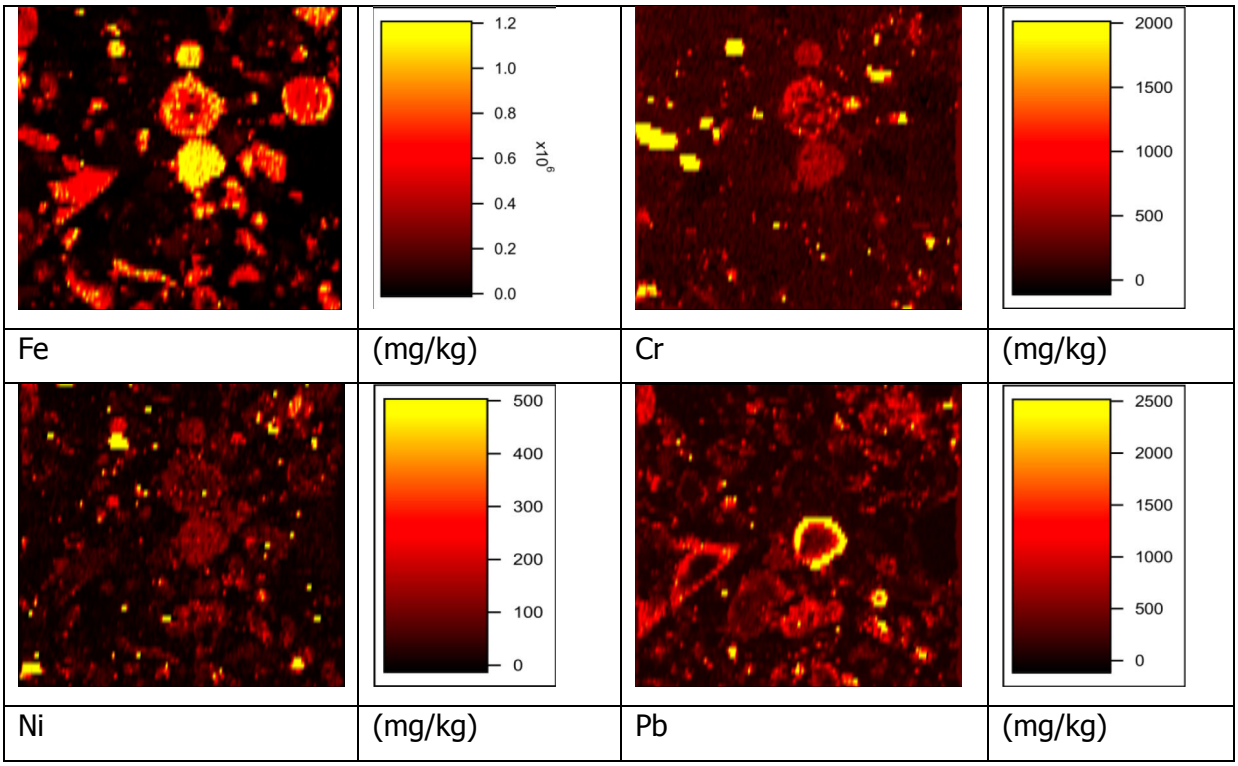

Figure 6 Magnetite containing heavy metals (Dust sample 5C)

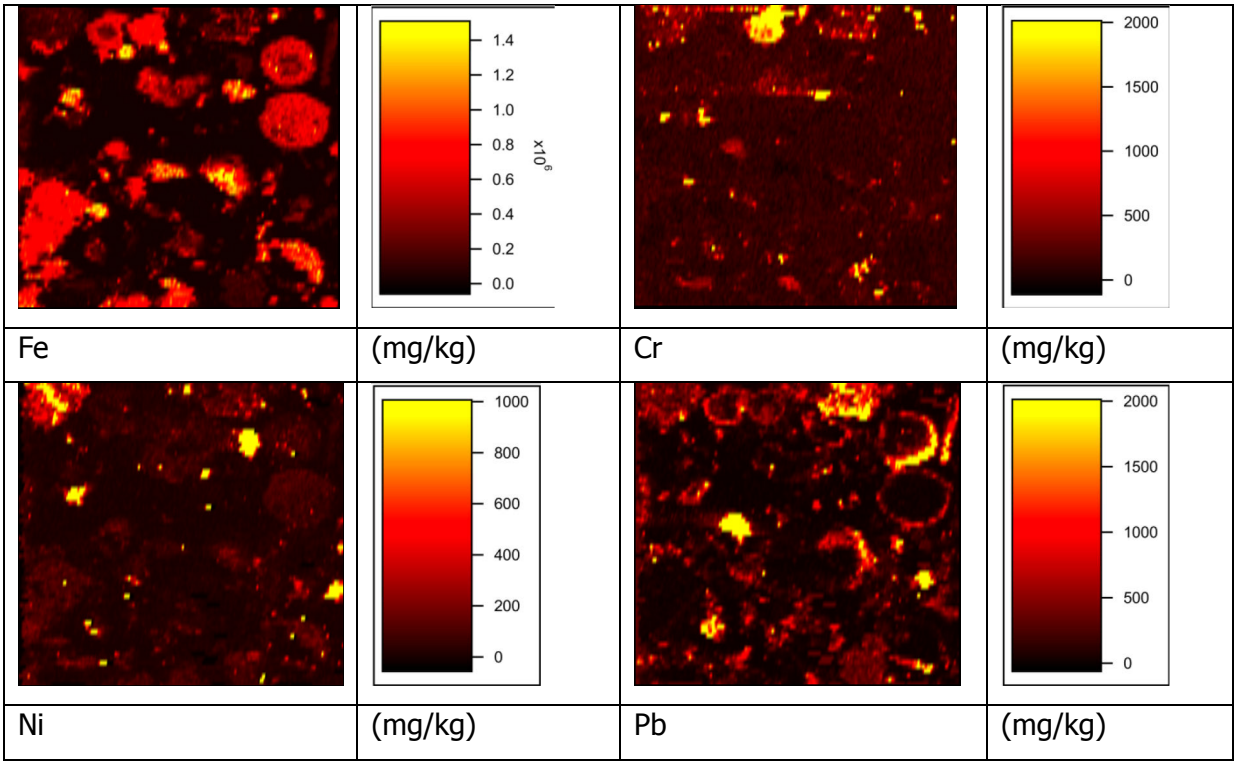

Figure 7 Dust sample containing flakes of nickel and chromium and Pb covered magnetites (5G)

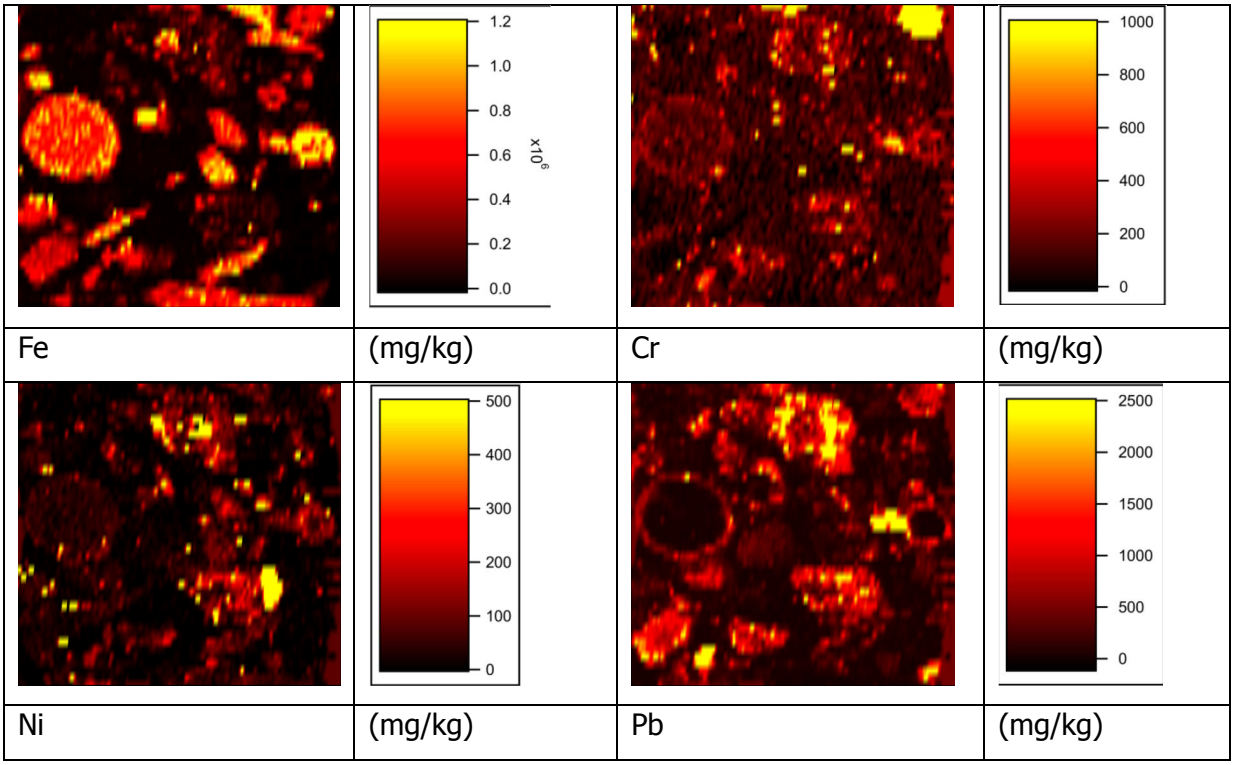

Fe	(mg/kg)	Cr	(mg/kg)
Ni	(mg/kg)	Pb	(mg/kg)

Figure 8 Magnetite covered by lead

From laser ablation study it is summarised that

- The magnetite particles contain chromium and nickel inside.
- Lead is surrounding most of the spherical and non-spherical particles in magnetic fraction as shown in Figure 2 and Figure 4. Condensation of more volatile lead on surface of sample has been identified.
- Beside spherical particles nickel and chromium were found in flakes and scales as well as shown in Figure 2-Figure 4.
- Chromium and nickel is found in magnetite spherules in both top (0-5 cm) and lower (5-10 cm) layers of soil and lead covering is also found in samples from both layer. It means that Pb covering is persistent over longer period of time.
- Dust particles which can be traced back to Voest-alpine also show similar kind of association of heavy metals (nickel and chromium) with spherical magnetites and covering of lead around them as shown in Figure 6-Figure 8.
- Some calcium rich spherules in soil and dust particles are also seen. Two of such spherules from dust samples are quantified (semi quantitative analysis) and for those two spherules, it is observed that Ca content remains same in them, but concentration of other elements, e.g., Fe, Al etc. varies as shown in Table 21.

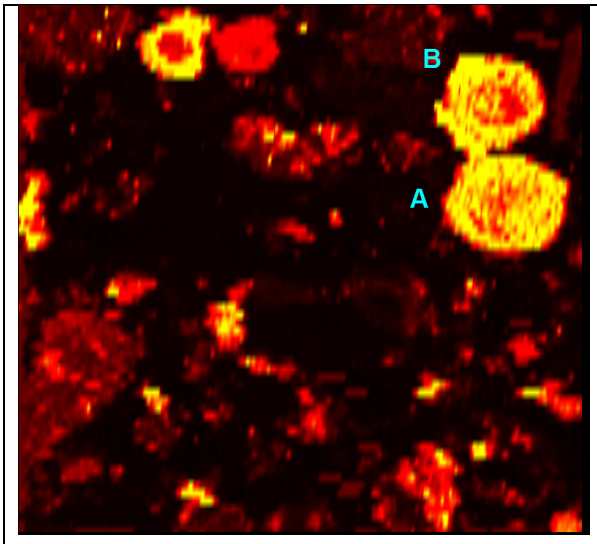

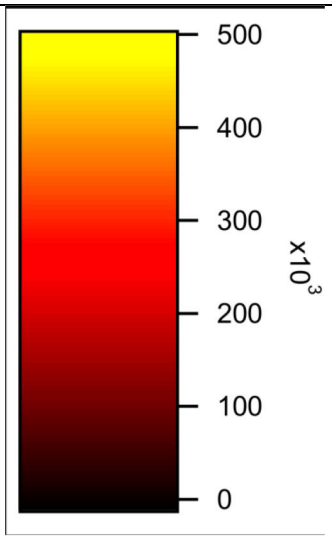

Ca	mg/kg

Figure 9 Ca-rich spherules

S.No.	Element	Spherule A concentration g/100g	Spherule B concentration g/100g
1	Mg	0.01	0.07
2	Al	3.59	1.43
3	Si	4.03	4.07
4	Ca	40.8	43.2
5	Cr	0.01	0.01
6	Mn	1.19	1.42
7	Fe	45.0	38.7
8	Ni	0.01	0.01
9	Zn	1.06	0.17

Table 21 Semi quantitative analysis of Ca-rich spherules in dust sample

5. Conclusions

Detailed geochemical, geophysical and mineralogical study on sediments of a river 'Vordernbergerbach' flowing in an alpine area of Steiermark, Austria has been made. Magnetic susceptibility meter (MS2-Bartington) with loop sensor, was used in the field and in studied river profile, areas of Vordernberg and Leoben are found with high magnetic signals 100-750 SI [10^{-5}] and 50-550 SI [10^{-5}] respectively.

Mass specific magnetic susceptibility of fine fraction of collected samples was determined in Petrophysics lab (Montanuniversität) Leoben. Mass specific susceptibility (X) showed similar trend as volume susceptibility measurements (in field) showed revealing the fact of higher values in area of Vordernberg >500 ($10^{-8}m^3$/kg) and Leoben >100 ($10^{-8}m^3$/kg). So these two areas are marked as hot spots by means of magnetic measurements.

Duplicate sediment test portion of laboratory samples from 24 points taken from Vordernbergerbach were geochemically analyzed with X-Ray Fluorescence spectrometer (XRF) and Inductively Coupled Plasma-Mass Spectrometer (ICP-MS). Concentration of iron, chromium, nickel and lead was found higher than background concentration values for Styrian soils on contaminated sites. Scatter plots between mass specific magnetic susceptibility and heavy metals showed that at contaminated sites show different trend (with higher susceptibility values) than for non-contaminated sites (with lower susceptibility values). Scatter plots indicate that the source/origin of heavy metals is different than the source of non-contaminated sites. Higher concentration values of heavy metals and magnetic susceptibility at hot spots convinces that magnetic susceptibility meter is a useful, quick and economical tool to mark the areas which are contaminated due to heavy metal's deposition caused by steel industry because of the association of heavy metals with magnetites. Average of concentration, in samples taken from area of Präbichl is decided as baseline, as there is/was not any anthropogenic source of contamination in that region. Concentrations chromium at contaminated sites 190 mg/kg at Friedauwerk location (TF1), 170 mg/kg in Leoben region (LE1) and 140 mg/kg in lower Trofaiach region (TF3-TF6) higher than safe limits (100 mg/kg) is found. Concentration of Fe_2O_3 near Friedauwerk is >8 % and >10 % in Donwaitz Leoben, which are higher than baseline of this river (6.5 %). Trofaiach and St. Peter/Freienstein contain iron bearing non-magnetic minerals. Concentration of nickel in contaminated areas is 90 mg/kg (Vordernberg region) and in Donawitz/Leoben is more but closer to safe limit (60 mg/kg). Concentration of lead at contaminated sites is 60 mg/kg and 80 mg/kg in Vordernberg and Donawitz/Leoben

respectively, which is more than normal background of Styrian soils (40 mg/kg) but still below safe limit (100 mg/kg). Concentration of zinc is found less than styrian soil's background values (140 mg/kg) in all regions except Leoben having concentration values more than the safe limit (300 mg/kg). Detailed mineralogy of contaminated sites and non-contaminated/less contaminated region between Vordernberg and Leoben is studied. The amount of heavy minerals in heavy mineral concentrate present in sediments at three sampled locations was found different i.e. 41 % at Friedauwerk, 13 % at St. Peter/Freienstein and 34 % at Leoben. The amount of sediment fraction (<1.4 mm) collected for preconcentrate of heavy minerals, in Leoben was almost double than that at Gmeingrube. Mineralogical study was done with reflection microscope and electron microprobe analyzer (EMPA) at Mineralogy institute (Montanuniversität Leoben). Maximum amount of anthropogenic particles (globular, scale, blast furnace slag, steel work slag and sinter) is found in heavy minerals, extracted from sample collected from Donawitz, relatively less at Friedauwerk and least at Gmeingrube. Anthropogenic particles which carry heavy metals in them are mostly magnetite (spherical, non-spherical), ferrosilicon, Ca-ferrite, Ca-Al ferrite, hematite, iron hydroxide, steel mill slag and iron work slag/blast furnace slag. Beside anthropogenic sources, some natural/ geogenic minerals like chromite, olivine, serpentine and rutile contain heavy metals in them. Difference in chromite type at studied locations is observed, at Gmeingrube only chromite type I is found, and sediments from Donawitz/Leoben contain chromite of both types, type I (without zinc) and type II (with zinc). All three studied sampling location have magnetite of anthropogenic origin in abundance. Abundance of geogenic magnetites at Gmeingrube are relatively more than they are found in other areas investigated in this work. Iron bearing minerals which are found in non-magnetic phase are pyrite, siderite etc. So the higher concentration level of heavy metals at contaminated sites is of anthropogenic origin mainly. The sources of anthropogenic contamination at polluted area of Vordernberg and surrounding is identified as iron activity which had been in progress in 17-19th centuries at Friedauwerk and steel production plant 'Voest-alpine' at Donawitz/Leoben.

Heavy minerals from Friedauwerk are Mn-rich because of processing siderite ore brought from Eisenerz contains high Mn content. To see the impact of steel production plant 'Voest-alpine' detailed study on soil samples from a residential area 'Judaskreuzsiedlung' situated near steel mill Donawitz/Leoben was made.

Soil samples of two depth levels, top layer (0-5 cm) and lower layer (5-10 cm) from two residential plots Judaskreuzsiedlung (JKS) 6 and JKS 8 were analyzed. Magnetic extract of

soil from suspension of soil in milli-Q water was more than 20 % for each site. Mass specific magnetic susceptibility of non-separated, magnetic and non-magnetic separation was determined with MS2-Bartington at Petrophysics lab (Montanuniversität Leoben). Mass specific susceptibility values of soil at JKS6 for non-separated measured samples lie in the range of 1500 to 3500 (10^{-8} m^3/kg), for magnetic fractions lie from 8500 to 11000 (10^{-8} m^3/kg) while for non-magnetic fraction from 250 to 550 (10^{-8} m^3/kg). Mass specific susceptibility measurements of soil at JKS8 for non-separated measured samples lie in the range of 2000 to 3000 (10^{-8} m^3/kg), for magnetic fractions lie from 7000-11000 (10^{-8} m^3/kg) and for non-magnetic fraction from 500-800 (10^{-8} m^3/kg). Concentration of heavy metals in soil was measured with XRF and ICP-MS in analytical chemistry lab (Montanuniversität Leoben). There is not any noticeable difference in concentration of heavy metals in soil from top and lower layer, showing that the extent of deposition for iron and other heavy metals is similar over a longer period of time. Concentrations of elements in soil from JKS 6 and JKS 8 are in same range. The concentration of heavy metals was more concentrated in magnetic fraction and less in non-magnetic fraction. Iron oxide is 15 g/100g in non- separated soils, <10 g/100g in non-magnetic and >30 g/100g in magnetic soils. The concentration of chromium in non-separated soil is 130 mg/kg. The average concentrations for lead and zinc soils at Judaskreuzsiedlung are 120 mg/kg and 430 mg/kg respectively. Pb was concentrated in magnetic phase more than non-magnetic i.e. lead was associated with magnetic phase. Concentration of nickel is 60 mg/kg in un-separated soil and more than 90 mg/kg in magnetic fraction while non-magnetic fraction contains less than 60 mg/kg concentration of nickel. Scatter plots and linear correlation of elements with Fe_2O_3 and with magnetic susceptibility was plotted. A perfect correlation of magnetic susceptibility and Fe_2O_3 is observed. Significant correlations of nickel and lead with Fe_2O_3 and magnetic susceptibility measurements are observed. But chromium and zinc showed different kind of correlation with magnetic susceptibility and Fe_2O_3. It is because, chromium and zinc are not only originated from anthropogenic source but also naturally present as chromite type II (with zinc) in abundance. Curie point measurement with Multi-Function Kappabridge for soils obtained ~585 °C, confirming the dominating phase of soil is magnetite. Anthropogenic globular magnetites were found in abundance and non-spherical but still anthropogenic magnetites were also observed in soil. These spherical magnetites are of various diameter sizes (<10 µm to 100 µm in sieved and grinded samples, however upper range of size can be higher as well). Morphology of spherules is also very different from each other, rimmed surface, with patches and spherules with pyramidal building units are observed.

Geogenic magnetites are there but very few as compared to abundant anthropogenic (mostly spherical) magnetite. Heavy metals are associated with spherical magnetites mainly. Laser ablation of globular magnetites confirmed the presence of Cr and Ni inside the particles. Lead was found as a covering around around anthropogenic particles of spherical and non-spherical shape. In addition to spherical particles, heavy metals are present as flakes or scales as well. Globular particles covered by Pb and having nickel and chromium inside the spherical magnetite are found in top and bottom layers (magnetic fractions). It is clear that anthropogenic deposition of heavy metals is in progress since longer time (few decades). Moreover it seems that lead is persistent over longer period of time. Some Ca-rich spherules with about 40 % calcium and varying amount of other elements, e.g., Al, Fe etc. are also observed. Particles with same type of components, with same pattern of distribution of heavy metals within the particles have been observed in dust particles as well. All the study convinces us that heavy metals especially nickel; chromium and lead are associated with anthropogenic magnetites mainly. However chromium is some time present in geogenic chromite along with zinc in them at the area of leoben. These anthropogenic particles are the carrier of heavy metals and are found in dust particles as well and can be traced back to Voest-alpine.

From all the work done it can be concluded that magnetic susceptibility meter is a useful, quick and economical tool to mark the area contaminated due to heavy metal deposition from iron and steel industry because of association of heavy metals with magnetite particles. Magnetic measurements along with geochemical measurements may indicate the different origin of minerals carrying heavy metals. Anthropogenic and geogenic minerals remain stable over river bed on sediments over centuries and remain an issue for longer period of time i.e., centuries. Lead is more stable in on surface of profile as compared to river sediments. The content of heavy metals, e.g., Pb, Zn and Fe concentration in a soil profile in the same area Donawitz/Leoben is greater than river sediments and almost similar for chromium and nickel, thus the heavy metals namely Pb, Zn and Fe are more stable in soil while nickel and chromium are equally stable in both medium.

Concentration of heavy metals and abundance of anthropogenic particles in Donawitz/Leoben show that the heavy metals deposition due to Voest-alpine is greater than the historical iron smelters in area of Vordernberg and Trofaiach. Heavy metals content in dust is even greater than the soil samples, which confirms the anthropogenic contamination of heavy metals by Voest-alpine mainly.

Since no changes in the immissions in the vicinity of the steel plant have been observed it is recommended to continue monitoring studies. Applying magnetic simple susceptibility meters is an adequate tool for mapping the extent and to quantify the immission of anthropogenic dust particles.

6. References

Agency for Toxic Substances and Disease Registry, **2000**. Case Studies in Environmental Medicine: Chromium Toxicity,, US Department of Health and Human Services, Public Health Services, pp. 1-36.

Arunachalam, R., Paulkumar, K., Ranjitsingh, A.J.A., Annadurai, G., **2009**. Environmental Assessment due to Air Pollution near Iron Smelting Industry. Journal of Environmental Science and Technology 2, 179-186.

Bityukova, L., Scholger, R., Birke, M., **1999**. Magnetic susceptibility as indicator of environmental pollution of soils in Tallinn. Physics and Chemistry of the Earth, Part A: Solid Earth and Geodesy 24, 829-835.

Blaha, U., Appel, E., Stanjek, H., **2008**. Determination of anthropogenic boundary depth in industrially polluted soil and semi-quantification of heavy metal loads using magnetic susceptibility. Environmental Pollution 156, 278-289.

Bućko, M., Magiera, T., Pesonen, L., Janus, B., **2010**. Magnetic, Geochemical, and Microstructural Characteristics of Road Dust on Roadsides with Different Traffic Volumes—Case Study from Finland. Water, Air, & Soil Pollution 209, 295-306.

Burke, T., Fagliano, J., Goldoft, M., Hazen, R.E., Iglewicz, R., McKee, T., **1991**. Chromite ore processing residue in Hudson County, New Jersey. Environ Health Perspect 92.

Canbay, M., Aydin, A., Kurtulus, C., **2010**. Magnetic susceptibility and heavy-metal contamination in topsoils along the Izmit Gulf coastal area and IZAYTAS (Turkey). Journal of Applied Geophysics 70, 46-57.

Chaparro, M., Sinito, A., Ramasamy, V., Marinelli, C., Chaparro, M., Mullainathan, S., Murugesan, S., **2008**. Magnetic measurements and pollutants of sediments from Cauvery and Palaru River, India. Environmental Geology 56, 425-437.

Chaparro, M.A.E., Bidegain, J.C., Sinito, A.M., Gogorza, C.S.G., Jurado, S., **2003**. Preliminary Results of Magnetic Measurements on Stream-Sediments from Buenos Aires Province, Argentina. Studia Geophysica et Geodaetica 47, 121-145.

Chaparro, M.A.E., Bidegain, J.C., Sinito, A.M., Jurado, S.S., Gogorza, C.S.G., **2004a**. Magnetic studies applied to different environments (soils and stream sediments) from a relatively polluted area in Buenos Aires Province, Argentina. Environmental Geology 45, 654-664.

Chaparro, M.A.E., Bidegain, J.C., Sinito, A.M., Jurado, S.S., Gogorza, C.S.G., **2004b**. Relevant Magnetic Parameters and Heavy Metals from Relatively Polluted Stream Sediments - Vertical and

Longitudinal Distribution Along a Cross-City Stream in Buenos Aires Province, Argentina. Studia Geophysica et Geodaetica 48, 615-636.

Çıftcı, H., Ölcücü, A., Çıftcı, T., **2007**. The Determination of Nickel in Some Plants with Reversed-Phase High Performance Liquid Chromatography (HPLC). International Journal of Science & Technology 2, 105-108.

Dalvi, A.D., Bacon, W.G., Osborne, R.C., **2004**. The past and the future of nickel laterites, PDAC 2004 International Convention, Trade Show & Investors Exchange, p. 27.

Darrie, G., **2001**. Commercial Extraction Technology and Process Waste Disposal in the Manufacture of Chromium chemicals From Ore. Environmental Geochemistry and Health 23, 187-193.

Desenfant, F., Petrovský, E., Rochette, P., **2004**. Magnetic Signature of Industrial Pollution of Stream Sediments and Correlation with Heavy Metals: Case Study from South France. Water, Air, & Soil Pollution 152, 297-312.

Doig, L.E., Liber, K., **2007**. Nickel speciation in the presence of different sources and fractions of dissolved organic matter. Ecotoxicology and Environmental Safety 66, 169-177.

El Baghdadi, M., Barakat, A., Sajieddine, M., Nadem, S., **2011**. Heavy metal pollution and soil magnetic susceptibility in urban soil of Beni Mellal City (Morocco). Environmental Earth Sciences, 1-15.

Environmental Protection Agency, U.S., **1991**. Nickel subsulfide (CASRN 12035-72-2) Integrated Risk Information System.

Evanko, C.R., Dzombak, D.A., **1997**. Remediation of metals-contaminated soils and groundwater, GWR Technology evaluation report. Ground-Water Remediation Technologies Analysis Center, pp. 1-53.

Farmer, J.G., Thomas, R.P., Graham, M.C., Geelhoed, J.S., Lumsdon, D.G., Paterson, E., **2002**. Chromium speciation and fractionation in ground and surface waters in the vicinity of chromite ore processing residue disposal sites. Journal of Environmental Monitoring 4, 235-243.

Frank, R., Stonefield, K.I., Suda, P., Potter, J.W., **1982**. Impact of nickel contamination on the production of vegetables on an organic soil, Ontario, Canada, 1980–1981. Science of The Total Environment 26, 41-65.

Gautam, P., Blaha, U., Appel, E., **2005**. Magnetic susceptibility of dust-loaded leaves as a proxy of traffic-related heavy metal pollution in Kathmandu city, Nepal. Atmospheric Environment 39, 2201-2211.

Georgeaud, V.M., Rochette, P., Ambrosi, J.P., Vandamme, D., Williamson, D., **1997**. Relationship between heavy metals and magnetic properties in a large polluted catchment: The Etang de Berre (south of France). Physics and Chemistry of The Earth 22, 211-214.

Gómez, V., Callao, M.P., **2006**. Chromium determination and speciation since 2000. TrAC Trends in Analytical Chemistry 25, 1006-1015.

Goodarzi, F., Huggins, F.E., Sanei, H., **2008**. Assessment of elements, speciation of As, Cr, Ni and emitted Hg for a Canadian power plant burning bituminous coal. International Journal of Coal Geology 74, 1-12.

Hanesch, M., Rantitsch, G., Hemetsberger, S., Scholger, R., **2007**. Lithological and pedological influences on the magnetic susceptibility of soil: Their consideration in magnetic pollution mapping. Science of The Total Environment 382, 351-363.

Hanesch, M., Scholger, R., Rey, D., **2003**. Mapping dust distribution around an industrial site by measuring magnetic parameters of tree leaves. Atmospheric Environment 37, 5125-5133.

Hanesch, M.H., Scholger, R.S., **2002**. Mapping of heavy metal loadings in soils by means of magnetic susceptibility measurements. Environmental Geology 42, 857-870.

Heller, F., Strzyszcz, Z., Magiera, T., **1998**. Magnetic record of industrial pollution in forest soils of Upper Silesia, Poland. J. Geophys. Res. 103, 17767-17774.

Hemetsberger, S., **2006**. Magnetic signature of pollution particles in soils. Montanuniversität Leoben, Ph.D thesis., pp 85.

Hu, S., Duan, X., Shen, M., Blaha, U., Roesler, W., Yan, H., Appel, E., Hoffmann, V., **2008**. Magnetic response to atmospheric heavy metal pollution recorded by dust-loaded leaves in Shougang industrial area, western Beijing. Chinese Science Bulletin 53, 1555-1564.

Jordanova, D., Veneva, L., Hoffmann, V., **2003**. Magnetic Susceptibility Screening of Anthropogenic Impact on the Danube River Sediments in Northwestern Bulgaria - Preliminary Results. Studia Geophysica et Geodaetica 47, 403-418.

Kapička, A., Petrovský, E., Ustjak, S., Macháčková, K., **1999**. Proxy mapping of fly-ash pollution of soils around a coal-burning power plant: a case study in the Czech Republic. Journal of Geochemical Exploration 66, 291-297.

Karimi, R., Ayoubi, S., Jalalian, A., Sheikh-Hosseini, A.R., Afyuni, M., **2011**. Relationships between magnetic susceptibility and heavy metals in urban topsoils in the arid region of Isfahan, central Iran. Journal of Applied Geophysics 74, 1-7.

Knab, M., Hoffmann, V., Petrovský, E., Kapička, A., Jordanova, N., Appel, E., **2006**. Surveying the anthropogenic impact of the Moldau river sediments and nearby soils using magnetic susceptibility. Environmental Geology 49, 527-535.

Krainer, W., **2000**. Bodenschutzbericht 2000, in: Köck, M. (Ed.). Landwirtschaftliches Versuchszentrum Steiermark, Amt der Steiermärkischen Landesregierung, p. 80.

Leece, B., Rifat, S., **1998**. Assement of potential health risk of reported soil levels of nickel, coppe and cobalt in Port Colborne and vicintiy. Ontario Ministry of the Environment; Standards Development Branch, Ontario, Canada, pp 52.

Lu, S.G., Bai, S.Q., Xue, Q.F., **2007**. Magnetic properties as indicators of heavy metals pollution in urban topsoils: a case study from the city of Luoyang, China. Geophysical Journal International 171, 568-580.

Maier, G., Scholger, R., **2004**. Demonstration of connection between pollutant dispersal and atmospheric boundary layers by use of magnetic susceptibility mapping, St. Jacob (Austria). Physics and Chemistry of the Earth, Parts A/B/C 29, 997-1009.

Maier, G., Scholger, R., Schön, J., **2006**. The influence of soil moisture on magnetic susceptibility measurements. Journal of Applied Geophysics 59, 162-175.

McNear Jr, D.H., Chaney, R.L., Sparks, D.L., **2007**. The effects of soil type and chemical treatment on nickel speciation in refinery enriched soils: A multi-technique investigation. Geochimica et Cosmochimica Acta 71, 2190-2208.

Meisel, T., Schöner, N., Paliulionyte, V., Kahr, E., **2002**. Determination of Rare Earth Elements, Y, Th, Zr, Hf, Nb and Ta in Geological Reference Materials G-2, G-3, SCo-1 and WGB-1 by Sodium Peroxide Sintering and Inductively Coupled Plasma-Mass Spectrometry. Geostandards Newsletter 26, 53-61.

MMC Norilsk Nickel, **2010**. Metals in Our Lives, Annual Review of MMC Norilsk Nickel for 2010, p. 223.

Morton-Bermea, O., Hernandez, E., Martinez-Pichardo, E., Soler-Arechalde, A.M., Santa-Cruz, R.L., Gonzalez-Hernandez, G., Beramendi-Orosco, L., Urrutia-Fucugauchi, J., **2009**. Mexico City topsoils: Heavy metals vs. magnetic susceptibility. Geoderma 151, 121-125.

Mukherjee, A.B., **1998**. Chromium in the environment of Finland. Science of The Total Environment 217, 9-19.

Nriagu, J.O., Pacyna, J.M., **1988**. Quantitative assessment of worldwide contamination of air, water and soils by trace metals. Nature 333, 134-139.

Papp, J.F., **1994**. Chromium life cycle study. Bureau of Mines, United States, pp 94.

Papp, J.F., **2012**. Chromium, U.S. Geological Survey, Mineral Commodity Summaries. USGS, pp. 42-43.

Prasad, B., Jaiprakas, K.C., **1999**. Evaluation of heavy metals in ground water near mining area and development of heavy metal pollution index. Journal of Environmental Science and Health, Part A 34, 91-102.

Reyes, B., Bautista, F., Goguitchaichvili, A., Morton, O., **2011**. Magnetic monitoring of top soils of Merida (Southern Mexico). Studia Geophysica et Geodaetica 55, 377-388.

Schmidt, A., Yarnold, R., Hill, M., Ashmore, M., **2005**. Magnetic susceptibility as proxy for heavy metal pollution: a site study. Journal of Geochemical Exploration 85, 109-117.

Shtiza, A., Swennen, R., Cappuyns, V., Tashko, A., **2009**. ANC, BNC and mobilization of Cr from polluted sediments in function of pH changes. Environmental Geology 56, 1663-1678.

Shtiza, A., Swennen, R., Tashko, A., **2005**. Chromium and nickel distribution in soils, active river, overbank sediments and dust around the Burrel chromium smelter (Albania). Journal of Geochemical Exploration 87, 92-108.

Shtiza, A., Swennen, R., Tashko, A., **2008**. Chromium speciation and existing natural attenuation conditions in lagoonal and pond sediments in the former chemical plant of Porto-Romano (Albania). Environmental Geology 53, 1107-1128.

Sponza, D., Karaoğlu, N., **2002**. Environmental geochemistry and pollution studies of Aliağa metal industry district. Environment International 27, 541-553.

Sprynskyy, M., Kosobucki, P., Kowalkowski, T., Buszewski, B., **2007**. Influence of clinoptilolite rock on chemical speciation of selected heavy metals in sewage sludge. Journal of Hazardous Materials 149, 310-316.

Strzyszcz, Z., Magiera, T., **1998**. Magnetic susceptibility and heavy metals contamination in soils of Southern Poland. Physics and Chemistry of The Earth 23, 1127-1131.

Tirez, K., Brusten, W., Cluyts, A., Patyn, J., De Brucker, N., **2003**. Determination of hexavalent chromium by species specific isotope dilution mass spectrometry and ion chromatography-1,5-diphenylcarbazide spectrophotometry. Journal of Analytical Atomic Spectrometry 18, 922-932.

Valentinuzzi, M.C., Sánchez, H.J., Abraham, J., **2006**. Total reflection X-ray fluorescence analysis of river waters in its stream across the city of Cordoba, in Argentina. Spectrochimica Acta Part B: Atomic Spectroscopy 61, 1175-1179.

Velea, T., Gherghe, L., Predica, V., Krebs, R., **2009**. Heavy metal contamination in the vicinity of an industrial area near Bucharest. Environmental Science and Pollution Research 16, 27-32.

Vitale, R.J., Mussoline, G.R., Rinehimer, K.A., **1997**. Environmental Monitoring of Chromium in Air, Soil, and Water. Regulatory Toxicology and Pharmacology 26, 80-85.

Walterson, E., Chromium, Nickel and Molybdenum In Society and the Environment, pp 26.

Wang, X., Qin, Y., **2005**. Correlation between magnetic susceptibility and heavy metals in urban topsoil: a case study from the city of Xuzhou, China. Environmental Geology 49, 10-18.

WHO, **1991**. Nickel, nickel carbonyl, and some nickel compounds health and safety guide, Health and Safety Guide. World Health Organization.

Williams, S.P., **2001**. Occupational health and speciation using nickel and nickel compounds as an example, Trace Element Speciation for Environment, Food and Health. The Royal Society of Chemistry, pp. 297-307.

Wolf, R.E., Morrison, J.M., Goldhaber, M.B., **2007**. Simultaneous determination of Cr(iii) and Cr(vi) using reversed-phased ion-pairing liquid chromatography with dynamic reaction cell inductively coupled plasma mass spectrometry. Journal of Analytical Atomic Spectrometry 22, 1051-1060.

Wuana, R.A., Okieimen, F.E., **2011**. Heavy Metals in Contaminated Soils: A Review of Sources, Chemistry, Risks and Best Available Strategies for Remediation. ISRN Ecology 2011, 20.

Yang, L., Ciceri, E., Mester, Z., Sturgeon, R., **2006**. Application of double-spike isotope dilution for the accurate determination of Cr(III), Cr(VI) and total Cr in yeast. Analytical and Bioanalytical Chemistry 386, 1673-1680.

Yang, T., Liu, Q., Chan, L., Liu, Z., **2007**. Magnetic signature of heavy metals pollution of sediments: case study from the East Lake in Wuhan, China. Environmental Geology 52, 1639-1650.

Appendix

Sample Protocols

Date	20090923
Time	12:00
Sample ID	PB/1/V(20m)/ 090923/S/O
Collected by	MII + FRIPI
Place/Location	Between Leobnerhütte and Hirscheggsttl
GPS Data	N47° 32.134' E 14° 58.353' Precise Position: 47.535567, 14.972633
Photo Number	102 – 0125
Temperature	17 °C
Sediments description	Dry, Coarser, light brown
Magnetic Susceptibility Readings on MS2 meter	4.3 4.3 4.5 2.3 2.5 3.1 1.6 2.9 2.6 2.6 4.8 2.6 2.9 3.3 2.0 2.3 2.0 2.4 1.6 1.7 2.0

Date	20090916
Time	10:58
Sample ID	PB/2/VI(40m)/ 090916/SF/O
Collected by	MII + FRIPI
Place/Location	Crossing over Handlgraben and way to Leobnerhütte
GPS Data	N47° 31.995' E 14° 58.762' Precise Position: 47.53325, 14.979583
Photo Number	102 – 0074
Temperature	12 °C
Sediments description	Fine: Light brown Coarser: Dark brown with light inclusion
Magnetic Susceptibility Readings on MS2 meter	8.8 9.5 10.2 10.7 7.1 7.1 5.0 5.6 5.5 6.2 6.2 7.2 7.2 5.2 7.2 3.1 5.1 5.2 6.0

Date	20090909
Time	11:54
Sample ID	PB/3/X(30m)/ 090909/SF/O
Collectedby	MII + FRIPI
Place/Location	Downstream from Handlgraben (crossing near pedestrian path)
GPS Data	N47° 31.896' E 14° 58.601' Precise Position: 47.5316, 14.976617
PhotoNumber	101 – 0991 to 102 – 0073
Temperature	15 °C
Sediments description	<150 µm light brown <2 mm dark brown + light brown with inclusions
Magnetic Susceptibility Readings on MS2 meter	1.9 5.3 4.5 5.1 4.1 5.2 5.6 5.7 5.6 2.8 2.8 7.8 7.7 7.7 2.7 2.7 3.3 3.3 5.9 5.9 <2mm 5.4 5.0 5.6 5.6 5.6

Date	20090930
Time	11:50
Sample ID	PB/4/V(30m)/090930/S/O
Collectedby	MII + FRIPI
Place/Location	Bridge near Almhäuser
GPS Data	N47° 31.095' E 14° 58.405' Precise Position: 47.518267, 14.973550
PhotoNumber	102 – 0169
Temperature	20 °C
Sediments description	Light brown sediments (fine and coarser)
Magnetic Susceptibility Readings on MS2 meter	2.9 4.2 2.3 2.4 3.3 3.6 2.9 8.6 9.2 9.1 4.2 3.7 3.1 3.3 7.2 7.4 6.2 4.3 3.0 2.2 4.6 3.5 4.8

Date	20091118
Time	12:30
Sample ID	PB/5/IV(30m)/ 091118/S/O
Collectedby	MII + FRIPI
Place/Location	Downstream (Almhäuser)
GPS Data	N47° 30.832' E 14° 58.521' Precise Position: 47.513867, 14.973933
PhotoNumber	102 – 0970 to 102 – 0977 102 – 0978 to 102 – 0983
Temperature	6 °C
Sediments description	Coarser: Dark brown-black Fine: Finer than (PB1 to PB4)
Magnetic Susceptibility Readings on MS2 meter	43.8 46.8 35.1 38.2 12.0 12.4 20.9 21.2 22.4 62.8 73.6 20.3 26.3 19.9

Date	20091118
Time	11:25
Sample ID	PB/6/VI(20m)/091118/S/O
Collectedby	MII + FRIPI
Place/Location	Upstream power plant Steinhaus
GPS Data	N47° 30.646' E 14° 58.734' Precise Position: 47.510817, 14.976800
PhotoNumber	102 – 0961 to 102 – 0969; 102 – 0984; 102 – 0988 to 102 – 0990; 102 – 0993 to 102 – 0994; 103 – 0028
Temperature	6 °C
Sediments description	Black sediments with light inclusions
Magnetic Susceptibility Readings on MS2 meter	23.0 25.3 27.2 28.1 28.0 13.9 7.5 10.0 20.5 20.7 20.3 23.3 21.4 55.3 55.2 38.9

Date	20091118
Time	11:35
Sample ID	PB/7/IV(10m)/ 091118/S/O
Collectedby	MII + FRIPI
Place/Location	Wegscheid
GPS Data	N47° 30.382' E 14° 59.104' Precise Position: 47.506367, 14.983417
PhotoNumber	102 – 0951 to 102 – 0960 102 – 0991 to 102 – 0992
Temperature	6 °C
Sediments description	Sieved in lab with river water Brown mud with light stones
Magnetic Susceptibility Readings on MS2 meter	45.4 45.6 45.6 38.0 26.5 25.3 26.0 41.7 41.9 45.7 69.4 65.3 65.4

Date	20091202
Time	11:05
Sample ID	VB/1/IV(15m)/091202/S/O
Collectedby	MII + FRIPI
Place/Location	Vordernberg – St. Laurenti
GPS Data	N47° 30. 086' E 14° 59.375' Precise Position: 47.500717, 14.988767
PhotoNumber	103 – 0001 to 103 – 0027 103 – 0035 to 103 – 0038
Temperature	2 °C
Sediments description	Light Brown, lighter inclusions
Magnetic Susceptibility Readings on MS2 meter	17.3 19.0 25.2 20.4 27.1 67.1 49.6 57.1 33.6 40.3 34.4

Date	20091202
Time	12:15
Sample ID	VB/2/IV(10m)/ 091202/S/O
Collectedby	MII + FRIPI
Place/Location	Vordernberg (Laurentistraße)
GPS Data	N47° 29.846' E 14° 59.513' Precise Position: 47.497433, 14.990708
PhotoNumber	103 – 0012 to 103 – 0020 103 – 0032 to 103 – 0034
Temperature	2 °C
Sediments description	Fine sediments: brown with inclusions Roots and worms
Magnetic Susceptibility Readings on MS2 meter	129.4 128.2 121.8 51.4 75.0 65.1 65.7 70.1 109.1 101.7

Date	20091202
Time	10:00
Sample ID	VB/3/IV(20m)/ 091202/S/O
Collectedby	MII + FRIPI
Place/Location	Vordernberg (Municipal waste point)
GPS Data	N47° 29.474' E 14° 59.712' Precise Position: 47.491250, 14.994067
PhotoNumber	103 – 0005; 103 – 0011 103 – 0029; 103 – 0031
Temperature	2 °C
Sediments description	Coarse, colored
Magnetic Susceptibility Readings on MS2 meter	98.2 118.6 127.7 92.2 116.9 592.5 713.2 746.8 175.7 164.2

Date	20091209
Time	12:10
Sample ID	VB/4/III(10m)/ 091209/S/O
Collectedby	MII + FRIPI
Place/Location	Parking place near Barbara Saale
GPS Data	N47° 29.121' E 14° 59.546' Precise Position: 47.485383, 14.991450
PhotoNumber	103 – 0048 to 103 – 0054; 104 – 0058; 103 – 0059
Temperature	2 °C
Sediments description	Brown mud with worms and insects
Magnetic Susceptibility Readings on MS2 meter	298.3 71.4 223.5 525.9 663.9 805.1 481.4 126.9

Date	20091209
Time	11:15
Sample ID	VB/5/III(5m)/091209/S/O
Collectedby	MII + FRIPI
Place/Location	Vordernberg near railway bridge
GPS Data	N47° 28.945' E 14° 59.401' Precise Position: 47.482417, 14.988983
PhotoNumber	103 – 0043 to 103 – 0047; 103 – 0060; 103 – 0061
Temperature	3 °C
Sediments description	Much coarser, light colored sediments
Magnetic Susceptibility Readings on MS2 meter	272.4 159.4 415.2 547.6 521.6 620.9 257.6 294.5

Date	20091209
Time	10:45
Sample ID	VB/6/V(10m)/ 091209/S/O
Collectedby	MII + FRIPI
Place/Location	Upstream near railway station in Vordernberg
GPS Data	N47° 28.510' E 14° 59.299' Precise Position: 47.475133, 14.987233
PhotoNumber	103 – 0039 to 103 – 0042; 103 – 0062 to 103 – 0064
Temperature	4 °C
Sediments description	Much coarser, colored, light
Magnetic Susceptibility Readings on MS2 meter	423.2 675.7 629.6 96.2 132.2 467.5 478.1 910.7 920.4 326.3 348.9

Date	20100921
Time	10:15
Sample ID	TF/1/V(15m)/100921/S/O
Collectedby	MII + FRIPI
Place/Location	Friedauwerk
GPS Data	N47° 27′ 24.7″ E 14° 59′ 45.1″ Precise Position: 47.454083, 14.996740
PhotoNumber	103 – 0894 to 103 – 0900; 103 – 0913 to 103 – 0914; 103 – 0936 to 103 – 0938; 103 – 0968 to 103 – 0969
Temperature	12 °C
Sediment Description	colored
Magnetic Susceptibility Readings on MS2 meter	656.9 669.7 674.4 756.5 746.5 757.2 444.2 423.4 424.3 427.8 427.6 208.6 208.3

Date	20100921
Time	12:15
Sample ID	TF/2/V(20m)/100921/S/O
Collectedby	MII + FRIPI
Place/Location	Hafning – Gemeindeamt
GPS Data	N47° 26′ 28.7″ E 14° 59′ 58.8″ Precise Position: 47.439417, 14.999800
PhotoNumber	103 – 0901 to 103 – 0905; 103 – 0970; 103 – 0977 103 – 0919; 103 – 0937; 103 – 0939
Temperature	14 °C
Sediment Description	Very fine, brown
Magnetic Susceptibility Readings on MS2 meter	47.4 47.6 49.6 46.1 49.3 44.7 43.8 25.1 25.0 25.1 29.6 29.7 137.1 134.1 135.6 45.4 44.4

Date	20100921
Time	13:00
Sample ID	TF/3/III(2m)/100921/S/O
Collectedby	MII + FRIPI
Place/Location	South of police station in Trofaiach
GPS Data	N47° 25′ 53.0″ E 15° 00′ 27.0″ Precise Position: 47.424967, 15.004500
PhotoNumber	103 – 906 to 103 – 912; 104 – 0062; 104 – 0063; 103 – 916; 103 – 972; 103 – 973
Temperature	16 °C
Sediment Description	Fine and coarser sediments: mixed
Magnetic Susceptibility Readings on MS2 meter	47.6 47.7 45.5 54.1 43.8 571.2 322.8 988.2

Date	20100928
Time	12:15
Sample ID	TF/4/III(1m)/100928/S/O
Collectedby	MII + FRIPI
Place/Location	In front of veterinary clinic Hüttor
GPS Data	N47° 25′ 37.6″ E 15 00′ 38.2″ Precise Position: 47.424800, 15.006367
PhotoNumber	103 – 0959 to 103 – 0962; 104 – 0064; 103 – 967; 104 – 0068
Temperature	13 °C
Sediment Description	Coarser and fine (mixed)
Magnetic Susceptibility Readings on MS2 meter	41.8 42.1 42.2 75.4 83.7 83.8 48.6 46.7

Date	20100928
Time	11:40
Sample ID	TF/5/II(2m)/100928/S/O
Collectedby	MII + FRIPI
Place/Location	Behind pharmacy Trofaiach (2nd order stream)
GPS Data	N47° 25' 33.4" E 15° 00' 1.4" Precise Position: 47.425250, 15.002667
PhotoNumber	103 – 0950 to 103 – 0958; 103 – 0974; 104 – 0069; 104 – 0065
Temperature	12.5 °C
Sediment Description	Much coarser fraction is available. Fine sediments are rare here.
Magnetic Susceptibility Readings on MS2 meter	5.2 5.3 5.5 3.3 3.8 3.9

Date	20100928
Time	11:00
Sample ID	TF/6/II(1m)/100928/S/O
Collectedby	MII + FRIPI
Place/Location	South of Trofaiach. Crossing of Lanital and bus stop "Gmeingrube"
GPS Data	N47° 24' 44.0" E 15° 01' 31.2" Precise Position: 47.412222, 15.022870
PhotoNumber	103 – 0942 to 103 – 0944; 103 – 0944; 104 – 0066; 104 – 0070; 104 – 0075
Temperature	12 °C
Sediment Description	Coarse, dark sediments with light stones
Magnetic Susceptibility Readings on MS2 meter	116.2 124.5 126.1 (measured in bucket)

Date	20101011
Time	13:50
Sample ID	SP/1/I(1m)/101011/S/O
Collectedby	MII + FRIPI
Place/Location	(St. Peter Freienstein) North of round about near water fall (closer to water flow measuring station)
GPS Data	N47° 23' 41.6" E 15° 02' 2.2" Precise Position: 47.390517, 15.038000
PhotoNumber	104 – 0159 to 104 – 0169 104 – 0216; 104 – 0212
Temperature	13.5 °C
Sediment Description	Fine sediment are abundant
Magnetic Susceptibility Readings on MS2 meter	9.6 9.5 9.5

Date	20101011
Time	13:15
Sample ID	SP/2/IV(0m)/ 101011/S/O
Collectedby	MII + FRIPI
Place/Location	South of St. Peter Freienstein. North of Voest alpine. near sports ground
GPS Data	N47° 23' 29.4" E 15° 02' 19.2" Precise Position: 47.390944, 15.03778
PhotoNumber	104 – 0156 to 104 – 0158; 104 – 0770; 104 – 0171; 104 – 0218; 104 – 0219
Temperature	13 °C
Sediment Description	Very fine and dark grey sediments
Magnetic Susceptibility Readings on MS2 meter	15.8 15.9 16.0 19.1 19.2 19.3 20.1 20.1 22.8 23.4 23.5 23.5

Date	20101011
Time	12:15
Sample ID	SP/3/VI(10m)/ 101011/S/O
Collectedby	MII + FRIPI
Place/Location	Donawitz
GPS Data	N47° 23′ 19.8″ E 15° 02′ 49.5″ Precise Position: 47.386000, 15.04579
PhotoNumber	104 – 0151 to 104 – 0155; 104 – 0172 to 104 – 0173; 104 – 0220 to 104 – 0221
Temperature	7.5 °C
Sediment Description	Less sediments, much coarser particles are present which seem like soil rather than sediments
Magnetic Susceptibility Readings on MS2 meter	9.4 9.5 9.6 9.4 9.5 9.5 48.2 48.1 37.8 37.9 95.3 95.3 31.8 31.8

Date	20101104
Time	10:45
Sample ID	LE/1/V(12m)/101104/S/O
Collectedby	MII + FRIPI
Place/Location	Judaskreuzsiedlung (Leoben)
GPS Data	N47° 22.688′ E 15° 04.757′ Precise Position: 47.378199, 15.079411
PhotoNumber	104 – 0266 to 104 – 0272; 104 – 0276 to 104 – 0277; 104 – 0356 to 104 – 0357; 104 – 0289
Temperature	10 °C
Sediment Description	Fine, Grey, compact
Magnetic Susceptibility Readings on MS2 meter	146.0 150.5 153.0 141.8 142.0 141.3 446.0 449.1 465.2 272.5 275.1 275.6 45.1 45.2 45.2

Date	20101104
Time	11:30
Sample ID	LE/2/III(4m)/ 101104/S/O
Collected by	MII + FRIPI
Place/Location	Leoben (near Interspar) along with small gardens
GPS Data	N 47° 22.797′ E 15° 05.366′ Precise Position: 47.379935, 15.089425
Photo Number	104 – 0273 to 104 – 0275; 104 – 0427 to 104 – 0428; 104 – 0278 to 104 – 0279; 104 – 0286
Temperature	13 °C
Sediment Description	Good, fine and abundant of sediments are present here
Magnetic Susceptibility Readings on MS2 meter	306.5 302.6 299.8 623.3 623.7 620.0 182.9 189.7 190.8

Maps

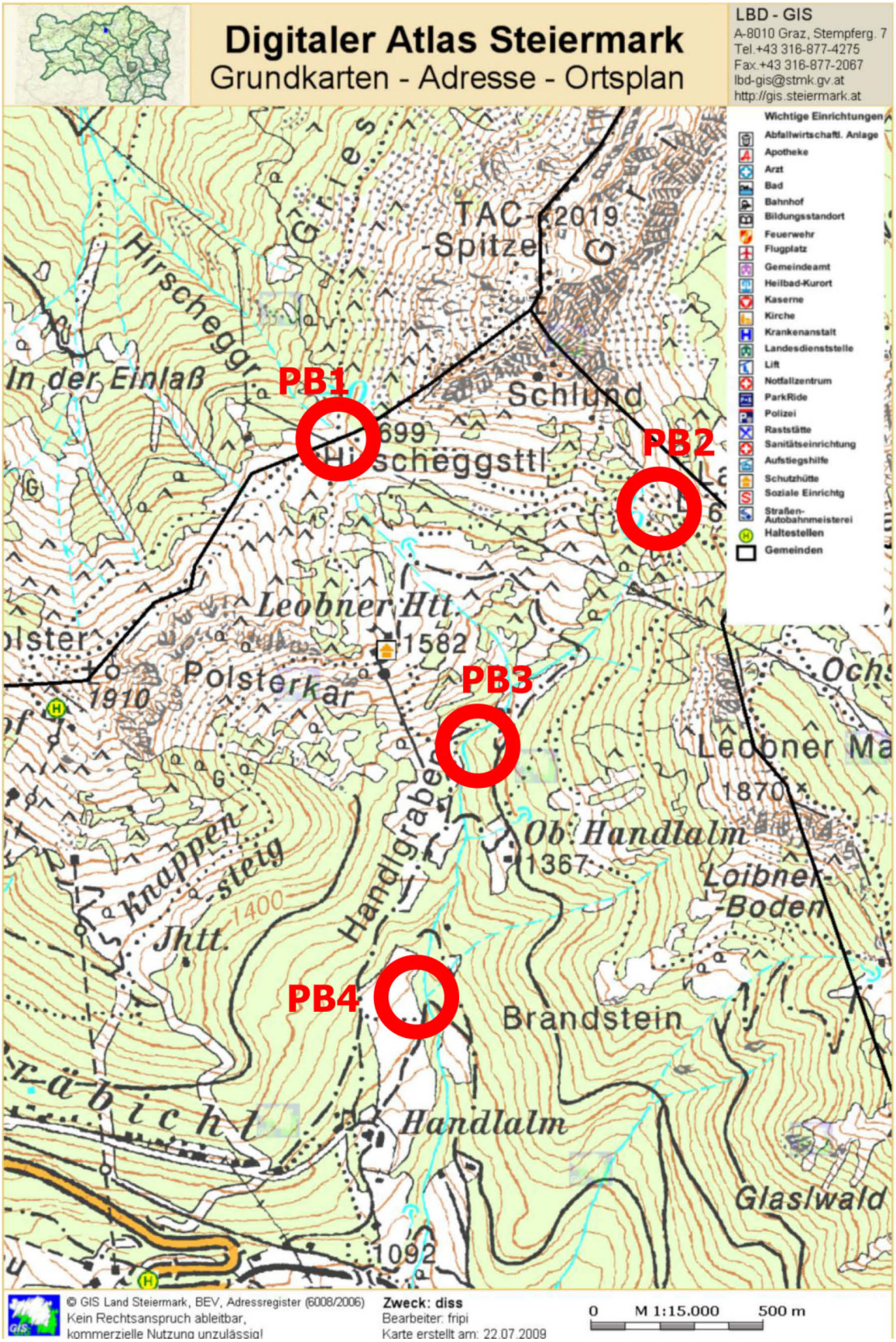
Digitaler Atlas Steiermark
Grundkarten - Adresse - Ortsplan
LBD - GIS
A-8010 Graz, Stempferg. 7
Tel.+43 316-877-4275
Fax.+43 316-877-2067
lbd-gis@stmk.gv.at
http://gis.steiermark.at
Wichtige Einrichtungen
Abfallwirtschaftl. Anlage
Apotheke
Arzt
Bad
Bahnhof
Bildungsstandort
Feuerwehr
Flugplatz
Gemeindeamt
Heilbad-Kurort
Kaserne
Kirche
Krankenanstalt
Landesdienststelle
Lift
Notfallzentrum
ParkRide
Polizei
Raststätte
Sanitätseinrichtung
Aufstiegshilfe
Schutzhütte
Soziale Einrichtg
Straßen-Autobahnmeisterei
Haltestellen
Gemeinden
PB1
PB2
PB3
PB4
In der Einlaß
Hirscheggr.
Gries
TAC-Spitze
2019
Schlund
699
Hirscheggsttl.
Leobner Htl.
1582
Polsterkar
1910
Handlgraben
Ob. Handlalm
1367
Loibner-Boden
1870
Knappen-steig
Jhtt.
1400
Brandstein
Handlalm
Glaslwald
1092
© GIS Land Steiermark, BEV, Adressregister (6008/2006)
Kein Rechtsanspruch ableitbar,
kommerzielle Nutzung unzulässig!
Zweck: diss
Bearbeiter: fripi
Karte erstellt am: 22.07.2009
0
M 1:15.000
500 m

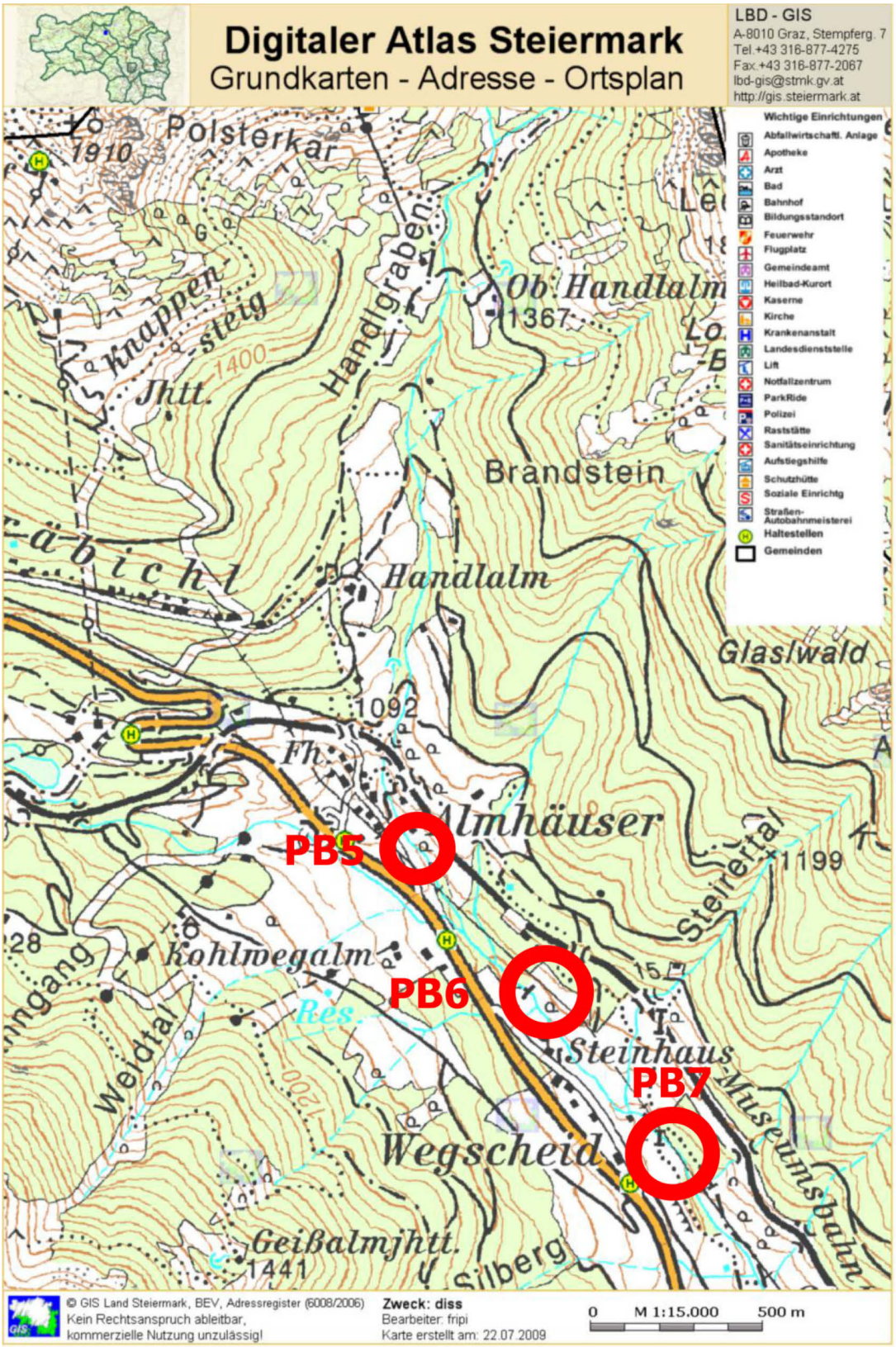
Digitaler Atlas Steiermark
Grundkarten - Adresse - Ortsplan
LBD - GIS
A-8010 Graz, Stempferg. 7
Tel.+43 316-877-4275
Fax.+43 316-877-2067
lbd-gis@stmk.gv.at
http://gis.steiermark.at
Wichtige Einrichtungen
Abfallwirtschaftl. Anlage
Apotheke
Arzt
Bad
Bahnhof
Bildungsstandort
Feuerwehr
Flugplatz
Gemeindeamt
Heilbad-Kurort
Kaserne
Kirche
Krankenanstalt
Landesdienststelle
Lift
Notfallzentrum
ParkRide
Polizei
Raststätte
Sanitätseinrichtung
Aufstiegshilfe
Schutzhütte
Soziale Einrichtg
Straßen-Autobahnmeisterei
Haltestellen
Gemeinden
Polsterkar
1910
Knappen-steig
Jhtt.
1400
Handlgraben
Ob. Handlalm
1367
Brandstein
Handlalm
Glaslwald
1092
Fh.
Almhäuser
PB5
1199
Steirertal
Kohlwegalm
PB6
Res.
Steinhaus
PB7
Weidtal
Wegscheid
Geißalmjhtt.
1441
Silberg
Museumsbahn
© GIS Land Steiermark, BEV, Adressregister (6008/2006)
Kein Rechtsanspruch ableitbar,
kommerzielle Nutzung unzulässig!
Zweck: diss
Bearbeiter: fripi
Karte erstellt am: 22.07.2009
0
M 1:15.000
500 m

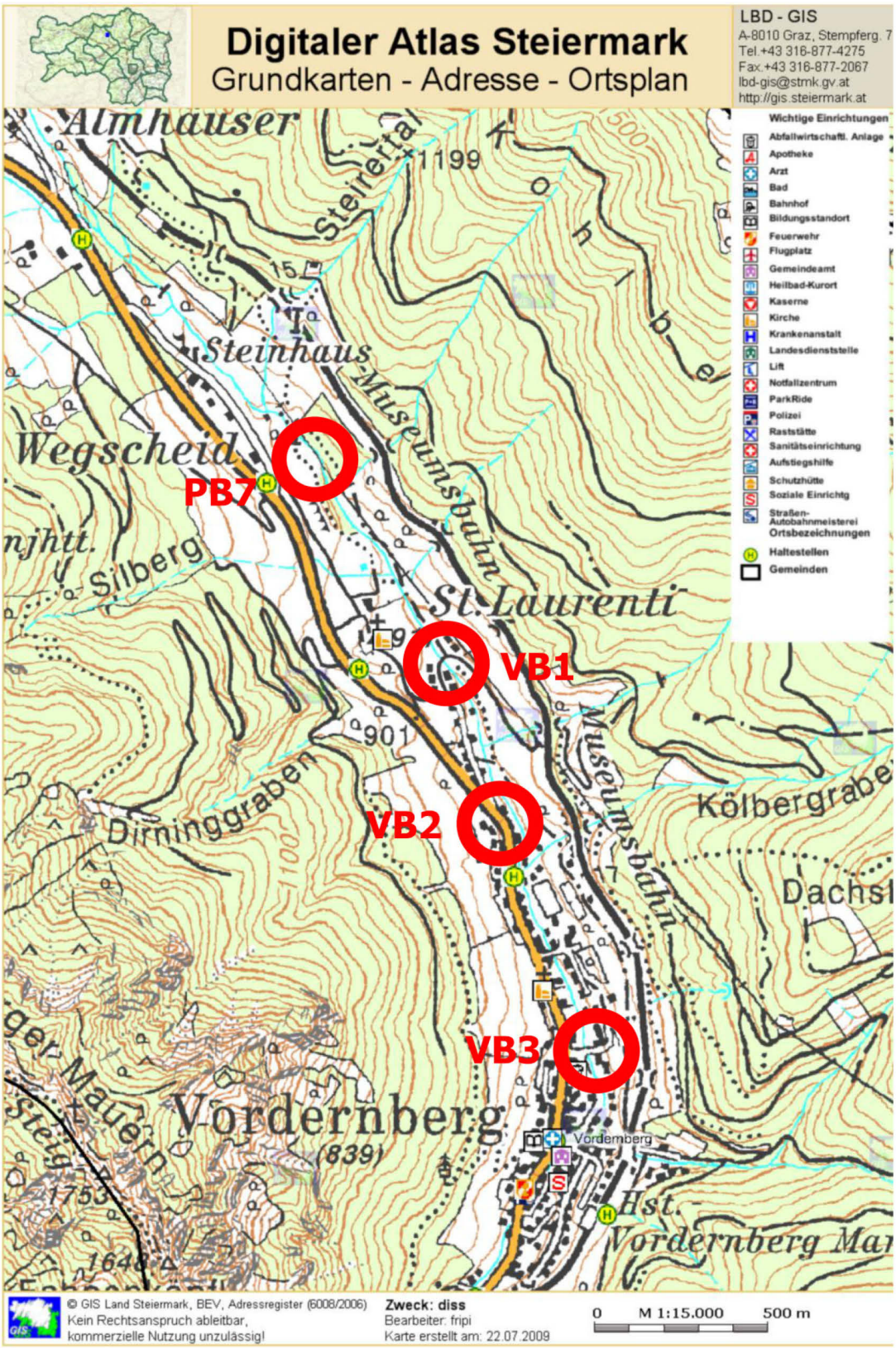
Digitaler Atlas Steiermark
Grundkarten - Adresse - Ortsplan
LBD - GIS
A-8010 Graz, Stempferg. 7
Tel.+43 316-877-4275
Fax.+43 316-877-2067
lbd-gis@stmk.gv.at
http://gis.steiermark.at
Wichtige Einrichtungen
Abfallwirtschaftl. Anlage
Apotheke
Arzt
Bad
Bahnhof
Bildungsstandort
Feuerwehr
Flugplatz
Gemeindeamt
Heilbad-Kurort
Kaserne
Kirche
Krankenanstalt
Landesdienststelle
Lift
Notfallzentrum
ParkRide
Polizei
Raststätte
Sanitätseinrichtung
Aufstiegshilfe
Schutzhütte
Soziale Einrichtg
Straßen-Autobahnmeisterei
Ortsbezeichnungen
Haltestellen
Gemeinden
Almhauser
Steiertal
1199
Steinhaus
Museumsbahn
Wegscheid
PB7
Silberg
St.Laurenti
VB1
901
VB2
Dirninggraben
Kölbergrabe
Dachsl
VB3
Vordernberg
(839)
Vordernberg
Hst.
1753
1648
© GIS Land Steiermark, BEV, Adressregister (6008/2006)
Kein Rechtsanspruch ableitbar,
kommerzielle Nutzung unzulässig!
Zweck: diss
Bearbeiter: fripi
Karte erstellt am: 22.07.2009
0
M 1:15.000
500 m

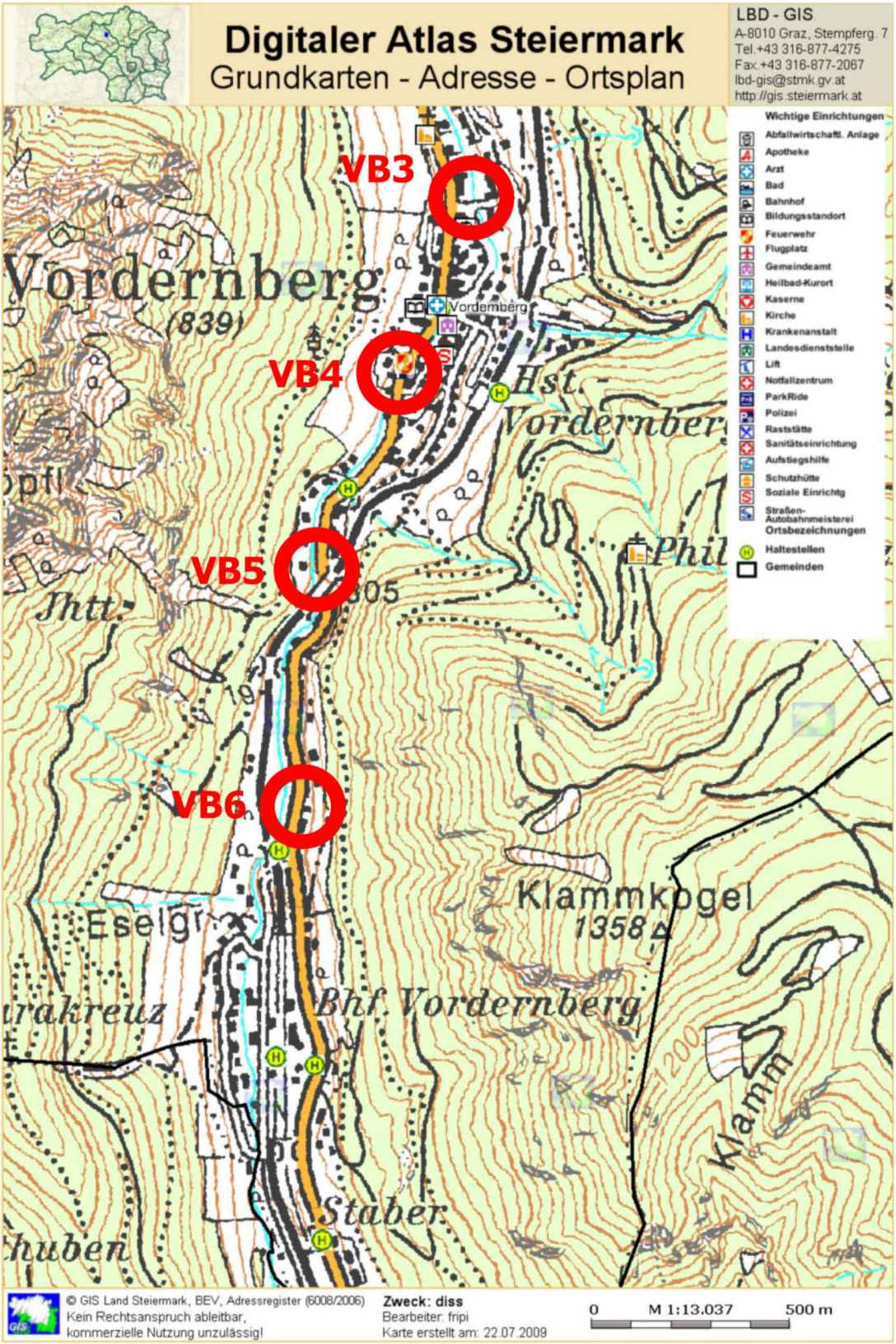
Digitaler Atlas Steiermark
Grundkarten - Adresse - Ortsplan
LBD - GIS
A-8010 Graz, Stempferg. 7
Tel.+43 316-877-4275
Fax.+43 316-877-2067
lbd-gis@stmk.gv.at
http://gis.steiermark.at
VB3
VB4
VB5
VB6
Vordernberg
(839)
Vordernberg
Hst. Vordernberg
Klammkogel
1358
Bhf. Vordernberg
Staber
Eselgr
Klamm
Wichtige Einrichtungen
Abfallwirtschaftl. Anlage
Apotheke
Arzt
Bad
Bahnhof
Bildungsstandort
Feuerwehr
Flugplatz
Gemeindeamt
Heilbad-Kurort
Kaserne
Kirche
Krankenanstalt
Landesdienststelle
Lift
Notfallzentrum
ParkRide
Polizei
Raststätte
Sanitätseinrichtung
Aufstiegshilfe
Schutzhütte
Soziale Einrichtg
Straßen-Autobahnmeisterei
Ortsbezeichnungen
Haltestellen
Gemeinden
© GIS Land Steiermark, BEV, Adressregister (6008/2006)
Kein Rechtsanspruch ableitbar,
kommerzielle Nutzung unzulässig!
Zweck: diss
Bearbeiter: fripi
Karte erstellt am: 22.07.2009
0
M 1:13.037
500 m

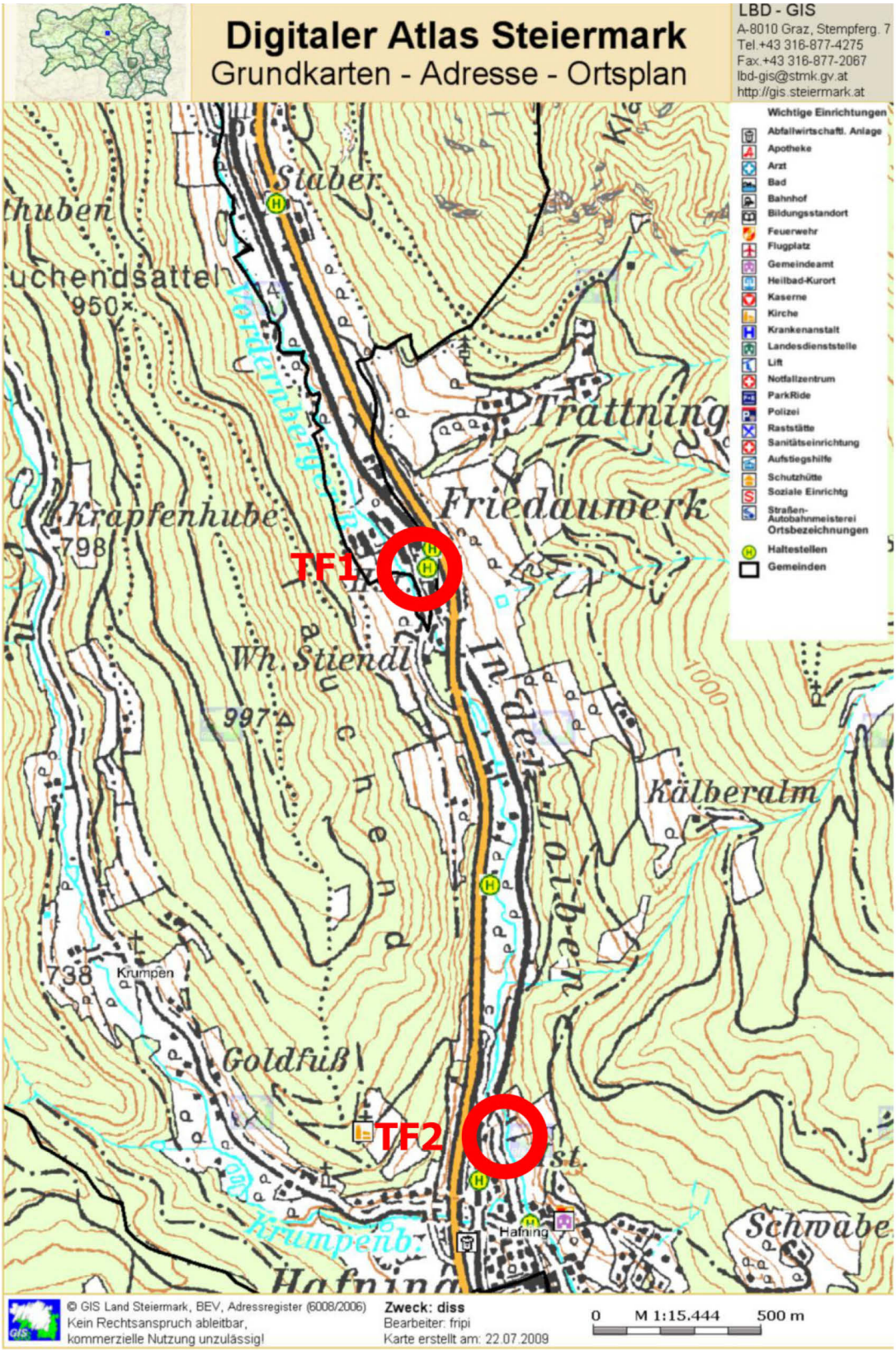
Digitaler Atlas Steiermark
Grundkarten - Adresse - Ortsplan
LBD - GIS
A-8010 Graz, Stempferg. 7
Tel.+43 316-877-4275
Fax.+43 316-877-2067
lbd-gis@stmk.gv.at
http://gis.steiermark.at
Wichtige Einrichtungen
Abfallwirtschaftl. Anlage
Apotheke
Arzt
Bad
Bahnhof
Bildungsstandort
Feuerwehr
Flugplatz
Gemeindeamt
Heilbad-Kurort
Kaserne
Kirche
Krankenanstalt
Landesdienststelle
Lift
Notfallzentrum
ParkRide
Polizei
Raststätte
Sanitätseinrichtung
Aufstiegshilfe
Schutzhütte
Soziale Einrichtg
Straßen-Autobahnmeisterei
Ortsbezeichnungen
Haltestellen
Gemeinden
Staber
Trattning
Friedauwerk
Krapfenhube
798
TF1
Wh. Stiendl
997
Kälberalm
738
Krumpen
Goldfuß
TF2
Hafning
Schwabe
© GIS Land Steiermark, BEV, Adressregister (6008/2006)
Kein Rechtsanspruch ableitbar,
kommerzielle Nutzung unzulässig!
Zweck: diss
Bearbeiter: fripi
Karte erstellt am: 22.07.2009
0
M 1:15.444
500 m

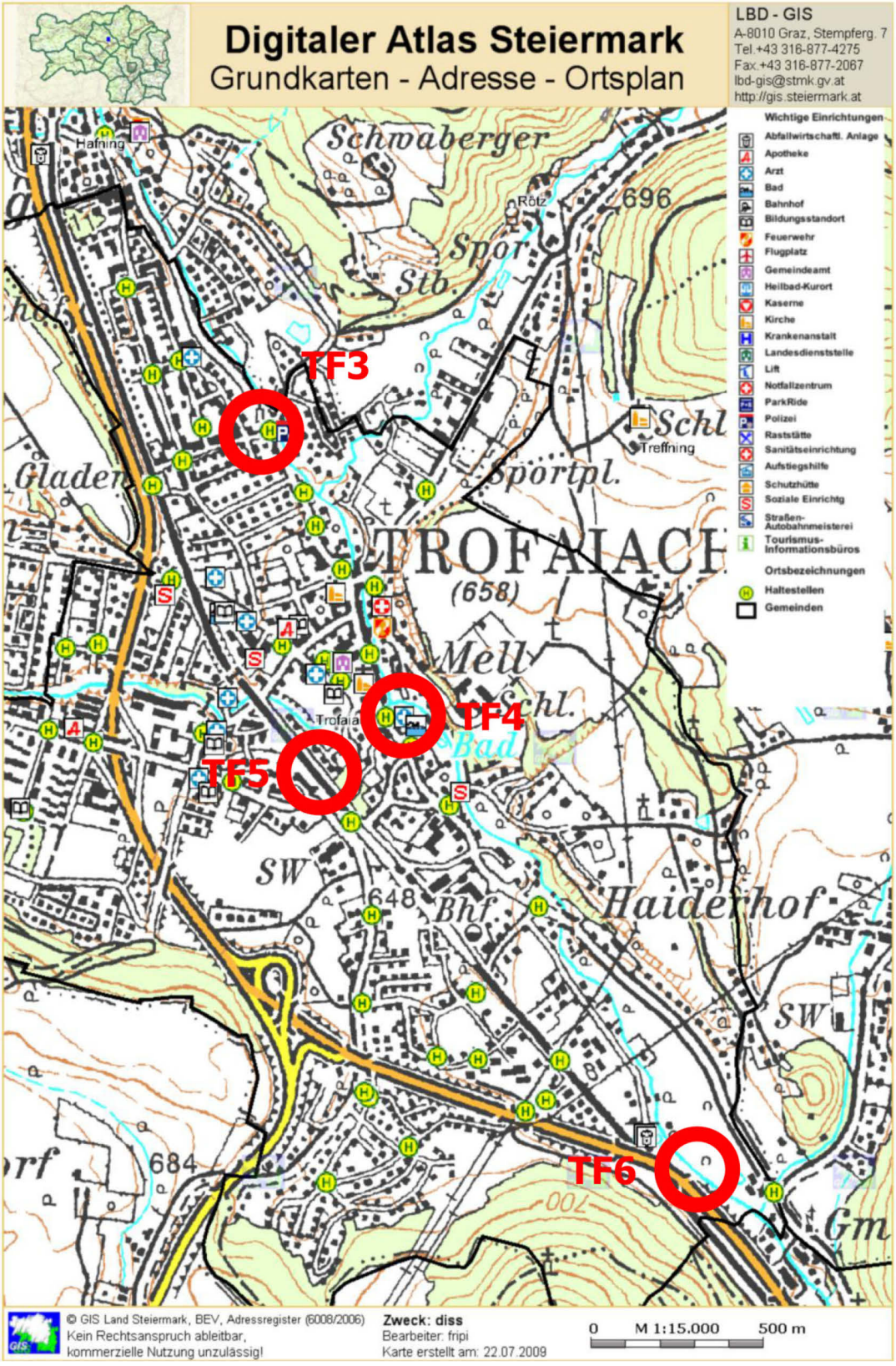
Digitaler Atlas Steiermark
Grundkarten - Adresse - Ortsplan
LBD - GIS
A-8010 Graz, Stempferg. 7
Tel.+43 316-877-4275
Fax.+43 316-877-2067
lbd-gis@stmk.gv.at
http://gis.steiermark.at
Wichtige Einrichtungen
Abfallwirtschaftl. Anlage
Apotheke
Arzt
Bad
Bahnhof
Bildungsstandort
Feuerwehr
Flugplatz
Gemeindeamt
Heilbad-Kurort
Kaserne
Kirche
Krankenanstalt
Landesdienststelle
Lift
Notfallzentrum
ParkRide
Polizei
Raststätte
Sanitätseinrichtung
Aufstiegshilfe
Schutzhütte
Soziale Einrichtg
Straßen-Autobahnmeisterei
Tourismus-Informationsbüros
Ortsbezeichnungen
Haltestellen
Gemeinden
TF3
TF4
TF5
TF6
TROFAIACH
(658)
Schwaberger
Rötz
696
Sport
Stb.
Hafning
Treffning
Sportpl.
Mell
Schl.
Bad
Trofaia
SW
648
Bhf.
Haiderhof
684
700
Gm
© GIS Land Steiermark, BEV, Adressregister (6008/2006)
Kein Rechtsanspruch ableitbar,
kommerzielle Nutzung unzulässig!
Zweck: diss
Bearbeiter: fripi
Karte erstellt am: 22.07.2009
0
M 1:15.000
500 m

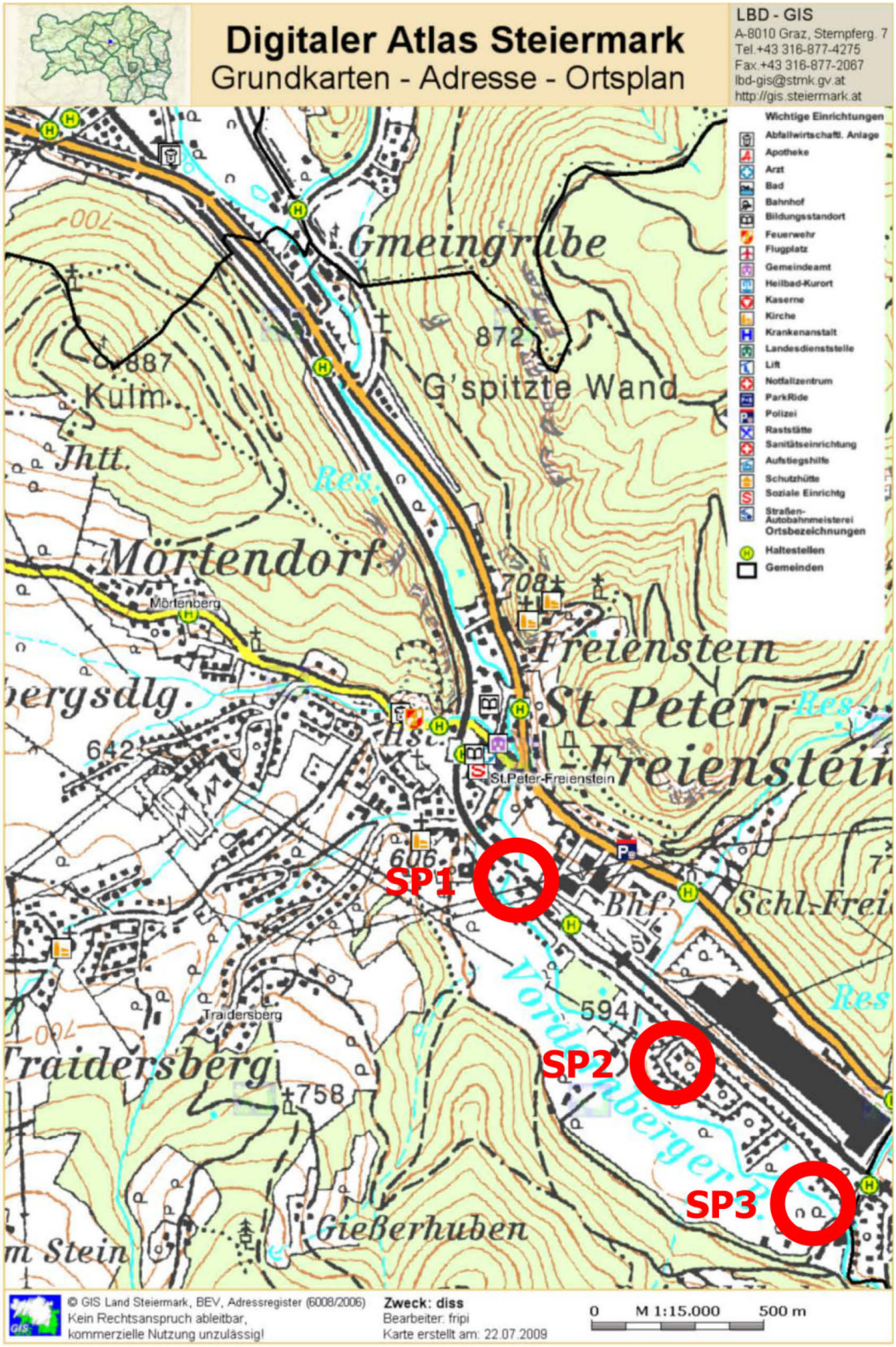
Digitaler Atlas Steiermark
Grundkarten - Adresse - Ortsplan
LBD - GIS
A-8010 Graz, Stempferg. 7
Tel.+43 316-877-4275
Fax.+43 316-877-2067
lbd-gis@stmk.gv.at
http://gis.steiermark.at
Wichtige Einrichtungen
Abfallwirtschaftl. Anlage
Apotheke
Arzt
Bad
Bahnhof
Bildungsstandort
Feuerwehr
Flugplatz
Gemeindeamt
Heilbad-Kurort
Kaserne
Kirche
Krankenanstalt
Landesdienststelle
Lift
Notfallzentrum
ParkRide
Polizei
Raststätte
Sanitätseinrichtung
Aufstiegshilfe
Schutzhütte
Soziale Einrichtg
Straßen-Autobahnmeisterei
Ortsbezeichnungen
Haltestellen
Gemeinden
Gmeingrube
872
G'spitzte Wand
887
Kulm
Mörtendorf
Mörtenberg
708
Freienstein
St.Peter-Freienstein
642
606
SP1
Bhf.
Schl-Frei
Traidersberg
594
SP2
758
SP3
Gießerhuben
© GIS Land Steiermark, BEV, Adressregister (6008/2006)
Kein Rechtsanspruch ableitbar,
kommerzielle Nutzung unzulässig!
Zweck: diss
Bearbeiter: fripi
Karte erstellt am: 22.07.2009
0
M 1:15.000
500 m

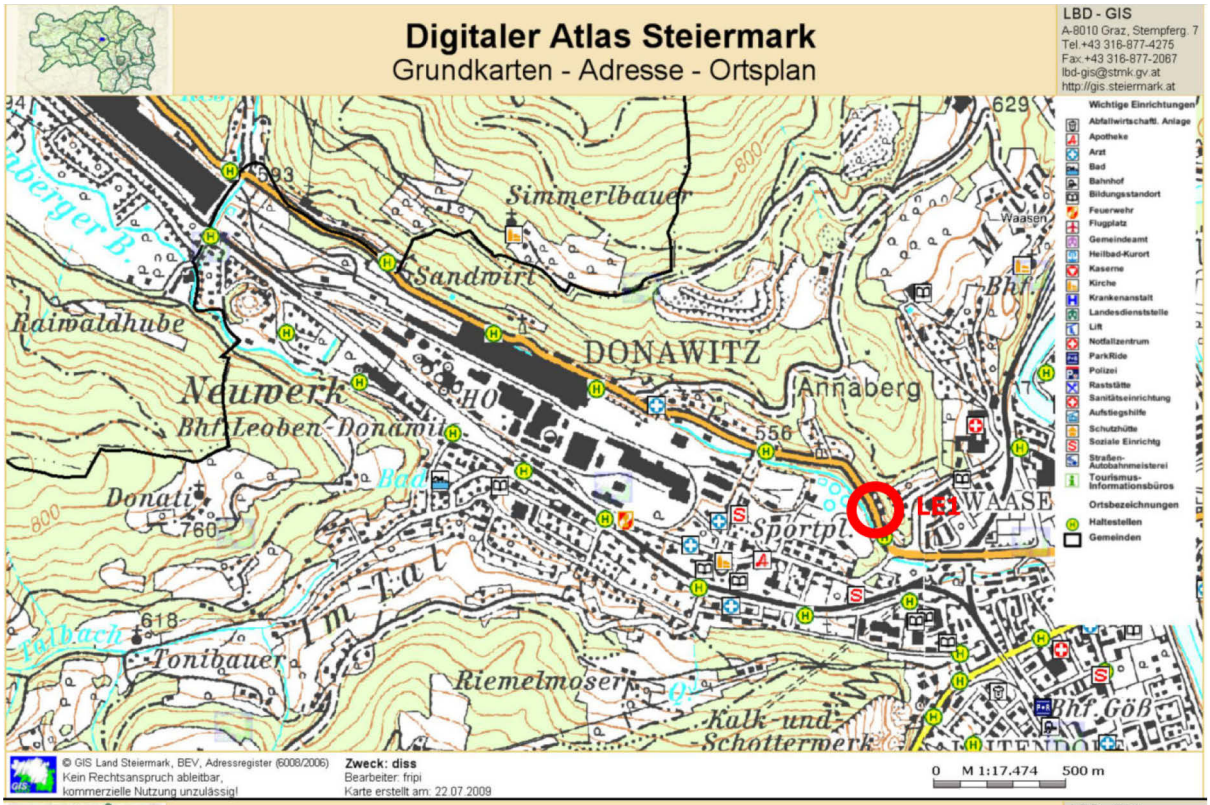
Digitaler Atlas Steiermark
Grundkarten - Adresse - Ortsplan
LBD - GIS
A-8010 Graz, Stempferg. 7
Tel.+43 316-877-4275
Fax.+43 316-877-2067
lbd-gis@stmk.gv.at
http://gis.steiermark.at
Wichtige Einrichtungen
Abfallwirtschaftl. Anlage
Apotheke
Arzt
Bad
Bahnhof
Bildungsstandort
Feuerwehr
Flugplatz
Gemeindeamt
Heilbad-Kurort
Kaserne
Kirche
Krankenanstalt
Landesdienststelle
Lift
Notfallzentrum
ParkRide
Polizei
Raststätte
Sanitätseinrichtung
Aufstiegshilfe
Schutzhütte
Soziale Einrichtg
Straßen-Autobahnmeisterei
Tourismus-Informationsbüros
Ortsbezeichnungen
Haltestellen
Gemeinden
Simmerlbauer
Sandwirt
Raimaldhube
Neuwerk
Bhf Leoben-Donawitz
DONAWITZ
Annaberg
WAASE
Sportpl.
Donati
760
618
Tonibauer
Im Tal
Riemelmoser
Kalk- und Schottermerk
Bhf. Göß
556
629
LE1
© GIS Land Steiermark, BEV, Adressregister (6008/2006)
Kein Rechtsanspruch ableitbar,
kommerzielle Nutzung unzulässig!
Zweck: diss
Bearbeiter: fripi
Karte erstellt am: 22.07.2009
0
M 1:17.474
500 m

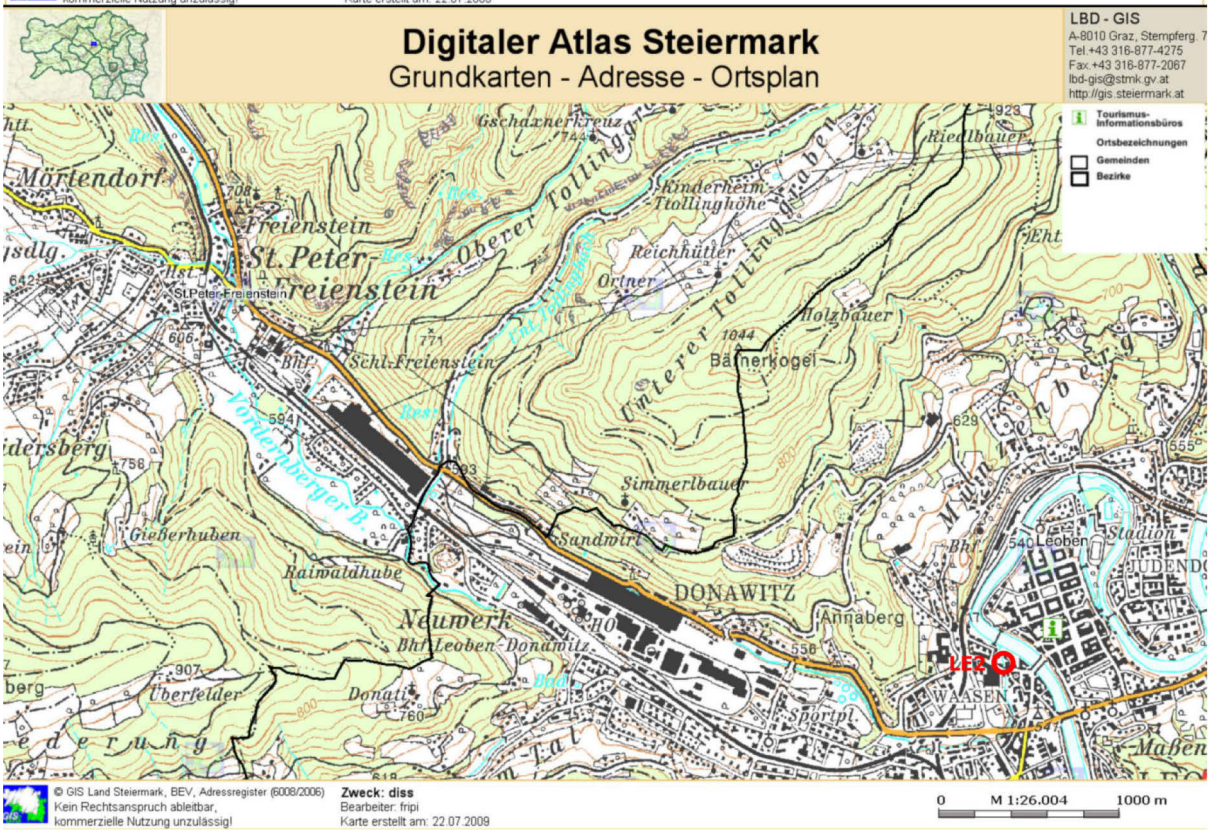
Digitaler Atlas Steiermark
Grundkarten - Adresse - Ortsplan
LBD - GIS
A-8010 Graz, Stempferg. 7
Tel.+43 316-877-4275
Fax.+43 316-877-2067
lbd-gis@stmk.gv.at
http://gis.steiermark.at
Tourismus-Informationsbüros
Ortsbezeichnungen
Gemeinden
Bezirke
Mörtendorf
Freienstein
St. Peter-Freienstein
Gschaxnerkreuz
Riedlbauer
Kinderheim Ttollinghöhe
Oberer Tollinggraben
Unterer Tollinggraben
Reichhütter
Ortner
Holzbauer
Bärnerkogel
Schl. Freienstein
Simmerlbauer
Sandwirt
Gießerhuben
Raimaldhube
Neuwerk
Bhf Leoben-Donawitz
DONAWITZ
Annaberg
Leoben
Stadion
WAASEN
Sportpl.
Donati
760
Überfelder
907
LE2
© GIS Land Steiermark, BEV, Adressregister (6008/2006)
Kein Rechtsanspruch ableitbar,
kommerzielle Nutzung unzulässig!
Zweck: diss
Bearbeiter: fripi
Karte erstellt am: 22.07.2009
0
M 1:26.004
1000 m

Geochemical data

Protrace Geo	CaO g/100g	Sc mg/kg	TiO_2 g/100g	V mg/kg	Cr mg/kg	MnO g/100g	Fe_2O_3 g/100g	Co mg/kg	Ni mg/kg	Cu mg/kg	Zn mg/kg	Ga mg/kg	Ge mg/kg	As mg/kg	Br mg/kg	Rb mg/kg	Sr mg/kg	Y mg/kg	Zr mg/kg	Nb mg/kg	Mo mg/kg
PB1	0.14	13.6	0.89	104.4	79.9	0.26	6.45	17.4	39.9	37.5	30.6	17.7	1.35	24.25	0.80	162.7	46.6	37.1	239	14.2	0.85
PB2	0.92	12.6	0.78	98.3	74.2	0.16	5.94	15.0	30.8	22.0	57.7	19.7	1.25	22.65	3.65	163.0	51.1	30.6	211	14.5	1.20
PB3	0.84	13.3	0.85	110.1	84.2	0.22	6.36	16.1	39.3	23.3	38.1	19.4	1.45	20.20	1.40	178.7	46.6	31.1	198	13.3	1.00
PB4	3.10	11.1	0.79	91.3	66.7	0.26	6.19	14.9	32.9	25.1	37.4	15.7	1.10	15.85	4.00	126.9	69.7	34.2	290	13.2	1.20
PB5	3.71	12.4	0.78	91.1	78.0	0.22	5.94	15.4	39.5	25.9	38.0	15.0	0.95	14.30	3.45	127.2	65.6	32.7	318	13.0	1.05
PB6	4.31	11.8	0.72	95.6	70.5	0.37	7.39	17.3	42.4	34.9	67.8	13.9	0.95	18.70	15.10	113.5	54.7	35.7	267	12.8	1.65
PB7	4.35	11.8	0.76	92.5	85.8	0.31	6.58	17.1	44.6	26.8	73.7	14.3	1.10	17.45	3.80	120.4	50.6	33.3	318	13.1	1.50
VB1	4.30	11.1	0.70	84.3	75.3	0.27	5.98	15.0	41.0	24.1	43.5	13.8	0.60	15.75	3.70	114.5	48.6	29.0	236	12.1	1.35
VB2	4.81	11.3	0.72	83.3	93.6	0.27	5.93	14.3	53.6	22.4	50.4	13.1	1.10	14.20	5.10	106.3	51.7	32.6	326	12.7	1.60
VB3	5.10	12.3	0.73	84.4	102.2	0.28	6.01	15.4	53.4	23.1	59.8	12.8	0.85	16.25	5.25	105.2	52.5	32.6	357	12.5	1.40
VB4	7.28	12.0	0.72	80.5	155.7	0.39	7.13	15.8	75.1	33.0	124.3	12.3	0.90	12.90	5.10	95.4	66.0	30.2	383	12.4	1.50
VB5	6.54	10.9	0.70	82.7	151.4	0.33	6.82	16.5	66.8	38.9	120.6	13.7	1.10	12.40	7.25	104.1	64.5	28.9	333	11.9	1.50
VB6	7.43	11.9	0.73	80.2	190.5	0.38	7.28	17.3	84.1	35.9	104.9	12.4	0.85	11.80	8.45	92.8	65.3	33.3	509	12.8	1.40
MUS1	4.20	12.5	0.74	91.4	99.2	0.29	6.47	15.9	49.0	27.7	64.6	14.4	1.20	16.60	5.95	118.5	56.1	32.8	314	12.6	1.30
TF1	6.64	12.8	0.81	88.9	188.3	0.62	8.54	16.0	65.2	31.6	79.2	14.2	0.85	17.25	3.95	101.5	68.4	33.1	534	13.7	1.55
TF2	7.12	11.8	0.78	82.3	170.5	0.52	7.59	14.4	65.7	27.1	72.8	12.9	0.65	14.90	3.55	94.0	66.5	31.4	489	13.6	1.20
TF3	9.85	13.6	0.76	87.7	127.6	0.53	7.43	17.4	67.0	32.2	92.0	12.6	0.60	16.75	7.15	87.5	69.0	28.3	292	12.5	1.50
TF4	9.10	12.2	0.73	81.1	164.2	0.43	6.83	16.9	90.0	30.3	104.1	11.3	0.50	16.35	7.35	79.3	69.6	29.8	409	12.6	1.45
TF5	6.95	14.5	0.88	126.0	127.4	0.15	6.47	16.6	54.3	25.3	78.3	16.6	0.60	14.20	1.75	97.2	71.8	25.0	214	12.8	1.60
TF6	6.79	14.4	0.90	114.3	150.0	0.27	6.90	18.4	67.5	30.5	105.5	15.9	0.60	17.20	3.90	93.4	88.0	27.9	295	13.7	1.75
SP1	8.83	14.3	0.86	106.3	141.6	0.25	6.45	17.6	59.6	27.9	77.3	13.8	0.70	17.25	2.65	84.6	77.6	28.1	339	13.5	1.80
SP2	8.84	14.1	0.86	106.0	114.5	0.22	6.10	17.2	56.3	25.9	68.0	14.3	0.50	14.90	1.85	84.9	75.7	26.1	251	13.1	1.85
SP3	9.27	13.9	0.85	106.6	120.4	0.26	6.36	17.0	58.8	31.0	86.0	14.2	0.40	16.05	4.65	84.7	77.6	27.7	251	12.7	1.70
LE1	8.41	15.0	0.90	112.0	172.7	0.81	10.64	15.9	66.7	48.3	238.2	13.7	0.45	22.05	5.75	78.4	82.1	29.6	410	13.2	3.00
LE2	8.91	14.0	0.85	111.8	124.6	0.40	9.31	15.2	63.6	36.0	393.2	13.8	0.40	18.50	3.05	79.1	76.4	25.6	203	11.8	2.55
MUS1	4.23	12.4	0.75	91.5	104.4	0.30	6.56	16.8	49.4	29.2	66.0	15.1	1.05	19.60	6.40	120.0	56.6	33.0	318	13.2	1.25

Protrace Geo	Sn	Sb	I	Cs	Ba	La	Ce	Nd	Sm	Yb	Hf	Ta	W	Hg	Tl	Pb	Th	U
	mg/kg	mg/kg	mg/kg	mg/kg	mg/kg	mg/kg	mg/kg	mg/kg	mg/kg	mg/kg	mg/kg	mg/kg	mg/kg	mg/kg	mg/kg	mg/kg	mg/kg	mg/kg
PB1	7.30	2.05	11.2	16.6	552	37.7	77.4	31.1	5.95	4.65	5.10	1.25	3.35	2.05	1.25	13.05	10.40	4.35
PB2	8.00	1.05	11.5	18.1	441	33.5	70.6	26.8	5.65	2.10	6.80	1.10	4.05	1.55	1.20	25.45	11.85	4.60
PB3	8.50	4.85	12.4	12.3	508	35.7	77.7	30.0	2.60	1.25	5.60	1.50	3.90	2.95	2.30	13.80	10.35	4.50
PB4	7.05	4.05	14.6	11.8	438	32.5	68.6	26.5	5.25	3.05	8.20	1.80	3.35	2.95	2.10	15.80	9.90	4.80
PB5	8.70	4.20	11.1	10.6	430	34.6	62.8	25.6	2.25	3.30	9.00	1.25	2.20	2.50	1.65	18.10	9.70	4.75
PB6	10.35	1.55	16.8	10.3	498	33.3	77.0	32.9	2.65	3.70	7.30	0.10	1.00	3.40	1.45	34.20	9.45	4.90
PB7	10.15	4.75	11.5	9.8	463	30.0	71.5	26.7	6.80	1.60	8.50	2.60	3.55	3.45	1.40	21.15	9.10	4.25
VB1	8.50	3.75	10.3	10.2	440	35.8	63.7	28.6	5.90	1.75	6.70	0.05	3.55	1.30	1.80	16.40	9.55	4.20
VB2	8.55	3.70	14.5	6.0	424	33.2	70.7	26.8	6.05	2.55	8.35	1.85	3.45	2.40	1.25	19.70	9.65	4.45
VB3	8.90	3.75	13.8	11.0	442	31.3	68.3	26.4	1.00	2.65	8.80	1.20	3.45	2.05	1.45	20.80	8.75	4.40
VB4	12.60	1.45	11.9	8.8	473	38.2	70.7	28.1	4.05	2.75	9.30	1.40	2.20	3.70	1.65	50.60	9.10	4.50
VB5	14.70	3.60	13.7	8.4	484	31.9	68.5	29.9	2.40	1.80	8.85	2.20	3.20	2.90	2.35	45.35	9.35	4.30
VB6	16.60	4.80	17.3	7.9	448	39.4	78.2	27.6	4.50	1.80	12.25	1.80	4.50	3.40	1.35	50.55	10.95	4.60
MUS1	10.20	3.70	14.6	15.1	472	34.2	71.0	28.3	3.05	2.95	7.80	1.70	3.30	2.95	2.15	25.80	9.85	5.20
TF1	14.35	0.65	14.7	8.2	521	42.2	86.2	36.4	5.25	3.45	15.55	2.15	2.85	5.20	4.80	39.25	14.20	6.40
TF2	12.95	1.15	12.3	3.4	460	36.0	78.5	27.6	6.40	0.65	12.60	2.55	4.10	4.10	3.35	36.50	13.15	4.35
TF3	9.65	1.60	13.1	8.1	466	28.2	66.4	24.2	3.10	-0.20	5.95	2.90	3.15	18.50	3.95	30.00	12.10	4.00
TF4	7.05	0.30	14.5	7.8	401	30.6	66.7	27.7	3.05	-0.40	11.55	2.00	3.65	16.25	3.45	27.90	10.70	4.50
TF5	3.60	-0.65	13.6	8.2	475	31.9	52.7	21.8	2.60	-0.05	7.10	2.10	3.70	3.45	3.90	12.75	9.40	4.55
TF6	7.30	2.00	13.5	9.9	495	33.6	61.9	24.2	3.50	1.75	8.10	2.15	2.75	5.90	3.95	23.95	11.05	4.25
SP1	6.10	-0.35	14.0	5.4	425	28.6	63.4	26.8	2.10	0.60	9.35	3.15	3.80	7.60	3.30	21.15	10.25	3.75
SP2	5.55	0.55	11.9	7.4	420	32.4	59.3	22.1	1.60	-0.25	7.20	2.60	3.25	5.25	3.10	16.25	10.75	4.55
SP3	4.05	-0.75	13.6	7.3	426	29.2	63.9	24.5	2.70	0.00	7.00	2.90	3.35	5.70	3.35	20.00	9.90	5.40
LE1	15.15	2.75	18.3	8.6	464	31.5	74.0	27.1	6.15	0.90	11.70	1.50	4.55	9.75	5.25	63.65	11.45	4.75
LE2	10.15	2.10	17.7	8.6	477	26.9	63.1	23.6	2.20	-1.60	5.25	2.75	5.35	5.45	5.90	74.95	10.70	4.40
MUS1	6.50	2.35	11.3	11.9	475	31.9	66.6	24.3	5.60	1.75	7.85	3.05	3.75	3.55	3.15	23.00	12.30	-2.30

	Na_2O	MgO	Al_2O_3	SiO_2	P_2O_5	SO_3	K_2O	CaO	Sc	TiO_2	V	Cr	MnO	Fe_2O_3	Co	Ni	Cu	Zn	Ga	Rb	Sr	Y	Zr	Nb	Ba	La	Ce	Pb	Th
GeoWSU	g/100g	g/100g	g/100g	g/100g	g/100g	g/100g	g/100g	g/100g	mg/kg	g/100g	mg/kg	mg/kg	g/100g	g/100g	mg/kg	mg/kg	mg/kg	mg/kg	mg/kg	mg/kg	mg/kg	mg/kg	mg/kg	mg/kg	mg/kg	mg/kg	mg/kg	mg/kg	mg/kg	mg/kg
PB1	0.59	0.85	15.3	68.1	0.16	-0.01	3.70	0.18	13.79	0.93	112.7	72.0	0.27	6.57	17.7	42.3	45.4	32.2	19.13	169.3	47.5	40.7	257	14.7	577	45.0	77.3	14.6	12.4
PB2	0.58	2.73	16.2	60.9	0.17	0.03	4.24	1.14	11.36	0.82	102.2	70.3	0.16	6.00	15.7	31.4	26.6	59.6	19.28	174.3	53.0	32.5	229	15.9	479	43.2	88.5	30.8	18.0
PB3	0.43	1.20	16.3	64.5	0.14	0.01	4.21	1.01	14.53	0.86	115.6	84.3	0.23	6.43	15.7	42.3	24.8	43.2	18.09	191.1	44.0	33.0	212	16.7	540	25.6	82.2	15.4	19.0
PB4	0.50	1.59	13.2	62.9	0.19	0.04	3.20	3.49	11.93	0.82	93.9	61.5	0.26	6.21	18.6	35.3	28.7	40.0	15.29	134.6	72.8	36.0	315	15.6	449	35.0	95.4	18.7	13.7
PB5	0.48	1.82	12.9	62.8	0.18	0.04	3.18	4.15	12.04	0.81	93.9	76.1	0.22	5.97	18.8	43.5	31.0	41.2	14.86	136.8	66.3	33.6	353	15.5	459	33.8	87.8	24.9	14.9
PB6	0.47	1.79	11.8	58.9	0.24	0.10	2.90	4.64	12.39	0.74	96.7	71.0	0.38	7.40	21.8	45.6	37.6	71.8	13.42	122.5	56.4	37.7	305	14.5	497	41.5	94.1	36.9	13.4
PB7	0.46	1.83	12.1	61.6	0.21	0.07	3.04	4.71	8.05	0.77	99.2	90.4	0.32	6.60	18.3	46.9	30.9	76.7	13.54	129.5	48.8	36.0	346	14.9	474	46.0	73.8	23.6	15.8
VB1	0.47	1.77	11.7	63.8	0.19	0.05	2.93	4.70	8.70	0.73	87.7	79.1	0.28	6.04	16.4	45.0	24.6	44.0	12.42	125.8	48.6	31.8	264	13.7	455	27.5	89.5	16.6	15.0
VB2	0.55	2.12	11.2	62.3	0.21	0.07	2.72	5.17	8.44	0.75	85.1	110.2	0.28	5.98	17.7	59.5	26.3	53.2	13.21	112.5	52.2	35.1	361	15.8	454	32.6	74.5	21.5	13.9
VB3	0.54	2.15	11.1	62.4	0.21	0.09	2.69	5.33	10.33	0.76	84.3	121.3	0.29	6.07	19.0	58.2	28.3	60.5	10.56	114.1	50.4	34.1	434	17.0	437	36.2	71.7	27.1	15.8
VB4	0.64	2.73	10.8	57.5	0.23	0.11	2.51	7.32	9.41	0.73	83.1	181.0	0.41	7.22	21.5	82.7	39.1	128.1	9.67	103.4	64.5	31.0	429	14.7	484	36.3	82.2	60.1	15.3
VB5	0.63	2.49	11.5	57.7	0.21	0.11	2.72	6.74	8.47	0.71	85.6	165.0	0.35	6.91	16.9	75.0	42.3	126.5	12.42	115.1	61.6	29.5	376	15.0	504	32.0	108.4	55.8	17.8
VB6	0.67	2.82	10.6	56.7	0.23	0.12	2.42	7.44	13.31	0.74	80.6	227.5	0.40	7.37	19.4	94.2	39.8	108.1	10.99	98.8	61.1	35.0	571	15.9	445	44.9	93.9	59.5	13.7
MUS1	0.54	2.00	12.3	61.3	0.20	0.08	3.01	4.57	14.11	0.78	94.8	107.8	0.31	6.55	18.6	53.5	32.3	67.3	10.91	125.9	56.9	34.5	360	14.3	476	39.7	83.4	32.3	12.8
TF1	0.70	2.25	11.6	55.8	0.22	0.08	2.65	6.64	11.88	0.79	85.2	204.9	0.66	8.60	20.4	62.6	35.6	83.4	11.47	108.6	63.6	34.2	591	14.4	512	47.0	94.5	46.4	14.9
TF2	0.71	2.37	10.9	57.5	0.21	0.08	2.47	7.12	12.40	0.78	82.1	196.0	0.55	7.67	17.1	63.5	30.9	75.2	9.18	103.9	61.1	34.3	551	14.9	454	45.7	101.4	44.2	17.3
TF3	0.73	2.30	10.6	53.1	0.24	0.08	2.29	9.43	10.16	0.75	88.7	139.2	0.56	7.38	17.4	64.5	38.4	95.2	9.72	100.6	67.7	28.3	327	15.4	445	44.3	75.5	38.6	18.6
TF4	0.75	2.69	9.5	54.9	0.24	0.15	2.02	8.68	8.10	0.75	78.5	182.5	0.44	6.76	20.7	90.6	29.2	104.2	7.93	87.8	63.0	31.7	476	13.8	394	40.7	98.0	29.7	13.3
TF5	1.35	2.42	13.7	55.0	0.23	0.05	2.69	7.33	14.76	0.89	133.2	134.6	0.15	6.47	18.4	49.6	29.4	83.5	16.45	108.3	69.0	24.8	232	14.6	495	30.5	88.3	17.4	14.0
TF6	1.24	2.46	12.5	51.6	0.25	0.12	2.32	6.62	10.80	0.87	114.2	149.5	0.27	6.52	16.5	61.0	30.8	101.8	13.02	96.9	87.2	28.6	312	17.4	480	34.7	59.0	26.2	11.9
SP1	1.17	2.28	11.6	55.7	0.26	0.14	2.28	8.74	14.46	0.87	109.3	139.9	0.26	6.46	17.4	55.5	28.7	79.7	11.44	96.4	65.1	28.9	385	17.0	432	36.6	78.8	29.9	13.8
SP2	1.19	2.24	11.6	56.0	0.25	0.11	2.28	8.79	11.89	0.87	110.6	119.0	0.23	6.05	17.9	51.9	30.7	70.5	10.81	90.2	78.0	28.3	276	15.6	426	34.4	77.5	22.2	10.3
SP3	1.16	2.25	11.6	53.5	0.27	0.14	2.30	9.18	14.42	0.86	111.4	125.4	0.27	6.33	21.3	57.4	31.5	89.2	13.06	91.5	80.6	29.4	277	14.0	431	45.0	64.0	29.6	11.6
LE1	1.05	2.61	11.1	51.7	0.30	0.14	2.07	7.98	13.94	0.87	108.4	175.8	0.81	10.94	18.9	64.0	53.2	236.0	9.85	92.8	73.4	30.2	455	15.7	433	42.1	65.6	70.0	18.1
LE2	1.11	2.28	10.8	52.8	0.25	0.11	2.13	8.60	10.88	0.82	105.9	125.5	0.40	10.03	18.2	61.0	42.6	380.7	10.25	89.3	69.2	26.0	248	14.6	439	40.7	81.4	79.5	17.4
MUS1	0.50	1.97	12.1	60.6	0.21	0.06	2.98	4.55	10.95	0.78	93.0	117.5	0.30	6.52	17.7	44.4	29.9	71.3	12.41	127.3	52.2	35.1	368	15.8	481	36.5	65.6	33.4	16.2

ICP-MS Geol01	^{7}Li	^{9}Be	^{24}Mg	^{27}Al	^{43}Ca	^{43}Ca	^{45}Sc	^{47}Ti	^{51}V	^{51}V	^{52}Cr	^{52}Cr	^{53}Cr	MnO	Fe_2O_3	Fe_2O_3	^{59}Co	^{59}Co	^{60}Ni	^{60}Ni	^{63}Cu	^{65}Cu
	T1	T1	T1	T1	T1	T2	T2	T1	T1	T2	T1	T2	T2	T1#55	T2#56	T2#57	T1	T2	T1	T2	T2	T2
			g/100g	g/100g	g/100g	g/100g	mg/kg	g/100g	mg/kg	mg/kg	mg/kg	mg/kg	mg/kg	g/100g	g/100g	g/100g	mg/kg	mg/kg	mg/kg	mg/kg	mg/kg	mg/kg
PB1	61.4	2.70	0.73	14.3	0.15	3.32	32.2	0.86	55.6	52.6	39.4	40.7	38.6	0.31	6.42	6.31	17.7	18.4	43.3	43.2	37.9	50.4
PB2	79.8	3.01	2.42	15.3	0.97	3.39	28.9	0.76	53.0	48.9	36.7	37.8	35.8	0.33	5.79	5.65	15.4	15.7	34.3	33.5	30.9	40.5
PB3	53.8	2.87	1.05	15.2	0.95	3.58	30.8	0.81	58.7	55.0	40.8	42.9	40.1	0.34	6.20	6.08	16.7	17.2	41.2	40.3	87.4	119.9
PB4	40.7	2.28	1.41	12.5	3.14	4.66	29.3	0.80	48.5	45.2	30.7	32.6	31.1	0.36	6.09	5.97	16.9	17.5	36.2	35.5	27.6	35.9
PB5	38.8	2.18	1.60	12.2	3.69	4.80	28.4	0.79	48.3	44.9	38.2	39.8	37.7	0.30	5.85	5.75	16.6	17.1	42.7	41.9	33.8	44.7
PB6	35.3	2.10	1.54	10.9	4.00	5.57	32.4	0.80	48.6	45.1	34.3	36.0	34.1	0.47	7.13	6.95	18.6	19.3	45.2	44.3	37.6	50.0
PB7	36.2	2.11	1.62	11.5	4.25	5.34	30.2	0.82	48.9	45.3	46.3	47.5	45.4	0.44	6.45	6.30	18.7	19.2	48.9	47.9	30.4	40.1
VB1	38.2	2.11	1.63	11.5	4.39	5.13	28.2	0.75	46.4	42.8	38.7	39.4	37.5	0.35	5.95	5.84	16.5	16.7	44.9	44.2	27.0	34.6
VB2	38.4	2.12	2.02	11.4	5.25	5.55	29.3	0.80	46.4	43.2	53.7	54.5	52.2	0.40	6.15	6.05	17.8	18.0	62.8	61.4	30.7	40.1
VB3	34.2	1.92	1.90	10.6	5.04	5.45	28.5	0.78	44.1	41.2	56.7	58.2	55.3	0.38	6.03	5.88	17.5	18.0	62.1	61.4	27.4	35.6
VB4	29.5	1.78	2.41	10.2	6.86	6.80	31.7	0.80	42.3	38.8	85.0	86.3	82.2	0.59	7.05	6.85	18.8	19.1	85.0	82.3	35.6	47.2
VB5	31.4	1.93	2.21	11.0	6.32	6.33	30.7	0.77	44.3	40.7	76.1	77.5	74.7	0.56	6.66	6.52	17.7	17.8	72.0	69.4	37.5	49.7
VB6	29.1	1.81	2.49	10.0	6.99	6.86	32.3	0.82	41.8	38.6	107.0	110.4	105.8	0.56	7.16	6.96	19.5	19.9	91.3	88.6	35.6	47.2
TF1	30.4	1.97	2.00	11.2	6.11	7.09	37.2	0.83	45.2	41.9	95.3	99.0	94.2	0.57	8.42	8.15	18.7	19.4	68.7	67.2	29.2	38.4
TF2	30.5	1.85	2.12	10.4	6.45	6.74	33.2	0.77	41.1	38.3	86.8	89.0	84.5	0.52	7.34	7.20	16.8	17.4	68.7	67.6	25.3	32.2
TF3	31.5	1.78	2.06	10.1	8.57	7.82	32.4	0.80	44.1	41.5	62.4	64.5	61.5	0.57	7.24	7.04	18.5	19.3	73.4	72.5	28.7	36.9
TF4	28.9	1.54	2.40	9.1	7.99	7.27	30.4	0.79	42.0	39.6	91.9	95.8	91.2	0.54	6.69	6.52	18.1	18.8	95.5	93.6	25.0	32.7
TF5	37.1	2.15	2.24	13.7	6.84	6.49	31.4	0.84	68.7	63.8	61.4	62.7	59.9	0.36	6.42	6.25	17.3	17.7	57.6	55.5	25.8	33.2
TF6	40.2	2.06	2.39	12.8	6.55	6.59	32.2	0.90	60.4	56.3	74.5	76.9	72.9	0.52	6.82	6.57	19.4	20.1	71.2	69.7	28.3	36.5
SP1	30.7	1.76	2.07	11.4	8.14	7.14	30.5	0.85	55.7	52.1	68.8	71.4	67.9	0.38	6.41	6.27	17.9	18.5	62.7	61.3	25.9	33.6
SP2	31.5	1.82	2.03	11.3	8.03	6.76	28.1	0.81	54.1	51.2	55.1	56.6	53.5	0.34	5.87	5.75	16.8	17.7	58.6	57.4	24.6	31.3
SP3	31.7	1.77	2.01	11.0	8.19	6.88	28.8	0.82	54.0	51.2	57.1	59.2	56.8	0.44	6.08	5.96	17.5	18.3	61.7	60.4	32.6	42.6
LE1	31.3	1.78	2.33	10.5	7.16	8.73	44.3	0.85	52.2	49.5	84.9	87.9	82.9	1.02	10.59	10.12	18.7	19.5	66.6	65.4	41.6	54.7
LE2	28.2	1.64	1.99	10.1	7.72	8.39	39.9	0.79	50.7	48.0	61.2	63.4	60.0	1.11	9.45	9.12	17.3	18.0	64.7	64.0	35.9	46.9
MUS1	40.7	2.19	1.78	11.8	4.05	5.28	30.3	0.80	48.4	44.5	54.5	55.8	53.3	0.39	6.45	6.27	17.7	18.2	53.8	52.4	29.6	38.5
Blank	0.1	0.00	0.00	0.0	0.00	0.05	0.3	0.01	2.1	0.7	1.0	1.5	1.7	0.12	0.04	0.04	0.0	0.1	1.4	1.7	5.8	5.0

ICP-MS Geol01	^{66}Zn	^{66}Zn	^{68}Zn	^{68}Zn	^{69}Ga	^{75}As	^{85}Rb	^{88}Sr	^{89}Y	^{90}Zr	^{93}Nb	^{95}Mo	^{111}Cd	^{121}Sb	^{133}Cs	^{137}Ba	^{139}La	^{140}Ce	^{141}Pr	^{145}Nd	^{146}Nd	^{147}Sm	^{149}Sm
	T1	T2	T1	T2	T1	T2	T1	T1	T1	T1	T1	T1	T1	T1	T1	T1	T1	T1	T1	T1	T1	T1	T1
	mg/kg	mg/kg	mg/kg	mg/kg	mg/kg	mg/kg	mg/kg	mg/kg	mg/kg	mg/kg	mg/kg	mg/kg	mg/kg	mg/kg	mg/kg	mg/kg	mg/kg	mg/kg	mg/kg	mg/kg	mg/kg	mg/kg	mg/kg
PB1	20.0	18.0	45.5	55.7	46.4	23.4	167.1	26.9	40.5	267	14.6	1.08	0.15	6.87	18.65	563	40.4	81.9	9.40	37.1	37.6	8.08	8.17
PB2	46.1	44.9	63.8	67.1	44.1	22.3	170.8	29.5	33.5	238	15.0	3.23	0.18	5.19	14.96	470	39.5	81.9	9.08	35.2	35.6	7.03	7.16
PB3	40.6	38.7	61.1	68.1	46.0	18.3	184.9	26.8	34.1	219	13.6	1.67	0.17	7.42	14.85	526	41.0	81.5	9.10	35.4	35.7	7.03	7.11
PB4	39.8	38.6	56.5	61.4	38.5	16.3	133.8	39.8	36.5	328	22.5	1.65	0.18	5.71	9.81	446	38.5	78.6	8.82	34.4	34.7	7.13	7.14
PB5	21.9	21.3	42.6	47.1	38.0	16.0	132.2	37.0	35.9	349	13.6	1.56	0.17	5.76	9.00	438	38.3	77.2	8.72	34.1	34.3	6.99	7.02
PB6	61.7	62.4	75.5	80.9	38.3	20.9	117.9	30.8	37.8	301	13.0	1.70	0.20	6.01	8.54	481	41.2	85.1	9.21	36.4	36.6	7.52	7.50
PB7	63.6	64.1	78.0	80.3	38.1	19.0	125.5	28.6	35.6	354	13.6	1.62	0.18	6.20	8.25	461	40.6	82.8	9.07	35.6	35.7	7.19	7.20
VB1	32.2	30.6	50.2	57.4	36.9	17.6	120.3	28.5	32.6	274	13.0	3.11	0.15	5.90	7.31	444	56.4	75.8	8.35	32.4	32.7	6.42	6.57
VB2	51.8	49.2	67.9	72.4	37.5	16.8	117.0	31.8	37.6	396	14.2	1.67	0.19	5.69	7.32	460	63.4	84.9	9.37	36.8	37.1	7.40	7.46
VB3	45.9	44.2	60.4	65.2	34.9	15.9	111.2	30.3	35.7	404	13.3	1.48	0.19	5.44	6.85	432	50.3	80.9	8.94	35.1	35.2	7.04	7.08
VB4	106.7	108.3	109.4	111.8	35.7	14.6	100.3	38.2	32.2	422	12.6	2.35	0.22	5.07	5.68	466	57.5	90.6	10.03	39.0	39.3	7.47	7.54
VB5	105.8	103.8	108.9	112.9	37.6	13.9	108.6	36.7	31.0	382	16.1	1.56	0.20	5.38	5.98	476	61.2	81.5	9.09	35.4	35.6	6.91	6.96
VB6	97.6	98.4	102.3	102.0	34.4	14.5	96.9	37.5	37.0	585	13.2	1.94	0.28	4.92	5.55	440	49.2	96.7	10.69	41.5	41.7	8.03	8.15
TF1	51.2	51.5	67.3	73.8	38.2	14.2	104.0	38.0	35.8	600	14.2	3.71	0.26	4.56	5.42	486	55.9	108.9	12.06	46.8	47.0	8.89	8.90
TF2	52.1	53.8	65.2	69.8	34.0	12.8	94.4	36.0	32.9	548	13.7	1.05	0.22	4.18	5.04	426	50.3	98.3	10.98	42.6	42.8	8.14	8.12
TF3	73.2	74.8	82.8	87.9	34.1	14.0	89.7	39.6	30.4	331	12.5	1.12	0.18	4.49	4.98	428	40.6	82.0	8.94	34.9	35.1	6.83	6.85
TF4	81.2	84.3	87.1	87.7	29.4	13.4	81.8	38.8	31.8	455	12.5	1.46	0.23	4.64	5.00	364	43.5	86.1	9.35	36.4	36.8	7.10	7.17
TF5	62.7	61.4	75.4	81.2	40.5	12.8	101.3	40.3	26.8	237	12.9	1.26	0.13	3.01	3.84	470	32.9	65.1	7.31	28.7	28.7	5.64	5.70
TF6	102.7	106.0	107.8	115.2	39.3	16.1	95.3	49.1	30.0	331	13.7	1.30	0.22	3.80	4.61	466	37.2	74.5	8.25	32.3	32.3	6.31	6.35
SP1	50.5	50.5	62.6	66.4	33.8	14.0	88.3	44.7	29.8	380	13.5	1.46	0.18	3.56	3.76	404	39.6	78.9	8.71	33.9	34.1	6.61	6.59
SP2	41.9	42.5	57.4	61.3	34.7	13.3	87.5	42.5	27.9	274	12.6	4.97	0.14	3.40	3.69	396	37.1	74.3	8.19	32.0	32.1	6.25	6.24
SP3	73.0	73.6	82.5	88.3	35.0	13.3	86.3	42.8	29.2	283	12.8	5.81	0.15	3.68	3.96	401	37.9	75.8	8.38	32.8	32.9	6.48	6.45
LE1	205.6	217.1	190.6	196.0	34.1	17.5	79.6	45.4	31.7	467	13.0	2.65	0.34	4.55	4.19	403	40.8	82.0	9.00	35.2	35.2	6.90	6.82
LE2	310.6	331.3	274.7	283.8	33.2	13.8	77.3	41.4	26.6	231	11.7	2.26	0.28	3.73	3.79	384	33.4	66.3	7.32	28.7	28.9	5.67	5.64
MUS1	43.2	42.0	60.5	65.2	37.6	17.7	124.7	32.5	36.1	354	15.9	1.70	0.19	5.74	8.93	458	40.8	83.1	9.19	36.0	36.1	7.31	7.34
Blank	<1	<1	<1	<1	<1	0.2	0.2	12.6	0.1	5	0.2	0.61	0.00	0.13	0.01	<1	<1	0.2	0.02	0.11	0.10	0.02	0.01

ICP-MS Geol01	^{151}Eu	^{153}Eu	^{157}Gd	^{159}Tb	^{160}Gd	^{161}Dy	^{163}Dy	^{165}Ho	^{166}Er	^{167}Er	^{169}Tm	^{172}Yb	^{173}Yb	^{175}Lu	^{178}Hf	^{181}Ta	^{182}W	^{205}Tl	^{206}Pb	^{207}Pb	^{208} Pb	^{209}Bi	^{232}Th	^{238}U
	T1	T1	T1	T1	T1	T1	T1	T1	T1	T1	T1	T1	T1	T1	T1	T1	T1	T1	T1	T1	T1	T1	T1	T1
	mg/kg	mg/kg	mg/kg	mg/kg	mg/kg	mg/kg	mg/kg	mg/kg	mg/kg	mg/kg	mg/kg	mg/kg	mg/kg	mg/kg	mg/kg	mg/kg	mg/kg	mg/kg	mg/kg	mg/kg	mg/kg	mg/kg	mg/kg	mg/kg
PB1	1.70	1.71	7.78	1.21	7.93	6.92	6.89	1.41	1.94	3.88	0.58	3.75	3.74	0.56	7.07	1.28	3.44	0.78	13.7	13.2	13.5	0.80	13.15	3.65
PB2	1.31	1.32	6.40	1.00	6.40	5.79	5.75	1.18	1.68	3.26	0.49	3.19	3.18	0.47	6.24	1.26	4.01	0.83	26.3	26.4	26.3	0.95	13.86	4.08
PB3	1.45	1.46	6.43	0.99	6.44	5.83	5.80	1.19	1.69	3.30	0.50	3.23	3.24	0.48	5.79	1.11	3.30	0.80	14.5	14.3	14.4	0.70	12.25	3.32
PB4	1.54	1.53	6.80	1.08	6.86	6.20	6.17	1.27	1.76	3.50	0.52	3.40	3.38	0.50	8.47	5.33	3.14	0.63	16.7	16.6	16.7	0.90	12.41	3.57
PB5	1.47	1.47	6.57	1.03	6.64	6.06	6.02	1.25	1.74	3.45	0.52	3.37	3.36	0.50	8.96	1.09	3.13	0.62	20.2	20.2	20.3	0.87	12.08	3.55
PB6	1.63	1.62	7.15	1.10	7.19	6.30	6.26	1.28	1.77	3.48	0.51	3.27	3.28	0.48	7.80	1.18	3.20	0.59	35.7	35.6	35.5	0.91	11.49	3.40
PB7	1.49	1.48	6.66	1.02	6.69	5.95	5.91	1.22	1.73	3.35	0.50	3.24	3.25	0.48	8.97	1.06	3.28	0.60	21.2	21.2	21.2	0.87	11.71	3.40
VB1	1.34	1.35	6.01	0.94	6.07	5.46	5.43	1.11	1.55	3.05	0.46	2.94	2.92	0.43	7.05	1.01	3.12	0.57	17.1	17.1	17.2	0.81	10.98	3.17
VB2	1.52	1.53	6.97	1.07	6.96	6.24	6.22	1.28	1.82	3.56	0.53	3.46	3.46	0.52	10.20	1.13	3.42	0.58	23.2	23.3	23.2	1.09	12.34	3.70
VB3	1.44	1.44	6.60	1.02	6.60	5.95	5.92	1.22	1.73	3.38	0.51	3.30	3.29	0.50	10.39	1.05	3.73	0.53	24.2	24.4	24.3	0.81	11.50	3.52
VB4	1.50	1.51	6.50	0.95	6.49	5.43	5.38	1.10	1.56	3.07	0.46	3.03	3.02	0.46	10.69	0.98	3.12	0.53	56.2	57.3	56.7	0.89	11.61	3.39
VB5	1.41	1.41	6.08	0.91	6.08	5.20	5.18	1.06	1.51	2.94	0.44	2.89	2.90	0.44	9.63	1.74	3.35	0.57	49.8	50.5	50.0	0.87	11.26	3.29
VB6	1.59	1.60	7.01	1.05	7.05	6.10	6.05	1.26	1.79	3.54	0.53	3.54	3.54	0.54	14.71	1.02	3.34	0.52	55.7	56.7	56.1	0.78	12.31	3.81
TF1	1.74	1.75	7.45	1.07	7.35	6.10	6.03	1.24	1.76	3.45	0.52	3.45	3.46	0.53	14.99	1.12	2.63	0.59	43.6	44.8	44.2	0.55	13.36	3.73
TF2	1.59	1.59	6.84	0.99	6.77	5.64	5.58	1.15	1.63	3.19	0.48	3.19	3.19	0.49	13.77	1.12	2.59	0.52	37.8	38.7	38.2	0.47	12.48	3.52
TF3	1.42	1.42	6.04	0.90	6.08	5.14	5.10	1.05	1.48	2.86	0.43	2.77	2.78	0.42	8.32	1.06	2.23	0.50	31.1	31.7	31.4	0.48	10.49	2.92
TF4	1.46	1.46	6.28	0.94	6.28	5.36	5.29	1.09	1.53	3.03	0.45	2.97	2.97	0.45	11.45	0.94	2.05	0.45	28.0	28.3	28.2	0.65	10.29	3.05
TF5	1.22	1.25	5.22	0.78	5.20	4.55	4.49	0.92	1.31	2.51	0.37	2.42	2.44	0.36	5.85	0.95	1.29	0.53	13.4	13.4	13.4	0.30	8.35	2.30
TF6	1.35	1.36	5.80	0.87	5.77	5.05	4.99	1.04	1.47	2.86	0.43	2.79	2.79	0.42	8.21	1.03	2.30	0.51	23.2	23.5	23.4	0.38	9.29	2.64
SP1	1.37	1.38	5.94	0.87	5.90	4.97	4.94	1.01	1.43	2.78	0.41	2.68	2.70	0.41	9.33	0.98	1.67	0.47	22.5	22.8	22.7	0.38	9.05	2.63
SP2	1.30	1.31	5.47	0.82	5.53	4.71	4.65	0.95	1.35	2.62	0.39	2.52	2.52	0.37	6.81	0.96	1.50	0.48	16.0	16.0	16.0	0.34	8.84	2.49
SP3	1.36	1.35	5.68	0.86	5.73	4.93	4.89	1.00	1.40	2.75	0.41	2.61	2.63	0.39	7.11	0.95	1.82	0.49	21.4	21.8	21.6	0.42	9.11	2.64
LE1	1.48	1.48	6.08	0.92	6.08	5.29	5.24	1.08	1.54	3.00	0.45	2.92	2.93	0.45	11.56	0.99	3.19	0.61	66.3	68.2	67.1	0.60	9.58	3.10
LE2	1.24	1.25	5.08	0.77	5.14	4.46	4.42	0.91	1.28	2.48	0.37	2.35	2.37	0.35	5.84	0.89	2.43	0.57	74.0	76.1	74.9	0.72	8.13	2.35
MUS1	1.51	1.51	6.80	1.05	6.80	6.07	6.02	1.24	1.73	3.40	0.51	3.27	3.28	0.49	9.02	2.47	2.79	0.60	27.5	27.8	27.7	0.84	11.96	3.54
Blank	0.00	0.00	0.01	0.00	0.01	0.02	0.02	0.00	16.88	0.01	0.00	0.01	0.00	0.00	0.05	0.02	0.27	0.01	0.3	0.2	0.3	0.13	0.03	0.00